UNIVERSITÀ DEGLI STUDI DI NAPOLI FEDERICO II

DEPARTMENT OF CIVIL, BUILDING AND ENVIRONMENTAL ENGINEERING

Ph.D. Course in CIVIL SYSTEMS ENGINEERING

XXXVI cycle

Harnessing magnetism and biogas micro-oxygenation to enhance the biomethane and fertilizing potential of sewage sludge

SSD: ICAR/03

Course Coordinator:

Prof. Andrea Papola

Ph.D. Student:

Nicola Di Costanzo

Supervisors:

Prof. Giovanni Esposito

Prof. Alessandra Cesaro

Prof. Francesco Di Capua

ABSTRACT

Sewage sludge, a byproduct of wastewater treatment, presents a significant challenge due to its volume, composition, and environmental impact. It is a complex mixture of organic and inorganic matter, its characteristics varying depending on the wastewater source and the treatment process employed. Over the years, the growing population and urbanization have fueled the expansion of wastewater treatment plants, leading to a concomitant surge in sewage sludge production. This trend has been further exacerbated by stricter effluent quality requirements, which necessitate more intensive treatment processes and, consequently, higher sludge generation. Anaerobic digestion (AD) is a promising alternative to traditional sewage sludge disposal methods. AD is a biological process that converts sewage sludge into methane gas, a valuable renewable energy source. The generation of biogas comes along with the production of anaerobic digestate with potential fertilizer properties due to the significant content of both macro- and micro-nutrients. It also helps to reduce the volume and weight of sewage sludge, making it easier to transport and dispose of. However, AD is not without its challenges. The complex organic matter (OM) composition of sewage sludge can make it difficult to digest anaerobically. Digested sludge tends to concentrate potential contaminants, thereby limiting its reuse in agriculture to fall within the limits set by the European directive 86/278/EEC. To overcome these challenges, several studies have implemented processes that can break down OM components increasing biodegradability, dewaterability of sewage sludge, and, consequently, biogas production or that can act positively on the agronomical and hygienic properties of sewage sludge. Among these, the application of static magnetic field (SMF) has been scarcely evaluated and recently has gained increasing interest. Also, the effects of SMF application on the agronomic properties of digestate have not yet been addressed.

Besides, inhibitory substances in the OM can also interfere with the anaerobic digestion process. Hydrogen sulfide (H_2S) is a common byproduct in biogas, produced through anaerobic digestion of sulfur-rich organics and the activity of sulfate-reducing bacteria (SRB). H_2S levels in biogas, which can range from hundreds to thousands of

ppm, are influenced by the feedstock's sulfur content and the microbial competition for organic substrates. Elevated H_2S levels not only harm biogas processing equipment but also lower its economic and reuse value. During combustion, H_2S gets converted to sulfur oxides (SO_x) and sulfuric acid (H_2SO_4), causing severe corrosion in infrastructure. Additionally, H_2S and SO_x can deactivate oxidation catalysts and inhibit methanogenic bacteria at concentrations above 50 mg/L, further stressing the need for careful management of H_2S in biogas systems. Microaeration has been reported as an efficient and cost-effective method for in-situ H_2S removal from biogas, but it leads to the dilution of the CH_4 produced during the process mainly due to the presence of nitrogen gas. Injecting small amounts of pure oxygen (micro-oxygenation) instead of air in the digester headspace to prevent nitrogen gas contamination of biogas, can turn in an important challenge if the target is biogas upgrading to biomethane. Several studies have demonstrated the efficacy and cost-effectiveness of microaeration in removing H_2S directly within biogas digesters. However, this approach suffers from methane dilution due to the presence of nitrogen gas introduced with air. To overcome this limitation and achieve efficient biogas upgrading to biomethane, micro-oxygenation - the controlled injection of pure oxygen into the digester headspace - emerges as a promising alternative. This method eliminates nitrogen gas contamination, thereby minimizing methane dilution and increasing the methane content of the upgraded biogas.

The primary objective of this doctoral thesis was to devise a comprehensive strategy for enhancing the AD of sewage sludge, particularly in terms of increased biomethane yield, nutrient recovery, and inhibitory compound removal. Towards this goal, the impact of SMF on AD processes and the biological biogas desulfurization via in-situ micro-oxygenation in real-scale anaerobic digesters were investigated.

The impact of SMF on AD of sewage sludge was evaluated in various settings: a) as post-treatment to improve the agricultural value of sewage sludge digestate by promoting the precipitation of valuable fertilizers (i.e., struvite); b) as pre-treatment to enhance the biomethane potential; c) during anaerobic digestion in a continuous side-stream recirculation system, ensuring uninterrupted sludge exposure to the SMF. Low-intensity SMF was found to be extremely effective in both batch and continuous

configurations, as it produced an improvement in biomethane production up to 12.7% and 48.3%, respectively. In contrast, high-intensity SMF (1.5 T) pre-treatment exhibited detrimental effects on methane generation, resulting in a 15.1% decline, indicating an inverse relationship between SMF intensity and biogas production. Nevertheless, high-intensity SMF post-treatment proved valuable in promoting the chemical precipitation of beneficial compounds with fertilizer properties (e.g., struvite) in anaerobically digested sludge, thereby enhancing its fertilizer potential.

This thesis work focused also on the biological removal of sulfur compounds from biogas, followed by biomethane production, using in-situ micro-oxygenation in large-scale anaerobic digesters that process high-solid AD under thermophilic conditions. A stable hydrogen sulfide (H_2S) removal efficiency of 98.2(±1.3) % was achieved with an oxygen (O_2) dose of 0.96 NL/Nm^3 biogas. At the lowest O_2 dose tested, removal efficiencies of 67.4(±0.7) % were observed. The response time of the biological desulfurization system to transient oxygen conditions was also evaluated through intermittent O_2 injection, proving that full recovery of desulfurization performance was within 10 hours. Moreover, by carefully introducing small amounts of O_2 into the anaerobic digester, the digestion performance was not negatively impacted and enabled the achievement of biogas quality that complies with the specifications for biomethane in terms of both O_2 and H_2S contents. Using a Next Generation Sequencing (NGS), targeting bacterial 16S rRNA gene, the main microbial families responsible for biological H_2S oxidation developing on the digester surface and internal walls were identified (*Lentimicrobiaceae*, *Caldicoprobacteraceae*, *DTU014*, *Syntrophomonadaceae*, and *Rhodobacteraceae).*

Therefore, by embracing the innovative treatments proposed in this thesis work, it seems possible to increase the environmental and economic benefits of sewage sludge management, turning it into a driving force for sustainable practices and resource conservation.

TABLE OF CONTENTS

[a] ***Chapter 6*** *is not included in this version of the thesis due to its inclusion in a patent application process. It will be made available once the process is complete.*

LIST OF FIGURES

LIST OF TABLES

List of tables

ABBREVIATIONS

AD	Anaerobic Digestion
ADS	Anaerobically Digested Sludge
CHP	Combined Heat and Power
COD	Chemical Oxygen Demand
CST	Capillary Suction Time
ED	Electrodialysis
FAN	Free Ammonia Nitrogen
FO	Forward Osmosis
HPM	High-Pressure Membrane
HSAD	High-Solids Anaerobic Digestion
HTC	Hydrothermal Carbonization
LPM	Low-Pressure Membrane
MD	Membrane Distillation
MF	Microfiltration
MR	Mixing Ratio
NF	Nanofiltration
NGS	Next Generation Sequencing
NMC	Number of Magnetization Cycles
PSA	Pressure Swing Adsorption
Q	Flow rate
RO	Reverse Osmosis
SBP	Specific Biomethane Production
sCOD	Soluble Chemical Oxygen Demand
SMF	Static Magnetic Field
SOB	Sulfur Oxidizing Bacteria
TAN	Total Ammonia Nitrogen
TFE	Thin Film Evaporator
TKN	Total Kjeldahl Nitrogen
TMP	Transmembrane Pressure

TS	Total Solids
UF	Ultrafiltration
VFA	Volatile Fatty Acid
VOC	Volatile Organic Compound
VS	Volatile Solids
WWTP	Wastewater Treatment Plant
XRD	X-ray Diffraction

CHAPTER 1

Introduction

Chapter 1

Sewage sludge is an unavoidable by-product of wastewater treatment, containing organic matter, nutrients and possibly pathogens and toxic substances such as organic pollutants and heavy metals. The management of this by-product is challenging due to the high investment and operational costs associated with its treatment and disposal [1]. The sludge produced by wastewater treatment plants represents only a few percent by volume of the treated wastewater, but its treatment accounts for up to 50% of total operating costs [2]. Conventional sewage sludge treatment involves volume reduction through thickening and dewatering, and biological stabilization through anaerobic digestion (AD). The latter produces a gaseous stream (the biogas) and a solid-liquid flow (the digestate). The biogas recovered from the AD of sewage sludge typically contains 55-65% methane (CH_4), 35-44% carbon dioxide, and small concentrations of other gases such as hydrogen, hydrogen sulfide, carbon monoxide and ammonia [3]. The digestate is a mixture of biomass, water and inert and undigested solids with potential fertilizer properties. Indeed, the biological degradation of the organic matter contained in the sludge during AD increases the concentration of soluble nutrient species, i.e., total ammonia nitrogen and ortho-phosphate [4]. Nevertheless, AD of sewage sludge is not always a viable option for small wastewater treatment plants or in developing countries due to high capital costs, large operating volumes and heating energy needs due to the high water content of the treated sludge, which often results in insufficient biogas production to sustain the energy requirements of the process [5]. In this scenario, undigested dewatered sludge can be collected and treated in centralized plants that perform a high-solids anaerobic digestion (HSAD) [6]. This process, usually characterized by a high total solids content of the feedstocks (typically greater than 15%$_{w/w}$), produces a particularly nutrient-rich digestate and is often carried out at thermophilic temperatures, resulting in better digestate sanitation compared to mesophilic AD [7]. Although, HSAD of sewage sludge has been claimed to be advantageous over traditional low-solid anaerobic digestion for several reasons (such as smaller reactor volume, lower energy requirements for heating, less material handling) [8], it poses some challenges due to the high concentration of ammonia nitrogen and/or hydrogen sulfide that can develop during the anaerobic conversion of organic matter (OM), which can slow down the biological kinetics andreduce the

economic value and reuse potential of biogas [9]. To mitigate the inhibition of the anaerobic process, specific treatments must be carried out. Moreover, the intricate composition of OM in sewage sludge poses challenges. To address these obstacles, various studies have explored methods to enhance the biodegradation and dewaterability of sewage sludge. Among the techniques examined, the use of static magnetic fields (SMF) has received limited attention but is now attracting growing interest. Also, as SMF application is known for its potential to precipitate solid compounds when applied to water, it might be useful to precipitate slow-release nutrient-rich solid compounds in the digestate, enhancing its fertilizing properties. Additionally, the removal of potential inhibitors during AD is fundamental to avoid inhibition and a reduction of process efficiency. A notable byproduct, hydrogen sulfide (H_2S), emerges from the anaerobic digestion of sulfur-rich organics and the action of sulfate-reducing bacteria (SRB). The concentration of H_2S in biogas, which can vary widely, depends on the sulfur content of the feedstock and the microbial dynamics competing for organic substrates. High levels of H_2S can damage biogas processing equipment and reduce its economic value and reuse potential. When burned, H_2S transforms into sulfur oxides (SO_x) and sulfuric acid, causing significant corrosion to infrastructure. Furthermore, H_2S and SO_x can deactivate oxidation catalysts and suppress methanogenic bacteria at concentrations exceeding 50 mg/L, underscoring the importance of managing H_2S levels in biogas systems. Microaeration has proven to be an effective and economical strategy for on-site H_2S removal from biogas, although it leads to CH_4 dilution primarily due to nitrogen gas inclusion. By introducing small amounts of pure oxygen into the digester headspace, microaeration represents a viable solution by preventing nitrogen gas contamination of the biogas.

This doctoral thesis aims to develop a comprehensive approach for enhancing the AD of sewage sludge, focusing on increasing biomethane production, recovering nutrients, and eliminating inhibitory substances. For this purpose, the research investigates the effects of SMF on AD processes and the biological desulfurization of biogas using in-situ micro-oxygenation in full-scale anaerobic digesters performing HSAD.

1.1. Static magnetic fields: a novel approach for enhancing anaerobic digestion of sewage sludge

Up to date, several studies implemented pretreatment processes to increase AD efficiency [5,10] but, among these, the application of static magnetic field (SMF) has been scarcely evaluated and recently has gained increasing interest. A static magnetic field envelops a region of space, exerting a constant magnetic influence that persists over time. Unlike dynamic fields, its strength and direction remain unchanging at every point. This technology demonstrates its efficacy in precipitating calcium carbonate from water [11] as well as its potential to synergize with aerobic biological processes, leading to enhanced nitrifying aerobic granulation [12]. Prior research has indicated also that SMF may influence the growth and metabolic processes of specific microbial species in varied ways [13], likely attributed to their distinct magnetic susceptibilities. SMF could amplify metabolic functions through the stimulation of interactions between metal ions and enzymes within cells, by the electrodynamic interplay between the magnetic force and the electrical currents present in living organisms, and by affecting cell membranes and transport mechanisms [14]. Enhanced biogas production during AD because of SMF was also reported. Zielinski et al. [15] investigated the impact of SMF on AD of dairy wastewater, observing that a SMF of about 20 mT enhanced biomethane production (373.2 $mL \cdot g_{VS}^{-1}$ compared to 200.2 $mL \cdot g_{VS}^{-1}$ in a control reactor) and methane content (56.8% compared to 49.1% in a control reactor). In a separate study, Zielinski et al. [16], evaluated the effect of SMF on AD of sewage sludge, revealing a substantial influence on methane production efficiency but no impact on cumulative biogas production. Dębowski et al. [17] evaluating the effect of the SMF on the anaerobic digestion of algal biomass, observed that a SMF exposure of 0.6 T for 216 $min \cdot d^{-1}$ exerted a positive effect on methane production, exceeding untreated condition by 11.4%, and content in biogas, 71% compared to 67% in the untreated condition. In a different study, Zhao et al. [18] employed a similar configuration that does not require external energy sources and features a flat circular permanent magnet to augment biogas production from corn stover substrate through anaerobic fermentation, demonstrating that a SMF of 11.4 mT (±2%) could increase

the total gas and methane volumes by 19.5% and 20%, respectively, compared to the control test. Moreover, SMF can also modify the interaction between metal ions [19]. The application of a SMF to sewage sludge destined to AD or to anaerobically digested sludge is expected to impact both the biogeneration of methane and the quality of the digestate, leading to the possible precipitation of compounds that may enhance the fertilizing properties of sewage sludge. Currently, to the best of our knowledge, the literature remains still restricted (**Table 1.1**) and has yet to uncover the mechanisms that explain how the SMF affects and improves the AD of sewage sludge.

Table 1.1 - Comprehensive overview of the existing literature concerning the integration of SMF into AD.

Substrate	Biomethane production			Methane content		SMF intensity	Exposure time	Reference
	SMF reactor	***Ctrl reactor***		***SMF reactor***	***Ctrl reactor***			
Dairy wastewater	373.2 L/kg_{VS}	200.2 L/kg_{VS}	+86.4%	56.8%	49.1%	20 mT	16.2 min/d	Zielinski et al. (2021)
Corn stover	14.8 L	11.9 L	+19.5%	67.2%	53.8%	11.4 mT	n.a.	Zhao et al. (2020)
Algal biomass	309.4 L/kg_{VS}	277.7 L/kg_{VS}	+11.4%	70.6%	67.2%	0.6 T	216 min/d	Debowski et al. (2016)
Sewage sludge	431±22 L/kg_{VS}	n.a.	n.a.	66.1%	n.a.	17.6 mT	144 min/d	Zielinski et al. (2021)

1.2. Headspace micro-oxygenation as a strategy for efficient biogas desulfurization

Micro-oxygenation of the headspace in anaerobic digesters is an advanced technique employed for the desulfurization of biogas. This process is specifically designed to mitigate the levels of H_2S within the biogas generated from the AD of organic substrates. Given the corrosive and toxic nature of H_2S, not only does its presence pose health risks, but it also significantly deteriorates the operational integrity and lifespan of biogas utilization equipment, such as engines and turbines intended for energy

conversion. Consequently, the strategic removal of H_2S is imperative for optimizing the performance and durability of biogas infrastructure.

The principle behind micro-oxygenation involves the precision-guided injection of O_2 into the headspace. Upon introduction, the O_2 engages in a series of chemical reactions with the H_2S present in the biogas. These reactions predominantly result in the conversion of H_2S into water and elemental sulfur (S^0), or into sulfateS (SO_4^{2-}), contingent upon the prevailing operational conditions within the digester. This transformative process effectively diminishes the H_2S concentration in the biogas, significantly enhancing its quality for subsequent applications. Typically, the most convenient and used option (**Table 1.1**) for providing O_2 in order to trigger the biological desulfurization is microaeration. For instance, Kraakman et al. [20] removed over 80% of the H_2S from the biogas under microaerobic condition at full scale by providing an amount of O_2 of about 0.26 – 0.70 L per L of feed sludge (i.e., 0.86 – 2.04 L of injected O_2 per Nm^3 of biogas produced). In another study, Jeníček et al. [21] reported that a H_2S removal efficiency of about 99% was achieved in 7 full-scale microaerobic digesters when 6.72 L of O_2 were fed per Nm^3 of biogas produced. Similarly, Kobayashi et al. [22] indicated a complete desulfurization at a O_2 dosage of 4.65 L per Nm^3 of biogas produced in a full-scale anaerobic digester. Ramos et al., (2014b, 2014a) in an industrial pilot-scale reactor applied microaerobic conditions by injecting around 0.6 m^3/week (i.e. 13.0 L of injected oxygen for Nm^3 of biogas produced) into the digester headspace and obtained a biogas efficiently desulphurised

Table 1.2 - Effect of air/O2 injections on H2S removal.

Digester Scale	**Feedstock**	**Working conditions**	**H_2S removal**	**gO_2/gH_2S**	**Reference**
Full-scale	Primary sludge + waste activated sludge	Air dose of 1.2 m^3/h	99.5%	2.02	Jeníček et al. (2017)

Full-scale	Dairy cow manure	Air dose of 20 m^3/d	68.2%	1.75	Kobayashi et al. (2012)
Lab-scale	Cow manure	Air dose with an O_2 load of 4.2 mL/gVS	99.7%	n.a.	Song et al. (2020)
Lab-scale	Primary sludge	Air dose of 20 mL/h	90%	n.a.	Andreides et al. (2021)
Pilot scale	Dairy manure	Air dose ranging from 5 to 150 mL/min	99%	n.a.	Mulbry et al. (2017)
Full-scale	High-solid sewage sludge	Air dose ranging from 0.09(± 0.02) to 0.77(± 0.13)	~100%	n.a.	Giordano et al. (2019)
Full-scale	High-solid sewage sludge	O_2 dose of 0.96(±0.03) NL/Nm^3 biogas	98.2%	3.99	*This work*

[1] n.a.: The data provided by the authors do not permit the computation of the value specified in the table.

Despite the use of air can be considered a suitable option it leads to the dilution of the CH_4 produced during the process mainly due to the presence of nitrogen. This can turn in an important challenge especially if the target is biogas upgrading to biomethane. From this perspective, micro-oxygenation has emerged as a particularly interesting and viable technology for both in-situ biological biogas desulfurization and facilitating the subsequent upgrading to biomethane.

1.3. Thesis scope and objective

The aim of this thesis was to develop an integrated approach to optimize the AD process of sewage sludge in terms of enhanced CH_4 production, nutrient recovery, and removal of inhibitory compounds.

Based on this, the following objectives were addressed (**Figure 1.1**):

- Investigating the effects of the implementation of a novel integrated technology to the AD of sewage sludge, i.e., the application of static magnetic fields. This technology was tested in different configurations: 1) as AD post-treatment, in order to enhance the agricultural properties of sewage sludge digestate promoting the precipitation of compounds with valuable fertilizing properties, such as struvite; 2) as AD pre-treatment, in order to increase the CH_4 production; 3) during AD of sewage sludge utilizing a continuous side-stream recirculation system that ensures uninterrupted sludge exposure to the applied SMF.
- Investigating the biological desulfurization of biogas and subsequent CH_4 generation via in-situ micro-oxygenation in real-scale anaerobic digesters treating high-solid sewage sludge under thermophilic conditions.

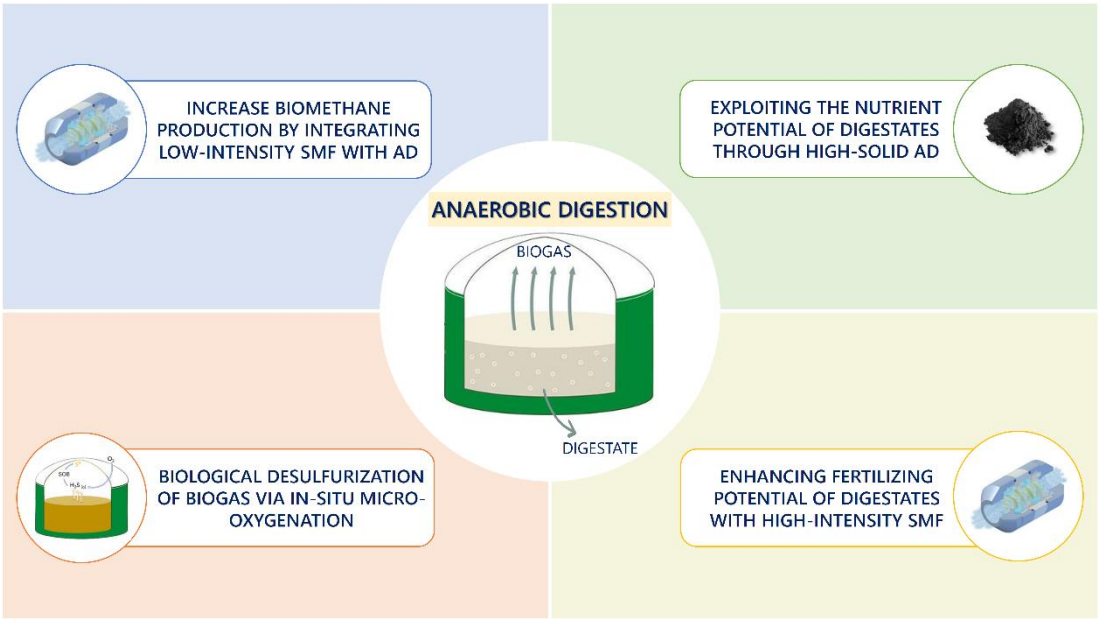

Figure 1.1 - A novel, integrated approach to potentiate the anaerobic digestion process of sewage sludge.

Accordingly, this Ph.D. thesis is composed of six chapters including a preliminary bibliographic study, five research chapters and a final section addressed to conclusive remarks and future perspectives. More specifically, the thesis is structured as follows:

Chapter 1 is a general introduction on the main topics of the thesis, in which the structure of the thesis is also described.

Chapter 2 proposes an overview on the current state of the art on nutrient recovery from sewage sludge anaerobic digestate, with a focus on opportunities and challenges related to nutrient reuse coupled to HSAD of sewage sludge.

Chapter 3 provides an initial assessment of the effectiveness of applying static magnetic fields as a pre-treatment to AD of sewage sludge, evaluating the impacts on the chemical composition of sewage sludge as well as on CH_4 generation during AD.

Chapter 4 explores the direct effects of high-intensity static magnetic field on the chemical properties of digestates originating from both AD and HSAD of sewage sludge.

Chapter 5 clarifies the effects of sludge exposure to low-intensity static magnetic field in terms of AD performance and evolution of fermentative and methanogenic communities.

Chapter 6 assesses both the stability and efficiency of CH_4 production under continuous exposure of digesting sludge to a low-intensity SMF of 20 mT utilizing a continuous side-stream recirculation.

Chapter 7 investigates biological biogas desulfurization via in-situ micro-oxygenation during the centralized digestion of sewage sludge and evaluates the impact of oxygen injection on biogas upgrading to CH_4.

Chapter 8 is a conclusion section that highlights the main findings of this doctoral thesis. This chapter also provides recommendations and perspectives for future research.

1.4. References

[1] S. Shaddel, H. Bakhtiary-Davijany, C. Kabbe, F. Dadgar, S.W. Østerhus, Sustainable sewage sludge management: From current practices to emerging nutrient recovery technologies, Sustain. 11 (2019). https://doi.org/10.3390/su11123435.

[2] M.C. Collivignarelli, A. Abbà, M.C. Miino, V. Torretta, What advanced treatments can be used to minimize the production of sewage sludge in WWTPs?, Appl. Sci. 9 (2019). https://doi.org/10.3390/app9132650.

[3] D. Nguyen, S. Nitayavardhana, C. Sawatdeenarunat, K.C. Surendra, S.K. Khanal, Biogas production by anaerobic digestion: Status and perspectives, 2nd ed., Elsevier Inc., 2019. https://doi.org/10.1016/B978-0-12-816856-1.00031-2.

[4] C. Vaneeckhaute, V. Lebuf, E. Michels, E. Belia, P.A. Vanrolleghem, F.M.G. Tack, E. Meers, Nutrient Recovery from Digestate: Systematic Technology Review and Product Classification, Waste and Biomass Valorization. 8 (2017) 21–40. https://doi.org/10.1007/s12649-016-9642-x.

[5] G. Zhen, X. Lu, H. Kato, Y. Zhao, Y.Y. Li, Overview of pretreatment strategies for enhancing sewage sludge disintegration and subsequent anaerobic digestion: Current advances, full-scale application and future perspectives, Renew. Sustain. Energy Rev. 69 (2017) 559–577. https://doi.org/10.1016/j.rser.2016.11.187.

[6] F. Di Capua, D. Spasiano, A. Giordano, F. Adani, U. Fratino, F. Pirozzi, G. Esposito, High-solid anaerobic digestion of sewage sludge: challenges and opportunities, Appl. Energy. 278 (2020) 115608. https://doi.org/10.1016/j.apenergy.2020.115608.

[7] A. Pigoli, M. Zilio, F. Tambone, S. Mazzini, M. Schepis, E. Meers, O. Schoumans, A. Giordano, F. Adani, Thermophilic anaerobic digestion as suitable bioprocess producing organic and chemical renewable fertilizers: A full-scale approach, Waste Manag. 124 (2021) 356–367. https://doi.org/10.1016/j.wasman.2021.02.028.

[8] N. Duan, B. Dong, B. Wu, X. Dai, High-solid anaerobic digestion of sewage sludge under mesophilic conditions: Feasibility study, Bioresour. Technol. 104

(2012) 150–156. https://doi.org/10.1016/j.biortech.2011.10.090.

[9] A. Giordano, F. Di Capua, G. Esposito, F. Pirozzi, Long-term biogas desulfurization under different microaerobic conditions in full-scale thermophilic digesters co-digesting high-solid sewage sludge, Int. Biodeterior. Biodegrad. 142 (2019) 131–136. https://doi.org/10.1016/j.ibiod.2019.05.017.

[10] V. Khanh Nguyen, D. Kumar Chaudhary, R. Hari Dahal, N. Hoang Trinh, J. Kim, S.W. Chang, Y. Hong, D. Duc La, X.C. Nguyen, H. Hao Ngo, W.J. Chung, D.D. Nguyen, Review on pretreatment techniques to improve anaerobic digestion of sewage sludge, Fuel. 285 (2021) 119105. https://doi.org/10.1016/j.fuel.2020.119105.

[11] M.C. Mascolo, Effect of magnetic field on calcium carbonate precipitated in natural waters with prevalent temporary hardness, J. Water Process Eng. 41 (2021) 102087. https://doi.org/10.1016/j.jwpe.2021.102087.

[12] H. Wang, L. Guo, X. Ren, M. Gao, C. Jin, Y. Zhao, J. Ji, Z. She, Enhanced aerobic granular sludge by static magnetic field to treat saline wastewater via simultaneous partial nitrification and denitrification (SPND) process, Bioresour. Technol. 350 (2022) 126891. https://doi.org/10.1016/j.biortech.2022.126891.

[13] J. Zhang, D. Zeng, C. Xu, M. Gao, Effect of low-frequency magnetic field on formation of pigments of Monascus purpureus, Eur. Food Res. Technol. 240 (2015) 577–582. https://doi.org/10.1007/s00217-014-2358-x.

[14] B. Hu, Y. Wang, J. Quan, K. Huang, X. Gu, J. Zhu, Y. Yan, P. Wu, L. Yang, J. Zhao, Effects of static magnetic field on the performances of anoxic/oxic sequencing batch reactor, Bioresour. Technol. 309 (2020). https://doi.org/10.1016/j.biortech.2020.123299.

[15] M. Zieliński, M. Zielińska, A. Cydzik-Kwiatkowska, P. Rusanowska, M. Dębowski, Effect of static magnetic field on microbial community during anaerobic digestion, Bioresour. Technol. 323 (2021). https://doi.org/10.1016/j.biortech.2020.124600.

[16] M. Zielinski, M. Debowski, J. Kazimierowicz, The effect of static magnetic field on methanogenesis in the anaerobic digestion of municipal sewage sludge,

Energies. 14 (2021). https://doi.org/10.3390/en14030590.

[17] M. Dębowski, M. Zieliński, M. Kisielewska, A. Hajduk, Effect of constant magnetic field on anaerobic digestion of algal biomass, Environ. Technol. (United Kingdom). 37 (2016) 1656–1663. https://doi.org/10.1080/09593330.2015.1126362.

[18] B. Zhao, H. Sha, J. Li, S. Cao, G. Wang, Y. Yang, Static magnetic field enhanced methane production via stimulating the growth and composition of microbial community, J. Clean. Prod. 271 (2020) 122664. https://doi.org/10.1016/j.jclepro.2020.122664.

[19] Y. Abbas, S. Yun, K. Wang, F. Ali Shah, T. Xing, B. Li, Static-magnetic-field coupled with fly-ash accelerant: A powerful strategy to significantly enhance the mesophilic anaerobic-co-digestion, Bioresour. Technol. 327 (2021) 124793. https://doi.org/10.1016/j.biortech.2021.124793.

[20] B. Kraakman, A. Romero, I. Diaz, Z. Wu, M. Noessen, R. Munoz, S.K. Khanal, P.H. Lee, Micro-Aerobic Digestion for Advanced Process Stability and Biogas Desulfurization, 95th Water Environ. Fed. Tech. Exhib. Conf. WEFTEC 2022. (2022) 1625–1642.

[21] P. Jeníček, J. Horejš, L. Pokorná-Krayzelová, J. Bindzar, J. Bartáček, Simple biogas desulfurization by microaeration – Full scale experience, Anaerobe. 46 (2017) 41–45. https://doi.org/10.1016/j.anaerobe.2017.01.002.

[22] T. Kobayashi, Y.Y. Li, K. Kubota, H. Harada, T. Maeda, H.Q. Yu, Characterization of sulfide-oxidizing microbial mats developed inside a full-scale anaerobic digester employing biological desulfurization, Appl. Microbiol. Biotechnol. 93 (2012) 847–857. https://doi.org/10.1007/s00253-011-3445-6.

[23] I. Ramos, R. Pérez, M. Reinoso, R. Torio, M. Fdz-Polanco, Microaerobic digestion of sewage sludge on an industrial-pilot scale: The efficiency of biogas desulphurisation under different configurations and the impact of O2 on the microbial communities, Bioresour. Technol. 164 (2014) 338–346. https://doi.org/10.1016/j.biortech.2014.04.109.

[24] I. Ramos, R. Pérez, M. Fdz-Polanco, The headspace of microaerobic reactors: Sulphide-oxidising population and the impact of cleaning on the efficiency of

biogas desulphurisation, Bioresour. Technol. 158 (2014) 63–73. https://doi.org/10.1016/j.biortech.2014.02.001.

[25] Y. Song, A. Mahdy, Z. Hou, M. Lin, W. Stinner, W. Qiao, R. Dong, Air Supplement as a Stimulation Approach for the in Situ Desulfurization and Methanization Enhancement of Anaerobic Digestion of Chicken Manure, Energy and Fuels. 34 (2020) 12606–12615. https://doi.org/10.1021/acs.energyfuels.0c01724.

[26] M. Andreides, L. Pokorná-Krayzelová, J. Říhová Ambrožová, E.I.P. Volcke, J. Bartáček, Key parameters influencing hydrogen sulfide removal in microaerobic sequencing batch reactor, Biochem. Eng. J. 168 (2021). https://doi.org/10.1016/j.bej.2021.107951.

[27] I. Díaz, S.I. Pérez, E.M. Ferrero, M. Fdz-Polanco, Effect of oxygen dosing point and mixing on the microaerobic removal of hydrogen sulphide in sludge digesters, Bioresour. Technol. 102 (2011) 3768–3775. https://doi.org/10.1016/j.biortech.2010.12.016.

[28] W. Mulbry, K. Selmer, S. Lansing, Effect of liquid surface area on hydrogen sulfide oxidation during micro-aeration in dairy manure digesters, PLoS One. 12 (2017) 1–12. https://doi.org/10.1371/journal.pone.0185738.

CHAPTER 2

Exploiting the nutrient potential of anaerobically digested sewage sludge: a review

The content of this chapter has been published as:
Di Costanzo N, Cesaro A, Di Capua F, Esposito G. Exploiting the Nutrient Potential of Anaerobically Digested Sewage Sludge: A Review. Energies. 2021; 14(23):8149. https://doi.org/10.3390/en14238149

Abstract

This chapter critically reviews the established and novel technologies, which are classified by their ability to recover a specific nutrient (ammonia stripping) or to allow the simultaneous recovery of multiple elements (struvite precipitation, ion exchange, membrane technologies, and thermal treatments). Specifically, this chapter compares the described technologies in terms of nutrient recovery efficiency, capital, and operational costs, as well as their feasibility for full-scale application, revealing the current state of the art and future perspectives on this topic.

2.1. Introduction

In recent decades, great attention has been devoted to the recovery of nutrients from secondary resources, such as waste streams, and to their use for sustainable agriculture [1]. This interest arises from the fact that the world population is growing, resulting in an increasing demand for food. In this context, the nexus 'water–energy–food' is at the center of the challenges arising from the growth of the world population, climate change, and the depletion of natural resources. This is also reflected in the development of strategies to facilitate the transition to a circular economy, based on renewable resources. From this point of view, the increasing need for nutrient compounds for agronomic utilization makes it necessary to identify technologies able to recover nutrients, limiting the consumption of natural resources [2].

Nitrogen (N), potassium (K), and phosphorus (P) have a key role in biological ecosystems [3–7]. Nitrogen is essential for the biological cycle of plants, being the main element responsible for their growth. Potassium facilitates water absorption and protects plants from parasites. Phosphorus, however, is useful for plant metabolism, by promoting a fast maturation. The first two nutrients are widely available in nature. Nitrogen is the fourth most abundant element in cellular biomass and comprises the majority of the Earth's atmosphere [8]. Before the development of the Haber–Bosch process, i.e., the industrial fixation of nitrogen gas (N_2) into ammonia (NH_3) in 1909 [9], the generation of reactive nitrogen species (e.g., NH_3) was exclusively possible through the activity of microbes fixing the inert N_2 of the atmosphere. Potassium is mainly derived from K-rich minerals mined from underground deposits, formed

millions of years ago from the evaporation of sea water [10]. Phosphorus is extracted from phosphate (PO_4^{3-}) rocks (phosphorites) rich in apatite (calcium phosphate minerals). The PO_4^{3-} obtained from the beneficiation (i.e., the separation of phosphatic minerals) of phosphate rocks is either solubilized to produce wet-process phosphoric acid, or smelted to produce elemental phosphorus [11]. Phosphorites are the main commercial source of phosphorus, but they also represent a critical resource, being limited and geographically concentrated, and they will inevitably be exhausted in the coming centuries [12].

On the other hand, the uncontrolled discharge of high levels of nutrients into water bodies causes a serious deterioration of environmental quality, due to eutrophication. This is even more detrimental when considering that these are valuable resources that could be recovered and brought back into the material chain, in accordance with the circular economy model (**Figure 1**). This model addresses the scarcity of raw materials, by promoting recovery of residual flows, thereby reducing their disposal and environmental impact. The new Circular Economy Action Plan - one of the main blocks of the European Green Deal, Europe's new agenda for sustainable growth - announces initiatives to foster sustainable consumption patterns and to ensure that resources are kept in the EU economy for as long as possible. In this framework, the EU Commission will consider reviewing directives on wastewater treatment and sewage sludge and will develop an integrated nutrient management plan, in order to ensure a more sustainable application of nutrients and to stimulate the market for recovered nutrients [13]. In view of this, handling sewage sludge is going to turn into a great opportunity, although some challenges still need to be tackled.

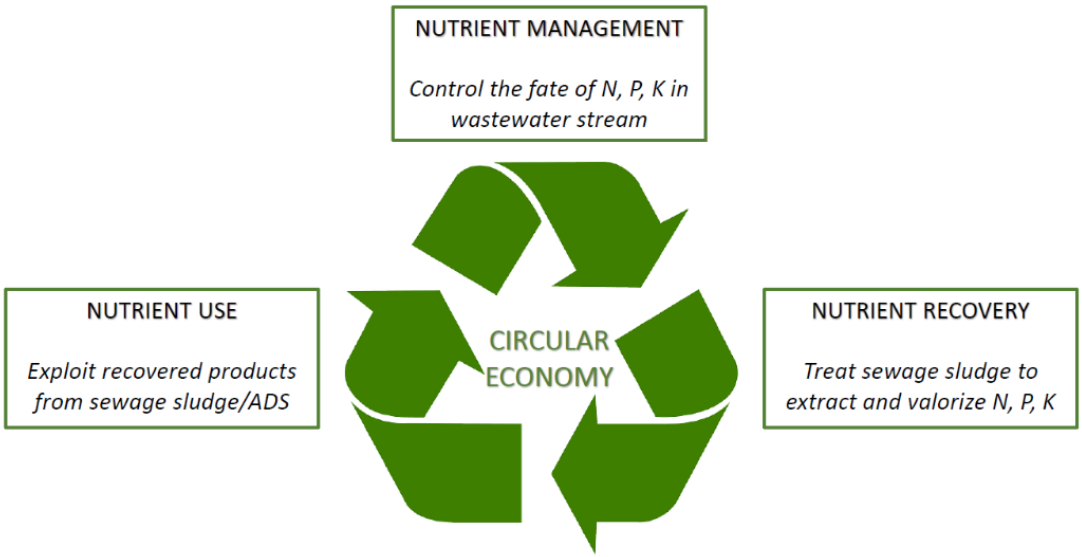

Figure 2.1 - Sustainable management of nutrient-containing wastewater according to the circular economy model.

Sewage sludge is an unavoidable by-product of wastewater treatment, holding organic matter, nutrients, and often pathogens and toxic substances, such as organic contaminants and heavy metals (HMs). The management of this by-product represents a challenge, due to the high investment and operational costs related to its treatment and disposal [14]. Sewage sludge is usually exploited through anaerobic digestion (AD), because it can realize sludge stabilization by converting a part of its organic content into biogas, which is a renewable energy source. However, AD of sewage sludge is not always practicable in small-scale wastewater treatment plants (WWTPs) or in developing countries, due to the large footprint requirement and high capital costs. In this case, dewatered sewage sludge can be collected and treated in centralized plants performing high-solid anaerobic digestion (HSAD), which can be followed by agricultural utilization of the ADS, as a strategy to reuse the nutrients contained in the sewage sludge [14]. In the scientific literature, there are many studies that describe the current technologies applied to efficiently recover nutrients from different residual flows, including wastewater [15–17], human urine [18–20], industrial effluents [21,22], and sewage sludge [1,23–26]. Notwithstanding the great number of existing studies on the topic of nutrient recovery, only a few are available on nutrient recovery

from ADS. Additionally, the latter are mainly focused on N and P recovery, whereas the fate and recovery of K from ADS has been poorly studied.

This review offers an overview on the current state of the art of nutrient recovery from ADS, with a focus on opportunities and challenges related to nutrient reuse coupled to HSAD of sewage sludge. Technologies for the recovery of nutrients from ADS are critically reviewed and compared, with a special attention to recent technological advances, in order to identify their state of application at industrial level, main advantages, and drawbacks, as well as to address future research directions.

2.2. Anaerobically digested sewage sludge: a nutrient source

Sewage sludge is the main residue of wastewater treatment and a major sink for the removed pollutants. It consists of a concentrated suspension of organic and inorganic solids and has a variable moisture content, depending on its origin. Conventional WWTPs generate primary and secondary sewage sludge, being different in organic and water content. Primary sludge derives from the primary sedimentation process and consists mainly of organic substances, with a content of solids in the range of 2–8%, typically 4% (96% humidity). Secondary sludge derives from secondary settling and contains mostly microbial biomass. It has a lower percentage of solids than primary sludge, with a typical value of 1% (99% humidity). Typically, sewage sludge treatment in the sludge streamline of a WWTP pursues volume reduction via thickening and dewatering, as well as a biological stabilization via digestion processes. In small plants, due to the need for operational simplicity and limited sewage sludge flows, the digestion process is either not performed or can be performed under aerobic conditions, while in medium and large plants, AD is more commonly implemented, since the energy recovery from sewage sludge can be substantial. AD generates a gaseous flow (the biogas) and a solid-liquid flow (the ADS). Biogas generated from AD of sewage sludge typically contains 55–65% methane (CH_4), 35–44% carbon dioxide (CO_2), and small concentrations of other gases, such as hydrogen, hydrogen sulfide, carbon monoxide, and ammonia [6,27]. As a result, biogas can be further processed to produce biomethane and/or thermal/electrical energy for plant operation, thereby eliminating or reducing the external supply of energy. However, anaerobic

digesters generally require huge operating volumes and heating energy, due to the high water content of the treated sludge, which often leads to insufficient biogas production to sustain the energy demand of the process [14,28]. Consequently, conventional AD is not always carried out in small WWTPs and highly urbanized areas with limited space [14,29]. In recent years, centralized AD plants collecting unstabilized dewatered sewage sludge from different WWTPs have been developed, with the aim of reducing the operating and capital costs for sludge treatment. These plants treat sewage sludge with a high concentration of TS (>6%): as a result, power consumption for heating is significantly reduced and more biogas is produced per liter of treated sludge, leading to energy-neutral or even net-energy-positive AD plants [14]. ADS is a mixture of biomass, water, and both inert and undigested solids, with potential fertilizer properties. During AD, the biological degradation of the organic matter contained in the sludge increases the concentration of soluble nutrients species, i.e., total ammonia nitrogen (TAN) and ortho-phosphate, which can be rapidly assimilated by plants for their growth [30] if the sludge is used for agricultural applications. Moreover, AD can ensure sufficient hygienization of sewage sludge, especially if performed under thermophilic conditions (50–55 °C) [31]. Although, pathogen reduction can also be achieved at mesophilic temperature (30–35 °C) [32], the latter has been reported to be less effective in reducing pathogens than thermophilic AD, due to lower operational temperatures. One of the most sustainable systems for the disposal of ADS is direct injection on agricultural land [33]. Reusing ADS as fertilizer fits the circular economy approach and has several advantages, which include the return of the organic materials and nutrients into the biocycle. Moreover, the use of ADS as a fertilizer allows reducing the demand for chemical fertilizers and, in turn, the costs for farmers.

In this context, HSAD can be considered the most direct and cost-effective pathway for the reuse of nutrients contained in sewage sludge. Indeed, HSAD generates an ADS particularly rich in nutrients and, thus, advantageous for application in agriculture [33]. Moreover, HSAD is often carried out at thermophilic temperatures, resulting in excellent hygienization of ADS, due to the higher levels of pH and ammonia compared to mesophilic conditions [31]. On the other hand, HSAD of sewage sludge presents certain challenges related to the high viscosity of ADS and concentration of organic

compounds containing nitrogen and sulfur, which may lead to the development of inhibitors (NH_3 and H_2S) that can slow down biological kinetics. To limit inhibition of the anaerobic process, specific treatments for ammonia and/or sulfide removal must be carried out, which can lead to the generation of agronomically valuable products, such as ammonium sulfate [33] and biogenic elemental sulfur [34]. Therefore, even though it is more challenging, thermophilic HSAD can lead to a sustainable recovery and reuse of nutrients from sewage sludge. Nonetheless, the quality of ADS must be carefully evaluated prior to its use in agriculture, as it carries not only nutrients, but may also contain organic and inorganic pollutants [1]. According to Directive 86/278/EEC, the use of ADS in agriculture is subjected to specific restrictions regarding the pH, homogeneity, purity, and contents of nutrients, dry matter, organic dry matter, biological (pathogenic) materials, and chemical pollutants [35]. The generation of poor-quality ADS would require proactive interventions, aimed at improving the quality of the sewage entering the WWTPs, in order to enable the direct utilization of digestate in agriculture. In the absence of remedial measures, nutrient recovery from ADS could be performed by adopting different techniques within the WWTP, in order to valorize a waste material, i.e., sewage sludge, and comply with the principles of a circular economy. It should be highlighted that nutrient recovery from ADS would be not economically profitable in the absence of incentives from national and European governments, due to the high process costs and low market value of recycled fertilizers. However, strategies for nutrient removal and recovery from ADS may be needed to avoid inhibition of the anaerobic process and/or to reduce emissions of N and P to the hydrosphere.

2.2.1. Nitrogen

Nitrogen in ADS mainly originates from the biological degradation of proteins in the feedstock. After anaerobic hydrolysis and fermentation, approximately 70% of organic nitrogen is mineralized to ammonium nitrogen ($N\text{-}NH_4^+$) and free ammonium nitrogen (FAN or $N\text{-}NH_3$), which constitute the TAN of the sludge. Di Capua et al. [14] reported average total Kjeldahl nitrogen (TKN) and FAN concentrations in ADS of 52-77 g/kg TS and 21-45 g/kg TS, respectively. TAN concentrations exceeding 1500 mg/L may

result in a strong inhibition of AD, even leading to process instability [36]. Thermophilic AD systems are more exposed to process instability, as the levels of FAN increase with temperature [37]. Ammonia inhibition proceeds through different mechanisms, i.e., proton imbalance, potassium deficiency, change of intracellular pH, increase of energy requirement, and inhibition of enzymatic reactions [14]. Typically, FAN enters microbial cells by passive diffusion, resulting in abnormal cell ectoplasm, and sodium potassium exchange balance; then, FAN entering into the cell by passive diffusion can indirectly lead to a change of pH, which affects cell stability [37]. In this way, the adoption of strategies for nitrogen recovery can be also seen as a method (if nitrogen is recovered before or during AD) of reducing the inhibitory effects of reduced nitrogen species on the anaerobic process and optimizing the process yield.

2.2.2. Phosphorus

Phosphorus is a fundamental and irreplaceable element for living organisms and has an essential role in global food production, as it is widely used by the fertilizer industry and as an additive for animal feed [38]. In 2015, according to data from the International Fertilizer Association (IFA), the total world production of phosphate rock was about 197 million tons; considering a nominal content of P_2O_5 of about 30%, this corresponds to about 26 million tons of P, with the highest production in China, Morocco, and USA [38]. The future trend of phosphorus production and consumption is currently one of the most debated issues among researchers. Based on current trends, it is estimated that the peak phosphorus production will occur by 2035 [38]. In this scenario, the need is clear for investments in innovative technologies capable of recovering phosphorus from secondary material, such as sewage sludge, wastewater, and urban and agro-industrial wastes [39]. The percentage of P in the dry fraction of sewage sludge can reach up to 10% in weight [40]. Based on this, sewage sludge is considered among the most abundant sources of this element among organic wastes [41]. The amount of phosphorus in sewage sludge depends on the type of wastewater treatment, since the phosphorus contained in wastewater has to be sequestrated into a solid to be removed. Conventional phosphorus removal works by fixing the phosphorus into the sludge in one of two ways: chemically or biologically. Chemical

processes are based on the use of coagulants that hydrolyze rapidly and form multicharged polynuclear complexes with enhanced adsorption characteristics; once suspended particles have flocculated into larger particles, they can be removed from the treated water by sedimentation [3]. Typically, precipitation of soluble phosphorus occurs with aluminum or iron salts, which convert it into insoluble P compounds [42]. Although easy to implement, chemical precipitation increases the cost of sewage treatment and the volume of sludge to be managed [43]. Biological processes exploit the ability of phosphorus accumulating organisms (PAO) to accumulate $P\text{-}PO_4^{3-}$ as polyphosphates in amounts exceeding their metabolic need [42]. The most widely used technology for biological treatment is conducting alternating aerobic and anaerobic processes, enabling the combined removal of carbon, nitrogen, and phosphorus. The first step is to carry out the anaerobic process, during which PAO hydrolyze polyphosphates and release phosphorus from cells in the form of ortho-phosphates, to gain energy for the uptake of organic carbon, which is absorbed as simple organic compounds (e.g., volatile fatty acids) and stored within the cell as polyhydroxyalkanoates (PHA). Next, the activated sludge goes into an aerated basin, where PAO begin to uptake ortho-phosphates to be retained within their cells as polyphosphate, resulting in a net $P\text{-}PO_4^{3-}$ uptake [44,45]. The phosphorus sequestrated into bacterial cells ends up in the sludge streamline of the WWTP and eventually enters AD. Here, P is partly retained in solids and partly released in the liquid phase, due to PAO activity under anaerobic conditions and VS degradation. As a result, both liquid and solid fraction of ADS can be considered valuable sources of phosphorus.

2.2.3. Potassium

Similarly to nitrogen and phosphorus, potassium is one of the essential microminerals for plant survival. Potassium is of great importance for soil health, plant growth, and animal nutrition. Its primary function in plants consists in maintaining osmotic pressure and cell size, thus influencing photosynthesis and energy production [10]. Most potassium is found in the earth's crust in the form of minerals, such as orthoclase (potassium feldspar, a common rock-forming mineral), sylvite (KCl), carnallite ($KCl \cdot MgCl_2 \cdot 6H_2O$), kainite ($MgSO_4 \cdot KCl \cdot 3H_2O$), and langbeinite ($MgSO_4 \cdot K_2SO_4$). In

1980, the main mining area used for potassium salt extraction was in Germany, while today most of the potassium minerals (especially sylvite and carnallite) come from Canada, the United States, and Chile. The world production of extracted potassium is about 50 million tons, and the reserves are estimated to be over 10 billion tons [46]. Potassium-based fertilizer prices have increased by as much as four times during the last decade and there are issues around supply of K-based fertilizers to developing nations, due to the limited global distribution of potash ores (the main source of K) [3]. Potassium concentrations in sewage sludge and ADS range between 0.3% and 0.7% of K per weight of dry solids [14,25,47]. As indicated, the potassium content in the ADS is low, which is why potassium is typically recovered through technologies also applied for phosphorus and nitrogen recovery, in particular through K-struvite precipitation, membrane technologies, and thermal treatments.

2.3. Technologies for the recovery of nutrients from ADS

This section aims to give an overview of the different possible methods for recovering nitrogen, phosphorus, and potassium from ADS. These technologies can either target a specific nutrient (e.g., ammonia stripping) or allow the simultaneous recovery of multiple elements (e.g., struvite precipitation for $P\text{-}PO_4^{3-}$ and $N\text{-}NH_4^+$ or potassium recovery). Typically, nutrient recovery technologies are applied directly to the ADS (or sewage sludge) stream or to a ADS liquid fraction (e.g., centrate).

2.3.1. Selective nutrient recovery: ammonia stripping

This process removes part of the TAN contained in the sludge by shifting the NH_4^+/NH_3 equilibrium towards FAN, which is removed from the system by a gas stream. Ammonia stripping is conventionally executed in heated packed column reactors on the liquid fraction achieved from sludge dewatering [14]; the air blown in the column from the bottom (stripping gas), traveling along the surface of the contact material, carries the ammonia. The stripped ammonia is transported to an absorption unit, where it is absorbed into sulfuric (or nitric) acid solutions, resulting in the production of ammonium sulfate (or nitrate), a marketable platform chemical for the production of base fertilizers and other chemical products [47]. Recently, approaches

based on NH_3 stripping from ADS and the liquid fraction of ADS have been established and extended from lab-scale to full-scale around the world [48].

Ammonia stripping is established based on the change of physical conditions of the sludge, enabling the transition of NH_4^+ to NH_3, which must be efficiently removed from the liquid phase [49]. Increasing temperature and pH shifts the NH_4^+/NH_3 equilibrium towards FAN. It was shown that increasing the pH (up to 10), temperature, and flow rate of the stripping gas can significantly improve the amount of stripped nitrogen [50]. Nevertheless, effective ammonia stripping during AD of sewage sludge can be obtained without using alkaline reagents for pH increase, as the concomitant stripping of CO_2 helps increase the pH of the system and shift the NH_4^+/NH_3 equilibrium towards FAN [51]. The ammonia stripping process is strongly conditioned by the type of matrix being treated; the passage in the stripping column is suitable for low viscous fluids, such as wastewater and the liquid fraction of municipal sewage sludge. For high-viscosity fluids, however, reactors with packed materials are not suitable, as they would result in rapid clogging. Therefore, TS content plays a key role in choosing the most suitable technology for ammonia stripping, as if affects the rheological characteristics of the medium [52]. To overcome this issue, it is necessary to develop new technologies specifically suited to ADS, especially if it comes from HSAD. Due to the higher TS concentration compared to conventional AD, the operation of packed columns for direct ammonia removal from ADS is impossible. Moreover, the high TS concentration in HSAD results in much higher TAN and FAN levels inside the digester, which may inhibit the biological process. Therefore, TAN removal cannot be performed as a post-treatment only on the liquid fraction of ADS but should be foreseen as a side-stream process of HSAD. Side-stream ammonia stripping represents a strategy for reducing ammonia toxicity during AD. The HSAD of sewage sludge produces TAN levels as high as 4 g/L, due to the high concentrations of proteinaceous organic materials in the feedstock [53]. High ammonia concentrations may be responsible of inhibitory effects on AD, hindering and slowing down the digestion process. The ammonia toxicity is amplified when the process is conducted at thermophilic temperatures [14]. To solve the problem of ammonia inhibition, numerous techniques, including dilution, co-digestion, and side-stream ammonia

stripping, could be applied. The latter approach seems to be the most promising. During AD, a portion of the digested sludge is continually removed and treated in a stripping unit, where the ammonia produced from the digestion process is transferred to a gas phase (commonly biogas or air) and then put into contact with a sulfuric acid solution, to produce ammonium sulfate [54]. This process prevents the inhibition of the anaerobic process and simultaneously recovers ammonia as ammonium sulfate, which can be used as fertilizer. Costamagna et al. [55,56] proposed a thin film evaporator (TFE) as a suitable technology for the continuous side-stream stripping of ammonia from dewatered sewage sludge (12.5% TS) during thermophilic HSAD. As an alternative to conventional packed columns when treating dewatered sewage sludge, this technology does not require solid/liquid separation and avoids clogging issues [14]. With this technology, the ADS is continuously recirculated to the TFE column, which is thermally insulated and allows the contact between the ADS film (5–15 mm) and the uprising biogas flow, which is enriched in ammonia. The treated sludge is then recirculated to the digester and the ammonia-rich biogas collected from the TFE is fed to an absorption column to remove ammonia and producing ammonium sulfate. During the trial period, Costamagna et al. [55] could recover 4.1 g $N\text{-}NH_4^+$ per kg of sludge fed to the digester, i.e., 19.3 g $N\text{-}NH_4^+$ per kg TS fed to the digester, as ammonium sulfate. Side-stream ammonia stripping during HSAD couples process non-inhibition with the possibility of recycling nutrients from sewage sludge using a two-fold production of fertilizer, i.e., ammonium sulfate and high-solid ADS. Recently, Di Capua et al. [52] proposed the use of air as a stripping gas in the TFE during the HSAD of sewage sludge (TS 11.04% and VS 7.01%). In this process, ADS is continuously recirculated from the digester to the TFE, where ammonia is stripped by an air stream. The TFE performance was monitored for 140 days, by gradually increasing the specific airflow rate from 1.5 to 4.6 m^3 air/kg ADS. The authors demonstrated that ammonia removal from sewage sludge was primarily influenced by the airflow rate, as the removal efficiency increased from 17.1% to 33.3% when the flow rate was increased from 1.5 to 4.6 m^3 air/kg ADS. In contrast, changes in temperature (from 63.6 °C to 73.6 °C) and CO_2 concentration (between 5% and 17%) did not influence the ammonia stripping significantly. Use of air as a stripping gas did

not exert any inhibitory impact on methane production, even when 4.6 m^3 air were fed per kg of ADS, which was attributed to low residence time of 2.5 min in the TFE and small fraction of ADS (only 1.7% of the total digestion volume) fed daily to the TFE. The process allowed avoiding inhibition of the HSAD process and, at the same time, producing nutrient-rich ADS and ammonium sulfate, to be applied as fertilizers.

Ammonia stripping from sewage sludge has been carried out before or after AD. In the former case, it serves as a pretreatment and has the advantage of improving the AD process, limiting the problems related to ammonia inhibition in AD [56,57]. In the latter case (**Table 2.1**), the ammonia nitrogen produced from the digestion process can be recovered as ammonium sulfate/nitrate, since the air leaving the stripping tower, enriched in the ammonia transferred to the gaseous phase, can be treated in a scrubber with sulfuric/nitric acid to obtain ammonium sulfate/nitrate.

Table 2.1 - Removal and recovery of N-NH_4^+ from ADS streams through ammonia stripping.

Sludge Type	Type of Ammonia Stripping	TS (%)	Influent TAN (g/L)	T (°C)	N-NH_4^+ Removal (%)	Ref.
Digestates taken from an anaerobic digester	Down-stream	-	4.98	70	17–86	[58]
	In situ	-	6–6.3	35	58–90	
	Side-stream	-	3.98	70	34–84	
	Up-stream	-	6–6.25	70	44–88	
AD effluent	Up-stream	2 1	1.544	15	72.1–95.3	[56]
ADS	Side-stream with TFE	10.7	3.65	65	21.2	[54]
HSAD of sewage sludge	Side-stream with TFE	11.04	3.714	63.6–73.6	17.1–33.3	[51]

2.3.2. Multiple nutrient recovery

2.3.2.1. Struvite precipitation

Struvite is a crystalline mineral composed of equimolar concentrations of Mg^{2+}, NH_4^+, and PO_4^{3-}, with the chemical formula $MgNH_4PO_4 \cdot 6H_2O$. Struvite consists of PO_4^{3-} (tetrahedral), $Mg(6H_2O)^{2+}$ (octahedral), and NH_4^+ (tetrahedral) groups, which are held

together by hydrogen bonds [42]. The formation of struvite is controlled by two mechanisms: nucleation (the initial formation of the crystal) and crystal growth. This last phase is characterized by a mass transfer through the diffusive layer surrounding the crystal and by the capture of the solute inside the crystal. In most of the published works on the principles of struvite formation, it has been highlighted that supersaturation ratio and pH have been found to be the most influential parameters on the crystallization mechanism [59]. The crystal formation process is also strongly influenced by other parameters, such as the presence of other ionic species (e.g., Ca^{2+}, Na^{+}, K^{+}) that can interfere with crystal formation, replacing N-NH_4^{+} (e.g., K^{+}) or Mg^{2+} (e.g., Ca^{2+}) and leading to the formation of a mineral similar to struvite but different in composition. When K^{+} replaces N-NH_4^{+}, potassium struvite precipitation ($KMgPO_4 \cdot 6H_2O$) can occur [59]. This precipitate is also known as K-struvite, an isomorphous analogue of struvite that can also be used as slow-release fertilizer [60]. The physical and chemical properties of K-struvite are similar to those of typical struvite crystals (e.g., the needle-like shape and transparent to whitish appearance [61]), although the density of K-struvite (1.864 g/cm^3) is slightly higher than that of struvite (1.711 g/cm^3) [62]. A suitable pH range for K-struvite precipitation is between 9.0 and 11.0, which is moderately higher than the pH range for struvite formation (8.5–9.5) [63]. Struvite precipitation depends on several parameters, perhaps most notably pH and the molar ratio of NH_4^{+}, PO_4^{3-}, and Mg^{2+} in the liquid phase [64]. Several researchers investigated the pH of minimum solubility for struvite [65], reporting values ranging from 7.8 [66] to 10.3 [67]. Generally, struvite precipitation occurs when NH_4^{+}, PO_4^{3-}, and Mg^{2+} concentrations overcome the solubility product (Ksp) of struvite under alkaline conditions [68]. In the literature, different Ksp values are reported, ranging from 2.50·10−13 to 7.50·10−14 [65]. Struvite precipitation occurs spontaneously in many WWTPs, resulting in scale deposits that are a significant concern for plant operation. As a result, struvite formation is perceived as a nuisance, affecting the efficiency of treatment processes and causing maintenance problems. However, for intentional struvite precipitation, most of the potential struvite sources need an input of chemicals for a pH increase and/or for the adjustment of NH_4^{+}, PO_4^{3-}, and Mg^{2+} concentrations, to reach an optimal molar ratio (Mg^{2+}: PO_4^{3-}: NH_4^{+}). This

must be assessed case-by-case, as it strongly depends on the chemical-physical characteristics of wastewater [69]. Uysal et al. [70] observed that the optimal Mg^{2+}: PO_4^{3-}: NH_4^+ molar ratio for struvite precipitation from sewage sludge was near to the equimolar ratio, being 1.5:1:1 at a pH of about 9.0. A supply of Mg^{2+} is generally required to make struvite precipitation effective, due to the lack of adequate Mg^{2+} concentrations in the majority of potential struvite sources, including sewage sludge [71].

Table 2.2 shows data present in the literature regarding nutrient removal and recovery from ADS through struvite precipitation, in relation to the parameters described above. Munir et al. [72] showed an increase in phosphate recovery, due to an increase of pH, i.e., 7.1 mg/L at pH 8 compared to 10.5 mg/L at pH 9. This result was also confirmed by Marti et al. [73], where the PO_4^{3-} recovery was 152 mg/L at pH 7 compared to 164 mg/L at pH 8. Uysal et al. [70] and Zheng et al. [74] observed that as the ratio Mg:N:P changes, the nutrient removal/recovery efficiency varies as well, with the best results obtained for a molar ratio of 1.3:1:1.

Table 2.2 - Recovery of N, P, and K from ADS streams through struvite precipitation.

Sludge Type	TS (g/L)	pH	Mg:N:P	P Recovery (%)	N Recovery (%)	K Recovery (%)	Ref.
ADS	-	8	1:1:1	<0 [1]	85.42	-	[69]
		8.5	1:1:1	<0 [1]	89.16	-	
		9	1:1:1	47.1	88.79	22.2	
		9	1.3:1:1	92.5	89.35	32.5	
		9	1.5:1:1	95.0	89.35	24.7	
ADS	37.26 ± 8.4	6.8–7.2	1:1.7:1.2	58	-	-	[72]
Acidified ADS	-	9.6	1–1.4:1:0.8–1.2	96–100	75–90	-	[73]
ADS supernatant	1.309	10	1–3:1–7.871:1–2	20.9–99.6	29	-	[74]
ADS centrate	-	7.67	1–2:1:0.8–1	95.9–99.8	76.7–99.5	-	[75]

Sludge Type	TS (g/L)	pH	Mg:N:P	P Recovery (%)	N Recovery (%)	K Recovery (%)	Ref.
Liquid fraction of ADS	16–29.6	6.2–8.7	1–1.5:6.7–7.9:1	76.0–83.9 (35.4–72.6 as struvite)	-	-	[76]
ADS	29.3	9.5	1–1.2:1:1–1.2	81–86.7	92.6–96	-	[77]

[1] Negative values are due to H3PO4 addition, to obtain the desired Mg:N:P ratio.

Struvite is considered a valid fertilizing product, because it contains nutrients such as nitrogen and phosphorus (essential for plant growth) [78], and its low solubility induces a slow release of nutrients in the soil, which allows optimal plant growth and avoids potentially harmful overdose phenomena [2]. As a result, the crystallization of struvite has gained interest for phosphorus recovery [42] and to remove NH_4^+ [79] from waste streams, such as wastewaters and sewage sludge. Interestingly, struvite precipitation in HSAD digesters treating dewatered sewage sludge may have a double positive effect: (1) avoiding process inhibition, due to TAN removal, and (2) increasing the fertilizing potential of the produced ADS [14]. The occurrence and quantification of struvite precipitation during the HSAD of sewage sludge and the struvite content of the produced ADS should be investigated in future studies.

2.3.2.2. Ion exchange and adsorption

Ion exchange and adsorption are similar physical-chemical processes as they both utilize sorbents in a column bed to extract the target compounds from the feed solution. Adsorption is a mass transfer phenomenon, by which one or more constituents present in the liquid phase are fixed on a porous solid surface. Contrarily to ion-exchange, which is driven by ionic forces, adsorption occurs due to weak intermolecular forces, i.e., Van der Waals forces, and, thus, the process is considered reversible. In ion exchange, mobile ions of a solid matrix (adsorbent) are exchanged with ions having a similar electric charge present in the solution (adsorbate). Electrostatic forces allow

the bonding between the ions of the adsorbate and the charges present on the surface of the adsorbent. Ion exchange and adsorption may occur simultaneously in one media, such as zeolites, clays, and resins, whether or not chemically or thermally modified [80]. After a certain period, the sorbent reaches its capacity and must be regenerated. Regeneration can be achieved with various techniques, including washing with nitric acid (HNO_3) or sodium chloride (NaCl) [81]. Ion exchange through natural minerals (e.g., zeolites or bentonites) has gained importance because of its low cost and ease of use. Furthermore, ion exchange enables the recovery of N-NH_4^+ and its reuse for fertilizing purposes [82,83]. For example, the ammonium-zeolite complex can applied directly to soil as it is decomposed slowly by soil bacteria and released to the soil as a nutrient [80]. The high ion exchange capacity, large reserves, shortage of competing minerals, and relatively low market price make zeolite an attractive mineral for application at large scale [84]. Despite this, there are no applications at full-scale, but only at lab-scale, due to the rapid obstruction of the adsorbent bed (which makes zeolite treatment potentially feasible only for the liquid fraction of ADS), as well as the necessary maintenance of the capacity of the bed after multiple recovery/regeneration cycles, which can increase the operating costs. Zeolite minerals differ in silicon (Si) and aluminum (Al) contents. Zeolite minerals differ in silicon (Si) and aluminum (Al) contents; among natural zeolites, clinoptilolite (Si:Al ratio equal to 5.7) is usually used for ion exchange, due to its high sorption and ion-exchange capacity and selectivity [85]. Zeolites exert their ammonia removal action through two different mechanisms: (1) ion exchange for N-NH_4^+, and (2) adsorption of N-NH_3 [86]. Temperature and pH strongly influence the removal efficiency of ammonia: the higher the temperature, the higher the removal efficiency achieved; regarding pH, the removal efficiency is approximately constant between values of 4 and 8, and rapidly decreases outside this range [80]. Zeolites are used for both N-NH_4^+ and P-PO_4^{3-} removal [87]; P-PO_4^{3-} can be adsorbed by zeolite, although the removal efficiency has been reported to be much lower than that of N-NH_4^+ [88]. This is due to the fact that zeolite, or rather, clinoptilolite has a higher selectivity for monovalent ions such as N-NH_4^+ and K^+ [84,89–91]. The best results in terms of removal/recovery of N-NH_4^+ were obtained with the use of mesolite [92] and polymeric resins [91], of 95% and 98%, respectively.

Kocatürk-Schumacher et al. [93], using clinoptilolite, demonstrated that N-NH_4^+ and K^+ can be removed from the liquid fraction of digestate with high removal efficiencies, i.e., 86% and 78%, respectively. These authors also showed that preconditioning of clinoptilolite with sodium ions had no significant effect on the removal of N-NH_4^+ and K^+ and that increasing the initial loading ratio significantly increased the nutrient concentrations of clinoptilolite but decreased the nutrient removal efficiencies from the liquid fraction of the digestate. This result was also confirmed by Gong et al. [94], who observed that an increased initial load leads to a higher concentration of nutrients in the polymer resins, but results in a low removal efficiency (37%). The costs of ion exchange and adsorption depend on several factors, including the availability of the sorption material used, the applied recovery/regeneration method, and the regeneration frequency of the adsorption medium. To date, no cost–benefit analyses for nutrient recovery from ADS using zeolites or other sorbents have been reported in the literature [81].

2.3.2.3. Membrane technologies

Membrane filtration is generally applied to the liquid fraction of the ADS, which is forced through a membrane by means of pressure [82]. With a driven pressure applied, porous membranes can retain larger particles, while allowing smaller ones to pass through [95]. Membrane systems can be operated either with a constant permeate flux (flow rate per unit of membrane area, L/m^2 h) and variable transmembrane pressure (TMP) or with a constant TMP and variable permeate flux [96]. Membrane technology has evolved considerably in recent years and it can be applied in almost all industrial sectors [49], including nutrient recovery from waste streams such as sewage sludge and ADS (**Table 2.3**). Gerardo et al. [97] used membrane filtration coupled with acid treatment and dialysis techniques and showed that 271.11 mg/L N-NH_3 and 25.60 mg/L P-PO_4^{3-} could be recovered from filtered ADS supernatant with initial concentrations of 686.2 mg/L N-NH_3 and 41.51 mg/L P-PO_4^{3-}. Membrane filtration effectively separates the ADS stream into a fraction rich in solids (retentate or concentrate) and an aqueous solution that passes through the membrane (permeate). Based on the operating TMP, membranes can be categorized as low-pressure

membranes (LPMs) and high-pressure membranes (HPMs). LPMs include microfiltration (MF) and loose ultrafiltration (UF) membranes, typically operated at TMPs below 200 kPa. Meanwhile, HPMs such as tight UF, nanofiltration (NF), and reverse osmosis (RO) membranes are operated at TMPs above 200 kPa [98]. MF and UF are mainly applied for the removal of suspended solids, microorganisms, and macro-molecules, while NF and RO are used for the removal of smaller organics and ions, including NH_4^+, PO_4^{3-}, and K^+ [97,99]. The main drawbacks of membrane processes is fouling, which leads to a rapid decline of the permeate flux over time; to maintain their separation performance, membranes must be cleaned and replaced periodically [82]. Recently, of the different membrane technologies, there are three processes: forward osmosis (FO), membrane distillation (MD), and electrodialysis (ED), showing promising results for nutrient recovery. Their selectivity is conducive to the formation of valuable nutrients, and their energy requirements and related costs are competitive with common pressure-driven membrane processes.

2.3.2.3.1. Nanofiltration and reverse osmosis

NF and RO have been widely applied, from laboratory to full scale, for potable water reclamation from wastewater and the removal of contaminants such as HMs and emerging organics [100–103]. In terms of nutrient removal and recovery from sewage sludge streams, NF and RO have been applied with the objective of recovering P by concentration in the retentate stream and precipitation with Ca ions. This process requires the use of acid-resistant and durable membranes, as cleaning with strong acids is periodically required to remove the Ca-P crystals attached to the membranes. Nitric acid is regarded as the best option, as it generates a solution rich in N and P, which can be locally applied as a fertilizer. Nir et al. [104] proposed a two stage NF/RO system for the simultaneous removal and recovery of P from WWTP secondary effluents, which could also be applied to the liquid fraction of ADS. In the first stage, a NF/RO treatment allows obtaining a permeate with high recovery ratio (i.e., ratio of permeate to influent flow). The obtained concentrate is sent to a second NF stage, where P and Ca ions exceed the supersaturation levels. Proper P precipitation is achieved in a crystallizer by adjusting the pH to reduce the formation of $CaCO_3$ crystals, which may

reduce the weight fraction of P in the precipitate. At a 95% recovery ratio, P recovery in the retentate could reach >90%. The costs of the proposed scheme, including membrane replacement and acid addition for pH adjustments, were estimated to be around 0.05 USD per m^3 of influent wastewater, being competitive with the conventional P removal and recovery method based on chemical P precipitation through addition of Al/Fe salts.

2.3.2.3.2. Forward osmosis

FO is carried out by placing a semipermeable membrane between two solutions with different solute concentrations: a concentrated draw solution, and a more diluted feed solution. Instead of hydraulic pressure, FO employs an osmotic pressure difference [105]. For this reason, unlike other membrane processes with a hydraulic pressure requirement, such as NF (3–20 bar) and RO (5–120 bar), FO has the advantage of low energy consumption. Moreover, FO has demonstrated a lower fouling propensity and higher fouling reversibility compared to pressure-driven RO [105–108].

The application of FO is promising, due to its distinctive advantages but, up to now, FO has only been assessed in laboratory-scale studies, and pilot and full-scale validations should be conducted. Nguyen et al. [109] evaluated the feasibility of applying FO on municipal wastewater sludge, showing recovery efficiencies of around 96% of N-NH_4^+ and 98% of P-PO_4^{3-}. Soler-Cabezas et al. [110] studied the recovery of nutrients in ADS centrate by FO using two industrial effluents as draw solutions; the results showed that NH_4^+ and K^+ could be concentrated with a factor (ratio between final and initial concentrations in ADS centrate) of 1.2 and 1.08, respectively. Conversely, phosphorous cannot be concentrated because of its spontaneous precipitation as calcium phosphate during FO.

2.3.2.3.3. Membrane distillation

Membrane distillation (MD) utilizes low-grade heat to drive separation. In this process, the feed stream is separated from the distillate by a hydrophobic and microporous membrane, which cannot be penetrated by the liquid [104]. The transport mechanism through the membrane occurs only in the vapor phase, and it is driven by

a difference in the partial vapor pressure; consequently, MD can offer complete rejection of all non-volatile constituents in the feed solution [111]. From this point of view, MD can be used for the recovery of valuable components, concentrating them either in the feed or in the permeate. For example, non-volatile inorganic nutrient ions, such as K^+ and PO_4^{3-}, can be concentrated in the feed stream to make the following nutrient precipitation easier [80], while NH_3, being more volatile, can be transported through the hydrophobic membrane pores along with the vapor. Xie et al. [106,107] reported that over 96% of the ammonia could be recovered from the ADS centrate in the form of an aqueous solution, which could then be reused as fertilizer. To further enhance the capture of ammonia vapor in contact with MD, a low concentration of sulfuric acid (H_2SO_4 0.1 M) was used on the permeate side; in this way, ammonia recovery was improved up to 99%, with ammonium sulfate produced as a fertilizer. Kim et al. [112] applied a MD process, on laboratory scale, to treat the supernatant of ADS produced from the treatment of livestock wastewater. The authors, performing a short-term distillation for 90 min with a feed solution (pH 8.5) at 60 °C and permeate stream at 20 °C, achieved a more than 99% rejection of phosphorus and 90.3% rejection of TN. Xie et al. [106,107] demonstrated the extraction of phosphorus from ADS centrate by a hybrid FO−MD system with a $MgCl_2$ draw solution. In this FO−MD hybrid process, FO concentrates $P\text{-}PO_4^{3-}$ and $N\text{-}NH_4^+$ for the following nutrient recovery in the form of struvite, while MD is used to recover the draw solution. The reverse Mg^{2+} permeation (reverse Mg^{2+} flux of 12 mmol/m^2 h) was also important, which substantially increased the feed Mg^{2+} concentration in the system, thereby supplementing Mg^{2+} for struvite formation. Struvite formation was not quantified but was indicated by the continuous decrease of solution pH and by the ionic product that was $10^{-5.77}$ M^3, above the struvite conditional solubility product. To prove this, the precipitates obtained in the hybrid process were verified to be struvite crystals by examining the crystal morphology, element composition, and crystal structure.

2.3.2.3.4. Electrodialysis

Electrodialysis (ED) is a membrane process in which semi-permeable membranes are applied to separate ions under the influence of an electric potential that allows cations

and anions to migrate towards the cathode and the anode, respectively. ED can selectively fraction nutrients from wastewater streams into high-quality nutrient products [104]. Ion separation is achieved by ion-exchange membranes, which comprise cation-selective, anion-selective, and bipolar membranes (which comprise a cation-selective and an anion-selective membrane). When bipolar membranes are used in an ED process, dissociation of solvent molecules, such as water, into H^+ and OH^- can be realized and this can diversify the final products and enhance the purity for nutrient recovery [104,113]. Combining H^+ and anions in certain chambers leads to the production of acids, while the combination of cations and OH^- leads to the production of the corresponding base. Wang et al. [114] employed the ED process with a bipolar membrane to convert the $P\text{-}PO_4^{3-}$ contained in sludge supernatant to purified phosphoric acid at a concentration of 0.075 mol/L. Wang et al. [113] conducted an experimental study on the recovery of ammonia and PO_4^{3-} by ED integrated with struvite precipitation; ED was mainly employed to obtain a concentrated nutrient salt solution that was fed into the precipitation reactor in order to precipitate N and P salts as struvite. By further treating the concentrate solution with ammonia stripping, the authors could obtain a removal ratio of about 95.8–100% for NH_3 and 86.1–94.4% for PO_4^{3-}. In the literature, no studies report on the recovery of potassium from ADS with ED. Nevertheless, there are some useful applications of K recovery from other organic waste substrates. Barros et al. [115], aiming at the generation of a potassium concentrated stream, were able to recover 72% of potassium from vinasse, which is characterized by a high concentration of K^+ (0.04–11 g/L).

Table 2.3 - Removal/recovery of N and P from sewage sludge and ADS streams through membrane technologies.

Sludge Type	TS (g/L)	pH	Membrane System	Influent $N\text{-}NH_4^+$ (mg/L)	Influent $P\text{-}PO_4^{3-}$ (mg/L)	N Removal (%)	P Removal (%)	Ref.
Wet-oxidized ADS and sewage sludge	5–20	1.5–2	UF-NF	-	87–152	-	68 [1]	[97]

Sludge Type	TS (g/L)	pH	Membrane System	Influent $N\text{-}NH_4^+$ (mg/L)	Influent $P\text{-}PO_4^{3-}$ (mg/L)	N Removal (%)	P Removal (%)	Ref.
Nutrient-enriched sewage sludge	-	7.2	FO	100–200	100–200	96–98	98–99	[108]
ADS centrate	-	7–8	FO-RO	1011	78	83–95	100	[116]
ADS centrate	1800	7.72	FO-MD-struvite precipitation	418	73	90	97	[112]

[1] assuming a permeate recovery of 90% and a rejection of 50%.

2.3.2.4. Thermal treatments

Thermal treatments include incineration, pyrolysis, gasification, and hydrothermal carbonization (HTC), depending on temperature, pressure, and oxygen conditions. Conversion of municipal sewage sludge by different thermal processes yields solid residuals (ashes and chars) with significant differences in their composition, values, and qualities [117,118]. Thermal treatments are not applied only to raw sewage sludge, but can also be carried out on ADS, providing an energetically favorable treatment cycle, which includes sending the sewage sludge to AD to produce biogas and then sending the ADS to thermal treatment [119]. Since the products of thermal processes retain most of the P, N, and K originally contained in the treated sludge, it is possible to use them directly as soil improvers or to further treat them via chemical and thermochemical routes to release the nutrients [3].

2.3.2.4.1. Incineration

Due to a significant reduction of the sewage sludge volume, thermal degradation of toxic components, and high energy efficiency, incineration is one of the most applied thermal technologies for sewage sludge treatment [118,120]. During the incineration process, combustible material is oxidized and energy is released as thermal energy in the flue gas, while the organic pollutants, endocrine disruptors, and pathogens contained in sewage sludge are destroyed, and volatile HMs, such as quicksilver, are

transferred to the flue gas. Nutrients, especially P, are not transferred to the flue gas, as they are kept in the incinerator ash [121]. The content of P in sewage sludge is estimated to range from 1% to 5%, while the P content in sewage sludge ash can reach 20% [41]. As a result, more phosphorus can be recovered per kg of ashes than of sewage sludge. Unfortunately, incineration appears economically viable only in large WWTPs, mainly because of the large capital costs associated with the compliance with ecological criteria. An opportunity could be to exploit existing incineration plants in the vicinity of the WWTPs. Moreover, during the combustion process, phosphorus is transferred into low-solubility mineral phases with low availability for plants. It is therefore necessary to transfer the $P\text{-}PO_4^{3-}$ by means of a suitable thermochemical reaction to a plant-available form [121]. Adam et al. [122] suggested a two-step thermal treatment based on (1) mono-incineration of municipal sewage sludge, and (2) thermochemical treatment of the resulting ashes. The authors were able to completely remove the critical organic pollutants from mono-incineration, obtaining, as a product, ashes with a P_2O_5 content of 21.4%, comparable with conventional P-fertilizers. However, the phosphorus in the raw ashes has a poor bioavailability and high HMs concentrations. Therefore, in a second thermochemical step, HMs are removed and P is transferred into mineral phases available for plants. Smol et al. [123] thermochemically treated sewage sludge ashes coming from mono-incineration, together with sodium additives and a reducing agent (dried sewage sludge), to remove HMs and transform the insoluble P present in the sewage sludge ashes into CaNaPO4, which is available to plants. The authors also made a comparison between the P solubility in the raw ashes and in the thermochemically treated ashes, using neutral ammonium citrate as a bioavailability indicator, and found that the P solubility was significantly increased from 19.7–45.7% to 76.5–100%. Nevertheless, P recovery processes mainly aim at separating HMs from the valuable P and at converting P to a form readily available to plants for reuse as fertilizer or into a raw material for the P-industry.

Two categories of P recovery technologies are available from sewage sludge ashes: wet chemical approaches, and thermal approaches. Thermal approaches separate P and HMs at temperatures of 1000-2000 °C and transform P into a plant-available form

[121,122,124], while wet chemical approaches include acid and alkaline dissolution techniques. Chemical extraction is the most used method for its high efficiency and low cost, but it also leaches metal/metalloids present in sewage sludge ashes. To recover P from the leachate, it can be precipitated by adjusting the pH to 4, but it is necessary to add cations to transform the metal-P precipitates into plant-available fertilizer [124]. However, due to P losses during the purification process, the conventional method for P extraction results in a low recovery efficiency [125]. To solve this problem, it is necessary to find suitable leaching agents to separate P from metals/metalloids. Organic acids induce chelating effects that greatly increase the leaching of metals/metalloids from ash and soil [124]. Inorganic acids leach alkali metal oxides and release all phases containing P, of which sulfuric acid and nitric acid proved to have a high P releasing capacity [126,127]. In order to ameliorate these drawbacks, Petzet et al. [124] developed a combined acid–base extraction procedure: the investigated process requires an acidic pre-treatment in which the P fraction of the raw sewage sludge ashes that is bound as calcium phosphate is converted into aluminum phosphate. This newly formed aluminum phosphate can be dissolved via alkaline treatment and easily separated from the leachate via precipitation of calcium phosphate. The described sequential treatment process yields P-recovery rates as high as 70–77%. Currently, the recovery of phosphorus from fly ashes is more expensive than the production of P from phosphorus ores; the former is, therefore, not economically feasible [41,121]. At the same time, a price increase is expected for phosphorus from natural deposits in the future, which may make the costs for phosphorus recovery from sewage sludge more competitive [41,128]. N and K cannot be effectively recovered through incineration, as N is lost as N_2 during combustion, while K is generally water-soluble and not incorporated into the sewage sludge ash [129].

2.3.2.4.2. Pyrolysis and gasification

Pyrolysis is the thermal process by which organic material decomposes under oxygen-free atmosphere at ambient pressure and temperatures between 400 and 800 °C [130]. Differently from incineration, which occurs in the presence of oxygen and above 800

°C, pyrolysis operates in the absence of oxygen and at lower temperatures [3]. Moreover, compared to the incineration process, which is highly exothermic, pyrolysis is endothermic, of the order of 100 kJ/kg dry solids [131]. This process generates gas and vapors, and liquid (bio-oil and tar) and solid (biochar) products [132] in a ratio which depends on the process parameters [118]. Due to the anoxic conditions, most of the carbon substances (e.g., cellulose, starch, lignin, and glucose) can be hydrolyzed and converted to biochar, with non-vapor elements coexisting [133]. Pyrolysis can be applied to convert raw, digested and waste-activated sewage sludge into syngas and biochar as by-products. It has been estimated that AD of sewage sludge followed by pyrolysis yields higher rates of energy recovery than stand-alone AD or pyrolysis [134]. Cao and Pawlowski [134] assessed the energy conversion efficiency of two parallel sludge-to-energy pathways: one pathway was based on AD followed by pyrolysis; the other pathway was based on pyrolysis alone. To characterize the energetic performance of the two pathways two indicators were used: the apparent energy efficiency (AEE), i.e., the ratio of the energy content in the target products to the energy content of the sludge feedstock, and the gross energy efficiency (GEE), which also considers the energy in process by-products (e.g., biochar). The results proved that the combination of AD and pyrolysis achieves higher energy efficiency (AEE 71.4%–GEE 92.5%) compared to the pathway employing pyrolysis alone (AEE 60.4%–GEE 89.8%). Although similar to pyrolysis, gasification usually transforms organic materials to combustible gas or syngas, using between 20% and 40% of the oxygen required for total combustion [135,136]. Gasification can limit the problems commonly faced in the incineration process, such as the need for a supplemental fuel; emissions of SOx, NOx, HMs, and fly; ash as well as the potential production of chlorinated dibenzodioxins and dibenzofurans. The gasification syngas, which is a mixture of CO, H_2, and other gases, has a heating value typically in the range of 4–12 MJ/Nm^3. Syngas is limited to local consumption, because its compression, storage, and transport are not economically attractive [135]. To date, pyrolysis and gasification are still poorly applied worldwide for full-scale valorization of sewage sludge. The main limitation to the spreading of these processes is the low quality of the obtained products, which require significant treatment before being used for energy and/or

material recovery. For instance, tar is a complex mixture of condensable hydrocarbons, phenolic compounds, and HMs, and may cause various operational problems within the plant, e.g., blockage of filters, fuel lines, valves, and fuel injectors of engines. Moreover, tar compounds are a serious concern if released into the environment, being toxic and potentially carcinogenic [137]. The syngas obtained from sewage sludge may contain high levels of corrosive gases, i.e., H_2S and HCl, and has a lower calorific value compared to biogas (up to 40 MJ/Nm^3) [133]. Utilization of char in agriculture may be limited by the high concentration of HMs, being mostly retained in the solid residue and concentrated because of the mass reduction resulting from thermal degradation [138].

In terms of nutrient recovery, both pyrolysis and gasification of sewage sludge could be coupled for efficient P removal and recovery. Indeed, the solid residues from pyrolysis and gasification are a sanitized source of minerals and some organic elements, including valuable fertilizing components, such as P_2O_5, K_2O, MgO, and Fe_2O_3, which makes them a potential substitute for natural phosphorus ore [139]. Pyrolysis can be designed and operated to retain most of the P and K and some of the N in the solid or liquid by-products. Bridle and Pritchard [140] showed that pyrolysis of dried sewage sludge pellets performed at 450 °C at a pressure of 1.5 kPa retained 99% of P and K and 55% of N in the char. Results from this study showed that the phosphorus in the char was in its soluble form, available for plants, while nitrogen was in an insoluble form and, thus, less available for plant use. Based on these results, it appears that there is the potential to use pyrolysis as an effective means of recovering and reusing both the energy and phosphorus present in sewage sludge [88]. Vali et al. [141] showed that over 90% of the phosphorus contained in sewage sludge was retained in the char after pyrolysis at temperatures up to 850 °C, while higher temperature led to the formation of gaseous P compounds. At the same time, the concentration of HMs in the char decreased significantly (except Cu and Zn), as most of them were volatilized in the gas phase or solubilized into the aqueous phase. As reported in **Table 2.4**, K was also retained in the char at all tested temperatures. The obtained char could be used as soil improver or for further refinery in the fertilizer industry. Atienza-Martínez et al. [142] recovered nearly all phosphorus contained in

the gasification ash of sewage sludge by extraction with sulfuric and oxalic acid at stoichiometric concentrations. Likewise, Gorazda et al. [139] demonstrated that acidic extraction (with nitric and/or phosphoric acid) was able to recover P with extraction efficiencies of 73–82%, transferring it from solid residue of ADS gasification into a plant-available form in leachates, which can be used for fertilizer production. Other studies confirm the presence of K in the gasification ashes of sewage sludge [143]: 0.55wt% [144], 4.63wt% [145], and 1.11wt% [146]. Nevertheless, these studies did not focus on the recovery of this element. The recovery of N through gasification is not possible, as it is diluted in the form of N_2 in the produced syngas [121].

2.3.2.4.3. Hydrothermal carbonization

HTC is a hydro-thermal process that takes place in liquid water at temperatures of 180–250 °C, pressure of 60–100 bar, and in the absence of oxygen. HTC requires lower temperatures than pyrolysis and gasification, but very high pressure [118,120]. During the HTC reaction, water, carbon dioxide, and other compounds are generated from the biomass, producing, in less than 10 h, a carbonaceous solid, the biocarbon (or hydrochar-HC), with characteristics similar to lignite, and an aqueous residue rich in the nutrients previously contained in the raw material (process water). The use of water as a solvent is a key factor for HTC, due to its good heat transfer and solvent properties [5]. In recent years, HTC has emerged as a promising technology for sustainable sewage sludge minimization and valorization of the solid products [147,148]. It can significantly reduce sewage sludge volume, decompose organic pollutants by hydrolysis and carbonization reactions, and generate valuable byproducts, including the hydrochar and process water [149]. In particular, HTC process water from sewage sludge is characterized by a higher nitrogen content than that resulting from the HTC of other biomasses [147,148,150]. HTC releases energy through carbonization and increases or maintains the reaction temperature in the HTC reactor, not requiring much additional energy input after the initial heating phase if the reactor energy losses are minimized. Escala et al. [151] calculated the energy balance based on assumptions regarding potential recoverable energy and showed that no additional external energy input is needed to support the reaction process for sewage sludge. These results were

also confirmed by Aragón-Briceño et al. [152]; the authors demonstrated that the integration of the HTC process to the AD of sewage sludge showed a positive energy balance, with a maximum net energy production of 312.9 kWh per ton of treated sludge if the hydrochar is considered as a fuel source; increasing the net energy production 10 times compared to when only biogas is used as energy source.

HTC process water is commonly regarded as a wastewater and needs to be appropriately treated. However, it has a high soluble concentration of both organics and nutrients (particularly NH_4^+ and K^+), allowing a potential application in liquid organic fertilizer production [153]. During HTC, nitrogen and phosphorus migrate from the raw sewage sludge to the process water in the form of NH_4^+ and PO_4^{3-}, which can be precipitated as struvite. Munir et al. [72] reported that struvite precipitation used as a post-treatment on liquid residue, after sewage sludge hydrothermal treatment, was a cost-effective option for P-PO_4^{3-} recovery. P-PO_4^{3-} was recovered by adding $MgCl_2$ solution (1000 ppm) at pH 9 to facilitate precipitation of struvite. In this way, the struvite production was 9.5 kg/m^3 and P-PO_4^{3-} recovery of 80% was obtained. According to Aragón-Briceño et al. [152,154], the best scenarios for struvite production showed that 0.06 kg of struvite could be produced per ton of sewage sludge when coupling HTC to AD for sewage sludge treatment.

Table 2.4 - Recovery of N, P, and K from ADS and sewage sludge streams through thermal treatments.

Sludge Type	System	T (°C)	Pressure (kPa)	Extraction Method	N, P and K Recovery	Ref.
Municipal sewage sludge	Incineration/ gasification	1000	-	-	$(\%P)_{ASHES}$ = 11–25 $(\%K)_{ASHES}$ = 0.6–2.8	[122]
Sewage sludge	Pyrolysis	450	1.5	Sequential extraction	$(\%N)_{IN\ CHAR}$ = 55 $(\%P)_{IN\ CHAR}$ = 100	[140]
Char from pyrolysis of sewage sludge	Combustion/ Gasification	600–900	-	Leaching with oxalic acid	$(\%P)_{IN\ LEACHATE} \geq 90$	[142]
Dry ADS	Gasification	800–1000	-	Leaching with nitric	$(\%P)_{IN\ SOLID\ RESIDUE}$ = 8.76	[139]

Sludge Type	System	T (°C)	Pressure (kPa)	Extraction Method	N, P and K Recovery	Ref.
				and/or phosphoric acid	$(\%P)_{IN\ LEACHATE}$ = 73.5–81.5 $(\%K)_{IN\ SOLID\ RESIDUE}$ = 0.703	
Sewage sludge	HTC	200	2100	-	(mg/L $_{in\ liquid\ fraction}$) N: 2392–2419 P: 804–813 K: 1516–1519	[155]

2.4. Comparative assessment of the strategies for exploiting the nutrient potential of ADS.

Based on the above compiled information, a critical comparative overview of the described technologies and strategies for exploiting the nutrient content of ADS is given in this section.

Struvite precipitation/crystallization and ammonia stripping are the most applied technologies for nutrient removal and recovery from ADS at full scale and are typically performed on the liquid fraction of ADS, obtained from the solid–liquid separation commonly carried out within the WWTP by screw press separators, screening drum presses, or decanter centrifuges. Solid–liquid separation reduces the transportation cost of the digestate [156] and avoids clogging in the struvite crystallizer (usually a fluidized-bed or a mechanically stirred reactor) [157] and stripping column (being fed with the liquid fraction only) [158].

Table 2.5 lists the costs of the different technologies that can be applied for nutrient recovery from ADS. Struvite crystallization is the most expensive approach for nutrient recovery, although it results in the production of the most valuable recovery product (struvite) from ADS processing. Both struvite precipitation and ammonia stripping from the liquid fraction of ADS are not viable strategies when the removal of ammonia must be carried out to avoid inhibition of the process, such as during HSAD of sewage sludge, due to the high sludge viscosity. The application of a new technology, i.e., TFE, enables directly stripping ammonia from the digesting sludge

[52,55,56], resulting in a powerful means for simultaneous process non-inhibition and two-fold production of fertilizers (high-solid ADS and ammonium sulfate) at full scale. Moreover, struvite precipitation during HSAD further increases the agronomic value of the produced ADS, promoting its application and public acceptance as a fertilizer, and can be also regarded as an alternative method of avoiding ammonia inhibition during HSAD of sewage sludge, as it can limit the build-up of ammonia in the digester. Mg is commonly the limiting element for struvite precipitation. To promote the application of struvite precipitation at real scale, a cheaper source of Mg should be utilized. This could be obtained by combining struvite precipitation with other technologies, e.g., coupling struvite precipitation to ion exchange with zeolite. Natural zeolite can be modified by incorporating magnesium salts, and the Mg^{2+} released from the adsorption process can promote struvite crystallization [159]. In the hybrid process, zeolite rich in N and P removed from ADS could be used as a nutrient source for fertilizer production, partly recovering the costs for the purchase of zeolites. This would promote the use of zeolite for nutrient recovery, as, to date, no application has been reported at full-scale and no cost-benefit analyses exist in the literature for nutrient recovery from ADS using zeolites. Future research could be directed towards an assessment of the market value of recovered N- and P-rich zeolite, to be used as a slow-release fertilizer.

Membrane technologies can efficiently concentrate nutrients. However, the operating costs of the process at full scale, which are closely linked to power consumption, cleaning frequency, and membrane replacement, need further investigation. Future studies will have to find solutions to improving membrane filtration performance, in terms of chemical and energy requirements, which can be achieved by limiting the fouling problem and utilizing renewable energy sources. It is worth highlighting that a comprehensive analysis of the costs of membrane filtration should consider the possible final reuse of the permeate and concentrate, which in turn are region specific. However, membrane processes are not as versatile for nutrient recovery as other options discussed in this study; for instance, high-solid substrates are not likely to be conveniently addressed by this technology because they would worsen fouling issues and increase the process complexity.

Table 2.5 - Cost estimation of different strategies for nutrient recovery from ADS.

Technology	Process Cost	Marketing Value of Recovered End-Products	Ref.
Side-stream ammonia stripping coupled to HSAD	1.17–1.83 €/kg N	0.77 €/kg N [1]	This study [160]
Ammonia stripping	2–7 €/kg N	0.77 €/kg N	[160,161]
Struvite precipitation	9–49 €/kg N 4–22 €/kg P	0.79–5.50 €/kg N 0.36–2.49 €/kg P	[81,162]
Membrane filtration	4–5 €/kg P [2]	0.11–0.42 €/kg N [3] 2.0–2.1 €/kg P [3] 0.11–0.30 €/kg K [3]	[81,103]
Thermal treatment	2–6 €/kg P [4]	0.85–4.25 €/kg P	[160,163–165]

[1] potential revenue associated with the sale of ammonium sulfate; [2] NF; [3] with reference to RO concentrate; [4] cost of wet-chemical leaching of sewage sludge.

From a wider perspective, it should be also noted that most technologies for nutrient recovery have been investigated on both sewage sludge and ADS. The advantage of using ADS within these processes lays in the possibility of taking the greatest advantage of the sewage sludge by exploiting not only its nutrient content, but also its biochemical potential for biogas generation. HSAD of sewage sludge seems the most efficient strategy for exploiting the nutrient potential of sewage sludge, as it results in the production of ADS with a significant agronomic value in terms of humified organic matter and nutrient concentrations, which can be directly injected into the soil (if compliant with the established regulations), and ammonium sulfate/nitrate as an additional fertilizer. Thermal treatments allow obtaining ash/char, from which a high recovery rate of nutrients can be reached. Nevertheless, thermal treatments are highly energy-consuming and require expensive emission control and further downstream gas treatment for pollutant mitigation. Due to these drawbacks, which increase the complexity of the process and capital costs and reduce the energy conversion efficiency, this technology seems the least promising. However, to improve the energy

balance of the cycle, thermal treatments could be integrated with AD, in order to generate biogas as well as energy and nutrient-rich products. From this point of view, the choice of coupling thermal treatments to AD could represent a convenient alternative to direct sewage sludge treatment, although in some cases it represents an obvious choice, for example when the produced ADS cannot be directly used in agriculture, due to low quality (e.g., high concentrations of HMs and/or other contaminants) or not being compatible with the local regulation for agricultural use.

2.5. Conclusions

This review outlines the potential for nutrient recovery from sewage sludge and its anaerobically digested form in a sustainable context. Various technologies were classified for their ability to recover a specific nutrient (e.g., nitrogen with ammonia stripping) or to allow the simultaneous recovery of multiple nutrients (struvite precipitation, ion exchange, membrane technologies, and thermal treatments followed by nutrient extraction techniques) and critically discussed to shed light on the state of the art, recent advances, opportunities, challenges, and feasibility for full-scale application.

It is evident that both sewage sludge and ADS can be considered as a resource to be exploited from a circular economy perspective. The use of ADS appears as the more convenient option, as it allows both the recovery of energy via biogas generation and nutrients via different strategies, resulting in a positive energy balance and wider applicability for nutrient recycling. From this perspective, HSAD can be considered as a promising and convenient option for simple, direct, and full exploitation of the nutrient potential of ADS, due to the possibility of producing a digestate that, compared to the conventional one, has a higher agronomic value. Nevertheless, HSAD needs further technological improvements, in terms of the energy recovery from sewage sludge, as well as a wider acceptance of ADS utilization in agriculture, which needs to be enhanced both at social and legislative levels. Further research is also needed in the field of struvite precipitation from ADS, since this can be regarded as a strategy to recover valuable nutrients, while reducing the formation of undesired deposits within the digesters. In this context, lab scale trials to unveil the formation

and precipitation mechanisms should be combined with full-scale investigations to address the definition of sustainable technical solutions, fully implementing circular economy principles in sewage sludge management.

2.6. References

[1] S. Shaddel, H. Bakhtiary-Davijany, C. Kabbe, F. Dadgar, S.W. Østerhus, Sustainable sewage sludge management: From current practices to emerging nutrient recovery technologies, Sustain. 11 (2019). https://doi.org/10.3390/su11123435.

[2] A. Siciliano, C. Limonti, G.M. Curcio, R. Molinari, Advances in struvite precipitation technologies for nutrients removal and recovery from aqueous waste and wastewater, Sustain. 12 (2020). https://doi.org/10.3390/su12187538.

[3] C.M. Mehta, W.O. Khunjar, V. Nguyen, S. Tait, D.J. Batstone, Technologies to recover nutrients from waste streams: A critical review, Crit. Rev. Environ. Sci. Technol. 45 (2015) 385–427. https://doi.org/10.1080/10643389.2013.866621.

[4] D. Bolzonella, F. Fatone, M. Gottardo, N. Frison, Nutrients recovery from anaerobic digestate of agro-waste: Techno-economic assessment of full scale applications, J. Environ. Manage. 216 (2018) 111–119. https://doi.org/10.1016/j.jenvman.2017.08.026.

[5] M.J. Alhnidi, D. Wüst, A. Funke, L. Hang, A. Kruse, Fate of Nitrogen, Phosphate, and Potassium during Hydrothermal Carbonization and the Potential for Nutrient Recovery, ACS Sustain. Chem. Eng. 8 (2020) 15507–15516. https://doi.org/10.1021/acssuschemeng.0c04229.

[6] A. Raheem, V.S. Sikarwar, J. He, W. Dastyar, D.D. Dionysiou, W. Wang, M. Zhao, Opportunities and challenges in sustainable treatment and resource reuse of sewage sludge: A review, Chem. Eng. J. 337 (2018) 616–641. https://doi.org/10.1016/j.cej.2017.12.149.

[7] V. Lebuf, F. Accoe, C. Vaneeckhaute, E. Meers, E. Michels, G. Ghekiere, Nutrient recovery from digestates: techniques and end-products, Venice 2012 Fourth Int. Symp. Energy from Biomass Waste. (2012) 18.

[8] C.J. Stevens, Nitrogen in the environment, Science (80-.). 363 (2019) 578–580. https://doi.org/10.1126/science.aav8215.

[9] L.Y. Stein, M.G. Klotz, The nitrogen cycle, Curr. Biol. 26 (2016) R94–R98. https://doi.org/10.1016/j.cub.2015.12.021.

[10] R.L. Mikkelsen, Managing potassium for organic crop production, Horttechnology. 17 (2007) 455–460. https://doi.org/10.21273/horttech.17.4.455.

[11] F. Zapata, R.N. Roy, The use of phosphate rock for sustainable agriculture, FAO Fertil. Plant Nutr. Bull. 13 (2004). http://www.mdpi.com/1996-1073/2/3/556/.

[12] R.B. Chowdhury, G.A. Moore, A.J. Weatherley, M. Arora, Key sustainability challenges for the global phosphorus resource, their implications for global food security, and options for mitigation, J. Clean. Prod. 140 (2017) 945–963. https://doi.org/10.1016/j.jclepro.2016.07.012.

[13] European Commission, Circular economy action plan, Proc. Eur. Comm. (2020).

[14] F. Di Capua, D. Spasiano, A. Giordano, F. Adani, U. Fratino, F. Pirozzi, G. Esposito, High-solid anaerobic digestion of sewage sludge: challenges and opportunities, Appl. Energy. 278 (2020) 115608. https://doi.org/10.1016/j.apenergy.2020.115608.

[15] T.D. Saliu, N.A. Oladoja, Nutrient recovery from wastewater and reuse in agriculture: a review, Environ. Chem. Lett. 19 (2021) 2299–2316. https://doi.org/10.1007/s10311-020-01159-7.

[16] Y. Ye, H.H. Ngo, W. Guo, S.W. Chang, D.D. Nguyen, X. Zhang, J. Zhang, S. Liang, Nutrient recovery from wastewater: From technology to economy, Bioresour. Technol. Reports. 11 (2020) 100425. https://doi.org/10.1016/j.biteb.2020.100425.

[17] B. Macura, S.L. Johannesdottir, M. Piniewski, N.R. Haddaway, E. Kvarnström, Effectiveness of ecotechnologies for recovery of nitrogen and phosphorus from anaerobic digestate and effectiveness of the recovery products as fertilisers: A systematic review protocol, Environ. Evid. 8 (2019) 1–9. https://doi.org/10.1186/s13750-019-0173-3.

[18] N. Morales, M.A. Boehler, S. Buettner, C. Liebi, H. Siegrist, Recovery of N and P from urine by struvite precipitation followed by combined stripping with digester sludge liquid at full scale, Water (Switzerland). 5 (2013) 1262–1278. https://doi.org/10.3390/w5031262.

[19] S. Caspersen, Z. Ganrot, Closing the loop on human urine: Plant availability of zeolite-recovered nutrients in a peat-based substrate, J. Environ. Manage. 211 (2018) 177–190. https://doi.org/10.1016/j.jenvman.2018.01.053.

[20] B. Liu, A. Giannis, J. Zhang, V.W.C. Chang, J.Y. Wang, Air stripping process for ammonia recovery from source-separated urine: Modeling and optimization, J. Chem. Technol. Biotechnol. 90 (2015) 2208–2217. https://doi.org/10.1002/jctb.4535.

[21] E.L. Foletto, W.R.B. Dos Santos, M.A. Mazutti, S.L. Jahn, A. Gündel, Production of struvite from beverage waste as Phosphorus source, Mater. Res. 16 (2013) 242–245. https://doi.org/10.1590/S1516-14392012005000152.

[22] H. Huang, Q. Song, W. Wang, S. Wu, J. Dai, Treatment of anaerobic digester effluents of nylon wastewater through chemical precipitation and a sequencing batch reactor process, J. Environ. Manage. 101 (2012) 68–74. https://doi.org/10.1016/j.jenvman.2011.12.035.

[23] Healy M., D. Clarke, E.. Peyton, E.L.. Cummins, A.. Moynihan, P.. Martins, B. and O. Fenton;, Resource recovery from sewage sludge, 2015.

[24] C. Adam, G. Kley, F.-G. Simon, A. Lehmann, Recovery of nutrients from sewage sludge – Results of the European research-project SUSAN, Water Pract. Technol. 3 (2008). https://doi.org/10.2166/wpt.2008.001.

[25] A. Mulchandani, P. Westerhoff, Recovery opportunities for metals and energy from sewage sludges, Bioresour. Technol. 215 (2016) 215–226. https://doi.org/10.1016/j.biortech.2016.03.075.

[26] D. Hidalgo, F. Corona, J.M. Martín-Marroquín, J. del Álamo, A. Aguado, Resource recovery from anaerobic digestate: struvite crystallisation versus ammonia stripping, Desalin. Water Treat. 57 (2016) 2626–2632. https://doi.org/10.1080/19443994.2014.1001794.

[27] G. Zhen, X. Lu, H. Kato, Y. Zhao, Y.Y. Li, Overview of pretreatment strategies for enhancing sewage sludge disintegration and subsequent anaerobic digestion: Current advances, full-scale application and future perspectives, Renew. Sustain. Energy Rev. 69 (2017) 559–577. https://doi.org/10.1016/j.rser.2016.11.187.

[28] X. Liao, H. Li, Y. Zhang, C. Liu, Q. Chen, Accelerated high-solids anaerobic digestion of sewage sludge using low-temperature thermal pretreatment, Int. Biodeterior. Biodegrad. 106 (2016) 141–149. https://doi.org/10.1016/j.ibiod.2015.10.023.

[29] N. Duan, B. Dong, B. Wu, X. Dai, High-solid anaerobic digestion of sewage sludge under mesophilic conditions: Feasibility study, Bioresour. Technol. 104 (2012) 150–156. https://doi.org/10.1016/j.biortech.2011.10.090.

[30] B. Scaglia, F. Tambone, L. Corno, V. Orzi, Y. Lazzarini, G. Garuti, F. Adani, Potential agronomic and environmental properties of thermophilic anaerobically digested municipal sewage sludge measured by an unsupervised and a supervised chemometric approach, Sci. Total Environ. 637–638 (2018) 791–802. https://doi.org/10.1016/j.scitotenv.2018.04.426.

[31] B. Scaglia, G. D'Imporzano, G. Garuti, M. Negri, F. Adani, Sanitation ability of anaerobic digestion performed at different temperature on sewage sludge, Sci. Total Environ. 466–467 (2014) 888–897. https://doi.org/10.1016/j.scitotenv.2013.07.114.

[32] V. Orzi, B. Scaglia, S. Lonati, C. Riva, G. Boccasile, G.L. Alborali, F. Adani, The role of biological processes in reducing both odor impact and pathogen content during mesophilic anaerobic digestion, Sci. Total Environ. 526 (2015) 116–126. https://doi.org/10.1016/j.scitotenv.2015.04.038.

[33] A. Pigoli, M. Zilio, F. Tambone, S. Mazzini, M. Schepis, E. Meers, O. Schoumans, A. Giordano, F. Adani, Thermophilic anaerobic digestion as suitable bioprocess producing organic and chemical renewable fertilizers: A full-scale approach, Waste Manag. 124 (2021) 356–367. https://doi.org/10.1016/j.wasman.2021.02.028.

[34] D. Zhang, G. Du, D. Chen, G. Shi, W. Rao, X. Li, Y. Jiang, S. Liu, D. Wang, Effect of elemental sulfur and gypsum application on the bioavailability and redistribution of cadmium during rice growth, Sci. Total Environ. 657 (2019) 1460–1467. https://doi.org/10.1016/j.scitotenv.2018.12.057.

[35] M.S. Romero-güiza, J. Mata-alvarez, J. María, C. Rivera, Nutrient recovery technologies for anaerobic digestion systems : An overview Tecnologías de

recuperación de nutrientes para los sistemas de digestión anaeróbica : revisión Tecnologias de recuperação de nutrientes para os sistemas de digestão anaeróbia : r, Bucaramanga. 29 (2015) 7–26.

[36] G. Capson-Tojo, R. Moscoviz, S. Astals, Robles, J.P. Steyer, Unraveling the literature chaos around free ammonia inhibition in anaerobic digestion, Renew. Sustain. Energy Rev. 117 (2020) 109487. https://doi.org/10.1016/j.rser.2019.109487.

[37] H. Yuan, N. Zhu, Progress in inhibition mechanisms and process control of intermediates and by-products in sewage sludge anaerobic digestion, Renew. Sustain. Energy Rev. 58 (2016) 429–438. https://doi.org/10.1016/j.rser.2015.12.261.

[38] S. Daneshgar, A. Callegari, A.G. Capodaglio, D. Vaccari, The potential phosphorus crisis: Resource conservation and possible escape technologies: A review, Resources. 7 (2018). https://doi.org/10.3390/resources7020037.

[39] T. Pepè Sciarria, G. Vacca, F. Tambone, L. Trombino, F. Adani, Nutrient recovery and energy production from digestate using microbial electrochemical technologies (METs), Elsevier Ltd, 2019. https://doi.org/10.1016/j.jclepro.2018.10.152.

[40] M. Henze, G.A. van Loosdrecht, M.C. Ekama, Biological wastewater treatment., 2008.

[41] B. Cieślik, P. Konieczka, A review of phosphorus recovery methods at various steps of wastewater treatment and sewage sludge management. The concept of “no solid waste generation” and analytical methods, J. Clean. Prod. 142 (2017) 1728–1740. https://doi.org/10.1016/j.jclepro.2016.11.116.

[42] K.S. Le Corre, E. Valsami-Jones, P. Hobbs, S.A. Parsons, Phosphorus recovery from wastewater by struvite crystallization: A review, 2009. https://doi.org/10.1080/10643380701640573.

[43] I.S.A. Abeysiriwardana-Arachchige, S.P. Munasinghe-Arachchige, H.M.K. Delanka-Pedige, N. Nirmalakhandan, Removal and recovery of nutrients from municipal sewage: Algal vs. conventional approaches, Water Res. 175 (2020) 115709. https://doi.org/10.1016/j.watres.2020.115709.

[44] F. Iannacone, F. Di Capua, F. Granata, R. Gargano, G. Esposito, Shortcut nitrification-denitrification and biological phosphorus removal in acetate- and ethanol-fed moving bed biofilm reactors under microaerobic/aerobic conditions, Bioresour. Technol. 330 (2021) 124958. https://doi.org/10.1016/j.biortech.2021.124958.

[45] F. Iannacone, F. Di Capua, F. Granata, R. Gargano, G. Esposito, Simultaneous nitrification, denitrification and phosphorus removal in a continuous-flow moving bed biofilm reactor alternating microaerobic and aerobic conditions, Bioresour. Technol. 310 (2020) 123453. https://doi.org/10.1016/j.biortech.2020.123453.

[46] I. Öborn, Y. Andrist-Rangel, M. Askegaard, C.A. Grant, C.A. Watson, A.C. Edwards, Critical aspects of potassium management in agricultural systems, Soil Use Manag. 21 (2005) 102–112. https://doi.org/10.1079/sum2005297.

[47] F. Tambone, B. Scaglia, G. D'Imporzano, A. Schievano, V. Orzi, S. Salati, F. Adani, Assessing amendment and fertilizing properties of digestates from anaerobic digestion through a comparative study with digested sludge and compost, Chemosphere. 81 (2010) 577–583. https://doi.org/10.1016/j.chemosphere.2010.08.034.

[48] A. Giordano, F. Di Capua, G. Esposito, F. Pirozzi, Long-term biogas desulfurization under different microaerobic conditions in full-scale thermophilic digesters co-digesting high-solid sewage sludge, Int. Biodeterior. Biodegrad. 142 (2019) 131–136. https://doi.org/10.1016/j.ibiod.2019.05.017.

[49] L. Shi, W.S. Simplicio, G. Wu, Z. Hu, H. Hu, X. Zhan, Nutrient Recovery from Digestate of Anaerobic Digestion of Livestock Manure: a Review, Curr. Pollut. Reports. 4 (2018) 74–83. https://doi.org/10.1007/s40726-018-0082-z.

[50] J. Arogo, R.H. Zhang, G.L. Riskowski, L.L. Christianson, D.L. Day, Mass transfer coefficient of ammonia in liquid swine manure and aqueous solutions, J. Agric. Eng. Res. 73 (1999) 77–86. https://doi.org/10.1006/jaer.1998.0390.

[51] S. Guštin, R. Marinšek-Logar, Effect of pH, temperature and air flow rate on the continuous ammonia stripping of the anaerobic digestion effluent, Process Saf. Environ. Prot. 89 (2011) 61–66.

https://doi.org/10.1016/j.psep.2010.11.001.

[52] F. Di Capua, F. Adani, F. Pirozzi, G. Esposito, A. Giordano, Air side-stream ammonia stripping in a thin film evaporator coupled to high-solid anaerobic digestion of sewage sludge: Process performance and interactions, J. Environ. Manage. 295 (2021) 113075. https://doi.org/10.1016/j.jenvman.2021.113075.

[53] B. Drosg, W. Fuchs, T. Al Seadi, M. Madsen, B. Linke, Nutrient Recovery by Biogas Digestate Processing Bernhard, 2020.

[54] Y. Nakashimada, Y. Ohshima, H. Minami, H. Yabu, Y. Namba, N. Nishio, Ammonia-methane two-stage anaerobic digestion of dehydrated waste-activated sludge, Appl. Microbiol. Biotechnol. 79 (2008) 1061–1069. https://doi.org/10.1007/s00253-008-1501-7.

[55] P. Costamagna, A. Giordano, Y. Lazzarini, M. Delucchi, G. Busca, Process of ammonia removal from anaerobic digestion and associated ammonium sulphate production: Pilot plant demonstration, J. Environ. Manage. 259 (2020) 109841. https://doi.org/10.1016/j.jenvman.2019.109841.

[56] P. Costamagna, M. Delucchi, G. Busca, A. Giordano, System for ammonia removal from anaerobic digestion and associated ammonium sulfate production: Simulation and design considerations, Process Saf. Environ. Prot. 144 (2020) 133–142. https://doi.org/10.1016/j.psep.2020.05.055.

[57] X. Lei, N. Sugiura, C. Feng, T. Maekawa, Pretreatment of anaerobic digestion effluent with ammonia stripping and biogas purification, J. Hazard. Mater. 145 (2007) 391–397. https://doi.org/10.1016/j.jhazmat.2006.11.027.

[58] C. Pedizzi, J.M. Lema, M. Carballa, A combination of ammonia stripping and low temperature thermal pre-treatment improves anaerobic post-digestion of the supernatant from organic fraction of municipal solid waste treatment, Waste Manag. 78 (2018) 271–278. https://doi.org/10.1016/j.wasman.2018.05.051.

[59] B. Tansel, G. Lunn, O. Monje, Struvite formation and decomposition characteristics for ammonia and phosphorus recovery: A review of magnesium-ammonia-phosphate interactions, Chemosphere. 194 (2018) 504–514. https://doi.org/10.1016/j.chemosphere.2017.12.004.

[60] J.A. Wilsenach, C.A.H. Schuurbiers, M.C.M. van Loosdrecht, Phosphate and

potassium recovery from source separated urine through struvite precipitation, Water Res. 41 (2007) 458–466. https://doi.org/10.1016/j.watres.2006.10.014.

[61] T. Larsen, K.M. Udert, J. Lienert, Source Separation and Decentralization for Wastewater Management, 2013. https://doi.org/10.1002/9780470925386.ch5.

[62] K. Shih, H. Yan, The Crystallization of Struvite and Its Analog (K-Struvite) From Waste Streams for Nutrient Recycling, Elsevier Inc., 2016. https://doi.org/10.1016/B978-0-12-803837-6.00026-3.

[63] S. Graeser, W. Postl, H. Bojar, P. Berlepsch, T. Armbruster, T. Raber, K. Ettinger, F. Walter, Struvite-(K), KMgPO4·6H2O, the potassium equivalent of struvite – a new mineral, Eur. J. Miner. 20 (2008) 6269–633. https://doi.org/10.1127/0935-1221/2008/0020-1810.

[64] K. Xu, J. Li, M. Zheng, C. Zhang, T. Xie, C. Wang, The precipitation of magnesium potassium phosphate hexahydrate for P and K recovery from synthetic urine, Water Res. 80 (2015) 71–79. https://doi.org/10.1016/j.watres.2015.05.026.

[65] D. Lorick, B. Macura, M. Ahlström, A. Grimvall, R. Harder, Effectiveness of struvite precipitation and ammonia stripping for recovery of phosphorus and nitrogen from anaerobic digestate: a systematic review, Environ. Evid. 9 (2020) 1–20. https://doi.org/10.1186/s13750-020-00211-x.

[66] S. Dhakal, A laboratory study of struvite precipitation for phosphorus removal from concentrated animal feeding operation wastewater, J. Environ. Eng. 6724 (2008) 14–39. https://scholarsmine.mst.edu/masters_theses/6724.

[67] J. Wang, J.G. Burken, X. (Jackie) Zhang, Effect of Seeding Materials and Mixing Strength on Struvite Precipitation, Water Environ. Res. 78 (2006) 125–132. https://doi.org/10.2175/106143005x89580.

[68] S.A. Parsons, J.D. Doyle, Struvite formation, control and recovery, Water Res. 36 (2002) 3925–3940.

[69] K.P. Fattah, N. Sabrina, D.S. Mavinic, F.A. Koch, Reducing operating costs for struvite formation with a carbon dioxide stripper, Water Sci. Technol. 58 (2008) 957–962. https://doi.org/10.2166/wst.2008.722.

[70] A. Uysal, Y.D. Yilmazel, G.N. Demirer, The determination of fertilizer quality

of the formed struvite from effluent of a sewage sludge anaerobic digester, J. Hazard. Mater. 181 (2010) 248–254. https://doi.org/10.1016/j.jhazmat.2010.05.004.

[71] S. Kataki, H. West, M. Clarke, D.C. Baruah, Phosphorus recovery as struvite: Recent concerns for use of seed, alternative Mg source, nitrogen conservation and fertilizer potential, Resour. Conserv. Recycl. 107 (2016) 142–156. https://doi.org/10.1016/j.resconrec.2015.12.009.

[72] M.T. Munir, B. Li, I. Boiarkina, S. Baroutian, W. Yu, B.R. Young, Phosphate recovery from hydrothermally treated sewage sludge using struvite precipitation, Bioresour. Technol. 239 (2017) 171–179. https://doi.org/10.1016/j.biortech.2017.04.129.

[73] N. Marti, A. Bouzas, A. Seco, J. Ferrer, Struvite precipitation assessment in anaerobic digestion processes, Chem. Eng. J. 141 (2008) 67–74. https://doi.org/10.1016/j.cej.2007.10.023.

[74] W. Zheng, X. Li, B. Li, High-quality Magnesium Ammonium Phosphate produced from Digested Sewage Sludge by Adsorption, Fresenius Environ. Bull. 23 (2014) 755–761.

[75] L.D. Xavier, M.C. Cammarota, L. Yokoyama, I. Volschan, Study of the recovery of phosphorus from struvite precipitation in supernatant line from anaerobic digesters of sludge, Water Sci. Technol. Water Supply. 14 (2014) 751–757. https://doi.org/10.2166/ws.2014.033.

[76] G. Jia, H. Zhang, J. Krampe, T. Muster, B. Gao, N. Zhu, B. Jin, Applying a chemical equilibrium model for optimizing struvite precipitation for ammonium recovery from anaerobic digester effluent, J. Clean. Prod. 147 (2017) 297–305. https://doi.org/10.1016/j.jclepro.2017.01.116.

[77] L. Pastor, N. Marti, A. Bouzas, A. Seco, Sewage sludge management for phosphorus recovery as struvite in EBPR wastewater treatment plants, Bioresour. Technol. 99 (2008) 4817–4824. https://doi.org/10.1016/j.biortech.2007.09.054.

[78] S. Wacławek, K. Grübel, P. Dennis, V.T.P. Vinod, M. Černík, A novel approach for simultaneous improvement of dewaterability, post-digestion liquor

properties and toluene removal from anaerobically digested sludge, Chem. Eng. J. 291 (2016) 192–198. https://doi.org/10.1016/j.cej.2016.01.103.

[79] B. Li, I. Boiarkina, W. Yu, H.M. Huang, T. Munir, G.Q. Wang, B.R. Young, Phosphorous recovery through struvite crystallization: Challenges for future design, Sci. Total Environ. 648 (2019) 1244–1256. https://doi.org/10.1016/j.scitotenv.2018.07.166.

[80] R. Taddeo, S. Prajapati, R. Lepistö, Optimizing ammonium adsorption on natural zeolite for wastewaters with high loads of ammonium and solids, J. Porous Mater. 24 (2017) 1545–1554. https://doi.org/10.1007/s10934-017-0394-1.

[81] N. Krakat, R. Anjum, D. Dietz, B. Demirel, Methods of ammonia removal in anaerobic digestion: A review, Water Sci. Technol. 76 (2017) 1925–1938. https://doi.org/10.2166/wst.2017.406.

[82] C. Vaneeckhaute, V. Lebuf, E. Michels, E. Belia, P.A. Vanrolleghem, F.M.G. Tack, E. Meers, Nutrient Recovery from Digestate: Systematic Technology Review and Product Classification, Waste and Biomass Valorization. 8 (2017) 21–40. https://doi.org/10.1007/s12649-016-9642-x.

[83] P. Seruga, M. Krzywonos, J. Pyzanowska, A. Urbanowska, H. Pawlak-Kruczek, Ł. Niedźwiecki, Removal of ammonia from the municipal waste treatment effuents using natural minerals, Molecules. 24 (2019). https://doi.org/10.3390/molecules24203633.

[84] A. Zarebska, D. Romero Nieto, K. V. Christensen, L. Fjerbæk Søtoft, B. Norddahl, Ammonium fertilizers production from manure: A critical review, Crit. Rev. Environ. Sci. Technol. 45 (2015) 1469–1521. https://doi.org/10.1080/10643389.2014.955630.

[85] L. Lin, Z. Lei, L. Wang, X. Liu, Y. Zhang, C. Wan, D.J. Lee, J.H. Tay, Adsorption mechanisms of high-levels of ammonium onto natural and NaCl-modified zeolites, Sep. Purif. Technol. 103 (2013) 15–20. https://doi.org/10.1016/j.seppur.2012.10.005.

[86] M. Zabochnicka-Świątek, K. Malińska, Removal of ammonia by clinoptilolite, Glob. Nest J. 12 (2010) 256–261. https://doi.org/10.30955/gnj.000724.

[87] A.G. Capodaglio, P. Hlavinek, M. Raboni, Physico-chemical technologies for nitrogen removal from wastewaters: a review, Rev. Ambient. e Agua. 10 (2015) 481–498. https://doi.org/10.4136/1980-993X.

[88] I. Kabdaşlı, O. Tünay, Nutrient recovery by struvite precipitation, ion exchange and adsorption from source-separated human urine–a review, Environ. Technol. Rev. 7 (2018) 106–138. https://doi.org/10.1080/21622515.2018.1473504.

[89] C.A. Takaya, L.A. Fletcher, S. Singh, K.U. Anyikude, A.B. Ross, Phosphate and ammonium sorption capacity of biochar and hydrochar from different wastes, Chemosphere. 145 (2016) 518–527. https://doi.org/10.1016/j.chemosphere.2015.11.052.

[90] X. Guo, L. (L). Zeng, X. Li, H.S. Park, Ammonium and potassium removal for anaerobically digested wastewater using natural clinoptilolite followed by membrane pretreatment, J. Hazard. Mater. 151 (2008) 125–133. https://doi.org/10.1016/j.jhazmat.2007.05.066.

[91] E. Polat, M. Karaca, H. Demir, a N. Onus, Use of natural zeolite (clinoptilolite) in agriculture, J. Fruit Ornam. Plant Reserarch. 12 (2004) 183–189.

[92] T. Wirthensohn, F. Waeger, L. Jelinek, W. Fuchs, Ammonium removal from anaerobic digester effluent by ion exchange, Water Sci. Technol. 60 (2009) 201–210. https://doi.org/10.2166/wst.2009.317.

[93] N.P. Kocatürk-Schumacher, S. Bruun, K. Zwart, L.S. Jensen, Nutrient Recovery From the Liquid Fraction of Digestate by Clinoptilolite, Clean - Soil, Air, Water. 45 (2017) 1–7. https://doi.org/10.1002/clen.201500153.

[94] H. Gong, Z. Wang, X. Zhang, Z. Jin, C. Wang, L. Zhang, K. Wang, Organics and nitrogen recovery from sewage via membrane-based pre-concentration combined with ion exchange process, Chem. Eng. J. 311 (2017) 13–19. https://doi.org/10.1016/j.cej.2016.11.068.

[95] H. Ma, Y. Guo, Y. Qin, Y.Y. Li, Nutrient recovery technologies integrated with energy recovery by waste biomass anaerobic digestion, Bioresour. Technol. 269 (2018) 520–531. https://doi.org/10.1016/j.biortech.2018.08.114.

[96] W. Guo, H.H. Ngo, J. Li, A mini-review on membrane fouling, Bioresour. Technol. 122 (2012) 27–34. https://doi.org/10.1016/j.biortech.2012.04.089.

[97] M.L. Gerardo, M.P. Zacharof, R.W. Lovitt, Strategies for the recovery of nutrients and metals from anaerobically digested dairy farm sludge using cross-flow microfiltration, Water Res. 47 (2013) 4833–4842. https://doi.org/10.1016/j.watres.2013.04.019.

[98] M.L. Gerardo, N.H.M. Aljohani, D.L. Oatley-Radcliffe, R.W. Lovitt, Moving towards sustainable resources: Recovery and fractionation of nutrients from dairy manure digestate using membranes, Water Res. 80 (2015) 80–89. https://doi.org/10.1016/j.watres.2015.05.016.

[99] C. Blöcher, C. Niewersch, T. Melin, Phosphorus recovery from sewage sludge with a hybrid process of low pressure wet oxidation and nanofiltration, Water Res. 46 (2012) 2009–2019. https://doi.org/10.1016/j.watres.2012.01.022.

[100] F. Waeger, T. Delhaye, W. Fuchs, The use of ceramic microfiltration and ultrafiltration membranes for particle removal from anaerobic digester effluents, Sep. Purif. Technol. 73 (2010) 271–278. https://doi.org/10.1016/j.seppur.2010.04.013.

[101] J. Mamo, M.J. García-Galán, M. Stefani, S. Rodríguez-Mozaz, D. Barceló, H. Monclús, I. Rodriguez-Roda, J. Comas, Fate of pharmaceuticals and their transformation products in integrated membrane systems for wastewater reclamation, Chem. Eng. J. 331 (2018) 450–461. https://doi.org/10.1016/j.cej.2017.08.050.

[102] K. Chon, H. KyongShon, J. Cho, Membrane bioreactor and nanofiltration hybrid system for reclamation of municipal wastewater: Removal of nutrients, organic matter and micropollutants, Bioresour. Technol. 122 (2012) 181–188. https://doi.org/10.1016/j.biortech.2012.04.048.

[103] G. Asik, T. Yilmaz, F. Di Capua, D. Ucar, G. Esposito, E. Sahinkaya, Sequential sulfur-based denitrification/denitritation and nanofiltration processes for drinking water treatment, J. Environ. Manage. 295 (2021) 113083. https://doi.org/10.1016/j.jenvman.2021.113083.

[104] O. Nir, R. Sengpiel, M. Wessling, Closing the cycle: Phosphorus removal and recovery from diluted effluents using acid resistive membranes, Chem. Eng. J. 346 (2018) 640–648. https://doi.org/10.1016/j.cej.2018.03.181.

[105] D.L. Shaffer, J.R. Werber, H. Jaramillo, S. Lin, M. Elimelech, Forward osmosis: Where are we now?, Desalination. 356 (2015) 271–284. https://doi.org/10.1016/j.desal.2014.10.031.

[106] M. Xie, L.D. Nghiem, W.E. Price, M. Elimelech, Toward Resource Recovery from Wastewater: Extraction of Phosphorus from Digested Sludge Using a Hybrid Forward Osmosis-Membrane Distillation Process, Environ. Sci. Technol. Lett. 1 (2014) 191–195. https://doi.org/10.1021/ez400189z.

[107] M. Xie, H.K. Shon, S.R. Gray, M. Elimelech, Membrane-based processes for wastewater nutrient recovery: Technology, challenges, and future direction, Water Res. 89 (2016) 210–221. https://doi.org/10.1016/j.watres.2015.11.045.

[108] Q. Li, M. Elimelech, Organic fouling and chemical cleaning of nanofiltration membranes: Measurements and mechanisms, Environ. Sci. Technol. 38 (2004) 4683–4693. https://doi.org/10.1021/es0354162.

[109] N.C. Nguyen, S.S. Chen, H.Y. Yang, N.T. Hau, Application of forward osmosis on dewatering of high nutrient sludge, Bioresour. Technol. 132 (2013) 224–229. https://doi.org/10.1016/j.biortech.2013.01.028.

[110] J.L. Soler-Cabezas, J.A. Mendoza-Roca, M.C. Vincent-Vela, M.J. Luján-Facundo, L. Pastor-Alcañiz, Simultaneous concentration of nutrients from anaerobically digested sludge centrate and pre-treatment of industrial effluents by forward osmosis, Sep. Purif. Technol. 193 (2018) 289–296. https://doi.org/10.1016/j.seppur.2017.10.058.

[111] A. Alkhudhiri, N. Darwish, N. Hilal, Membrane distillation: A comprehensive review, Desalination. 287 (2012) 2–18. https://doi.org/10.1016/j.desal.2011.08.027.

[112] S. Kim, D.W. Lee, J. Cho, Application of direct contact membrane distillation process to treat anaerobic digestate, J. Memb. Sci. 511 (2016) 20–28. https://doi.org/10.1016/j.memsci.2016.03.038.

[113] X. Wang, X. Zhang, Y. Wang, Y. Du, H. Feng, T. Xu, Simultaneous recovery of ammonium and phosphorus via the integration of electrodialysis with struvite reactor, J. Memb. Sci. 490 (2015) 65–71. https://doi.org/10.1016/j.memsci.2015.04.034.

[114] X. Wang, Y. Wang, X. Zhang, H. Feng, C. Li, T. Xu, Phosphate recovery from excess sludge by conventional electrodialysis (CED) and electrodialysis with bipolar membranes (EDBM), Ind. Eng. Chem. Res. 52 (2013) 15896–15904. https://doi.org/10.1021/ie4014088.

[115] L.B.M. Barros, L.H. Andrade, J.E. Drewes, M.C.S. Amaral, Investigation of electrodialysis configurations for vinasse desalting and potassium recovery, Sep. Purif. Technol. 229 (2019) 115797. https://doi.org/10.1016/j.seppur.2019.115797.

[116] R.W. Holloway, A.E. Childress, K.E. Dennett, T.Y. Cath, Forward osmosis for concentration of anaerobic digester centrate, Water Res. 41 (2007) 4005–4014. https://doi.org/10.1016/j.watres.2007.05.054.

[117] T.P. Thomsen, Z. Sárossy, J. Ahrenfeldt, U.B. Henriksen, F.J. Frandsen, D.S. Müller-Stöver, Changes imposed by pyrolysis, thermal gasification and incineration on composition and phosphorus fertilizer quality of municipal sewage sludge, J. Environ. Manage. 198 (2017) 308–318. https://doi.org/10.1016/j.jenvman.2017.04.072.

[118] D. Durdević, M. Trstenjak, I. Hulenić, Sewage sludge thermal treatment technology selection by utilizing the analytical hierarchy process, Water (Switzerland). 12 (2020). https://doi.org/10.3390/W12051255.

[119] F. Facchini, G. Mummolo, M. Vitti, Scenario Analysis for Selecting Sewage Sludge-to-Energy/Matter Recovery Processes, Energies. 14 (2021). https://doi.org/doi.org/10.3390/en14020276.

[120] D. Durdević, P. Blecich, Ž. Juri´, Energy Recovery from Sewage Sludge : The Case, Energies. 12 (2019) 1–19. doi:10.3390/en12101927.

[121] A. Tsybina, C. Wuensch, Analysis of sewage sludge thermal treatment methods in the context of circular economy, Detritus. 2 (2018) 3–15. https://doi.org/10.31025/2611-4135/2018.13668.

[122] C. Adam, G. Kley, F.G. Simon, Thermal treatment of municipal sewage sludge aiming at marketable P-fertilisers, Mater. Trans. 48 (2007) 3056–3061. https://doi.org/10.2320/matertrans.MK200707.

[123] M. Smol, C. Adam, S.A. Kugler, Thermochemical treatment of Sewage Sludge

Ash (SSA)-potential and perspective in Poland, Energies. 13 (2020) 1–17. https://doi.org/10.3390/en13205461.

[124] S. Petzet, B. Peplinski, P. Cornel, On wet chemical phosphorus recovery from sewage sludge ash by acidic or alkaline leaching and an optimized combination of both, Water Res. 46 (2012) 3769–3780. https://doi.org/10.1016/j.watres.2012.03.068.

[125] L. Fang, J. shan Li, M.Z. Guo, C.R. Cheeseman, D.C.W. Tsang, S. Donatello, C.S. Poon, Phosphorus recovery and leaching of trace elements from incinerated sewage sludge ash (ISSA), Chemosphere. 193 (2018) 278–287. https://doi.org/10.1016/j.chemosphere.2017.11.023.

[126] B.K. Biswas, K. Inoue, H. Harada, K. Ohto, H. Kawakita, Leaching of phosphorus from incinerated sewage sludge ash by means of acid extraction followed by adsorption on orange waste gel, J. Environ. Sci. 21 (2009) 1753–1760. https://doi.org/10.1016/S1001-0742(08)62484-5.

[127] M. Baldi, A. Martinotti, S. Sorlini, I.A. Katsoyiannis, A. Abbà, M.C. Miino, M.C. Collivignarelli, Extraction and purification of phosphorus from the ashes of incinerated biological sewage sludge, Water (Switzerland). 13 (2021) 1–11. https://doi.org/10.3390/w13081102.

[128] P. Guedes, E.P. Mateus, J. Almeida, A.R. Ferreira, N. Couto, A.B. Ribeiro, Electrodialytic treatment of sewage sludge: Current intensity influence on phosphorus recovery and organic contaminants removal, Chem. Eng. J. 306 (2016) 1058–1066. https://doi.org/10.1016/j.cej.2016.08.040.

[129] H. Kirchmann, G. Börjesson, T. Kätterer, Y. Cohen, From agricultural use of sewage sludge to nutrient extraction: A soil science outlook, Ambio. 46 (2017) 143–154. https://doi.org/10.1007/s13280-016-0816-3.

[130] E. Monfet, G. Aubry, A.A. Ramirez, Nutrient removal and recovery from digestate: a review of the technology, Biofuels. 9 (2018) 247–262. https://doi.org/10.1080/17597269.2017.1336348.

[131] B. Khiari, F. Marias, F. Zagrouba, J. Vaxelaire, Analytical study of the pyrolysis process in a wastewater treatment pilot station, Desalination. 167 (2004) 39–47. https://doi.org/10.1016/j.desal.2004.06.111.

[132] K.B. Cantrell, P.G. Hunt, M. Uchimiya, J.M. Novak, K.S. Ro, Impact of pyrolysis temperature and manure source on physicochemical characteristics of biochar, Bioresour. Technol. 107 (2012) 419–428. https://doi.org/10.1016/j.biortech.2011.11.084.

[133] J. Oladejo, K. Shi, X. Luo, G. Yang, T. Wu, A review of sludge-to-energy recovery methods, Energies. 12 (2019) 1–38. https://doi.org/10.3390/en12010060.

[134] Y. Cao, A. Pawłowski, Sewage sludge-to-energy approaches based on anaerobic digestion and pyrolysis: Brief overview and energy efficiency assessment, Renew. Sustain. Energy Rev. 16 (2012) 1657–1665. https://doi.org/10.1016/j.rser.2011.12.014.

[135] M.C. Samolada, A.A. Zabaniotou, Comparative assessment of municipal sewage sludge incineration, gasification and pyrolysis for a sustainable sludge-to-energy management in Greece, Waste Manag. 34 (2014) 411–420. https://doi.org/10.1016/j.wasman.2013.11.003.

[136] S.A. Hoang, N. Bolan, A.M.P. Madhubashini, M. Vithanage, V. Perera, H. Wijesekara, H. Wang, P. Srivastava, M.B. Kirkham, B.S. Mickan, J. Rinklebe, K.H.M. Siddique, Treatment processes to eliminate potential environmental hazards and restore agronomic value of sewage sludge: A review, Environ. Pollut. 293 (2022). https://doi.org/10.1016/j.envpol.2021.118564.

[137] G. Calì, P. Deiana, C. Bassano, S. Meloni, E. Maggio, M. Mascia, A. Pettinau, Syngas production, clean-up and wastewater management in a demo-scale fixed-bed updraft biomass gasification unit, Energies. 13 (2020). https://doi.org/10.3390/en13102594.

[138] M. Seggiani, M. Puccini, G. Raggio, S. Vitolo, Effect of sewage sludge content on gas quality and solid residues produced by cogasification in an updraft gasifier, Waste Manag. 32 (2012) 1826–1834. https://doi.org/10.1016/j.wasman.2012.04.018.

[139] K. Gorazda, B. Tarko, S. Werle, Z. Wzorek, Sewage sludge as a fuel and raw material for phosphorus recovery: Combined process of gasification and P extraction, Waste Manag. 73 (2018) 404–415.

https://doi.org/10.1016/j.wasman.2017.10.032.

[140] T.R. Bridle, D. Pritchard, Energy and nutrient recovery from sewage sludge via pyrolysis, Water Sci. Technol. 50 (2004) 169–175. https://doi.org/10.2166/wst.2004.0562.

[141] N. Vali, L.E. Åmand, A. Combres, T. Richards, A. Pettersson, Pyrolysis of municipal sewage sludge to investigate char and phosphorous yield together with heavy-metal removal—experimental and by thermodynamic calculations, Energies. 14 (2021). https://doi.org/10.3390/en14051477.

[142] M. Atienza-Martínez, G. Gea, J. Arauzo, S.R.A. Kersten, A.M.J. Kootstra, Phosphorus recovery from sewage sludge char ash, Biomass and Bioenergy. 65 (2014) 42–50. https://doi.org/10.1016/j.biombioe.2014.03.058.

[143] N. Gao, K. Kamran, C. Quan, P.T. Williams, Thermochemical conversion of sewage sludge: A critical review, Prog. Energy Combust. Sci. 79 (2020) 100843. https://doi.org/10.1016/j.pecs.2020.100843.

[144] A. Smoliński, N. Howaniec, Co-gasification of coal/sewage sludge blends to hydrogen-rich gas with the application of simulated high temperature reactor excess heat, Int. J. Hydrogen Energy. 41 (2016) 8154–8158. https://doi.org/10.1016/j.ijhydene.2015.10.145.

[145] J.G. Zhu, Y. Yao, Q.G. Lu, M. Gao, Z.Q. Ouyang, Experimental investigation of gasification and incineration characteristics of dried sewage sludge in a circulating fluidized bed, Fuel. 150 (2015) 441–447. https://doi.org/10.1016/j.fuel.2015.02.031.

[146] D. Schwitalla, M. Reinmöller, C. Forman, C. Wolfersdorf, M. Gootz, J. Bai, S. Guhl, M. Neuroth, B. Meyer, Ash and slag properties for co-gasification of sewage sludge and coal: An experimentally validated modeling approach, Fuel Process. Technol. 175 (2018) 1–9. https://doi.org/10.1016/j.fuproc.2018.02.026.

[147] M. Volpe, L. Fiori, F. Merzari, A. Messineo, G. Andreottola, Hydrothermal carbonization as an efficient tool for sewage sludge valorization and phosphorous recovery, Chem. Eng. Trans. 80 (2020) 199–204. https://doi.org/10.3303/CET2080034.

[148] F. Merzari, M. Langone, G. Andreottola, L. Fiori, Methane production from process water of sewage sludge hydrothermal carbonization. A review. Valorising sludge through hydrothermal carbonization, Taylor & Francis, 2019. https://doi.org/10.1080/10643389.2018.1561104.

[149] E. Danso-Boateng, G. Shama, A.D. Wheatley, S.J. Martin, R.G. Holdich, Hydrothermal carbonisation of sewage sludge: Effect of process conditions on product characteristics and methane production, Bioresour. Technol. 177 (2015) 318–327. https://doi.org/10.1016/j.biortech.2014.11.096.

[150] R. Ferrentino, F. Merzari, L. Fiori, G. Andreottola, Coupling hydrothermal carbonization with anaerobic digestion for sewage sludge treatment: Influence of HTC liquor and hydrochar on biomethane production, Energies. 13 (2020). https://doi.org/10.3390/en13236262.

[151] M. Escala, T. Zumbühl, C. Koller, R. Junge, R. Krebs, Hydrothermal carbonization as an energy-efficient alternative to established drying technologies for sewage sludge: A feasibility study on a laboratory scale, Energy and Fuels. 27 (2013) 454–460. https://doi.org/10.1021/ef3015266.

[152] C.I. Aragón-Briceño, A.B. Ross, M.A. Camargo-Valero, Mass and energy integration study of hydrothermal carbonization with anaerobic digestion of sewage sludge, Renew. Energy. 167 (2021) 473–483. https://doi.org/10.1016/j.renene.2020.11.103.

[153] X. Zhuang, Y. Huang, Y. Song, H. Zhan, X. Yin, C. Wu, The transformation pathways of nitrogen in sewage sludge during hydrothermal treatment, Bioresour. Technol. 245 (2017) 463–470. https://doi.org/10.1016/j.biortech.2017.08.195.

[154] C. Aragón-Briceño, A.B. Ross, M.A. Camargo-Valero, Evaluation and comparison of product yields and bio-methane potential in sewage digestate following hydrothermal treatment, Appl. Energy. 208 (2017) 1357–1369. https://doi.org/10.1016/j.apenergy.2017.09.019.

[155] P. Saetea, N. Tippayawong, Recovery of Value-Added Products from Hydrothermal Carbonization of Sewage Sludge, ISRN Chem. Eng. 2013 (2013) 1–6. https://doi.org/10.1155/2013/268947.

[156] R. Delzeit, U. Kellner, The impact of plant size and location on profitability of biogas plants in Germany under consideration of processing digestates, Biomass and Bioenergy. 52 (2013) 43–53. https://doi.org/10.1016/j.biombioe.2013.02.029.

[157] B. Saerens, S. Geerts, M. Weemaes, Phosphorus recovery as struvite from digested sludge – experience from the full scale, J. Environ. Manage. 280 (2021) 111743. https://doi.org/10.1016/j.jenvman.2020.111743.

[158] F. Guilayn, M. Rouez, M. Crest, D. Patureau, J. Jimenez, Valorization of digestates from urban or centralized biogas plants: a critical review, Springer Netherlands, 2020. https://doi.org/10.1007/s11157-020-09531-3.

[159] H. Huang, D. Xiao, R. Pang, C. Han, L. Ding, Simultaneous removal of nutrients from simulated swine wastewater by adsorption of modified zeolite combined with struvite crystallization, Chem. Eng. J. 256 (2014) 431–438. https://doi.org/10.1016/j.cej.2014.07.023.

[160] C. Brienza, I. Sigurnjak, T. Meier, E. Michels, F. Adani, O. Schoumans, C. Vaneeckhaute, E. Meers, Techno-economic assessment at full scale of a biogas refinery plant receiving nitrogen rich feedstock and producing renewable energy and biobased fertilisers, J. Clean. Prod. 308 (2021) 127408. https://doi.org/10.1016/j.jclepro.2021.127408.

[161] E.M. Barampouti, S. Mai, D. Malamis, K. Moustakas, M. Loizidou, Exploring technological alternatives of nutrient recovery from digestate as a secondary resource, Renew. Sustain. Energy Rev. 134 (2020) 110379. https://doi.org/10.1016/j.rser.2020.110379.

[162] T. Dockhorn, About the economy of phosphorus recovery, in: Int. Conf. Nutr. Recover. from Wastewater Streams, IWA Publishing, London, UK, 2009: pp. 145–158.

[163] L. Egle, H. Rechberger, J. Krampe, M. Zessner, Phosphorus recovery from municipal wastewater: An integrated comparative technological, environmental and economic assessment of P recovery technologies, Sci. Total Environ. 571 (2016) 522–542. https://doi.org/10.1016/j.scitotenv.2016.07.019.

[164] L. Luyckx, S. Geerts, J. Van Caneghem, Closing the phosphorus cycle: Multi-

criteria techno-economic optimization of phosphorus extraction from wastewater treatment sludge ash, Sci. Total Environ. 713 (2020) 135543. https://doi.org/10.1016/j.scitotenv.2019.135543.

[165] O.F. Schoumans, W.H. Rulkens, O. Oenema, P.A.I. Ehlert, Phosphorus recovery from animal manure : technical opportunities and agro-economical perspectives, Alterra, 308, CWK - Integraal Waterbeheer, , 2010. https://edepot.wur.nl/163684.

CHAPTER 3

Impact of high-intensity static magnetic field on chemical properties and anaerobic digestion of sewage sludge

The content of this chapter has been published as:

Di Costanzo, N., Di Capua, F., Cesaro, A. et al. Impact of High-Intensity Static Magnetic Field on Chemical Properties and Anaerobic Digestion of Sewage Sludge. Waste Biomass Valor 14, 2469–2479 (2023). https://doi.org/10.1007/s12649-022-01891-x

Abstract

This chapter aims to determine the effects of a 1.5 T SMF on the chemical composition of sewage sludge as well as on methane generation during anaerobic digestion. The main parameters influencing the static magnetic field (SMF) (i.e., flow rate, mixing ratio of magnetized to non-magnetized sludge, number of pumping cycles, and total solid content) were varied to evaluate the impact of different exposure conditions on the chemical characteristics and methane potential of sewage sludge. The outcomes of the present chapter suggest that high-intensity SMF, although negatively influencing methane generation, can promote the precipitation, and possibly the recovery/recycle of valuable compounds from sewage sludge, enhancing its proper management in a circular economy perspective.

3.1. Introduction

The growing demand for wastewater treatment has led to a rapid increase in the production of an unavoidable by-product, i.e., sewage sludge, holding organic matter, nutrients, and often pathogens as well as toxic substances such as organic contaminants and heavy metals [1]. Typically, sewage sludge treatment pursues a volume reduction via thickening and dehydration as well as a biological stabilization via digestion processes, usually performed under anaerobic conditions. The anaerobic digestion process generates a gaseous flow, the biogas, and a solid–liquid flow, the digestate or anaerobically digested sludge (ADS). The biogas is a well-known energetically valuable product containing around 55–65% of methane (CH_4), and it can be further processed to produce biomethane and/or thermal/electrical energy for plant operation, thereby eliminating or reducing the external supply of energy and related costs. On the other hand, ADS is a valuable source of organic matter and nutrients, and its reuse as a fertilizer is among the most attractive strategies fitting the principles of circular economy [2]. The management of this by-product represents a challenge due to the high investment and operating costs for its treatment and disposal. Both ADS management and agricultural valorization are key factors for the economic and environmental sustainability of wastewater treatment plants (WWTPs).

In the past decades, many studies have been carried out with the aim to select the best strategies to enhance the energetic valorization of sewage sludge through anaerobic digestion. These strategies include mechanical methods such as sonication [3] and lysis-centrifuge [4], thermal hydrolysis carried out at high (> 140 °C) [5] and at low temperatures (50–90 °C) [6], chemical methods such as ozonation [7] as well as biological methods such as bacterial pretreatment [8] and microaeration [9,10]. These different strategies, although they showed good performance in improving the anaerobic digestion process, are characterized by high costs for energy and/or chemicals, which are not always compensated by an increased biogas production and prevent a wider application in WWTPs. In this scenario, it therefore seems interesting to search for innovative and more sustainable technologies.

Recently, the impact of static magnetic field (SMF) on the anaerobic digestion of sewage sludge has gained increasing interest [11–13]. In the past, some studies focused on the effects of low-intensity SMF on the aerobic degradation of organic matter and denitrification. The application of a weak SMF (13 mT) was shown to increase by 10% the efficiency of the biological decomposition of organics in activated sludge at low temperature (5 °C) [14]. Similar results were obtained by Filipič et al. [15] who demonstrated that 17 mT SMF could enhance the enzymatic activity and organic matter degradation by wastewater bacteria. In another study, it was demonstrated that a SMF with an intensity of 30 mT can improve the denitrification performance of immobilized bacteria [16].

More recently, Zieliński et al. [11] evaluated the effect of the SMF on the anaerobic digestion of municipal sewage sludge. These authors observed that a low-intensity SMF of 17.6 mT exerted a positive effect on CH_4 production efficiency and content in biogas, which was attributed to an increased proportion of methanogenic archaea in the digester mixed culture [13]. Also, the application of a weak SMF was shown to determine positive effects on solid separation, e.g., removal of sludge flocs from the bioreactor effluent, and on sludge properties, improving sludge sedimentation and dewaterability. In the literature, it is reported that these effects may depend on the SMF intensity and frequency [17], its static or oscillating nature, waveform, as well as on type and condition of the exposed cells [18]. Also, it has been proven that a strong

SMF affects properties of liquids such as surface tension, density, viscosity, light extinction and wettability of solid substances [19]. Although positive impacts of low-intensity SMF on anaerobic digestion have been highlighted, the current literature lacks information regarding the effects induced by high magnetic intensities on the chemical composition and the anaerobic degradation of sewage sludge. Moreover, changes of the chemical composition of sewage sludge exposed to high-intensity SMF have not been yet investigated. As this kind of technology is used to reduce water hardness by promoting the precipitation of ionic species, its application could likely exert a similar effect on the ionic species present in sewage sludge and promote the potential precipitation of struvite, a crystalline mineral composed of magnesium, nitrogen and phosphorus with good fertilizing properties [1,20].

The aim of this work was to determine the impact of a high-intensity (1.5 T) SMF on sewage sludge in terms of its chemical composition and CH_4 production by anaerobic digestion. The effects of the main parameters influencing SMF intensity were investigated at laboratory scale and used to discuss practical applications of this technique for enhancing nutrient recovery and recycle from sewage sludge.

3.2. Materials and Methods

3.2.1. Sewage sludge origin and composition

The sewage sludge was collected at the WWTP of Nola (Italy) during two sampling exercises and used to run two separate experimental phases, i.e., stage 1 (S1) and stage 2 (S2). Nola WWTP treats wastewater of predominantly municipal origin and, to a lesser extent, industrial wastewater from the nearby industrial area of Nola - Marigliano. The plant is based on a conventional activated sludge system operated at long solid retention time (> 20 days). The sewage sludge was collected from the lower withdrawal point of the pre-thickener, placed in plastic containers, transported to the laboratory, and used for the experiments. The characteristics of the sewage sludge used in this study are listed in **Table 3.1**.

Table 3.1 - Characteristics of the sewage sludge used for the experiments.

Parameter	Unit	Stage 1	Stage 2
pH	-	6.9±0.1	7.0±0.1
Total solids	%	5.0±0.2	4.9±0.15
Volatile solids	%	3.8±0.3	3.6±0.2
Chemical oxygen demand (COD)	mg/L	11496±62	11579±49
Soluble COD	mg/L	4887±99	4990±56
Ammonium (NH_4^+)	mg/L	180±2	179±6
Phosphate (PO_4^{3-})	mg/L	375.5±3.3	357.3±1.6
Nitrate (NO_3^-)	mg/L	17.6±0.4	19.2±2.2
Sulfate (SO_4^{2-})	mg/L	13.7±1.2	15.1±0.8
Magnesium (Mg^{2+})	mg/L	3.8±0.3	4.2±0.7

3.2.2. Magnetic pretreatment of sewage sludge

The SMF was generated by a patented Purak magnetic polarizer provided by AMS company (Italy) (V. Ruggero, Magnetic polarizer. Italian patent company (2004) Patent N.0001351125; V. Ruggero, Magnetic polarizer. Italian patent company (2015) Patent N.102015000013842), which was composed of magnetic rings made with a mixture of rare earth metals embedded in a ceramic base and sintered. The technical parameters of the magnetic polarizer are as follows: nominal diameter = 50 mm, height = 125 mm, weight = 1.5 kg and nominal intensity of the induced SMF = 1.5 T. Sewage sludge magnetization was applied as a pretreatment to anaerobic digestion and carried out by pumping a volume of 2L of the sludge through the polarizer. For this purpose, the magnetic polarizer was installed on a circuit (**Figure 3.1**) made with a plastic tube (diameter = 1.5 cm) and connected to a pumping system. The latter consisted of a 520Du peristaltic pump (Watson-Marlow, UK) when the flow rate was in the lower range (0.1–0.5 L/min), while a submersible water pump (Comet, USA) was used for the higher flow rate.

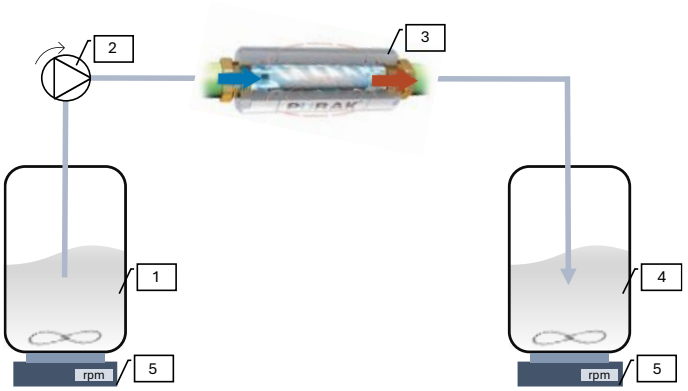

Figure 3.1 - Scheme of the experimental set-up: 1 - feedstock; 2 - peristaltic pump; 3 - magnetic polarizer; 4 - treated sewage sludge; 5 - magnetic stirrer.

3.2.3. Anaerobic digestion tests with magnetized sewage sludge

Anaerobic digestion experiments were conducted in triplicate and performed in 500 mL Schott glass bottles (Duran, Germany). Each bioreactor was sealed by screw caps with two sampling ports for daily CH_4 quantification and withdrawal of liquid samples, placed in a thermostatic bath at 35 °C and monitored for 42 days. Mixing of each bioreactor was performed manually once/day before sampling. The experimental work was divided in two stages: the first was carried out with partially magnetized sewage sludge (S1) and the second with completely magnetized sewage sludge (S2). In S1 tests, the effect of different values of magnetized sewage sludge total solid (TS) concentration (2.5% and 5%), mixing ratio (MR) of magnetized to non-magnetized sludge (0.5 and 2 in terms of VS) and number of magnetization cycles (NMC) (1 and 10) was evaluated at a constant flow rate (Q) of 0.5 L/min. In S2 the tests were carried out at Q of 0.1, 0.5 and 10 L/min, TS concentration of 2.5% and 5% and NMC of 1 and 10. The experimental design of S1 is shown in **Table 3.2**.

Table 3.2 - Design of anaerobic digestion tests with partially magnetized sludge (S1).

Test	Q (L/min)	TS (%)	MR	NMC
A	0.5	5	0.5	1
B				10
C			2	1
D				10
E		2.5	0.5	1

F				10
G			2	1
H				10
Ctrl	-	5	-	-

Experiments were carried out with 9 different tests, including a control test to which the SMF was not applied. **Supplementary Table 3.1** shows the organic load for S1 and S2 tests. From each test bottle, the daily CH_4 production was quantified 5 times/week and liquid samples (12 mL) were withdrawn once a week to measure the concentrations of volatile fatty acids (VFA), ammonium (NH_4^+), phosphate (PO_4^{3-}), nitrate (NO_3^-) and sulfate (SO_4^{2-}). These analyses, along with the chemical oxygen demand (COD) concentration, were also carried out on the feedstock after the magnetic pretreatment as well as on the digestate at the end of the tests.

Following the results from S1, in S2 the effect of SMF on the anaerobic digestion of sewage sludge was evaluated considering 8 tests with completely magnetized sludge, including 2 control tests at different TS concentrations. In S2 conditions of maximum ($Q = 10$ L/min, NMC = 10), medium ($Q = 0.5$ L/min, NMC = 10) and minimum ($Q = 0.1$ L/min, NMC = 1) exposure to the SMF during the pretreatment were investigated. The experimental design of S2 tests is shown in **Table 3.3**.

Table 3.3 - Design of anaerobic digestion tests with completely magnetized sludge (S2).

Test	Q (L/min)	TS (%)	NMC
A	10	5	10
B		2.5	
C	0.5	5	
D		2.5	
E	0.1	5	1
F		2.5	
Ctrl 1	-	5	-
Ctrl 2	-	2.5	-

The daily CH_4 production of each bioassay and control reactor was quantified 5 times/week. The concentrations of TAN, anions, TS, VS and COD were measured on

the feedstock after magnetization and on the final digestate. Moreover, after the pretreatment, a sample (100 mL) for each condition was collected for the solid-phase analysis.

3.2.4. Analytical methods

The daily CH_4 production was quantified with the water displacement method by using a two-column system: the first column was filled with a 15% NaOH solution to allow carbon dioxide trapping and it was connected at the top to a second column filled with tap water. The concentrations of COD, TS and VS were analyzed according to the Standard Methods [21]. The concentration of ammonium nitrogen ($N\text{-}NH_4^+$) was evaluated as total ammonium nitrogen (TAN), being the fraction of free ammonia nitrogen (FAN) negligible (< 0.5%) at the temperature and pH conditions of the sludge during pretreatment (**Supplementary Table 3.2**). TAN was determined by steam distillation followed by titration by a semi-automated distillation unit (UDK 132, VELP, Italy). The titrations were performed by using an automated titrator (TTT80 Radiometer, Copenhagen). VFA concentration was determined by high-performance liquid chromatography (HPLC) using a UVD 340U HPLC system (Dionex, Sunnyvale, CA, USA) equipped with a diode array detector and a Metrosep organic acid column 250/7.8 (Metrohm, Switzerland). Anionic concentrations were measured by ion chromatography (IC) as described by Di Capua et al. [22]. Magnesium concentration was measured by ICP-MS (Perkin Elmer Nexion 300, USA) operating in dual detector mode.

Mineralogical characterization of sewage sludge was performed by X-ray diffraction (XRD) analysis using a Philips diffractometer and Cu Kα radiation. For this purpose, films were prepared with the different samples using the Doctor Blade Coating technique. Once the films of material were obtained, they were dried in the air for a time sufficient to achieve a constant mass.

3.3. Results and discussion

3.3.1. Impact of high-intensity SMF pretreatment on the chemical composition of sewage sludge

The application of a 1.5 T SMF as pretreatment led to a decrease of the monitored ionic concentrations in the liquid phase of sewage sludge. Increasing the NMC from 1 to 10 during S1 pretreatment enhanced precipitation at both TS concentrations of 5% and 2.5%: in particular, all monitored ionic concentrations in the liquid phase decreased by 8–14.9% at NMC = 1 and 9.3–20.1% at NMC = 10 in the tests at 5%TS, while in the tests at 2.5%TS a 11.2–17.2% decrease was observed at NMC = 1 and a 14–31.4% decrease was observed at NMC = 10 (**Figure 3.2**).

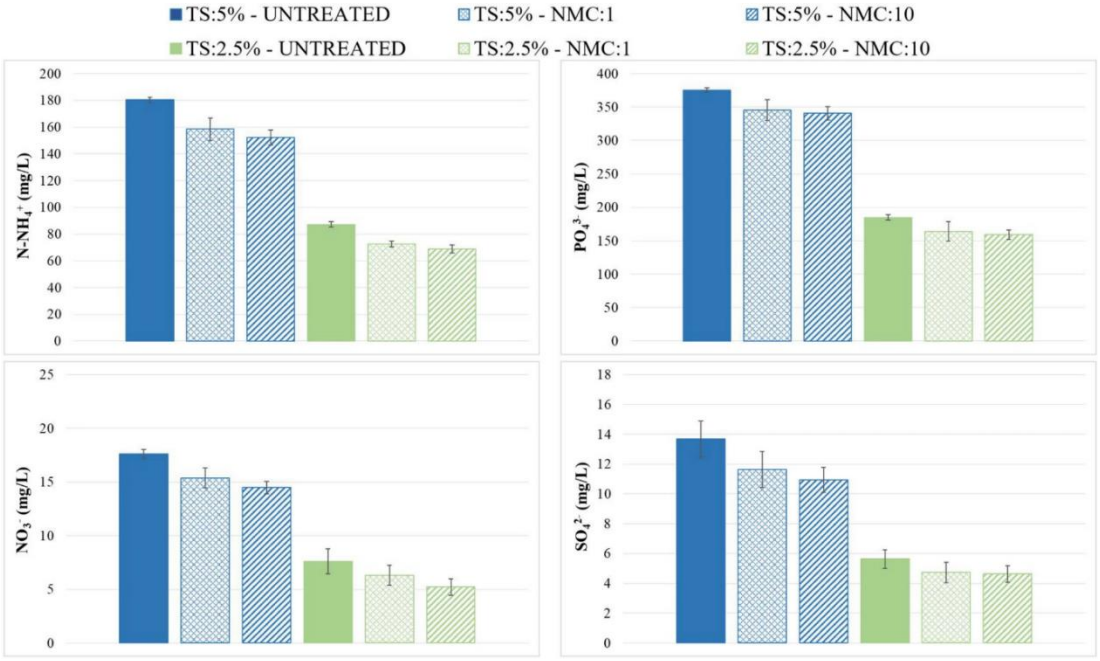

Figure 3.2 - Concentrations of NH_4^+, NO_3^-, PO_4^{3-} and SO_4^{2-} before and after SMF pretreatments in S1.

These results show that the increase of NMC increases the tendency of the ions to form new aggregates. However, no significant differences were observed in terms of solid concentration before and after the application of the SMF (**Supplementary Table 3.3**). It can be also observed that the highest reduction percentage of ionic concentration was obtained at 2.5%TS, which could be explained considering that the main effect of magnetic treatment consists in the associations of ionic species which are present in the solution, with consequent formation of precipitates, and this effect is more pronounced for solutions characterized by a lower ions concentration [23]. From this

point of view, the obtained results show that sewage sludge at 2.5%TS is a less complex matrix over which the impact of the SMF can be more effective compared to sludge at 5%TS.

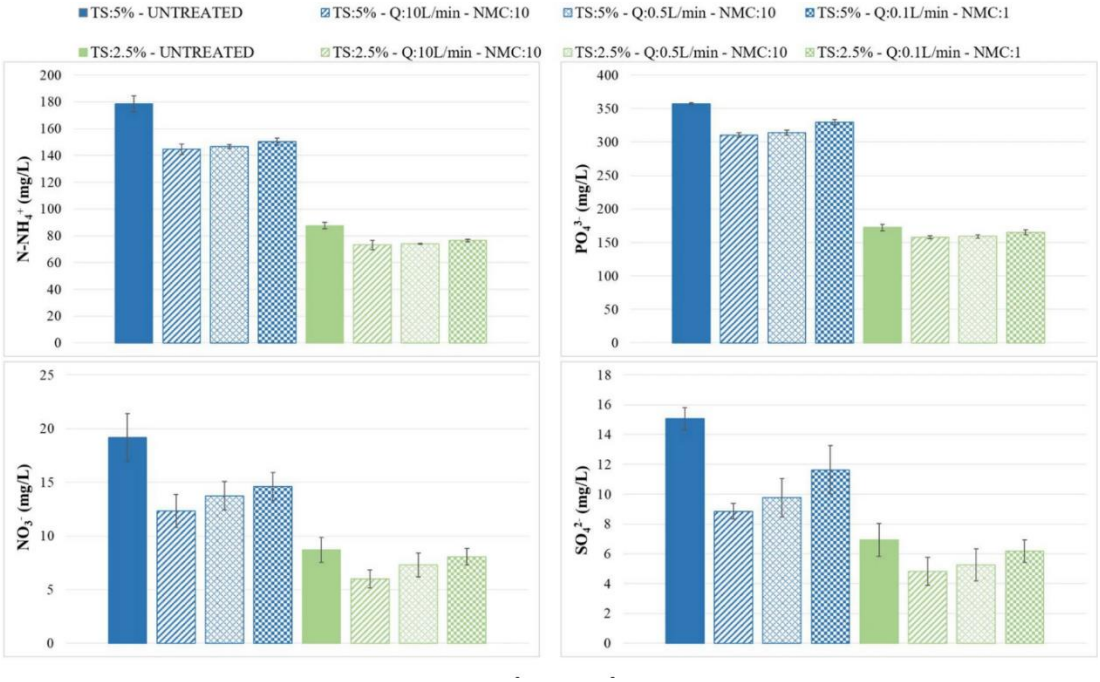

Figure 3.3 - Concentrations of NH_4^+, NO_3^-, PO_4^{3-} and SO_4^{2-} before and after SMF pretreatments in S2.

Figure 3.3 shows the data obtained from S2 tests. As observed during S1, increasing the NMC from 1 to 10 led to greater reductions of ionic concentrations at both of 5%TS and 2.5%TS. Moreover, results from S2 shows that increasing Q from 0.5 to 10 L/min at the same NMC enhanced the reduction of the ionic concentration in the liquid phase at both TS concentrations. Comparing the results obtained at Q = 10 L/min and NMC = 10 to those obtained at Q = 0.5 L/ min and NMC = 10, the difference in terms of NH_4^+, NO_3^-, PO_4^{3-} and SO_4^{2-} removal efficiency was 1.2%, 7.4%, 0.9%, 6.2%, respectively, in the tests a 5%TS, while in the tests at 2.5%TS this difference was respectively of 1.0%, 14.8%, 0.8%, 6.2%. S2 tests also include a condition of minimum exposure to the SMF (Q = 0.1 L/min, NMC = 1), which also resulted in a reduction of NH_4^+, NO_3^-, PO_4^{3-} and SO_4^{2-} concentrations respectively by 15.9%,

23.9%, 7.8% and 22.7% in the tests at 5%TS, and by 12.6%, 7.3%, 4.2% and 10.6% in the tests at 2.5%TS. However, these reductions were less pronounced than those obtained at higher Q and NMC values. These results indicate that increasing sewage sludge exposure to the applied high-intensity SMF promotes the precipitation of different ionic species, which is consistent with observations on S1 experiments. Similar results are reported in studies dealing with calcium carbonate precipitates in natural waters [23,24], where increasing the exposure of the treated matrix to the SMF resulted in an improved precipitation of calcium carbonate. Magnesium concentration was also monitored during S2 (**Figure 3.4**) to have an indication on the possible precipitation of struvite.

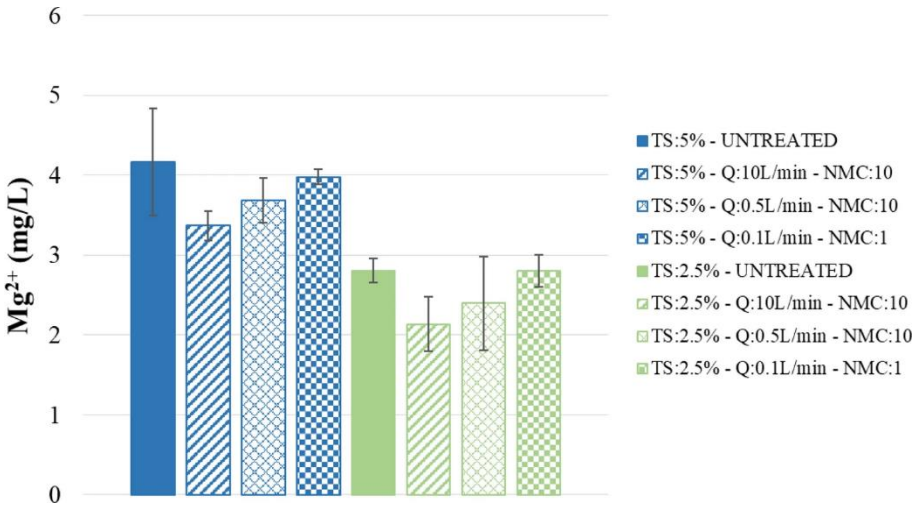

Figure 3.4 - Concentrations of Mg2+ before and after SMF pretreatments in S2.

Results indicate that, as already observed for the other ions, the higher reduction of Mg^{2+} in solution was obtained at the conditions of maximum exposure to the applied SMF (Q = 10 L/min, NMC = 10), resulting in aver- age reduction of Mg^{2+} concentration by 19.2% at 5%TS and by 23.9% at 2.5%TS, respectively.

3.3.2. Impact of the SMF on the solid phase of sewage sludge

A mineralogical characterization of the solid phase was carried out by XRD analysis to verify the co-precipitation of different crystalline phases due to the application of

the high-intensity SMF. **Figure 3.5** shows the XRD patterns of the solid phases related to S2 tests at 2.5%TS (**Figure 3.5a**) and 5%TS (**Figure 3.5b**).

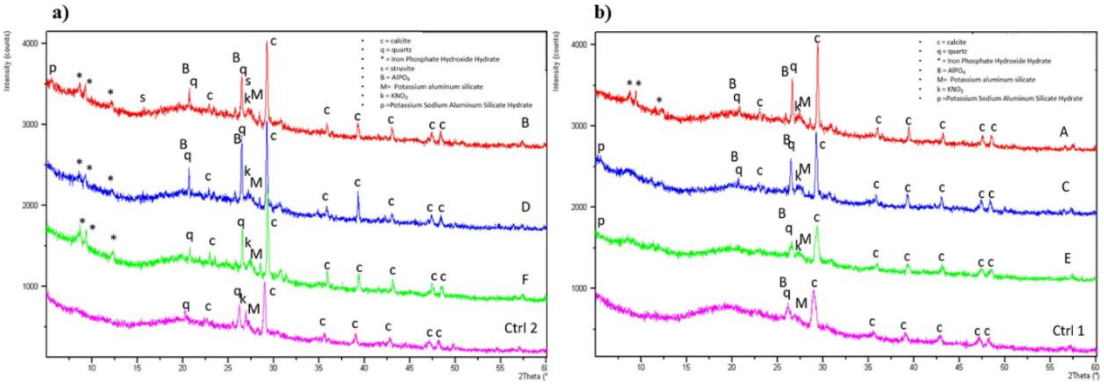

Figure 3.5 - XRD patterns for S2 tests (A–H) at a) 2.5%TS and b) 5%TS.

All samples show an amorphous band in the 2θ range equal to 15–35° due to the presence of an amorphous phase. Moreover, there are multiple diffraction peaks that can be associated with the co-presence of different crystalline phases. In particular, there are diffraction peaks of calcite ($CaCO_3$) [JPCDS card no. 1–72-1214] and quartz (SiO_2) [JPCDS card no. 1–83-2466], which were the main crystalline phases identified at both TS concentrations. Furthermore, there are other crystalline phases associable with phosphate precipitates, i.e., struvite ($MgNH_4PO_4 \cdot 6H_2O$) [JPCDS card no. 1–77-2303]), aluminum phosphate ($AlPO_4$) [JPCDS card no 1–76-226], iron phosphate ($Fe_3H_{8.5}O_{13.5}P_2$) [JPCDS card no 17–472], potassium phosphorus nitride sulfide ($K_6N_{14}P_{12}S_{12}$) [JPCDS card no 1–70-222]), iron nitrate hydrate ($Fe_4NO_3(OH)_{11} \cdot 2H_2O$) [JPCDS card no. 44–519], potassium nitrate (KNO_3) [JPCDS card no. 2–991]) and silicoaluminates ($KAlSi_3O_8$ [JPCDS card no. 1–84-1455], $Al_2H_2K_2Na_2O_8Si$ [JPCDS card no. 43–47]). As the peak area is proportional to the weight percentage of the corresponding crystalline phase, it can be observed that the amount of crystalline precipitates increases when exposure to the applied SMF increases (higher Q and NMC values). This effect is even more evident with the increase of the flow rate and, at the same flow rate, with the increase of the NMC, in agreement with the literature [23]. The application of the SMF to sewage sludge at 5%TS (**Figure 3.5b**) has determined effects similar to those verified at 2.5%TS in terms of type of precipitates, except for

struvite, being the related peaks more visible at 2.5%TS than at 5%TS. In general, peak intensities were slightly higher at 2.5%TS than at 5%TS. This is justified by the fact that the effect of the magnetic treatment on the precipitation process is more pronounced for solutions characterized by a lower concentration of ions. For this reason, to increase the quantity of precipitates in sewage sludge at high solid content it is necessary to increase the SMF intensity or sewage sludge exposure by applying higher values of Q and NMC [23].

3.3.3. Impact of the SMF on methane production

Figure 3.6 compares the cumulative CH_4 production obtained from the anaerobic digestion tests performed in S1.

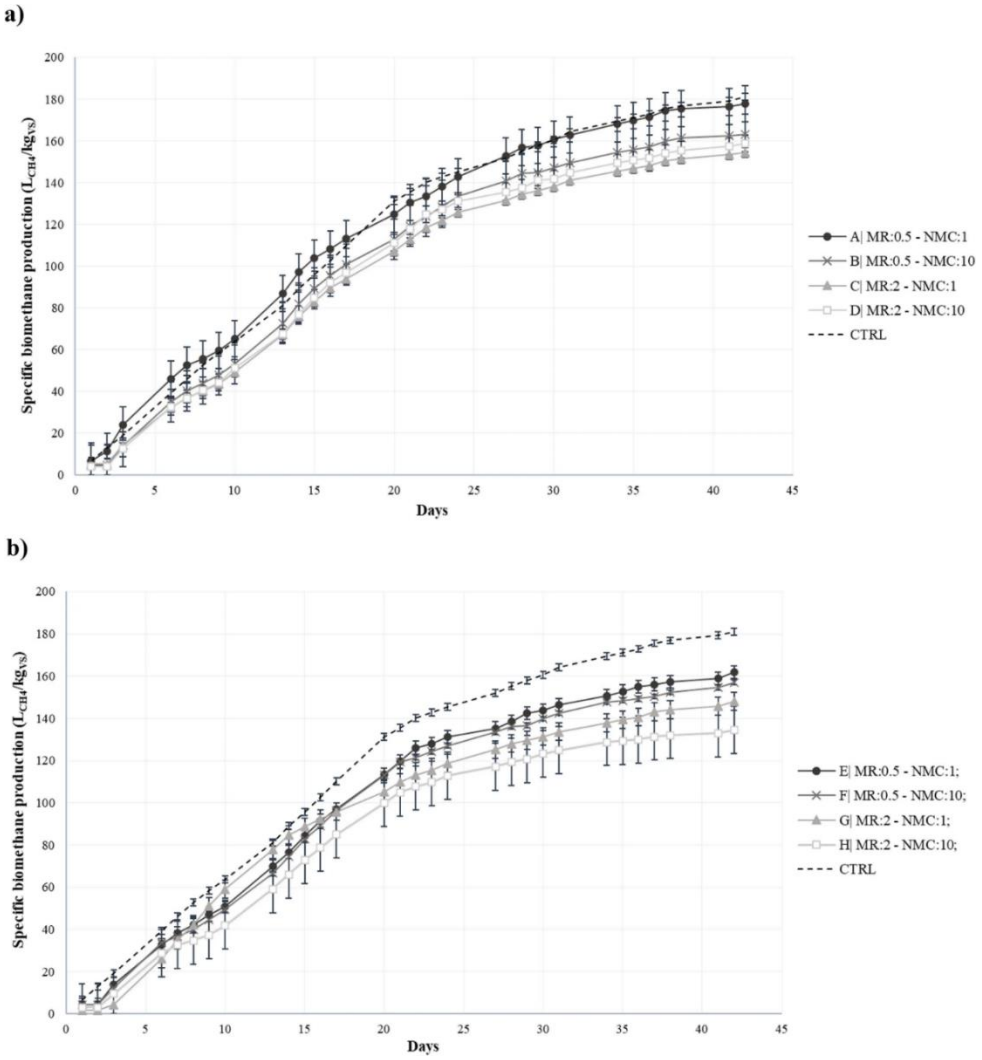

Figure 3.6 - Biomethane production of S1 tests at a) 5%TS and b) 2.5%TS.

Results show that the application of 1.5 T SMF negatively affected the CH_4 production. The highest CH_4 production of 181(±2) L_{CH4}/kg_{VS} was obtained with non-magnetized sludge (control test), while feeding the reactors with partially magnetized sludge resulted in 1.8–25.7% lower biomethane potential. The increase of MR decreased CH_4 production in all tests at similar TS concentration and NMC, e.g., at 2.5%TS and NMC = 1, only 135(±11) L_{CH4}/kg_{VS} was produced when the MR was 2 (test H), while methane production was 162(± 3) L_{CH4}/kg_{VS} (test E) at MR of 0.5. Observing the trend of the specific biomethane production (**Figure 3.6**), an initial lag-phase of 2 days can be observed for each production curve subjected to the application of the SMF. This suggests that, although resulting in lower methane generation, the high-intensity SMF is not lethal for micro-organisms. It is possible that the SMF induced an adaptive phase on the microbial community followed by the recovery of CH_4 production. Comparing the different final biomethane productions (**Supplementary Table 3.4**), slightly lower productions can be noted for the tests conducted at 2.5%TS compared to the tests conducted at 5%TS. This could be likely due to a lower intake of micro- and macro-nutrients available to microorganisms during the digestion process, which can be linked to the formation of precipitates discussed above and is in agreement with studies reported in the literature [25–27] highlighting that micro and macro nutrients are essential for the growth of microorganisms, to survive and carry out their cell metabolism. No significant effects of NMC were observed on CH_4 production at the tested values. Therefore, it can be concluded that the MR was the key parameter influencing CH_4 production of the magnetized sludge, as increasing the share of magnetized over non-magnetized sewage sludge negatively affected methane production. Nonetheless, the differences in methane generation at different MR values were not enormous due to the presence of a certain amount of non-magnetized sewage sludge. Magnetization produced no differences in terms of pH, as the pH of magnetized and non-magnetized sludge of S1 was the same (6.9±0.1) (**Supplementary Table 3.5**). Similarly, no significant differences due to magnetization were observed in the profiles and accumulation of VFA during the anaerobic digestion process (**Supplementary Figure 3.1**). Indeed, the maximum concentration of all VFA identified in S1 tests (acetic, propionic, butyric,

and citric) remained well below the inhibitory thresholds for methanogens [28]. Therefore, the detrimental impact of high-intensity magnetization to the anaerobic digestion process could depend on inhibition of bacterial growth due to direct impact of magnetic field [29,30] and/ or to the lack of micronutrients as discussed above. The results of anaerobic digestion tests performed in S2 confirmed the detrimental impact of magnetization, which was even more significant compared to S1 as anaerobic digestion reactors in S2 were loaded with the sole magnetized sludge under the selected operating conditions. **Figure 3.7** shows that the highest decrease of CH_4 production over the control bioreactors was observed in test A (24%) performed at the maximum exposure conditions (Q = 10 L/ min, NMC = 10), followed by C (22%) and E (9%) for the tests at 5%TS.

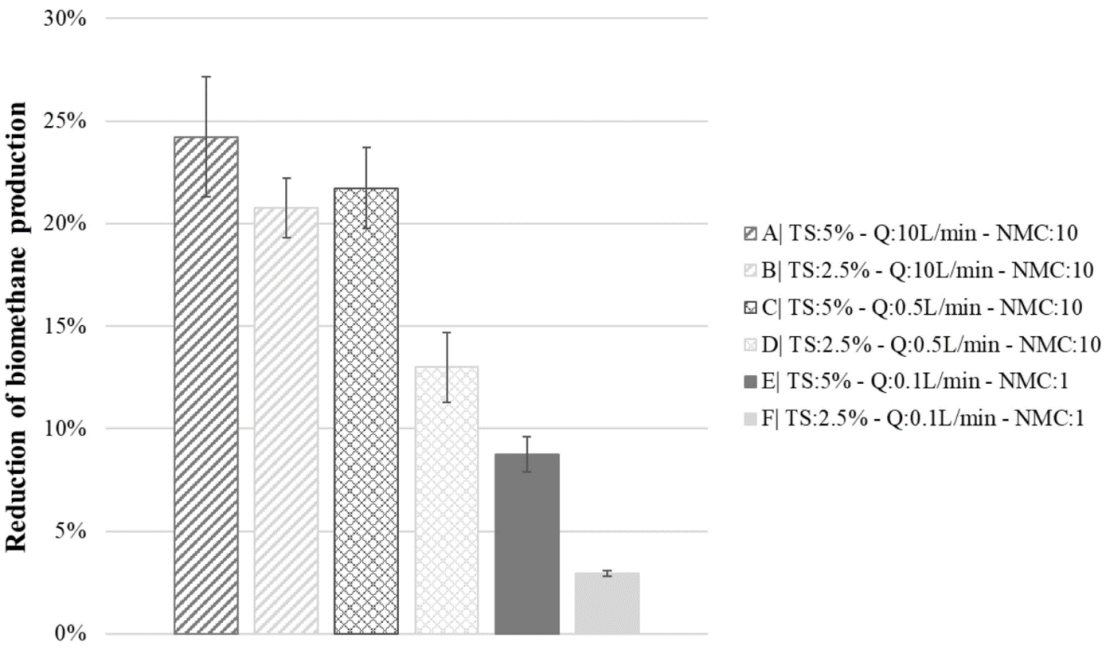

Figure 3.7 - Reduction in CH_4 production of anaerobic digestion tests in S2.

Similar results were obtained at 2.5%TS, as the maximum reduction was observed for test B (21%), followed by D (13%) and F (3%). These results further confirm that the greater is the exposure to the applied SMF, the lower is the production of CH_4. Furthermore, it can be observed that, under the same NMC, the greater reduction in CH_4 production was obtained when the applied Q was higher (A vs C and B vs D).

These results are in agreement with Mascolo [23], highlighting that the exposure to the magnetic field and the consequent induced effect is more evident at higher flow rates.

3.4. Practical implications and future research perspectives

Our study clearly indicates that the application of a high-intensity (1.5 T) SMF has a detrimental impact on anaerobic digestion in terms of methane production. However, this negative impact is reduced or even ruled out if sludge exposure to SMF is limited, i.e., when $Q \leq 0.1$ L/min, $MR \leq 0.5$ and $NMC = 1$ are applied for magnetization. Further research should elucidate the primary cause of anaerobic digestion inhibition following exposure to the high-intensity SMF. On the other hand, this study shows for the first time that applying a high-intensity SMF significantly reduces ionic concentrations in the sludge and leads to the precipitation of nutrient-based compounds with potential fertilizing properties such as struvite. This suggests a potential application of high-intensity magnetization on sewage sludge digestate, which could be exploited in a circular economy perspective. Indeed, agricultural application of hygienized sewage sludge is considered a best practice, as it couples the recycling of nutrients and organic matter and reduces landfilling of sewage sludge, resulting also in lower disposal costs for WWTPs [31]. By applying magnetization directly on the digestate, struvite precipitation could be promoted after digestion, avoiding accumulation within the digester and pumping systems. This work also shows that the TS content of sewage

sludge influences the extent of precipitation, which may reduce struvite crystallization when high-solid digestate, which is often applied in agriculture, is magnetized. Additional research should be carried out to investigate the impact of magnetization on the chemical composition of sewage sludge digestate and elucidate the impact of TS content on struvite precipitation in magnetized sludge.

3.5. Conclusions

This study explores the effects of a high-intensity (1.5 T) SMF on the composition and anaerobic digestion of sewage sludge was explored. The experimental results show

that the high-intensity SMF is disadvantageous for anaerobic digestion but promotes the precipitation of ionic species, including NH_4^+, NO_3^-, PO_4^{3-}, SO_4^{2-} and Mg^{2+}, and the generation of struvite. Higher exposure of sewage sludge to the SMF, provided by increasing Q, MR and NMC, resulted in the higher reduction of ionic concentrations in the liq- uid phase (up to 19.1% for NH_4^+, 35.7% for NO_3^-, 13% for PO_4^{3-}, 41.2% for SO_4^{2-} and 23.9% for Mg^{2+}) and in lower methane generation. The detrimental effect on anaerobic digestion could be due to an adverse impact of the high- intensity SMF on the structure/metabolism of bacterial com- munities as well as on the decreased availability of micro- and macro-nutrients in the liquid phase after magnetization. Notwithstanding the negative effects in terms of methane generation, experimental evidence seems promising when focused on the formation of precipitates: among others, the generation of struvite was, indeed, observed in this study in magnetized sewage sludge at low TS content (2.5%TS). This may be of strategic importance if the application of the SMF is considered as a post-treatment on ADS to improve its fertilizing properties. In this regard, further studies are necessary to better understand the mechanisms promoting the formation of target precipitates and consequently the recovery of valuable compounds according to the principles of circular economy and sustainable development.

3.7. Supplementary information

Supplementary Table 3.1 - Organic load in S1 and S2 tests.

Test	$kg_{VS}/m^3_{(S1)}$
Ctrl	37.9
A	37.9
B	
C	
D	
E	28.4
F	
G	22.7
H	

Test	$kg_{VS}/m^3_{(S2)}$
Ctrl 1	36.5
Ctrl 2	18.3
A	36.5
B	18.3
C	36.5
D	18.3
E	36.5
F	18.3

Supplementary Table 3.2 - Values of FAN of S1 tests (a) and S2 tests (b) calculated at T=293K. FAN is been calculated according to [1].

a)

	TAN (mg/L)	pH	FAN (mg/L)	$N\text{-}NH_4^+$ (mg/L)	% FAN/TAN	% $N\text{-}NH_4^+$/TAN
TS:5% - UNTREATED	180,4	6,9	0,5	179,8	0,3%	99,7%
TS:5% - NMC:1	158,4	6,9	0,5	157,9	0,3%	99,7%
TS:5% - NMC:10	152,1	6,8	0,4	151,7	0,3%	99,7%
TS:2.5% - UNTREATED	87,2	6,9	0,3	86,9	0,3%	99,7%
TS:2.5% - NMC:1	72,6	7,0	0,3	72,3	0,4%	99,6%
TS:2.5% - NMC:10	68,8	6,9	0,2	68,6	0,3%	99,7%

b)

	TAN (mg/L)	pH	FAN (mg/L)	$N\text{-}NH_4^+$ (mg/L)	% FAN/TAN	% $N\text{-}NH_4^+$/TAN
TS:5% - UNTREATED	178,7	7,0	0,7	178,0	0,4%	99,6%
TS:5% - Q:10L/min - NMC:10	144,6	6,9	0,4	144,1	0,3%	99,7%
TS:5% - Q:0.5L/min - NMC:10	146,8	6,9	0,5	146,3	0,3%	99,7%
TS:5% - Q:0.1L/min - NMC:1	150,3	6,9	0,5	149,8	0,3%	99,7%
TS:2.5% - UNTREATED	87,6	7,0	0,3	87,2	0,4%	99,6%
TS:2.5% - Q:10L/min - NMC:10	73,2	6,9	0,2	73,0	0,3%	99,7%
TS:2.5% - Q:0.5L/min - NMC:10	74,1	6,9	0,3	73,8	0,3%	99,7%
TS:2.5% - Q:0.1L/min - NMC:1	76,5	6,9	0,3	76,2	0,3%	99,7%

Supplementary Table 3.3 - TS, VS before and after SMF treatment.

		TS (%)	VS (%)
S1	BEFORE SMF TREATMENT	5.0±0.2	3.8±0.3
	AFTER SMF TREATMENT	5.1±0.1	3.8±0.3
S2	BEFORE SMF TREATMENT	4.9±0.2	3.6±0.2
	AFTER SMF TREATMENT	4.9±0.2	3.7±0.3

Supplementary Table 3.4 - Biomethane production of S1 tests.

Test	Q (L/min)	TS (%)	NMC	Biomethane production (L_{CH4}/kg_{VS})
Ctrl	-	5	-	181±2
A	0.5	5	1	178±9
B			10	163±10
C			1	155±2
D			10	159±4
E		2.5	1	162±3

F			10	157±1
G			1	148±4
H			10	135±11

Supplementary Table 3.5 - pH of magnetized and non-magnetized sludge of S1.

Test	Q (L/min)	TS (%)	NMC	pH
Ctrl	-	5	-	6.87±0.08
A	0.5	5	1	6.94
B			10	6.87
C			1	6.85
D			10	6.81
E		2.5	1	6.98
F			10	6.92
G			1	6.98
H			10	6.86

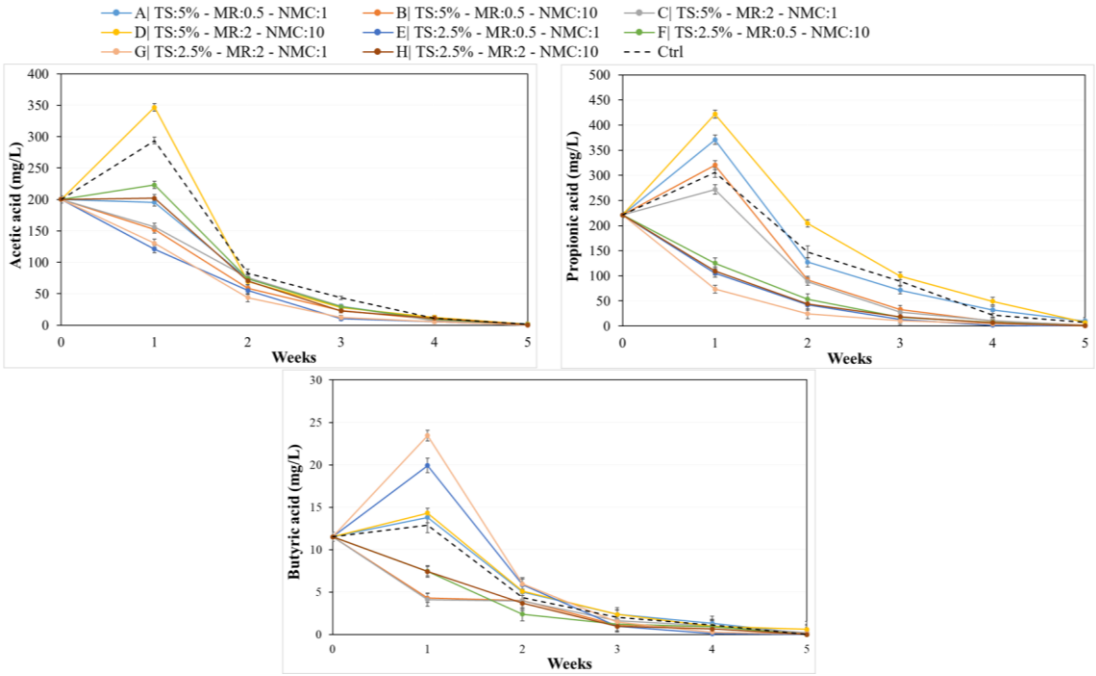

Supplementary Figure 3.1 – Evolution of VFA concentration in S1 tests.

3.7. References

[1] F. Di Capua, D. Spasiano, A. Giordano, F. Adani, U. Fratino, F. Pirozzi, G. Esposito, High-solid anaerobic digestion of sewage sludge: challenges and opportunities, Appl. Energy. 278 (2020) 115608. https://doi.org/10.1016/j.apenergy.2020.115608.

[2] F. Di Capua, F. Adani, F. Pirozzi, G. Esposito, A. Giordano, Air side-stream ammonia stripping in a thin film evaporator coupled to high-solid anaerobic digestion of sewage sludge: Process performance and interactions, J. Environ. Manage. 295 (2021) 113075. https://doi.org/10.1016/j.jenvman.2021.113075.

[3] S. Pilli, P. Bhunia, S. Yan, R.J. LeBlanc, R.D. Tyagi, R.Y. Surampalli, Ultrasonic pretreatment of sludge: A review, Ultrason. Sonochem. 18 (2011) 1–18. https://doi.org/10.1016/j.ultsonch.2010.02.014.

[4] H. Carrère, C. Dumas, A. Battimelli, D.J. Batstone, J.P. Delgenès, J.P. Steyer, I. Ferrer, Pretreatment methods to improve sludge anaerobic degradability: A review, J. Hazard. Mater. 183 (2010) 1–15. https://doi.org/10.1016/j.jhazmat.2010.06.129.

[5] C. Bougrier, J.P. Delgenès, H. Carrère, Combination of thermal treatments and anaerobic digestion to reduce sewage sludge quantity and improve biogas yield, Process Saf. Environ. Prot. 84 (2006) 280–284. https://doi.org/10.1205/psep.05162.

[6] I. Ferrer, S. Ponsá, F. Vázquez, X. Font, Increasing biogas production by thermal (70 °C) sludge pre-treatment prior to thermophilic anaerobic digestion, Biochem. Eng. J. 42 (2008) 186–192. https://doi.org/10.1016/j.bej.2008.06.020.

[7] B. Otieno, S. Apollo, J. Kabuba, B. Naidoo, G. Simate, A. Ochieng, Ozonolysis pre-treatment of waste activated sludge for solubilization and biodegradability enhancement, J. Environ. Chem. Eng. 7 (2019) 1–8. https://doi.org/10.1016/j.jece.2019.102945.

[8] J. Merrylin, S.A. Kumar, S. Kaliappan, I.-T. Yeom, J.R. Banu, Biological pretreatment of non-flocculated sludge augments the biogas production in the anaerobic digestion of the pretreated waste activated sludge, Environ. Technol.

34 (2013) 2113–2123. https://doi.org/10.1080/09593330.2013.810294.

[9] R. Morello, F. Di Capua, L. Pontoni, S. Papirio, D. Spasiano, U. Fratino, F. Pirozzi, G. Esposito, Microaerobic digestion of low-biodegradable sewage sludge: Effect of air dosing in batch reactors, Sustain. 13 (2021) 1–11. https://doi.org/10.3390/su13179869.

[10] A. Giordano, F. Di Capua, G. Esposito, F. Pirozzi, Long-term biogas desulfurization under different microaerobic conditions in full-scale thermophilic digesters co-digesting high-solid sewage sludge, Int. Biodeterior. Biodegrad. 142 (2019) 131–136. https://doi.org/10.1016/j.ibiod.2019.05.017.

[11] M. Zielinski, M. Debowski, J. Kazimierowicz, The effect of static magnetic field on methanogenesis in the anaerobic digestion of municipal sewage sludge, Energies. 14 (2021). https://doi.org/10.3390/en14030590.

[12] M. Zieliński, M. Zielińska, A. Cydzik-Kwiatkowska, P. Rusanowska, M. Dębowski, Effect of static magnetic field on microbial community during anaerobic digestion, Bioresour. Technol. 323 (2021). https://doi.org/10.1016/j.biortech.2020.124600.

[13] M. Zieliński, P. Rusanowska, M. Dębowski, A. Hajduk, Influence of static magnetic field on sludge properties, Sci. Total Environ. 625 (2018) 738–742. https://doi.org/10.1016/j.scitotenv.2017.12.226.

[14] C. Niu, J. Geng, H. Ren, L. Ding, K. Xu, W. Liang, The strengthening effect of a static magnetic field on activated sludge activity at low temperature, Bioresour. Technol. 150 (2013) 156–162. https://doi.org/10.1016/j.biortech.2013.08.139.

[15] J. Filipič, B. Kraigher, B. Tepuš, V. Kokol, I. Mandic-Mulec, Effects of low-density static magnetic fields on the growth and activities of wastewater bacteria Escherichia coli and Pseudomonas putida, Bioresour. Technol. 120 (2012) 225–232. https://doi.org/10.1016/j.biortech.2012.06.023.

[16] L. Hou, Y. Liu, S. Fan, J. Li, Magnetic field enhanced denitrification efficiency of immobilized bacterial particles, Water Sci. Technol. 81 (2020) 622–629. https://doi.org/10.2166/WST.2020.156.

[17] L. Dini, L. Abbro, Bioeffects of moderate-intensity static magnetic fields on

cell cultures, Micron. 36 (2005) 195–217. https://doi.org/10.1016/j.micron.2004.12.009.

[18] A. Yadollahpour, S. Rashidi, Z. Ghotbeddin, M. Jalilifar, Z. Rezaee, Electromagnetic fields for the treatments of wastewater: A review of applications and future opportunities, J. Pure Appl. Microbiol. 8 (2014) 3711–3719.

[19] M. Krzemieniewski, M. Dębowski, W. Janczukowicz, J. Pesta, Effect of the constant magnetic field on the composition of dairy wastewater and domestic sewage, Polish J. Environ. Stud. 13 (2004) 45–53.

[20] F. Di Capua, S. de Sario, A. Ferraro, A. Petrella, M. Race, F. Pirozzi, U. Fratino, D. Spasiano, Phosphorous removal and recovery from urban wastewater: Current practices and new directions, Sci. Total Environ. 823 (2022) 153750. https://doi.org/10.1016/j.scitotenv.2022.153750.

[21] A.P.H.A. American Public Health Association, A.W.W.A. American Water Works Association, W.E.F. Water Environment Federation, Standard Methods for the Examination of Water and Wastewater, 24th ed., APHA Press, Washington DC, 2023.

[22] F. Di Capua, M.C. Mascolo, F. Pirozzi, G. Esposito, Simultaneous denitrification, phosphorus recovery and low sulfate production in a recirculated pyrite-packed biofilter (RPPB), Chemosphere. 255 (2020) 126977. https://doi.org/10.1016/j.chemosphere.2020.126977.

[23] M.C. Mascolo, Effect of magnetic field on calcium carbonate precipitated in natural waters with prevalent temporary hardness, J. Water Process Eng. 41 (2021) 102087. https://doi.org/10.1016/j.jwpe.2021.102087.

[24] S. Kobe, G. Dražić, A.C. Cefalas, E. Sarantopoulou, J. Stražišar, Nucleation and crystallization of CaCO3 in applied magnetic fields, Cryst. Eng. 5 (2002) 243–253. https://doi.org/10.1016/S1463-0184(02)00035-7.

[25] Y.Y. Choong, I. Norli, A.Z. Abdullah, M.F. Yhaya, Impacts of trace element supplementation on the performance of anaerobic digestion process: A critical review, Bioresour. Technol. 209 (2016) 369–379. https://doi.org/10.1016/j.biortech.2016.03.028.

[26] B.C. Maharaj, M.R. Mattei, L. Frunzo, E.D. van Hullebusch, G. Esposito, A general framework to model the fate of trace elements in anaerobic digestion environments, Sci. Rep. 11 (2021) 1–19. https://doi.org/10.1038/s41598-021-85403-2.

[27] P.M. Thanh, B. Ketheesan, Z. Yan, D. Stuckey, Trace metal speciation and bioavailability in anaerobic digestion: A review, Biotechnol. Adv. 34 (2016) 122–136. https://doi.org/10.1016/j.biotechadv.2015.12.006.

[28] Y. Wang, Y. Zhang, J. Wang, L. Meng, Effects of volatile fatty acid concentrations on methane yield and methanogenic bacteria, Biomass and Bioenergy. 33 (2009) 848–853. https://doi.org/10.1016/j.biombioe.2009.01.007.

[29] Y. Ji, Y. Wang, J. Sun, T. Yan, J. Li, T. Zhao, X. Yin, C. Sun, Enhancement of biological treatment of wastewater by magnetic field, Bioresour. Technol. 101 (2010) 8535–8540. https://doi.org/10.1016/j.biortech.2010.05.094.

[30] S. Mousavian-Roshanzamir, A. Makhdoumi-Kakhki, The Inhibitory Effects of Static Magnetic Field on Escherichia coli from two Different Sources at Short Exposure Time., Reports Biochem. Mol. Biol. 5 (2017) 112–116.

[31] N. Di Costanzo, A. Cesaro, F. Di Capua, G. Esposito, Exploiting the nutrient potential of anaerobically digested sewage sludge: A review, Energies. 14 (2021) 1–25. https://doi.org/10.3390/en14238149.

CHAPTER 4

Application of high-intensity static magnetic field as a strategy to enhance the fertilizing potential of sewage sludge digestate

The content of this chapter has been published as:

N. Di Costanzo, A. Cesaro, F. Di Capua, M.C. Mascolo, G. Esposito, Application of high-intensity static magnetic field as a strategy to enhance the fertilizing potential of sewage sludge digestate, Waste Manag. 170 (2023) 122–130. https://doi.org/10.1016/j.wasman.2023.08.005.

Abstract

This chapter aims to determine the effects of a high-intensity static magnetic field (SMF) (1.5 and 2 T) on the chemical composition of sewage sludge anaerobic digestate. Several strategies (i.e., number of magnetization cycles, addition of different sources and quantities of magnesium, and digestate aeration) have been applied to evaluate the possible formation of compounds with valuable fertilizing properties in the digestate. The proposed results highlight that SMF application can increase the fertilizing potential of sewage sludge digestate and promote its valorization in a sustainable and circular perspective.

4.1. Introduction

Sewage sludge management has recently become a key task for wastewater treatment plant operation due to a considerable increase in sludge production, high disposal costs (160–210 €/t dry matter), and other many legal, social, and environmental constraints [1]. Different sludge management choices are practiced globally including landfills, biological stabilization, incineration, pyrolysis, and gasification. In this framework, anaerobic digestion (AD) is certainly one of the most sustainable technologies to transform sewage sludge into renewable energy and a fertilizer. AD generates a gaseous (biogas) and a semi-solid product (digestate), the first being an energy vector which can be upgraded to biomethane, the second being a material that can be valorised in agriculture as a valuable source of nutrients [2,3]. During AD, the biological degradation of the organic matter contained in the sludge increases the concentration of soluble nutrients species, i.e., total ammonia nitrogen and ortho-phosphate (PO_4^{3-}), which are nutrient compounds that can be rapidly assimilated by plants for their growth.

Among the strategies reported for nutrient recovery [4] reusing sewage sludge digestate as a fertilizer fits the circular economy approach and has several advantages, which include the return of the organic materials and nutrients into the bio-cycle [5,6]. Indeed, the agronomic use of sludge-derived digestate has demonstrated to increase the portion of organic carbon in the soil, contributing to the improvement of its agronomic quality [7]. Moreover, the application of sludge digestate in agriculture

allows reducing the demand for chemical fertilizers and, in turn, the related costs for farmers. In the context of sewage sludge valorization, the high-solid anaerobic digestion (HSAD) represents an opportunity to improve the economical balance compared to conventional AD as it reduces treatment volumes, transportation costs, and energy consumption for heating, and generates a digestate with very good agronomic properties and hygienic properties [8,9]. From this point of view, HSAD can be considered the most sustainable pathway for the reuse of nutrients contained in sewage sludge.

A possible strategy to further enhance the agricultural properties of sewage sludge digestate is to promote the precipitation of valuable compounds, such as struvite and hydroxyapatite, that can effectively and slowly release the nutrients contained in the digestate to the soil [2]. In this way, plants can uptake the released nutrients more efficiently and the risk of nutrient overload and groundwater contamination can be reduced as well. Among the agronomic compounds of greatest interest, there is the struvite, a crystalline mineral composed of equimolar concentrations of magnesium (Mg^{2+}), ammonium (NH_4^+) and PO_4^{3-} with chemical formula $MgNH_4PO_4 \cdot 6H_2O$. Specifically, struvite is considered a valid fertilizing product because it contains essential nutrients for plant growth, which are slowly released into the soil due to its low solubility, thus limiting potentially harmful overdose phenomena [10]. Struvite precipitation depends on several parameters, i.e. most notably pH, Mg^{2+} source, and the molar ratio of Mg^{2+}, NH_4^+ and PO_4^{3-} in the liquid phase [11]. During AD of sewage sludge, struvite may precipitate spontaneously from the interaction of the mineralized Mg^{2+}, NH_4^+ and PO_4^{3-} originating from the degradation of organic material [12]. However, in practice, struvite precipitation needs a chemical input in the form of additional Mg^{2+}, being typically the limiting compound, and alkali for pH adjustment [13], both translating into high operational costs [14]. Previous studies have shown that other mineral phases containing macro- and micro-nutrients (such as newberyite, gwihabaite, brushite and potassium calcium magnesium sulphate) can improve of agronomic characteristics of soils [15,16]. Besides supplying essential nutrients for plant growth, these mineral phases possess a low/moderate solubility that leads to a

slow release of nutrients to the soil and mitigates the negative impact of fertilizers on the environment (e.g., leaching to groundwater) [17,18].

In this context, there is a legitimate need to seek alternative, prospective, and competitive methods enhancing the formation of struvite and other valuable precipitates in sewage sludge. Recent research has demonstrated that the application of high-intensity static magnetic field (SMF) can represent a novel option. The SMF has often been applied to reduce water hardness [19] by promoting the precipitation of ionic species and, more recently, Di Costanzo et al. [20] reported that it can be used as sewage sludge pretreatment to promote the precipitation of compounds with fertilizing properties, including struvite. On the other hand, applying strong SMF as sewage sludge pretreatment was shown to reduce methane production during the subsequent AD process [20]. In this perspective, applying the high-intensity SMF directly to the digestate can circumvent the negative impacts on methane generation during AD. Moreover, the precipitation effect induced by the SMF might be further improved under certain operating conditions, including those exploiting the paramagnetism of the oxygen molecule. Paramagnetism is the property observed when certain substances, whose molecules possess their own magnetic dipole moment, are immersed in a magnetic field. In the case of air, the paramagnetic effect is at the expense of the oxygen molecule, which possesses split electron doublets in its outer orbitals and makes it affine to the magnetic field. Unpaired electrons, when exposed to magnetic fields, align themselves with the field lines and amplify the effect of the magnetic field. Another strategy to improve the SMF effects may rely on the disturbance of the magnetic field flux lines, which in turn converts the magnetic fields from uniform to non-uniform. Both these strategies (i.e., the exploitation of the oxygen paramagnetism and the magnetic field disturbance) can be obtained by adding oxygen during the magnetization of sewage sludge digestate, thus enhancing the SMF effect and likely promoting the precipitation of valuable compounds.

Currently, literature lacks information regarding the impact of the SMF on the chemical composition of sewage sludge digestate. Similarly, no information regarding oxygen contribution to nutrient precipitation during SMF application is available. In this context, the present study explored for the first time the direct effects of high-

intensity SMF on the chemical properties of digestates originating from both AD and HSAD of sewage sludge. More specifically, the effects of magnetic exposure, amount and source of Mg^{2+}, and presence of oxygen during magnetization on the precipitation of valuable nutrients in the digestate were investigated at laboratory scale. The outcomes of this study were discussed with the aim to identify practical applications of the proposed methodology to improve nutrient recycling from sludge to agriculture and promote the use of alternatives to chemical fertilizers, thereby limiting the depletion of valuable resources as well as fertilization costs.

4.2. Materials and Methods

4.2.1 Origin and composition of sewage sludge digestate

Two different digestates obtained from HSAD and AD of sewage sludge were used in this study. The digestate from HSAD was provided by the "Acqua & Sole" digestion plant located in Lombardy Region (Italy) treating a high-solid feedstock (about 18.5 %), mainly composed of municipal sewage sludge. The plant performs a thermophilic (55 °C) HSAD process in three digesters (4,500 m^3 each) displaced in series. The digestate from AD was collected at the wastewater treatment plant (WWTP) of Mercato San Severino (Italy) that treats wastewater of predominantly municipal origin and, to a lesser extent, industrial wastewater. In this WWTP, sewage sludge is bio-stabilized via a conventional AD process operated under mesophilic conditions (35 °C). Both kinds of digestate were collected during two sampling campaigns (I and II) from the lower withdrawal point of both the HSAD and AD digesters, placed in plastic containers, and transported to the laboratory, where they were stored at 4°C until use. Prior to magnetic treatment, the HSAD digestate was diluted from a total solids (TS) content of 12 % to 7 %, to ensure the pumping within the magnetization circuit. **Table 4.1** lists the main characteristics of the digestates used for the experiments.

Table 4.1 - Characteristics of the digestates used for the experiments.

Parameter	**Unit**	**Digestate from HSAD**		**Digestate from AD**	
Sampling campaign		I	II	I	II
pH	-	8.3±0.3	8.1±0.1	6.8±0.1	6.8±0.2
Total solids (TS)	%	7.0±0.1	7.0±0.1	2.1±0.1	2.5±0.2

Volatile solids (VS)	%	3.7±0.2	3.7±0.1	1.0±0.1	1.5±0.2
NH_4^+	mg/L	510±2	329±1	283±1	296±1
PO_4^{3-}	mg/L	187±1	203±4	213±2	235±2
Nitrate (NO_3^-)	mg/L	38±1	40±1	9±0	11±0
Sulphate (SO_4^{2-})	mg/L	21±1	23±0	22±1	24±0
Mg^{2+}	mg/L	20±0	19±0	10±0	10±0
Mg^{2+}:NH_4^+:PO_4^{3-}	-	0.04:1:0.36	0.06:1:0.62	0.03:1:0.75	0.03:1:0.79

4.2.2 Experimental set-up for the magnetic treatment of digestates

Two SMF intensities, i.e., 1.5 T and 2 T, were applied to the sludge digestate samples. The SMF was generated by a patented Purak magnetic polarizer provided by AMS company (Italy) as described by Mascolo (2021). The magnetic polarizer was installed on a circuit made with a plastic tube (diameter = 1.5 cm) and connected to a submersible water pump (Comet, USA) as illustrated by Di Costanzo et al. [20].

4.2.3. Experimental design

To assess the impact of the high-intensity SMF, the following operating conditions were investigated: SMF intensity; number of magnetization cycles (NMC), which is the number of digestate passages within the magnetic polarizer; Mg^{2+}:NH_4^+:PO_4^{3-} molar ratio, which was varied by adding Mg^{2+} either as hydroxide ($Mg(OH)_2$) or as chloride hexahydrate ($MgCl_2 \cdot 6H_2O$), as well as PO_4^{3-} as phosphoric acid (H_3PO_4), to promote the precipitation of struvite; digestate aeration, under two alternative configurations (**Figure 4.1**). In the first one, air was supplied through an aquarium pump equipped with a porous stone directly into the sewage sludge digestate feeding tank (**Figure 4.1a**); in the second one, air was supplied directly within the magnetization circuit (*in-line oxygenation*) (**Figure 4.1b**). The first strategy was chosen to take advantage of the paramagnetic effect of the oxygen molecule. Specifically, the digestate saturated in oxygen and circulating in the polarizer is subjected to local increases of SMF intensity. Conversely, the in-line oxygenation strategy was considered to evaluate both the effect induced by the paramagnetism of the oxygen molecule and the effect of the airflow turbulence during the SMF application, which was expected to modify the magnetic field from uniform to non-uniform.

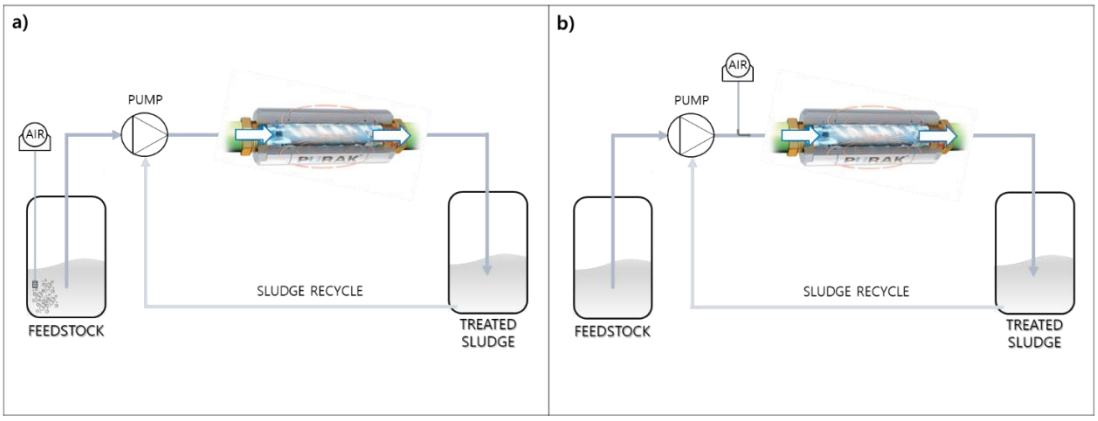

Figure 4.1 - Scheme of the experimental set-up for the magnetic treatment of digestates using direct air injection into the supply tank (a) or in-line aeration (b).

Two experimental phases i.e., phase 1 (P1) and phase 2 (P2), were carried out as detailed in **Table 4.2**. In P1 tests, the effect of a 1.5 T SMF on the digestates was evaluated at NMCs of 10 and 30 and Mg^{2+}:NH_4^+:PO_4^{3-} molar ratios of 1:1:1, 1.5:1:1 and 2:1:1. In order to assess the effect of Mg^{2+} source on precipitation, P1 tests on HSAD digestate were conducted twice, using initially $Mg(OH)_2$ and then $MgCl_2 \cdot 6H_2O$. In all tests, the pH was maintained around 8-9 dosing a 3M potassium hydroxide (KOH) solution after Mg^{2+} addition. For P1 tests, the flow rate Q of the digestate within the magnetization circuit was maintained constant at 10 L/min and no aeration was performed.

Table 4.2 - Design of P1 and P2 tests.

Experimental phase	Test	NMC	Mg^{2+}:NH_4^+:PO_4^{3-}	Mg^{2+} source	SMF intensity (T)	Qair (L/min)
P1	A	10	-	-	1.5	-
P1	B	30	-	-	1.5	-
P1	C	10	1:1:1	$Mg(OH)_2$ or $MgCl_2 \cdot 6H_2O$	1.5	-
P1	D	30	1:1:1	$Mg(OH)_2$ or $MgCl_2 \cdot 6H_2O$	1.5	-
P1	E	10	1.5:1:1	$Mg(OH)_2$ or $MgCl_2 \cdot 6H_2O$	1.5	-

P1	F	30	1.5:1:1	$Mg(OH)_2$ or $MgCl_2 \cdot 6H_2O$	1.5	-
P1	G	10	2:1:1	$Mg(OH)_2$ or $MgCl_2 \cdot 6H_2O$	1.5	-
P1	H	30	2:1:1	$Mg(OH)_2$ or $MgCl_2 \cdot 6H_2O$	1.5	-
P2	I	10	-	-	2	-
P2	J	30	-	-	2	-
P2	K	10	2:1:1	$MgCl_2 \cdot 6H_2O$	2	-
P2	L	30	2:1:1	$MgCl_2 \cdot 6H_2O$	2	-
P2	M	10	2:1:1	$MgCl_2 \cdot 6H_2O$	2	5
P2	N	30	2:1:1	$MgCl_2 \cdot 6H_2O$	2	5

In the second experimental phase (P2), digestate exposure to a higher SMF (2 T) was tested at NMCs of 10 and 30, using $MgCl_2 \cdot 6H_2O$ and maintaining the optimal Mg^{2+}:NH_4^+:PO_4^{3-} molar ratio of 2:1:1 obtained from P1 tests; these experimental settings were tested without aeration as well as by supplying an air flow rate of 5 L/min. Both in P1 and P2 control tests were carried out (test A and B in P1, test I and J in P2), i.e., tests in which the digestate was only magnetized.

After each treatment, the magnetized sludge was analysed in terms of nutrient (N, P) concentrations and the precipitates in the solid phase were identified to evaluate the effects of the applied SMF conditions on the generation of nutrient-based compounds with potential fertilizing properties.

4.2.4. Analytical methods

The concentrations of COD, TS and VS were analysed according to the Standard Methods [21]. NH_4^+ concentration was determined spectrophotometrically using the indophenol blue method [22]. Anionic concentrations were measured by ion chromatography (IC) as described by Di Capua et al. [23]. Mg^{2+} concentration was measured by ICP-MS (Perkin Elmer Nexion 300, USA) operating in dual detector mode. The mineralogical characterization of the digestates was performed by X-ray diffraction (XRD) analysis as reported by Di Costanzo et al. [20].

4.2.5. Statistical analysis

Statistical comparison of the reported data from the control and each samples under the different treatment conditions were compared by one-way analysis of variance (ANOVA) followed by the Tukey post hoc test [24,25]. All analyses were performed with Minitab 17 Statistical Software (Minitab LCC, USA), where a difference marked with a p-value lower than 0.05 was considered statistically significant.

4.3. Results and discussions

4.3.1. Impact of magnetization conditions on ionic precipitation in HSAD and AD digestates

4.3.1.1. SMF intensity and NMC

The exposure of the HSAD digestate to a high-intensity SMF led to a reduction of the monitored ionic concentrations in the liquid phase. At a SMF of 1.5 T, all monitored ionic concentrations decreased by 5-16 % at NMC = 10 and by 8-23 % at NMC = 30, indicating that increasing the NMC from 10 to 30 enhanced precipitation (**Figure 4.2a**). These results are in line with those outlined in a previous work [20], showing that increasing the NMC from 1 to 10 at a SMF of 1.5 T enhanced the reduction of ionic species in the liquid phase of pre-thickened sludge up to 20 %. These results further confirm that an NMC increase amplifies the SMF effect in terms of precipitation efficiency. A higher reduction in the concentration of ionic species was observed at a SMF intensity of 2 T both at an NMC of 10 (6-18%) and 30 (9-25%). This indicates that increasing the SMF intensity from 1.5 to 2 T had a significant impact on enhancing nutrient precipitation from HSAD digestate.

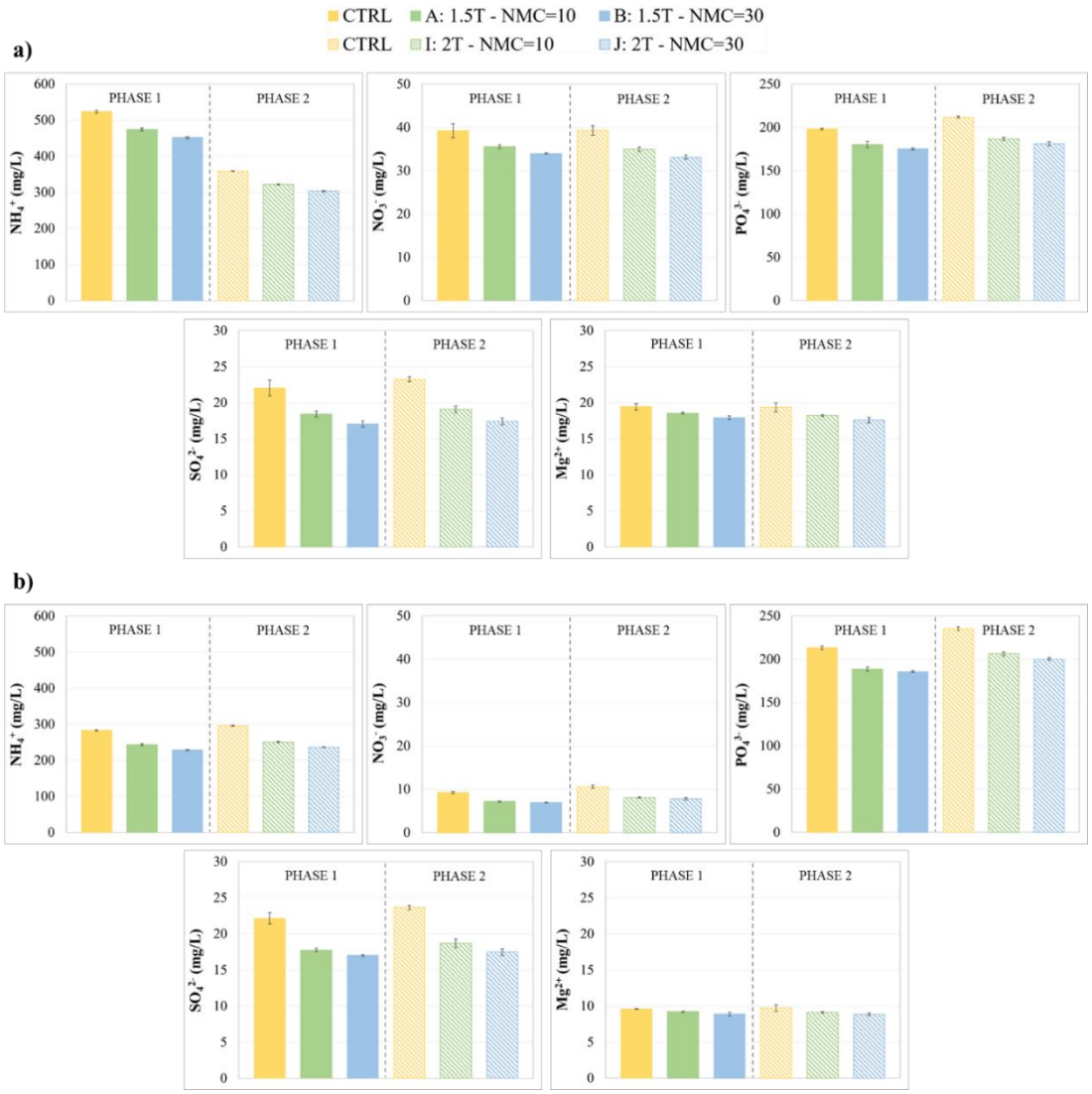

Figure 4.2 - Concentrations of NH_4^+, NO_3^-, PO_4^{3-}, SO_4^{2-}, Mg^{2+} in the HSAD digestate (**a**) and AD digestate (**b**) at the end of P1 and P2 tests with different SMF intensities and NMCs.

Figure 4.2b shows the results obtained from the same tests on the AD digestate. Likewise, it can be observed that at a SMF of 1.5 T all the monitored ionic concentrations in the liquid phase decreased by 4-22 % at NMC = 10 and by 7-25 % at NMC = 30, indicating that increasing the NMC from 10 to 30 improved ion precipitation. At the same time, at a SMF of 2 T, higher ionic species reduction was observed both at NMC of 10 (6-23 %) and 30 (9-26 %).

The reduction percentages of the ionic species observed for the AD digestate were slightly higher (+ 0.1-1%) compared to those obtained for the HSAD digestate. This effect is due to the fact that AD digestate is a less complex matrix than HSAD digestate, as it is characterised by a lower TS content and reduced interaction within the solid phase that can disturb the formation of precipitates, as previously found by Di Costanzo et al. [20]. As a consequence, the effect induced by the magnetic field on the aggregation and precipitation of ionic species is stronger.

4.3.1.2. Dose and source of magnesium

Figure 4.3a plots the concentrations of NH_4^+, NO_3^-, PO_4^{3-}, SO_4^{2-}, Mg^{2+} in the HSAD digestate at the end of P1 tests with $Mg(OH)_2$ as Mg^{2+} source. It can be observed that increasing the amount of added Mg^{2+} led to lower ionic concentrations at the end of the magnetization treatment: at NMC of 10, shifting from an equimolar Mg^{2+}:NH_4^+:PO_4^{3-} ratio of 1:1:1 to 2:1:1 increased the precipitation of NH_4^+, NO_3^-, PO_4^{3-}, SO_4^{2-} and Mg^{2+} by 2 %, 3 %, 4 %, 3 % and 10 %, respectively; at NMC of 30, the increase of the Mg^{2+}:NH_4^+:PO_4^{3-} ratio from 1:1:1 to 2:1:1 resulted in greater precipitation efficiency of 5 %, 7 %, 5 %, 11 %, and 10 % for NH_4^+, NO_3^-, PO_4^{3-}, SO_4^{2-} and Mg^{2+}, respectively.

Therefore, increasing the Mg^{2+} dose over the equimolar Mg^{2+}:NH_4^+:PO_4^{3-} ratio led to a higher precipitation of the monitored ionic species at both the NMC tested. This is attributable to the formation of new aggregates in the solid phase, as better discussed in section 3.2.1.

Not only the concentration, but also the source of Mg^{2+} can play an important role in terms of ion precipitation. Comparing the reduction percentages obtained with HSAD digestates treated under the same SMF conditions but supplied with a different Mg^{2+} source, i.e., $Mg(OH)_2$ (**Figure 4.3a**) and $MgCl_2 \cdot 6H_2O$ (**Figure 4.3b**), it can be seen that, in the latter case, the obtained values turned out to be 1-5 % higher. This result can be due to the much greater availability in the liquid phase of Mg^{2+} when added as chloride (468.7 g/L at 20 °C) than as hydroxide (9.12 mg/L at 25 °C), facilitating the formation of Mg^{2+} precipitates in the solution.

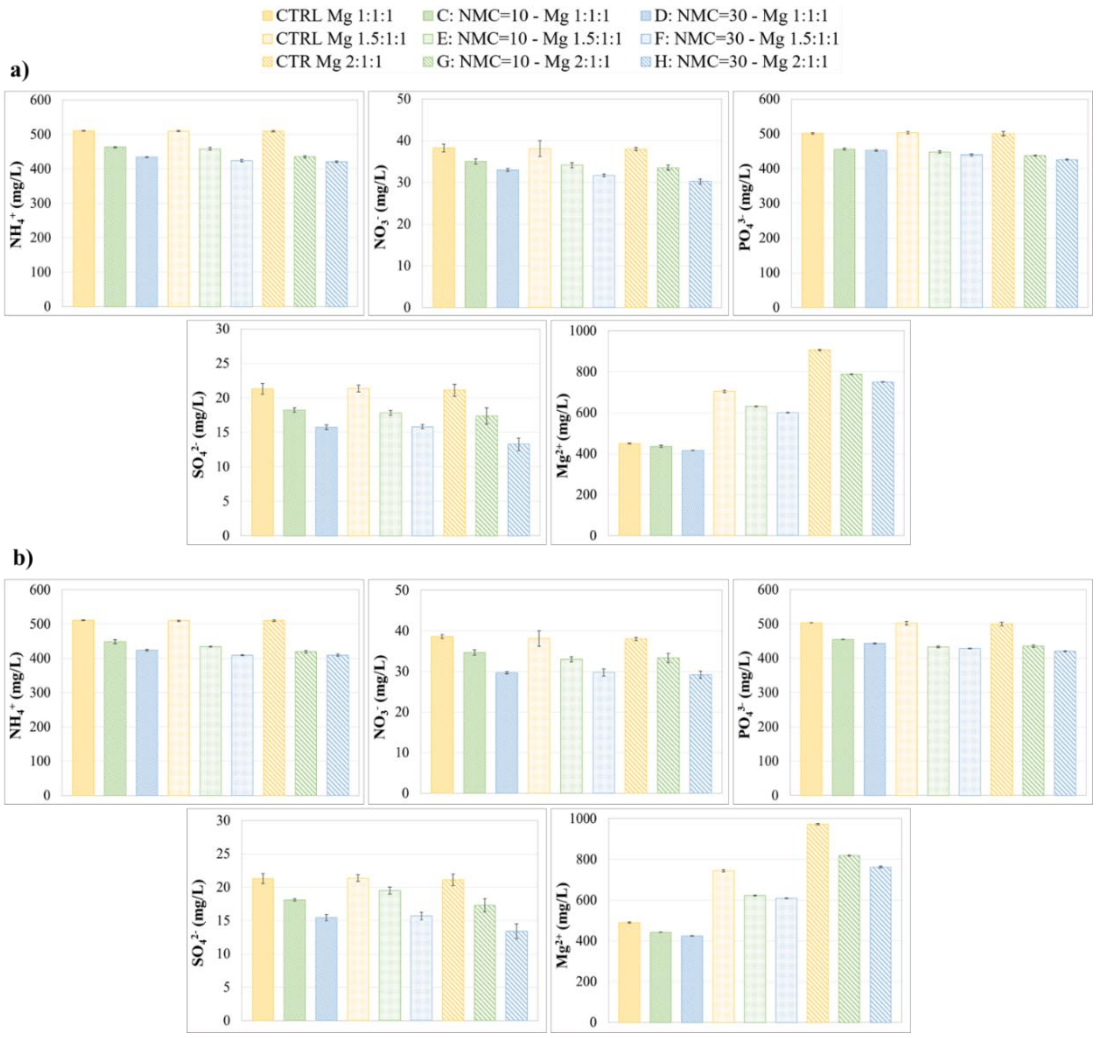

Figure 4.3 - Concentrations of NH_4^+, NO_3^-, PO_4^{3-}, SO_4^{2-}, Mg^{2+} in the HSAD digestate at the end of P1 tests with $Mg(OH)_2$ (**a**) and with $MgCl_2 \cdot 6H_2O$ (**b**) as Mg^{2+} source.

The same tests were also carried out on AD digestate (**Figure 4.4**) but only with $MgCl_2 \cdot 6H_2O$ as Mg^{2+} source, which was found to perform better in terms of ionic precipitation with HSAD digestate. At NMC = 30, switching from a Mg^{2+}:NH_4^+:PO_4^{3-} molar ratio of 1:1:1 to 2:1:1 improved the precipitation of NH_4^+, NO_3^-, PO_4^{3-}, SO_4^{2-} and Mg^{2+} concentrations by 3 %, 4 %, 4 %, 6 % and 8 %, respectively. Again, the effect of SMF application on a digestate with a lower TS content was more evident, which can be attributed to a reduced interaction between inorganic and organic phases and, therefore, to a higher availability of the ionic species to form new precipitates.

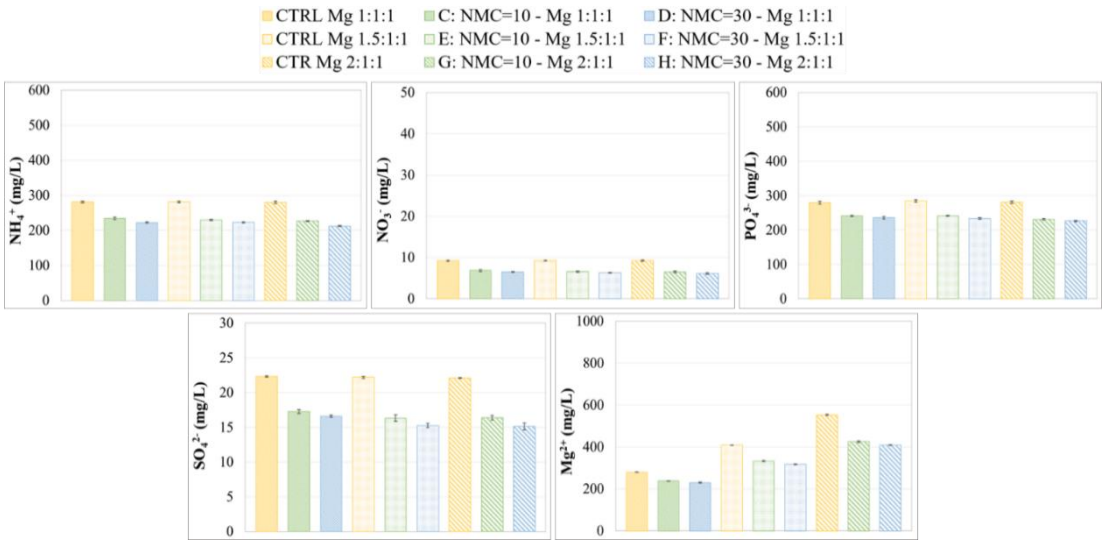

Figure 4.4 - Concentrations of NH_4^+, NO_3^-, PO_4^{3-}, SO_4^{2-}, Mg^{2+} in the AD digestate at the end of P1 tests with $MgCl_2 \cdot 6H_2O$ as Mg^{2+} source.

Once the best condition in terms of ions reduction (i.e., use of $MgCl_2 \cdot 6H_2O$ as Mg^{2+} source and of a Mg^{2+}:NH_4^+:PO_4^{3-} molar ratio of 2:1:1) were established at a SMF intensity of 1.5 T, the same experiments were also performed by applying a SMF with a higher intensity (2 T). **Figure 4.5** shows that the use of a higher SMF induced a reduction of ionic concentrations up to 21 % for NH_4^+, 24 % for NO_3^-, 18 % for PO_4^{3-}, 39 % for SO_4^{2-}, and 23 % for Mg^{2+} on HSAD digestate, and up to 27 % for NH_4^+, 35 % for NO_3^-, 20 % for PO_4^{3-}, 38 % for SO_4^{2-} and 27 % for Mg^{2+} on AD digestate. These precipitation efficiencies were higher than those obtained at a SMF of 1.5 T using the same Mg^{2+} dose and source, confirming that increasing the SMF intensity promotes precipitation.

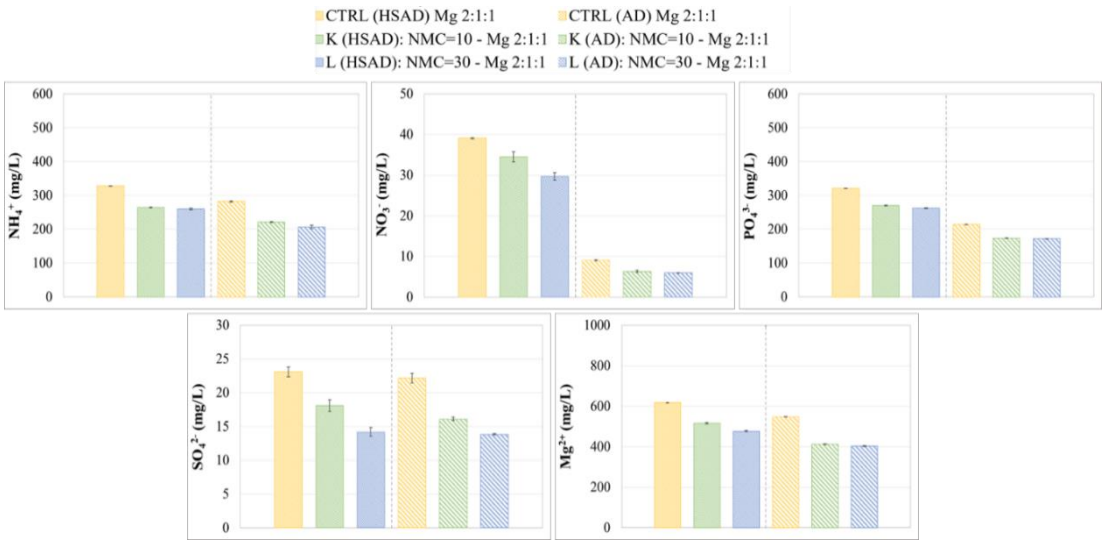

Figure 4.5 – Comparison in ionic concentration reduction of ionic species between HSAD and AD digestate after treatment with 2 T SMF using $MgCl_2 \cdot 6H_2O$ as Mg^{2+} source at a Mg^{2+}:NH_4^+:PO_4^{3-} molar ratio of 2:1:1 at different NMCs.

4.3.1.3. Aeration strategy

The effect of oxygen supply to the digestate on ionic precipitation was evaluated in the second experimental phase (P2) either by blowing air directly into the influent tank prior to SMF application or by injecting oxygen in the magnetization circuit (in-line aeration). A slight increase in the reduction of the ionic species in the liquid phase, ranging from 0.2 to 3 % for HSAD digestate (**Figure 4.6a**) and from 0.4 to 3 % for AD digestate (**Figure 4.6b**), were obtained with in-line aeration. This strategy has led to a reduction in the liquid phase of 23 % for NH_4^+, 28 % for NO_3^-, 32 % for PO_4^{3-}, 36 % for SO_4^{2-}, and 25 % for Mg^{2+} on HSAD digestate (**Figure 4.6a**) and 28 % for NH_4^+, 38 % for NO_3^-, 34 % for PO_4^{3-}, 39 % for SO_4^{2-}, and 31 % for Mg^{2+} on AD digestate (**Figure 4.6b**).

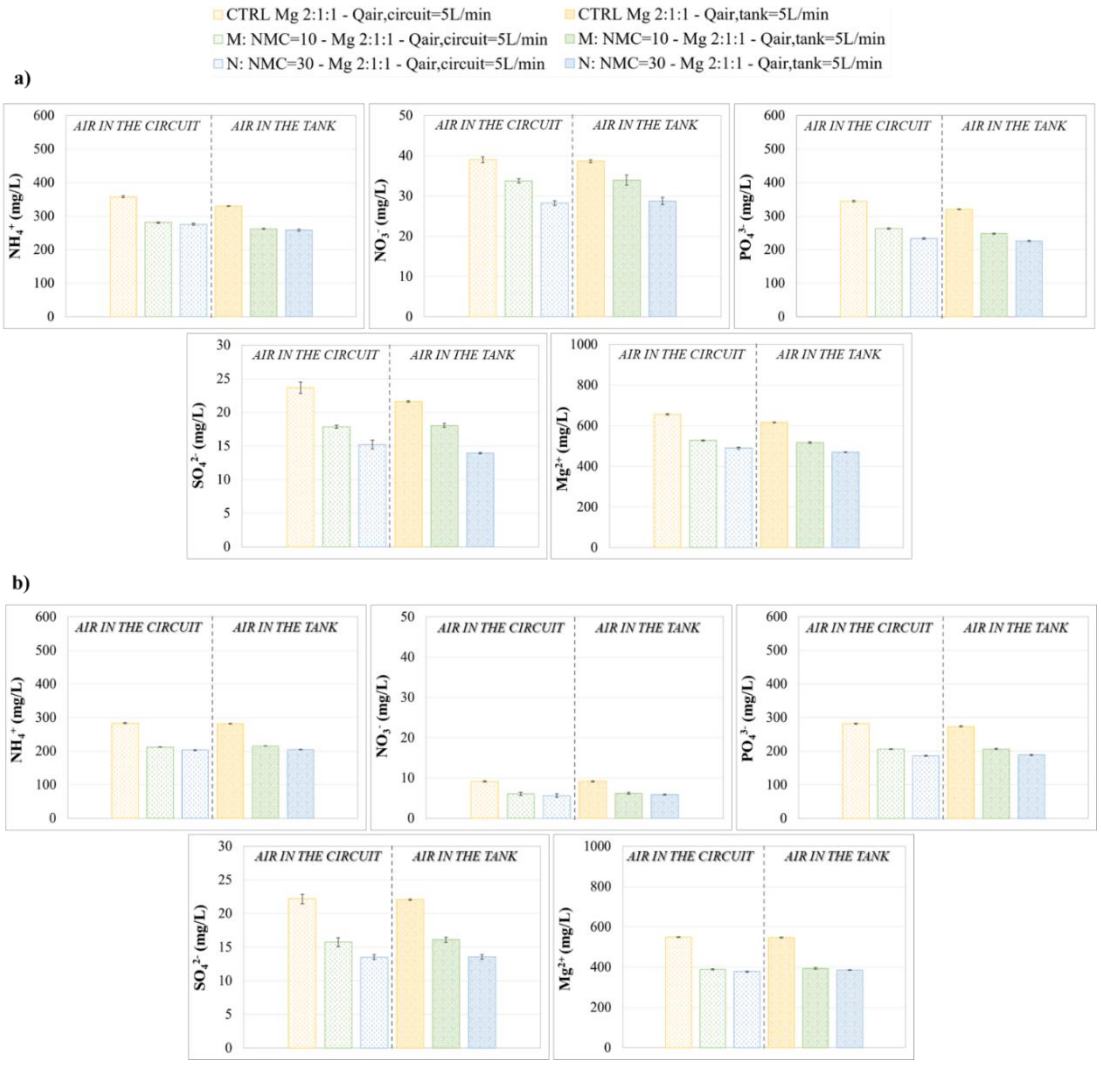

Figure 4.6 - NH_4^+, NO_3^-, PO_4^{3-}, SO_4^{2-}, Mg^{2+} concentrations in HSAD digestate (**a**) and in AD digestate (**b**) obtained at the end of the magnetization treatment with the two different aeration strategies tested.

4.3.2 Impact of magnetization conditions on precipitate formation in HSAD and AD digestates

4.3.2.1. NMCs and magnesium dose

From **Supplementary Figure 4.1**, it is possible to observe that SMF application on HSAD digestate both at NMC = 10 and NMC = 30, as well as the addition of increasing concentrations of $MgCl_2 \cdot 6H_2O$, enhanced the precipitation of the monitored ionic species compared to the control test, in agreement with the observed reductions in the liquid phase (**Figures 4.2a-4.3b**).

PO_4^{3-} reduction in the HSAD digestate treated at a SMF intensity of 1.5 T and NMC of 10 (**Supplementary Figure 4.1** A, C, E and G) is due to the precipitation of different phases including newberyte ($MgHPO_4(H_2O)_3$), sodium phosphate hydrate ($(NaPO_3)_4 \cdot H_2O$), and ammonium calcium phosphate hydrate ($(NH_4)_2Ca_3(P_2O_7)_2 \cdot 6H_2O$), whose XRD peaks are characterised for all samples by a higher intensity, and consequently a greater amount, than that of the control sample peaks. For samples treated with a SMF intensity of 1.5 T and NMC = 30 (**Supplementary Figure 4.1** B, D, F and H), the reduction of PO_4^{3-} ions in the liquid phase is additionally linked to the precipitation of struvite and other solid phases such as calcium iron magnesium hydroxide phosphate hydrate ($CaMgFe(OH)(PO_4)_2 \cdot (H_2O)_4$) and iron phosphate ($Fe_7(PO_4)_6$). Doubling the Mg^{2+} dose promoted the precipitation of these phases, as indicated by the intensity increase of the XRD peaks at a Mg^{2+}:NH_4^+:PO_4^{3-} dose of 2:1:1. By comparing the results obtained at similar Mg^{2+} doses but different NMCs (10 and 30), higher XRD peaks of struvite can be observed for samples treated at higher NMC, indicating a slightly higher content of this mineral.

The precipitation of NH_4^+ (**Figures 4.2a-4.3b**) was linked to the formation of: i) $(NH_4)_2Ca_3(P_2O_7)_2 \cdot 6H_2O$ in samples treated with NMC of 10 and 30, ii) ammonium calcium sulfate ($(NH_4)_2(CaSO_4)_5 \cdot SO_4 \cdot H_2O$) in samples B, D, F and H, iii) struvite in samples F and H, as well as to the presence of amorphous phases containing NH_4^+ (indicated by the amorphous band in the range 2θ = 15-35°).

SO_4^{2-} precipitation could be linked to the formation of several solid phases such as potassium calcium magnesium sulphate ($K_2CaMg(SO_4)_3$), sodium iron sulphide ($NaFeS_2$), and $(NH_4)_2(CaSO_4)_5 \cdot SO_4 \cdot H_2O$, which were not present in the control sample, and whose amount depends on the exposure to the applied magnetic field and the increasing $MgCl_2 \cdot 6H_2O$ concentrations. The higher precipitation of SO_4^{2-} obtained at a NMC of 30 compared to that observed at NMC of 10 can be justified by both the presence of $(NH_4)_2(CaSO_4)_5 \cdot SO_4 \cdot H_2O$, which was not detected in samples with NMC = 10, and the precipitation of amorphous SO_4^{2-} due to the presence of an amorphous band in the range 2θ = 15-35°, which is slightly more intense for magnetized samples.

The results of diffractometric analyses on AD digestate are given in **Supplementary Figure 4.2**. All samples were characterized by the presence of quartz, calcite, and microclines. From **Supplementary Figure 4.2** is also appreciable the presence of sodium magnesium sulphate hydrate ($Na_2Mg(SO_4)_2(H_2O)_4$), magnesium phosphate ($Mg_2P_4O_{12}$), sodium phosphate sulphide hydrate ($Na_3PSO_3 \cdot 9H_2O$), gwihabaite ($(NH_4K)NO_3$), potassium iron sulphide ($KFeS_2$) and aluminum phosphate ($AlPO_4$). The intensity increase of the XRD peaks, and consequently the amount of these phases compared to the control sample, follows both the increase in SMF exposure (NMC = 10 and 30) and the dose of $MgCl_2 \cdot 6H_2O$, and justifies the reductions of the various ionic species determined in the liquid phase (**Figures 4.2b-4.4**). Moreover, in the range 2θ = 5-35° there is an amorphous band whose intensity increases slightly when increasing the SMF exposure (NMC = 10 and 30) and the dose of $MgCl_2 \cdot 6H_2O$, indicating the precipitation of amorphous phases not identifiable by XRD analysis.

4.3.2.2. Impact of different aeration strategies on the solid phase of HSAD and AD digestate

Supplementary Figure 4.3 and **Supplementary Figure 4.4** shows the XRD patterns obtained from the magnetization tests at 2 T on HSAD and AD digestate, respectively, with Mg^{2+} addition at the best Mg^{2+}:NH_4^+:PO_4^{3-} molar concentration ratio of 2:1:1 (tests K and L), and include the XRD patterns of the tests with oxygenation (tests M and N) via pre-aeration ($Q_{air,tank}$) and in-line aeration ($Q_{air,circuit}$).

The increased reduction of PO_4^{3-} concentration in the liquid phase of HSAD and AD digestate due to oxygenation both at NMC = 10 and NMC = 30 was confirmed by the increase of P-based precipitates. In particular, it can be observed that at NMC = 30, the intensity of the struvite peaks in oxygenated samples increased compared to the non-oxygenated ones. For both digestates, the XRD peaks of other P-based compounds, i.e, $(NaPO_3)_4 \cdot H_2O$ and $MgHPO_4(H_2O)_3$, slightly increased in intensity both in the samples at NMC = 10 and NMC = 30 for oxygenated digestate compared to the corresponding samples without oxygenation.

Considering the oxygenated digestate by comparing the results obtained at similar Mg^{2+} doses and NMC = 30, higher XRD peaks of struvite can be observed for

digestates magnetized with in-line oxygenation compared to pre-aerated ones, suggesting that in-line oxygenation stimulates struvite precipitation. The higher PO_4^{3-} reduction observed in the liquid phase for AD digestate compared to HSAD digestate agrees with the additional presence of the XRD peaks of $Na_3PSO_3 \cdot 9H_2O$ and $AlPO_4$ in the AD digestate samples, as well as with a greater presence of amorphous PO_4^{3-} precipitates. Regarding NH_4^+, its precipitation in the solid phase of both HSAD and AD digestates can be linked to the presence of the XRD peaks of $(NH_4)_2(CaSO_4)_5 \cdot SO_4 \cdot H_2O$, which was slightly higher in the digestates subjected to oxygenation during the magnetization process compared to no oxygenation. The XRD peak intensities in all samples subjected to oxygenation are similar both at NMC = 10 and NMC = 30, indicating that the NMC did not exert a significant impact on NH_4^+ precipitation as crystalline forms at the tested values.

SO_4^{2-} precipitation in the solid phase can be linked to the presence of $NaFeS_2$ and $K_2CaMg(SO_4)_3$ in all collected samples. However, the XRD peak intensities related to these compounds are similar for both oxygenated and non-oxygenated digestates. Therefore, the effect of oxygenation in the solid phase should not be attributed to the above-mentioned mineralogical phases but to the precipitation of amorphous phases whose entity increased with oxygenation. In fact, the amorphous band included in the 2θ range between 15° and 35° is more intense in diffractograms of oxygenated samples than in those not subjected to air injection. Furthermore, the sample with in-line oxygenation shows a slightly more intense band than the other samples, indicating a greater presence of amorphous phases. Conversely, oxygenation seems to have played a role in the precipitation of crystalline SO_4^{2-} precipitates in AD digestate. The intensity of the XRD peaks of $Na_2Mg(SO_4)_2(H_2O)_4$, $KFeS_2$, and $Na_3PSO_3 \cdot 9H_2O$ phases are higher than those of the corresponding peaks in samples without oxygenation (**Supplementary Figure 4.4** K and L) in agreement with the higher SO_4^{2-} reductions observed in the liquid phase. For AD digestate also the NMC seems to have played a role on precipitation. While the intensities of the XRD peaks of $Na_2Mg(SO_4)_2(H_2O)_4$ and $Na_3PSO_3 \cdot 9H_2O$ in sample N (NMC = 30) are similar to those of the corresponding peaks of sample M (NMC =10), the intensity of the $KFeS_2$ peaks in sample N is greater than those in sample M, justifying the greater reduction of SO_4^{2-}

observed in the liquid phase at higher NMC. **Supplementary Figure 4.4** also highlights both XRD peaks of greater intensity and an amorphous band in the range 2θ = 15-25° more pronounced in the case of in-line oxygenation (M and N: $Q_{air,circuit}$) compared to pre-oxygenation (M and N: $Q_{air,tank}$).

4.3.3. Practical implications and future research perspectives

This study shows that the application of a high-intensity SMF to sewage sludge digestate significantly reduces ionic concentrations in the liquid phase, leading to the formation of nutrient-based compounds with potential fertilizing properties, such as struvite. Specifically, struvite precipitation was promoted by maximizing the exposure of HSAD and AD digestate to the SMF. The highest precipitation yield was observed at the highest intensity tested of 2 T, NMC = 30, Mg^{2+} addition at a Mg^{2+}:NH_4^+:PO_4^{3-} ratio of 2:1:1, and with in-line oxygenation of the digestate.

Compared to magnetization performed before AD, digestate magnetization avoids the detrimental impacts on methane production and reduces the potential accumulation of struvite within digesters and pumping systems. This novel approach can be exploited in a circular economy perspective to promote the agricultural application of the digestate, a solution that is considered a good practice as it couples the recycling of nutrients and organics and reduces the landfilling of sewage sludge, resulting in reduced disposal costs for wastewater treatment plants [2]. In this context, oxygenation of the digestate can help enhancing the precipitation of nutrient-based compounds with fertilizer properties. Future research should investigate additional strategies that can maximise the effect induced by the magnetic field on the formation of valuable precipitates. Moreover, the technical-economic feasibility of SMF application under different operating conditions at larger scale should be assessed to evaluate the potential scale-up of this technology as an integrated system to AD coupled to an oxygenation strategy. In full-scale digesters, pre-oxygenation of digesting sludge can be performed within the recirculation stream to control hydrogen sulfide (H_2S) production and limit its concentration in biogas [26]. To enhance the agronomic quality of the digestate, oxidative H_2S removal within the digesters could be fine-tuned to promote precipitation during the subsequent magnetization step. Furthermore, it is

also important to investigate the effect of alternative sources of Mg^{2+} to be added to promote struvite precipitation, perhaps by favouring recycled materials to make the process more competitive and sustainable.

4.4. Conclusions

This study demonstrates that combining the exposure of sewage sludge digestates from both AD and HSAD processes to a SMF at increasing intensity (from 1.5 to 2 T) and NMC (from 10 to 30), with the addition of $MgCl_2 \cdot 6H_2O$ as Mg^{2+} source at a Mg^{2+}:NH_4^+:PO_4^{3-} molar ratio of 2:1:1, enhances the precipitation of nutrient concentrations and promotes the precipitation of nutrient-based compounds that can improve the agronomic quality of sewage sludge digestate. At the maximum SMF exposure (SMF intensity of 2 T and NMC = 30), ionic precipitation efficiencies ranged from 18 to 39 % for HSAD digestate and from 20 to 39 % for AD digestate. Similarly, the formation of solid-phase compounds was stimulated at increasing SMF exposure, in agreement with the results of ionic precipitation. The best conditions for struvite formation were observed to be SMF intensity of 2 T for a NMC = 30 with Mg^{2+} addition in the optimum concentration as well as with in-line oxygenation, which also promoted the formation of other nutrient-based compounds with potential agronomic value such as $MgHPO_4(H_2O)_3$, $(NH_4K)NO_3$, $K_2CaMg(SO_4)_3$, $CaMgFe(OH)(PO_4)_2 \cdot (H_2O)_4$, and $((NH_4)_2Ca_3(P_2O_7)_2 \cdot 6H_2O)$, being characterized by the presence in their structure of macro- (N, P, K, S, Ca) and micro- (Fe, Mg, Na) nutrients.

4.6. Supplementary materials

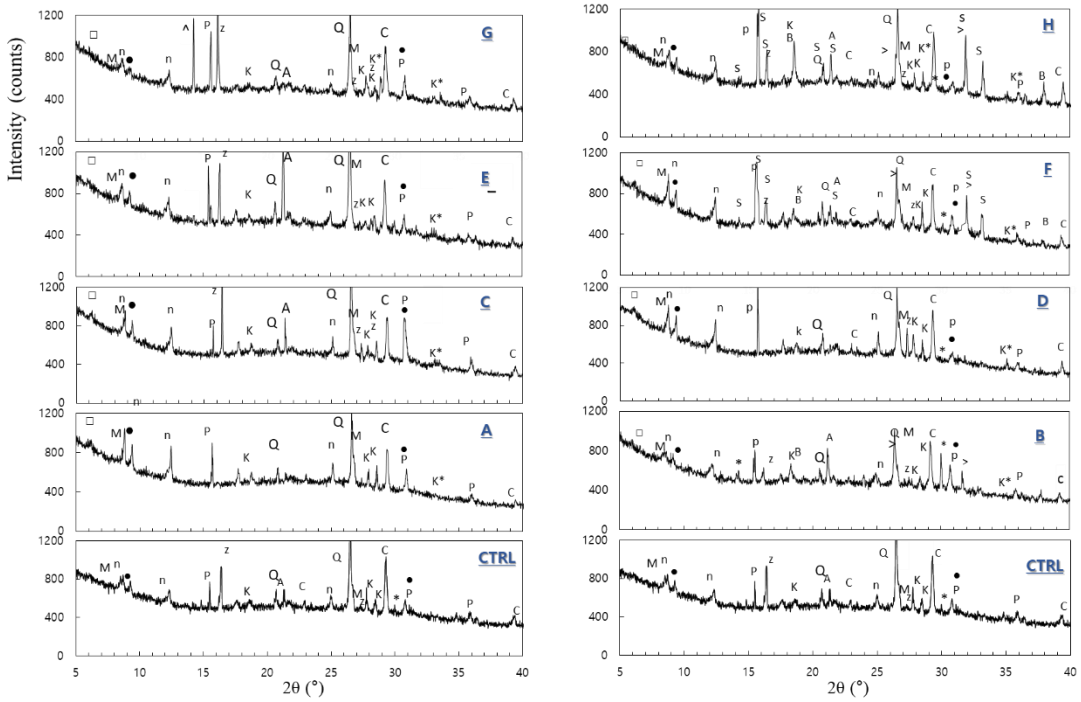

Supplementary Figure 4.1 - XRD patterns of HSAD digestate samples A, B, C, D, E F, G, H, and control listed in Table 2 with $MgCl_2 \cdot 6H_2O$ as magnesium source.

(C = Calcite; Q = Quartz; z = Sodium iron sulphide, $NaFeS_2$; k = Potassium calcium magnesium sulphate, $K_2CaMg(SO_4)_3$; > = Ammonium calcium sulphate, $(NH_4)_2(CaSO_4)_5 \cdot SO_4 \cdot H_2O$; n = Newberyte, $MgHPO_4 \cdot 3(H_2O)_3$; p = Sodium Phosphate Hydrate, $(NaPO_3)_4 \cdot H_2O$; k = Ammonium Calcium Phosphate Hydrate, $(NH_4)_2Ca_3(P_2O_7)_2 \cdot 6(H_2O)$; * = Iron Phosphate, $Fe_7(PO_4)_6$; ● = $CaMgFe(OH)(PO_4)_2 \cdot 4(H_2O)$; B = Brucite, $Mg(OH)_2$; S= struvite; M = Muscovite; ^ = Iron Hidroxide, $Fe(OH)_3$; A = Sodium Aluminum Silicate, $Na_{1.55}Al_{1.55}Si_{0.45}O_4$; □ = Magnesium Iron Aluminum Silicate Hydroxide, $Mg_{2.5}Fe_{1.65}Al_{1.5}Si_{2.2}Al_{1.8}O_{10}(OH)_8$).*

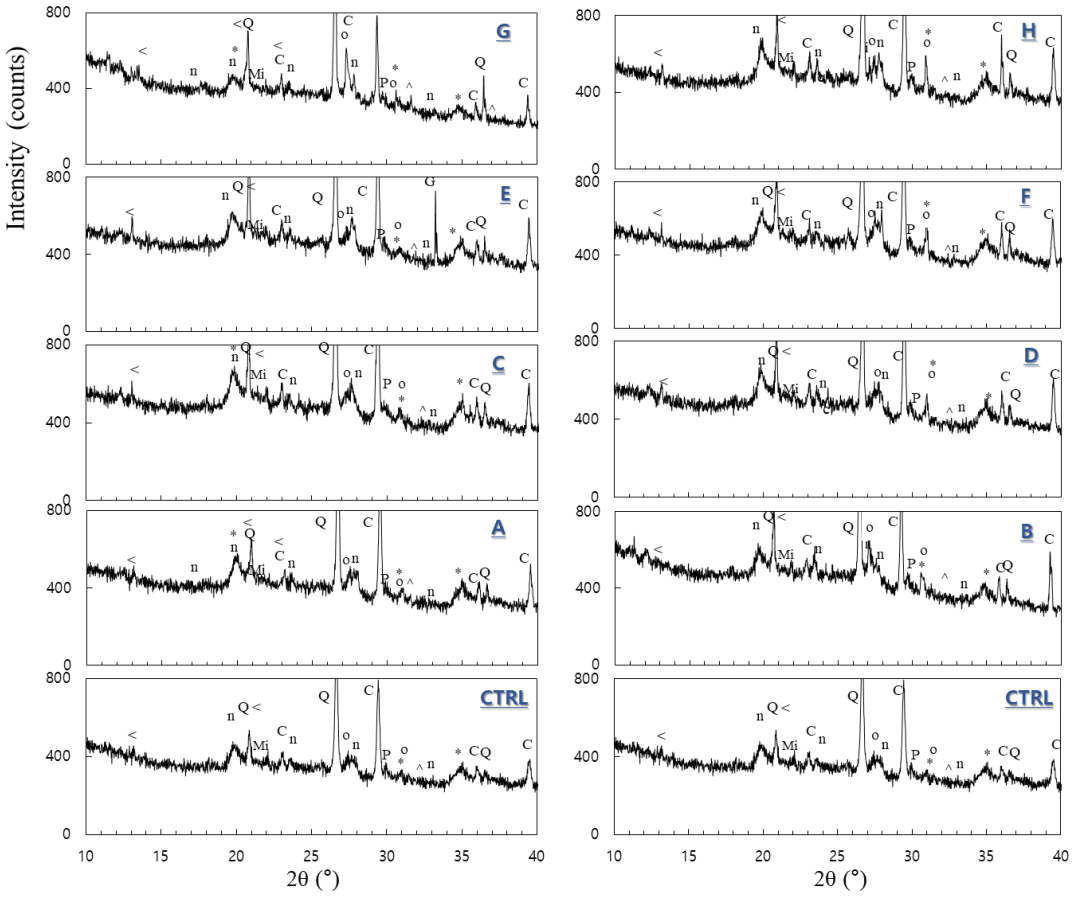

Supplementary Figure 4.2 - XRD patterns of AD digestate samples A, B, C, D, E F, G, H, and control listed in Table 2 with $MgCl_2 \cdot 6H_2O$ as magnesium source.

*(C = Calcite, $CaCO_3$; Q = Quartz, SiO_2; Mi = microcline, $KAlSi_3O_8$; n = Sodium Magnesium Sulphate Hydrate, $Na_2Mg(SO_4)_2(H_2O)_4$; * = Sodium Pophate sulphide Hydrate, $Na_3PSO_3 \cdot 9H_2O$; o = Potassium iron sulfide, $KFeS_2$; p = Magnesium Phosphate, $Mg_2P_4O_{12}$; < = Aluminum Phosphate, $AlPO_4$; ^ = Gwihabaite, $(NH_4, K)NO_3$).*

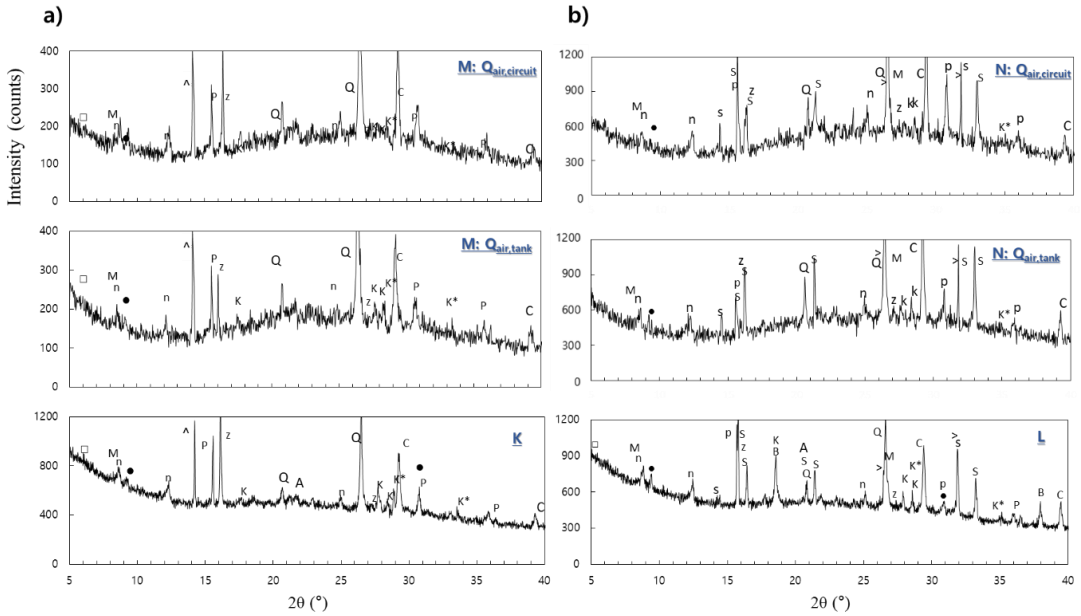

Supplementary Figure 4.3 - XRD patterns of HSAD digestate samples with $MgCl_2 \cdot 6H_2O$ (Mg^{2+}:NH_4^+:PO_4^{3-} = 2:1:1) as magnesium source without oxygenation (samples K and L), with pre-aeration (M: $Q_{air,tank}$ and N: $Q_{air,tank}$), and with in-line aeration (M: $Q_{air,circuit}$ and N: $Q_{air,circuit}$).

(C = Calcite; Q = Quartz; k = Potassium calcium magnesium sulphate, $K_2CaMg(SO_4)_3$; z = Sodium iron sulphide, $NaFeS_2$; ; > = Ammonium calcium solphate $(NH_4)_2(CaSO_4)_5 \cdot SO_4 \cdot H_2O$; n = Newberyte, $MgHPO_4 \cdot 3(H_2O)_3$; p = Sodium Phosphate Hydrate, $(NaPO_3)_4 \cdot H_2O$; k = Ammonium Calcium Phosphate Hydrate $(NH_4)_2Ca_3(P_2O_7)_2 \cdot 6(H_2O)$; * = Iron Phosphate, $Fe_7(PO_4)_6$; ● = $CaMgFe(OH)(PO_4)_2 \cdot 4(H_2O)$; B = Brucite, $Mg(OH)_2$; S= struvite, $(NH_4)MgPO_4 \cdot 6(H_2O)$; ; ^ = Iron Hidroxide, $Fe(OH)_3$; M = Muscovite; A Sodium Aluminum Silicate ($Na_{1.55}Al_{1.55}Si_{0.45}O_4$), □ = Magnesium Iron Aluminum Silicate Hydroxide ($Mg_{2.5}Fe_{1.65}Al_{1.5}Si_{2.2}Al_{1.8}O_{10}(OH)_8$)).*

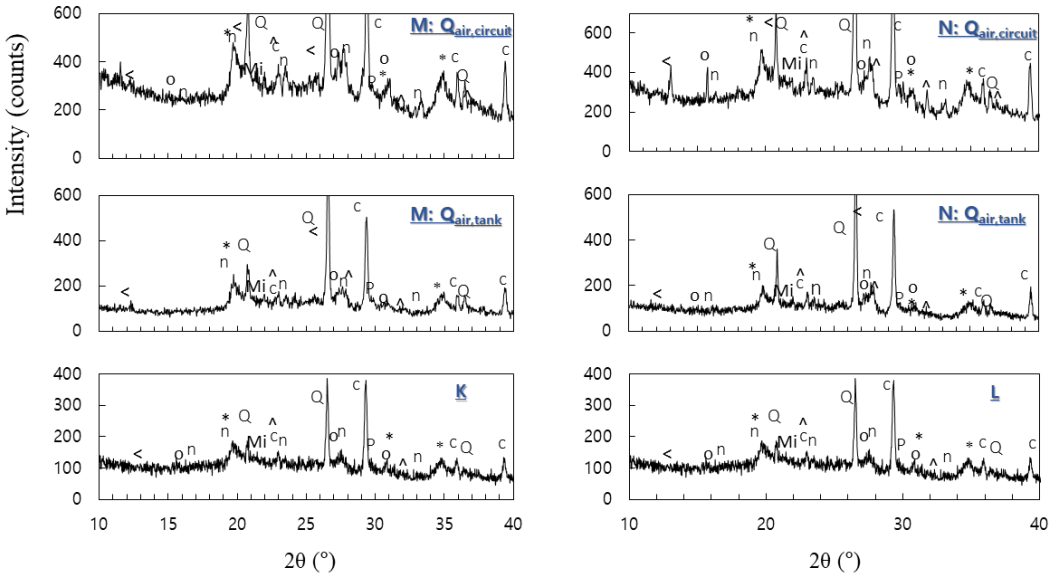

Supplementary Figure 4.4 - XRD patterns of AD digestate samples with $MgCl_2 \cdot 6H_2O$ (Mg^{2+}:NH_4^+:PO_4^{3-} = 2:1:1) as magnesium source without oxygenation (samples K and L), with pre-aeration (M: $Q_{air,tank}$ and N: $Q_{air,tank}$), and with in-line aeration (M: $Q_{air,circuit}$ and N: $Q_{air,circuit}$).

*(C = Calcite, $CaCO_3$; Q = Quartz, SiO_2; Mi = microcline, $KAlSi_3O_8$; n = Sodium Magnesium Sulfate Hydrate, $Na_2Mg(SO_4)_2(H_2O)_4$; * = Sodium Phosphate sulfide Hydrate, $Na_3PSO_3 \cdot 9H_2O$; o = Potassium iron sulfide, $KFeS_2$; p = Magnesium Phosphate, $Mg_2P_4O_{12}$; < = Aluminum Phosphate, $AlPO_4$; ^ = Gwihabaite, $(NH_4, K)NO_3$).*

4.6. References

[1] S. Shaddel, H. Bakhtiary-Davijany, C. Kabbe, F. Dadgar, S.W. Østerhus, Sustainable sewage sludge management: From current practices to emerging nutrient recovery technologies, Sustain. 11 (2019). https://doi.org/10.3390/su11123435.

[2] N. Di Costanzo, A. Cesaro, F. Di Capua, G. Esposito, Exploiting the nutrient potential of anaerobically digested sewage sludge: A review, Energies. 14 (2021) 1–25. https://doi.org/10.3390/en14238149.

[3] G. Siebielec, S. Siebielec, D. Lipski, Long-term impact of sewage sludge, digestate and mineral fertilizers on plant yield and soil biological activity, J. Clean. Prod. 187 (2018) 372–379. https://doi.org/10.1016/j.jclepro.2018.03.245.

[4] J. Stávková, J. Maroušek, Novel sorbent shows promising financial results on P recovery from sludge water, Chemosphere. 276 (2021). https://doi.org/10.1016/j.chemosphere.2021.130097.

[5] M. Zilio, A. Pigoli, B. Rizzi, A. Herrera, F. Tambone, G. Geromel, E. Meers, O. Schoumans, A. Giordano, F. Adani, Using highly stabilized digestate and digestate-derived ammonium sulphate to replace synthetic fertilizers: The effects on soil, environment, and crop production, Sci. Total Environ. 815 (2022) 152919. https://doi.org/10.1016/j.scitotenv.2022.152919.

[6] A. Kelessidis, A.S. Stasinakis, Comparative study of the methods used for treatment and final disposal of sewage sludge in European countries, Waste Manag. 32 (2012) 1186–1195. https://doi.org/10.1016/j.wasman.2012.01.012.

[7] B. Dubis, A. Szatkowski, K.J. Jankowski, Sewage sludge, digestate, and mineral fertilizer application affects the yield and energy balance of Amur silvergrass, Ind. Crops Prod. 175 (2022). https://doi.org/10.1016/j.indcrop.2021.114235.

[8] F. Di Capua, D. Spasiano, A. Giordano, F. Adani, U. Fratino, F. Pirozzi, G. Esposito, High-solid anaerobic digestion of sewage sludge: challenges and opportunities, Appl. Energy. 278 (2020) 115608. https://doi.org/10.1016/j.apenergy.2020.115608.

[9] A. Pigoli, M. Zilio, F. Tambone, S. Mazzini, M. Schepis, E. Meers, O. Schoumans, A. Giordano, F. Adani, Thermophilic anaerobic digestion as suitable bioprocess producing organic and chemical renewable fertilizers: A full-scale approach, Waste Manag. 124 (2021) 356–367. https://doi.org/10.1016/j.wasman.2021.02.028.

[10] A.J. Hertzberger, R.D. Cusick, A.J. Margenot, A review and meta-analysis of the agricultural potential of struvite as a phosphorus fertilizer, Soil Sci. Soc. Am. J. 84 (2020) 653–671. https://doi.org/10.1002/saj2.20065.

[11] D. Lorick, B. Macura, M. Ahlström, A. Grimvall, R. Harder, Effectiveness of struvite precipitation and ammonia stripping for recovery of phosphorus and nitrogen from anaerobic digestate: a systematic review, Environ. Evid. 9 (2020) 1–20. https://doi.org/10.1186/s13750-020-00211-x.

[12] S.A. Parsons, J.D. Doyle, Struvite formation, control and recovery, Water Res. 36 (2002) 3925–3940.

[13] H. Huang, D. Xiao, Q. Zhang, L. Ding, Removal of ammonia from landfill leachate by struvite precipitation with the use of low-cost phosphate and magnesium sources, J. Environ. Manage. 145 (2014) 191–198. https://doi.org/10.1016/j.jenvman.2014.06.021.

[14] B. Drosg, W. Fuchs, T. Al Seadi, M. Madsen, B. Linke, Nutrient Recovery by Biogas Digestate Processing Bernhard, 2020.

[15] X. Hao, C. Wang, M.C.M. Van Loosdrecht, Y. Hu, Looking beyond struvite for P-recovery, Environ. Sci. Technol. 47 (2013) 4965–4966. https://doi.org/10.1021/es401140s.

[16] B. Sniatala, T.A. Kurniawan, D. Sobotka, J. Makinia, M.H.D. Othman, Macro-nutrients recovery from liquid waste as a sustainable resource for production of recovered mineral fertilizer: Uncovering alternative options to sustain global food security cost-effectively, Sci. Total Environ. 856 (2023). https://doi.org/10.1016/j.scitotenv.2022.159283.

[17] C. Vogel, C. Adam, B. Peplinski, S. Wellendorf, Chemical reactions during the preparation of P and NPK fertilizers from thermochemically treated sewage sludge ashes, Soil Sci. Plant Nutr. 56 (2010) 627–635.

https://doi.org/10.1111/j.1747-0765.2010.00485.x.

[18] K. Lubkowski, Environmental impact of fertilizer use and slow release of mineral nutrients as a response to this challenge, Polish J. Chem. Technol. 18 (2016) 72–79. https://doi.org/10.1515/pjct-2016-0012.

[19] M.C. Mascolo, Effect of magnetic field on calcium carbonate precipitated in natural waters with prevalent temporary hardness, J. Water Process Eng. 41 (2021) 102087. https://doi.org/10.1016/j.jwpe.2021.102087.

[20] N. Di Costanzo, F. Di Capua, A. Cesaro, M.C. Mascolo, F. Pirozzi, G. Esposito, Impact of High-Intensity Static Magnetic Field on Chemical Properties and Anaerobic Digestion of Sewage Sludge, Waste and Biomass Valorization. 14 (2023) 2469–2479. https://doi.org/10.1007/s12649-022-01891-x.

[21] (APHA) American Public Health Association, (AWWA) American Water Works Association, (WEF) Water Environment Federation, Standard Methods for the Examination of Water and Wastewater Standard Methods for the Examination of Water and Wastewater, Public Health. 51 (1999) 940–940. https://doi.org/10.2105/AJPH.51.6.940-a.

[22] APAT CNR IRSA, Analytical Methods for Water, 2003.

[23] F. Di Capua, M.C. Mascolo, F. Pirozzi, G. Esposito, Simultaneous denitrification, phosphorus recovery and low sulfate production in a recirculated pyrite-packed biofilter (RPPB), Chemosphere. 255 (2020) 126977. https://doi.org/10.1016/j.chemosphere.2020.126977.

[24] A. Oliva, L.C. Tan, S. Papirio, G. Esposito, P.N.L. Lens, Effect of methanol-organosolv pretreatment on anaerobic digestion of lignocellulosic materials, Renew. Energy. 169 (2021) 1000–1012. https://doi.org/10.1016/j.renene.2020.12.095.

[25] S. Lee, D.K. Lee, What is the proper way to apply the multiple comparison test?, Korean J. Anesthesiol. 71 (2018) 353–360. https://doi.org/10.4097/kja.d.18.00242.

[26] P. Jeníček, J. Horejš, L. Pokorná-Krayzelová, J. Bindzar, J. Bartáček, Simple biogas desulfurization by microaeration – Full scale experience, Anaerobe. 46 (2017) 41–45. https://doi.org/10.1016/j.anaerobe.2017.01.002.

CHAPTER 5

Exploring the effects of static magnetic fields for enhanced valorization of sewage sludge via anaerobic digestion

Part of the content of this chapter has been published as:

Di Costanzo N., Cesaro A., Di Capua F., Mascolo M., Esposito G., 2023. Exploring the effects of static magnetic fields for the enhanced valorization of sewage sludge by anaerobic digestion. International Conference on Environmental Science and Technology (CEST) Proceedings. https://doi.org/10.30955/gnc2023.00090

Abstract

This chapter investigated the effect of low-intensity static magnetic field (SMF) (20 mT) on methane production and microbial communities involved in anaerobic digestion (AD) of sewage sludge, comparing it to the effect deriving from the application of a high-intensity SMF (1.5 T), in order to establish a potential integration between SMF and AD for the valorization of sewage sludge within a circular economy context.

5.1. Introduction

Sewage sludge is an inevitable byproduct of municipal wastewater treatment and represents a key issue in many countries due to its increasing volume and the impacts associated with its disposal [1]. In addition, the management and disposal of sewage sludge stands as a significant part of the total operating costs, up to 50% [2], of wastewater treatment plants [3]. For this reason, appropriate management strategies that are sustainable from an environmental and economic point of view are needed. In this perspective, anaerobic digestion (AD) is considered an effective, economical, and eco-friendly technology. AD stabilizes the sludge, reduces its solid content, aids in odor and pathogen removal [4], and generates a methane rich biogas that can be utilized for energy purposes [5]. The generation of biogas comes along with the production of anaerobic digestate with potential fertilizer properties due to the significant content of both macro- and micro-nutrients [6]. Several studies have implemented pretreatment processes increasing sludge biodegradability and dewaterability, leading to higher volumetric reduction and biogas production. Among these, the application of static magnetic field (SMF) has been recently shown to affect AD efficiency and digestate quality [7]. This technology has been applied for precipitating calcium carbonate in water [8] and has been proposed in combination with aerobic biological processes for the enhancement of nitrifying aerobic granulation [9]. The application of a SMF to sewage sludge destined to AD is expected to impact both the generation of methane and the quality of the digestate, leading to the possible precipitation of compounds that may enhance the fertilizing properties of sewage sludge [3].

Recently, Zieliński et al. [10] evaluating the effect of static magnetic field on the anaerobic digestion of dairy wastewater, observed that a static magnetic field of 8.1 mT resulted in higher biogas production and higher methane content compared to the control reactor; the same authors, in another study Zielinski et al. [11], assessed the effect of static magnetic field also on the anaerobic digestion of municipal sewage sludge and found that static magnetic field had a significant impact on methane production efficiency but did not affect cumulative biogas production; Zhao et al. [12] by using a flat circular permanent magnet to increase biogas production from corn stover substrate by anaerobic fermentation, showed that static magnetic field of 11.4 mT (±2%) increased the volumes of total gas and methane produced by 19.5% and 20% in comparison to the control test.

Currently, to the best of our knowledge, the literature has yet to uncover the mechanisms that explain how the magnetic field affects and improves the AD of sewage sludge. Additionally, there are no studies available that assess and compare the impact of different static magnetic field intensities on fermentative and methanogenic microbial communities and the metabolic pathways implicated. Consequently, this work clarifies the effects of sludge exposure to SMF in terms of AD performance and evolution of fermentative and methanogenic communities. The impacts observed at low intensity (20 mT) and high intensity (1.5 T) SMF on both biomethane production and chemical composition of the digestate were compared. Batch AD tests were carried out on both untreated and pretreated sewage sludge samples and experimental results were discussed to identify the possible integration of this novel technology within AD processes. The evolution of the microbial communities in the sludge were investigated through Next-Generation Sequencing (NGS) to evaluate the response of the anaerobic microbiota to the SMF pretreatment at different intensities.

5.2. Materials and methods

5.2.1. Sewage sludge origin and composition

The sewage sludge used in this study was collected from a wastewater treatment plant situated in Nola (Campania region, Italy), which treats wastewater mainly of municipal origin and, to a lesser extent, industrial wastewater from the nearby industrial area.

The plant is based on a conventional activated sludge system operated at long solid retention time (> 20 days). The sewage sludge was extracted from the lower withdrawal point of the pre-thickening unit, stored in plastic, and promptly employed for the experiments. The characteristics of the sewage sludge used are listed in **Table 5.1**.

Table 5.1 - Characteristics of the sewage sludge used for the experiments.

Parameter	Unit	Value
pH	-	7.42±0.15
Total solids (TS)	%	2.4±0.1
Volatile solids (VS)	%	1.1±0.1
Soluble chemical oxygen demand (sCOD)	$mg \cdot L^{-1}$	98.3±1.3
Ammonia nitrogen ($N\text{-}NH_4^+$)	$mg \cdot L^{-1}$	67.0±2.0
Nitrate (NO_3^-)	$mg \cdot L^{-1}$	10.5±0.5
Phosphate (PO_4^{3-})	$mg \cdot L^{-1}$	185.6±4.7
Sulphate (SO_4^{2-})	$mg \cdot L^{-1}$	9.5±0.3
Sodium (Na^+)	$mg \cdot L^{-1}$	99.1±4.4
Magnesium (Mg^{2+})	$mg \cdot L^{-1}$	5.9±0.7
Calcium (Ca^{2+})	$mg \cdot L^{-1}$	165.9±4.6

5.2.2. Magnetic pretreatment and AD *tests*

The SMF was generated by a magnetic polarizer provided by AMS company (Italy) and installed on a magnetization circuit as described by Di Costanzo et al. [7]. Sewage sludge magnetization as AD pretreatment was carried out by pumping 2 L of sludge at a flow rate of 0.1 $L \cdot min^{-1}$ through the polarizer. Two different polarizers were used in this study, i.e., one with a nominal SMF intensity of 20 mT and the other with a nominal SMF intensity of 1.5 T.

AD experiments were conducted in triplicate under mesophilic conditions (37±1 °C) and in 250 mL serum glass bottles (OCHS, Germany). Each bioreactor was sealed by a cap composed of rubber septum, aluminum crimp, and needles equipped with 1-way stopcocks (Masterflex, Germany) for gas and liquid sampling. Mixing of each bioreactor was performed manually once a day before sampling. Each bottle was filled with treated sludge only leveraging the endogenous microbiota in order to assess the specific effect of magnetic field pretreatment on the physico-chemical properties of

the sludge, leaving 100 mL as headspace volume for biogas accumulation. To ensure anaerobic conditions, each bottle was flushed with argon gas for 1 min and then vented to reach atmospheric pressure. Control tests, containing only sludge, were simultaneously carried out to evaluate methane generation from the sludge without magnetic pretreatment. The experimental design used for the tests is shown in **Table 5.2**.

Table 5.2 - Design of AD tests with different SMF intensities.

Test	SMF intensity (mT)	Flow rate ($L \cdot min^{-1}$)	Magnetization cycles
Control	-	-	-
A	20	0.1	1
B	1500	0.1	1

From each test bottle, the daily methane production was quantified 5 times per week and was recorded for 40 days. In addition, 2 mL liquid samples were withdrawn once a week to measure the concentrations of volatile fatty acids (VFAs), $N\text{-}NH_4^+$, NO_3^-, PO_4^{3-}, SO_4^{2-} and Mg^{2+}.

5.2.3. Analytical methods

The concentrations of TS and VS were analyzed according to Standard Methods [13]. Prior to the following analyses, all samples were centrifuged at 12,000 rpm for 15 min and the liquid fraction was filtered through 0.45 μm polypropylene-membrane syringe filters (VWR, Italy). The concentration of sCOD was determined by the closed reflux colorimetric method [13]. The concentration of NH_4^+ was analyzed spectrophotometrically through the indophenol blue method [14]. Established the ammonium ion concentration, $N\text{-}NH_4^+$ concentration was then calculated. Anionic concentrations were measured by ion chromatography as described by Di Capua et al. [15]. Metal concentrations were measured by ICP-MS (Perkin Elmer Nexion 300, USA) operating in dual detector mode. VFAs analysis was performed by a high-performance liquid chromatography using a UVD 340U system (Dionex, USA) equipped with a diode array detector and a Metrosep organic acid column 250/7.8 (Metrohm, Switzerland).

5.2.4. Statistical analysis

The statistical comparison of reported data was performed by one-way analysis of variance through Minitab 17 Statistical Software (Minitab LCC, USA), where a difference marked with a *p*-value lower than 0.05 was considered statistically significant.

5.2.5. Microbial community characterization using Next Generation Sequencing

Samples for the identification of microbial communities were collected before and after the magnetic pretreatment and stored at -20 °C. The DNA extraction was carried out in triplicate and the samples with a higher amount and purity of DNA were sequenced. The samples were pre-treated to avoid interference with the PCR and subsequent genomic sequencing of certain components (e.g., humic and fulvic acids). Pretreatment includes the use of glass beads and vortexing that helps to remove the biotic fraction from the solid sample, which is then concentrated in the supernatant. Based on this, to sequence the genome of the whole microbiota, first 10 g were aliquoted and centrifuged to extract DNA, transferring 2 mL supernatant in sterile vials containing 0.5 g glass beads. The recovery of total DNA was performed using CTAB extraction protocol [16]. Extracted DNA samples were amplified employing PCR, utilizing V3 and V4 primers, complementary to the V3-V4 variable region - the most adequate hypervariable region for archaea and bacteria -of 16S rRNA bacterial gene (V3: TCGTCGGCAGCGTCAGATGTGTATAAGAGACAGCCTACGGGNGGCWCGAG; V4: GTCTCGTGGGCTCGGAGATGTGTATAAGAGACAGGACTACHVGGGTATCTAATCC) and then sequenced with NGS analysis employing MiSeq Illumina platform, with 2 × 300 bp paired end, 600 cycles, according to manufacturer's instructions (Illumina MiSeq, USA). Methods and software used for precessing Sequencing data, quality control and taxonomic profiling are detailed in the supplementary materials. The diversities in the microbial community data were

evaluated using weighted UniFrac distance and ANOVA (using Bray Curtis distance, Mothur) by anosim [17].

5.3. Results and discussion

5.3.1. Impact of SMF pretreatment on biomethane production

Figure 5.1 reports the specific biomethane production (SBP) after 40 days of AD tests. The control test, with untreated sludge, showed a maximum SBP of 341±5 $L_{CH4} \cdot kg_{VS}^{-1}$, notably exceeding the value reported in *Chapter 3*. This discrepancy is attributed to observed load fluctuations within the wastewater treatment plant and reported malfunctions affecting the secondary sedimentation tank during the separate sampling campaigns. The low intensity pretreatment at 20 mT significantly increased the methane production compared to control test (p<0.05). In particular, the SBP reached 384±6 $L_{CH4} \cdot kg_{VS}^{-1}$. On the other hand, the use of a high intensity SMF (1.5 T) pretreatment resulted in a decrease of SBP by 15.1% compared to the control test, reaching 289±3 $L_{CH4} \cdot kg_{VS}^{-1}$. This result is in line with those outlined in a previous work [7], where high intensity SMF (1.5 T) resulted in 23.9% lower methane generation compared to tests with untreated sludge. Zieliński et al. [10] investigated biogas production in a reactor exposed continuously to static magnetic field of 8.1 mT and fed with dairy wastewater. The authors observed an increased biogas production significantly higher in the SMF reactor (373 ± 30 $L_{CH4} \cdot kg_{VS}^{-1}$) compared to the control reactor (200 ± 35 $L_{CH4} \cdot kg_{VS}^{-1}$). A higher increase in methane production observed by the authors (+86.5%) than in the present study (+12.7%) might be a result of the lower and the different exposure condition to the SMF. Zhao et al. [12], reported a comparable percentage increase in biogas production of 19.5% during anaerobic fermentation of non-pre-treated corn stover substrate, exposed a permanent SMF intensity of 11.4 mT (±2%).

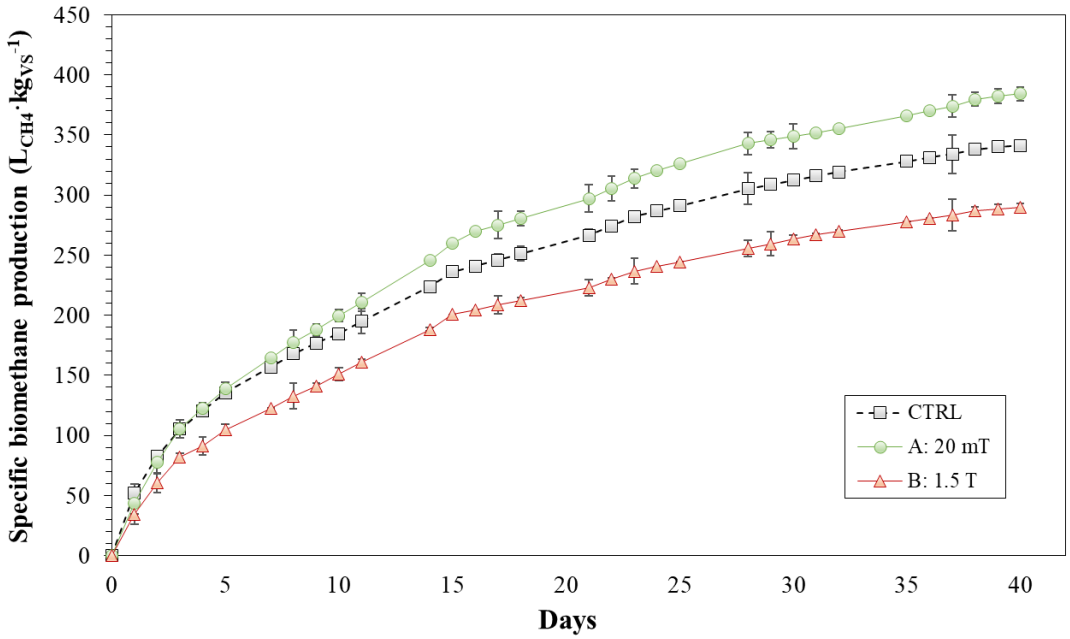

Figure 5.1 - SBP in AD tests.

After the pretreatment, a greater reduction of ionic concentrations in the liquid phase was observed at increasing SMF intensity (**Figure 5.2**). Specifically, sludge exposure to 1.5 T produced a maximum reduction of 8.7%, 39.8%, 31.6%, 40.3% and 16.6% for N-NH_4^+, NO_3^-, PO_4^{3-}, SO_4^{2-} and Mg^{2+} concentrations, respectively. Moreover, it can be observed that this reduction percentages persists throughout the duration of the AD tests. This effect, as reported in literature [8], can be linked to a magnetization memory, i.e., the persistence of the magnetization with time. This greater reduction affected the difference in SBP between the two pretreatment conditions. During AD, N-NH_4^+ originates from the hydrolysis of organic nitrogen in the substrate. It is widely reported that high concentrations of N-NH_4^+ (1.7-6.7 g·L^{-1} of N-NH_4^+) inhibit the AD process by several mechanisms, i.e. proton imbalance, potassium depletion, intracellular pH change, increased energy demand and inhibition of enzymatic reactions [1]. Despite this, N-NH_4^+ is an essential micronutrient for bacterial growth. Hence, the discrepancy in SBP can be attributed to the increased precipitation resulting from the high intensity magnetic pretreatment, compared to the low intensity magnetic pretreatment. Similarly, excessively reducing of NO_3^- and PO_4^{3-} levels with the pretreatment may result in either a reduction of VFAs and the metabolites during acidogenic

fermentation [18] or it could result in diminished methanogenic activity, a loss of buffer capacity and a shortage of essential nutrients for anaerobic degradation [19].

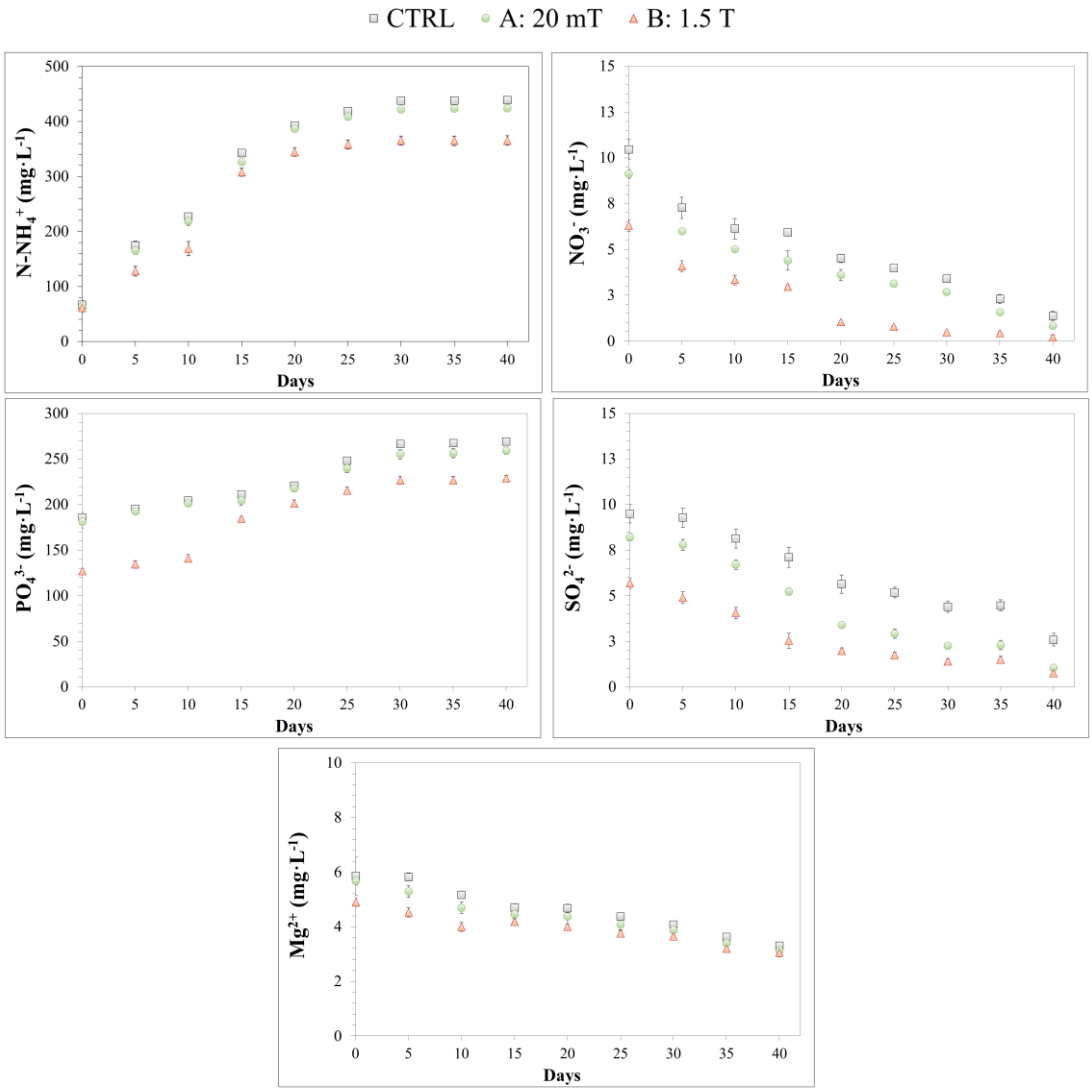

Figure 5.2 – Concentrations of $N\text{-}NH_4^+$, NO_3^-, PO_4^{3-}, SO_4^{2-} and Mg^{2+} after pretreatment (day 0) and during AD tests.

Figure 5.3 shows the variation of VFAs during AD tests. The concentration of VFAs is reported as the sum of acetic, propionic, iso-butyric and butyric acids expressed in $mg_{COD} \cdot L^{-1}$, considering the specific COD conversion coefficients (i.e., 1 g of acetic acid = 1.07g COD, 1 g of propionic acid = 1.51g COD, 1 g of butyric acid = 1.82 g

COD) [20]. From **Figure 5.3** it can be observed how magnetic pretreatment leads to changes in VFAs concentrations. Immediately after magnetic pretreatment (day 0), the total amount of VFAs for the low intensity pretreatment was higher (397±16 $mg \cdot L^{-1}$) than that measured in the untreated sludge (353±10 $mg \cdot L^{-1}$) and after the high intensity pretreatment (323±17 $mg \cdot L^{-1}$). These differences became even more evident at day 5, when the VFAs concentration after pretreatment at 20 mT reached 503 $mg \cdot L^{-1}$, 21% and 50% higher than that observed for the untreated sludge and after pretreatment at 1.5 T, respectively. Noticeably, VFAs accumulation in the bioreactors with the sludge pretreated at 20 mT evolved more rapidly than the high intensity pretreatment, reaching a peak at day 10. However, the highest VFAs concentration produced in these tests was well below the inhibitory limits for AD [21]. After day 5, the differences in VFA concentrations among the three conditions tested became less and less evident. The substantial increase in VFAs production strongly suggests an enhanced decomposition of organic materials during the early stages of the process. This implies that the low intensity SMF pretreatment likely promoted either or both the hydrolysis and acidification steps of AD, which could be the key factor for achieving a higher SBP.

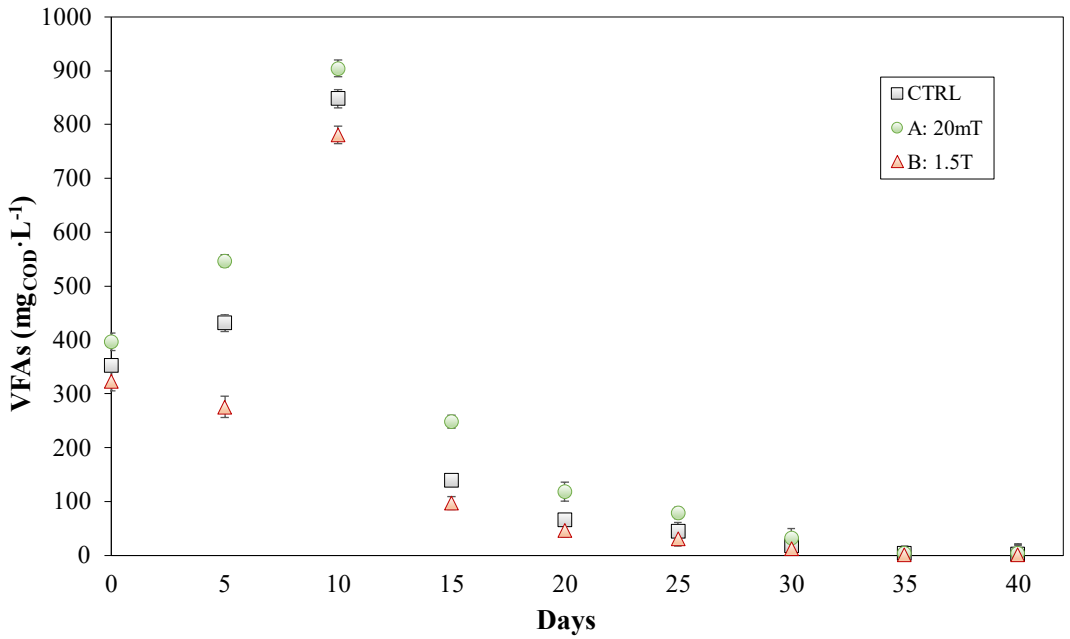

Figure 5.3 - Evolution of VFA production along the 40 days of AD tests.

5.3.2. Impact of SMF pretreatment on microbial communities

Considering the high number of detected taxa, only the taxonomic composition at genus level of the microbial communities with a relative abundance >1% is shown in **Figure 5.4**. The completed Taxonomy BarPlot generated with this analysis is showed in **Supplementary Figure 5.3** while the remaining genera are available in **Supplementary Table 5.4**.

In the sample not subjected to magnetic pretreatment, mainly 5 species, belonging to both the Archaea and Bacteria reigns, involved in methane metabolism were identified: *Methanoregula*, *Methyloparacoccus*, *Crenothrix*, *Methanosaeta* and *Methanobrevibacter*. Specifically, the indicated species are present at a relative abundance ranging between 0.01% and 0.04% and interact differently with the metabolic steps for methane production. For instance, *Methanoregula* strains are identified by the presence of the mcrA gene and encodes the alpha subunit of methyl-coenzyme M reductase, a key enzyme in the methane production pathway [22]; *Methanosaeta* uses different enzymes to catalyze the first steps of acetate methanogenesis [23]. Following the low intensity pretreatment, the relative abundance of the indicated species increases, ranging between 0.01% and 0.06%, along with the relative abundance of other species always involved in methanogenesis [24,25]: *Methylopilaceae, Methanobacterium and Methylosarcina*. On the other hand, considering the high intensity magnetic pretreatment, all the species participating in methanogenesis are nearly entirely inhibited: all the species mentioned above are at most 0.01%. The only exception being *Methanoregula*, which occurs at a relative abundance of 0.07%.

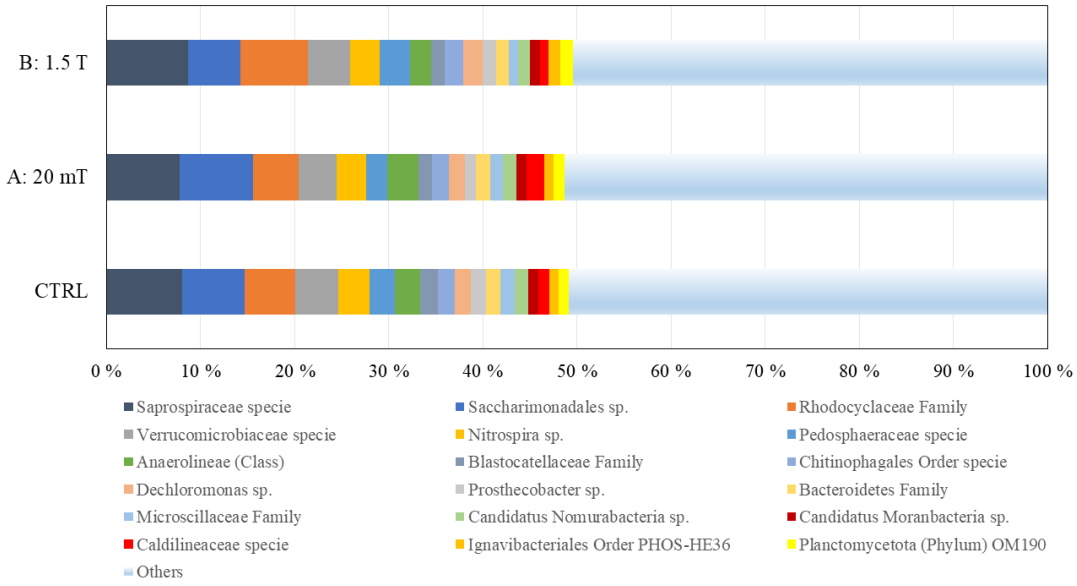

Figure 5.4 - Microbial community composition at genus level (relative abundances >1%).

Figure 5.5 shows the correlation between the microbiota composition and chemical metadata such as the SBP and the VFAs sum. Notably, the figure highlights how all the species mentioned above, despite their low percentage of relative abundance in comparison to the total population detected, exhibit trends of increase or decrease in response to the different treatments applied, specifically suggesting that the low intensity pretreatment was positively correlated with the SBP.

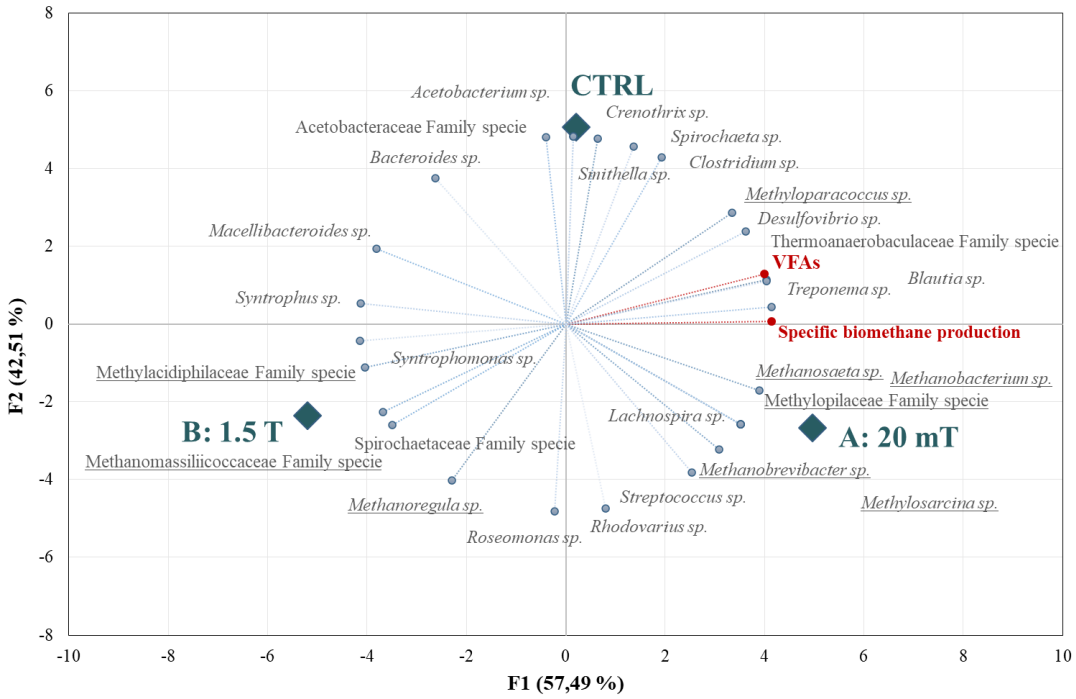

Figure 5.5 - Association of treated and untreated samples with microbiota composition and chemical metadata (Biplot; axes F1 and F2: 100%).

4. Conclusions

Our study demonstrates that low intensity SMF pretreatment is an effective technique for enhancing AD performance, attaining 12.7% improvement of methane production at 20 mT compared to the untreated sewage sludge. On the other hand, applying a high intensity SMF (1.5 T) is detrimental. Specifically, even at a minimal exposure, the latter determined a reduction in methane production of 15.1%. Microbial community analysis indicated that the low intensity SMF pretreatment results in differences in the microbiota structure, increasing the relative abundance of the species involved in the biomethane production. This study therefore proposes an innovative treatment opening up to future perspectives aimed at creating a system integrating SMF and AD for the valorization of sewage sludge in a circular economy perspective.

5.5. Supplementary materials

Methods and software used for processing Sequencing data, quality control and taxonomic profiling

After 16S amplification, a PCR clean-up was done to purify the V3-V4 amplicon from free primers and primer dimer species. A subsequent limited-amplification cycle was carried out to add multiplexing indices and Illumina sequencing adapters by using a Nextera XT Index Kit. A second step of clean-up was further performed and then libraries were normalized and pooled by denoising processes (**Supplementary Tables 5.1, 5.2 and 5.3**) and sequenced on Illumina MiSeq Platform.

Supplementary Table 5.1 - Denoising process: AmpliconStat by Qiime2.

Sample-id	Input	Filtered	Percentage of input passed filter	Denoised	Merged	Percentage of input merged	Non-chimeric	Percentage of input non-chimeric
CTR	124084	104879	84.52	88058	66764	53.81	61867	49.86
A	120761	101688	84.21	87770	71763	59.43	68530	56.75
B	88665	74934	84.51	61076	43735	49.31	40154	45.29

Supplementary Table 5.2 - Sequence Length Statistics.

Sequence Count	Min Lenght	Max Lenght	Mean Lenght	Range	Standard Deviation
2956	273	430	404.11	157	39.56

Supplementary Table 5.3 - Seven-Number Summary of Sequence Lengths

Percentile:	2%	9%	25%	50%	75%	91%	99%
Length*(nts)	273	401	403	419	426	427	428

QIIME 2 platform was used for microbiome analysis from raw DNA sequencing data. QIIME 2 analysis workflow was performed by demultiplexing, quality filtering, chimera removal, taxonomic assignment. Taxonomy was assigned using "home made" Naive Bayesian Classifier trained on V3-V4 16S sequences of SILVA 132 database. Frequencies per feature and per sample are shown in **Supplementary Figures 5.1, 5.2**.

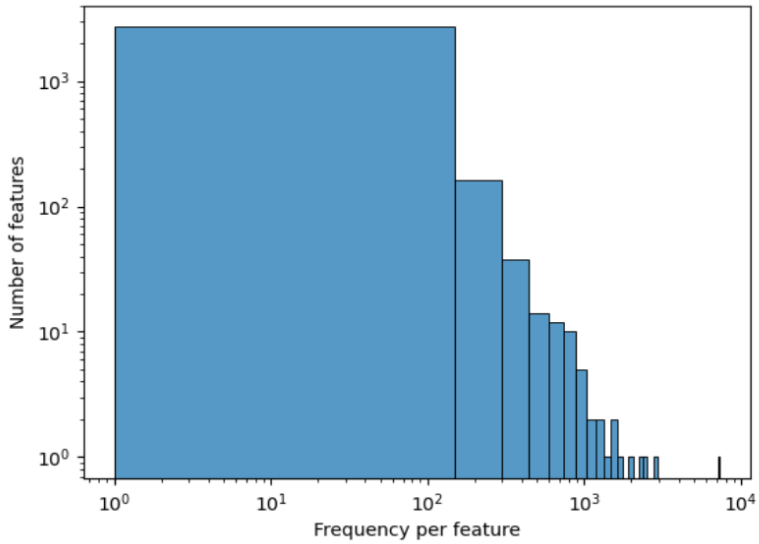

Supplementary Figure 5.1 - Distribution of ASV's frequencies.

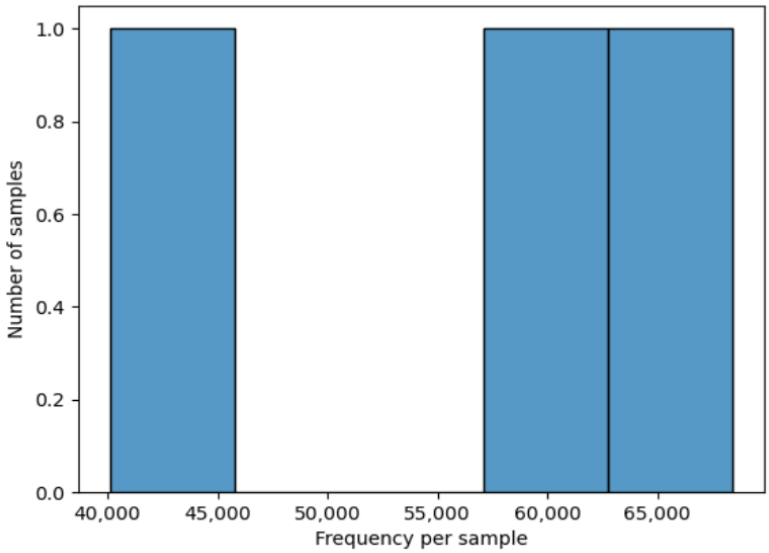

Supplementary Figure 5.2 - Distribution of ASV's frequencies for each sample.

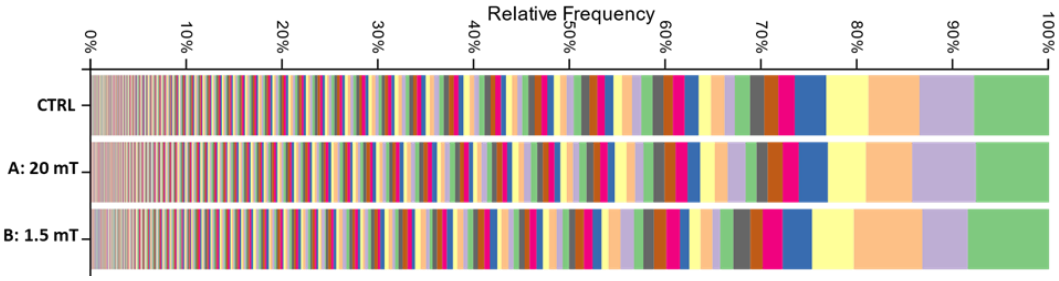

Supplementary Figure 5.3 – Complete Taxonomy BarPlot.

Supplementary Table 5.4 – Microbial community composition at genus level.

Genus level – Relative abundance (%)	**CTRL**	**A: 20 mT**	**B: 1.5 T**
Saprospiraceae specie	7.95	7.75	8.65
Saccharimonadales sp.	6.58	7.69	5.48
Rhodocyclaceae Family	5.38	4.85	7.14
Verrucomicrobiaceae specie	4.53	4.02	4.49
Nitrospira sp.	3.28	3.04	3.08
Pedosphaeraceae specie	2.73	2.27	3.23
Anaerolineae (Class)	2.65	3.25	2.20
Blastocatellaceae Family	1.83	1.48	1.44
Chitinophagales Order specie	1.78	1.76	1.97
Dechloromonas sp.	1.72	1.67	2.07
Prosthecobacter sp.	1.57	1.14	1.36
Bacteroidetes Family	1.54	1.60	1.38
Microscillaceae Family	1.51	1.33	0.98
Candidatus *Nomurabacteria* sp.	1.41	1.35	1.25
Candidatus *Moranbacteria* sp.	1.13	1.14	1.10
Caldilineaceae specie	1.09	1.88	0.83
Ignavibacteriales Order PHOS-HE36	1.04	0.90	1.26
Planctomycetota (Phylum) OM190	1.02	1.19	1.34
Zoogloea sp.	0.96	0.87	1.40
Vicinamibacteraceae sp.	0.91	0.76	0.95
Chloroflexi (Phylum)	0.88	0.82	0.69
Haliangium sp.	0.82	0.69	0.89
Ahniella sp.	0.78	0.73	0.65
Latescibacterota sp.	0.78	0.78	0.93
Phycisphaeraceae Family	0.78	0.65	0.64
Verrucomicrobiales FamilyDEV007	0.76	0.66	0.64
Comamonadaceae Family	0.75	0.73	0.89
Halieaceae Family	0.74	0.68	0.76

Lentimicrobium sp.	0.70	0.61	0.52
Flavobacteriales Family NS9_marine_group	0.68	0.66	0.65
Sphingobacteriales Family AKYH767	0.67	0.62	0.66
Hydrogenedensaceae sp.	0.67	0.59	0.60
Hassallia sp.	0.63	0.65	0.55
Candidatus *Soleaferrea* sp.	0.62	0.67	0.42
Ferruginibacter sp.	0.62	0.60	0.72
Polyangia (Class)	0.61	0.55	0.76
Rubinisphaeraceae Family specie	0.60	0.68	0.67
Parcubacteria sp.	0.60	0.52	0.60
Pirellulaceae Family specie	0.59	0.66	0.75
Synergistaceae Family specie	0.57	0.56	0.39
Vicinamibacterales Order specie	0.56	0.49	0.56
Thauera sp.	0.55	0.56	0.73
Blastocatellia (Class)	0.55	0.56	0.63
Sulfuritalea sp.	0.54	0.52	0.78
Candidatus *Accumulibacter* sp.	0.53	0.43	0.56
Bdellovibrionaceae Family OM27_clade	0.51	0.43	0.63
Gammaproteobacteria (Class) CCM19a	0.51	0.56	0.66
Pirellula sp.	0.50	0.72	0.54
Sphingorhabdus sp.	0.50	0.51	0.36
Fimbriimonadaceae sp.	0.49	0.57	0.32
Sphingobacteriales Order	0.49	0.50	0.56
Candidatus *Campbellbacteria* sp.	0.48	0.52	0.49
Novosphingobium sp.	0.46	0.52	0.32
Terrimonas sp.	0.46	0.41	0.56
Oligoflexia (Class) 0319-6G20	0.45	0.45	0.45
Oscillospirales Order	0.41	0.38	0.40
Candidatus *Competibacter* sp.	0.41	0.44	0.43
Woesearchaeales sp.	0.38	0.43	0.35
Bacteroidales Order	0.38	0.37	0.39
Anaerolinea sp.	0.38	0.35	0.22
Haliscomenobacter sp.	0.37	0.26	0.34
Phycisphaerae (Class) CCM11a	0.37	0.34	0.43
Gracilibacteria sp.	0.37	0.40	0.39
Burkholderiales Order	0.36	0.38	0.38
Defluviicoccus sp.	0.35	0.35	0.25
Rikenellaceae Family	0.34	0.33	0.29
Thermoanaerobaculaceae Family	0.33	0.34	0.32
Acidimicrobiia Order	0.32	0.34	0.32
Pseudomonadales (Class)	0.32	0.31	0.31

Anaerolineaceae Family specie	0.32	0.42	0.28
Planctomycetales Family specie	0.32	0.41	0.44
Blastopirellula sp.	0.31	0.37	0.25
Candidatus *Magasanikbacteria* sp.	0.31	0.24	0.24
Paludibaculum sp.	0.30	0.24	0.16
Tetrasphaera sp.	0.30	0.31	0.12
Lautropia sp.	0.30	0.31	0.25
Leptothrix sp.	0.29	0.25	0.30
Ignavibacteria (Class) SJA-28	0.28	0.25	0.40
Lentimicrobiaceae sp.	0.27	0.24	0.30
Saccharimonadaceae Family	0.27	0.31	0.24
Nitrosomonadaceae Family	0.27	0.29	0.32
Solirubrobacterales Order 67-14	0.25	0.28	0.18
Absconditabacteriales Order SR1	0.25	0.26	0.24
Elusimicrobia (Class)	0.24	0.25	0.23
Sphingomonadaceae specie	0.24	0.22	0.24
Hyphomonadaceae SWB02	0.24	0.18	0.10
Bdellovibrio sp.	0.24	0.29	0.19
Ottowia sp.	0.24	0.24	0.25
Acidobacteriae (Class)	0.24	0.26	0.12
Brevifollis sp.	0.24	0.17	0.22
Gemmatimonadaceae Family specie	0.23	0.21	0.22
Hirschia sp.	0.23	0.23	0.19
Stenotrophobacter sp.	0.23	0.25	0.20
Candidatus *Omnitrophus* sp.	0.23	0.22	0.27
Spirochaetaceae Family specie	0.23	0.23	0.26
Candidatus *Kaiserbacteria* sp.	0.21	0.23	0.28
Phaeodactylibacter sp.	0.21	0.15	0.26
Candidatu *Falkowbacteria* sp.	0.20	0.26	0.24
Reyranella sp.	0.20	0.24	0.13
Luteitalea sp.	0.20	0.21	0.15
Gemmataceae Family specie	0.20	0.21	0.25
Oikopleura sp.	0.19	0.14	0.19
Candidatus *Obscuribacter* sp.	0.19	0.15	0.24
Berkelbacteria sp.	0.18	0.25	0.17
Bryobacter sp.	0.18	0.17	0.13
Caldisericum sp.	0.18	0.14	0.12
Rhodoferax sp.	0.18	0.17	0.18
Parcubacteria (Class)	0.18	0.11	0.11
Paludibacter sp.	0.17	0.21	0.24
Spongiibacteraceae Family	0.17	0.14	0.16

Candidatus *Microthrix* sp.	0.17	0.41	0.12
Prolixibacteraceae Family specie	0.17	0.13	0.09
Sporomusaceae Family specie	0.17	0.20	0.20
Ilumatobacteraceae Family	0.17	0.17	0.12
Steroidobacteraceae Family specie	0.16	0.15	0.17
Hydrogenophilaceae Family specie	0.16	0.19	0.22
Alphaproteobacteria (Class) specie	0.16	0.15	0.11
Chitinivibrionia (Class) specie	0.16	0.20	0.14
Crocinitomix sp.	0.15	0.14	0.14
Marinilabiliaceae Family specie	0.15	0.16	0.14
Desulfobacterota (Phylum) specie	0.15	0.13	0.18
Nannocystis sp.	0.14	0.06	0.12
Longilinea sp.	0.14	0.18	0.10
Macellibacteroides sp.	0.14	0.06	0.15
Kapabacteriales sp.	0.14	0.11	0.14
Lacunisphaera sp.	0.13	0.13	0.16
Fimbriiglobus sp.	0.13	0.18	0.16
Kiritimatiellae (Class)	0.13	0.18	0.26
Spirochaetota (Phylum) MVP-15	0.13	0.11	0.17
Myxococcaceae Family	0.13	0.11	0.14
Gracilibacteraceae Family	0.13	0.13	0.14
Phaselicystis sp.	0.13	0.12	0.10
Christensenellaceae Family	0.13	0.16	0.11
Tepidisphaerales Order WD2101_soil_group	0.13	0.11	0.05
Trichococcus sp.	0.13	0.12	0.10
Desulfuromonadia (Class) PB19	0.12	0.09	0.13
Elusimicrobiota (Phylum)	0.12	0.11	0.11
Hahella sp.	0.12	0.09	0.12
WS4	0.12	0.11	0.06
LCP-89	0.11	0.14	0.12
Rhodanobacteraceae Family specie	0.11	0.06	0.14
Candidatus *Alysiosphaera* sp.	0.11	0.14	0.09
Sumerlaea sp.	0.11	0.16	0.10
Hungateiclostridiaceae Family specie	0.10	0.12	0.08
Polyangiales Order specie	0.10	0.09	0.19
Porticoccaceae Family C1-B045	0.10	0.07	0.12
Williamwhitmaniaceae Family Blvii28 wastewater sludge group	0.10	0.07	0.09
Holophagae (Class) Subgroup_7	0.10	0.10	0.10
Rhizobiales Incertae Sedis specie	0.10	0.09	0.07
Lactivibrio sp.	0.10	0.18	0.06
Opitutaceae Family	0.10	0.11	0.18

Blastocatella sp.	0.10	0.11	0.05
Desulfomicrobium sp.	0.09	0.09	0.11
Rhodopirellula sp.	0.09	0.11	0.07
Rhodobacter sp.	0.09	0.11	0.07
Vicinamibacteria (Class) Subgroup_17	0.08	0.11	0.10
Gemmata sp.	0.08	0.12	0.16
Aquabacterium sp.	0.08	0.06	0.10
Chitinophagaceae Family	0.08	0.02	0.05
Leptolinea sp.	0.08	0.11	0.00
Arenicellaceae specie	0.08	0.11	0.05
Sandaracinaceae specie	0.07	0.06	0.11
Halomonas sp.	0.07	0.08	0.07
Mycobacterium sp.	0.07	0.13	0.07
Thermomicrobiales Order	0.07	0.14	0.10
Microtrichales Order specie	0.07	0.09	0.05
Anaerovoracaceae Family	0.07	0.03	0.01
Actinomycetaceae Family specie	0.07	0.10	0.08
Sandaracinus sp.	0.07	0.05	0.07
Zixibacteria sp.	0.07	0.07	0.12
Izemoplasmataceae sp.	0.07	0.10	0.10
Pajaroellobacter sp.	0.07	0.07	0.07
Iamia sp.	0.07	0.09	0.06
Vampirovibrionales sp.	0.06	0.08	0.04
Acidovorax sp.	0.06	0.08	0.12
Halioglobus sp.	0.06	0.04	0.07
Microtrichaceae Family specie	0.06	0.09	0.05
Anaerovorax sp.	0.06	0.04	0.06
Obscuribacteraceae Family	0.06	0.06	0.09
Leptospiraceae Family RBG-16-49-21	0.06	0.07	0.04
Leptospiraceae sp.	0.06	0.05	0.03
Holophagaceae sp.	0.06	0.05	0.06
Peptostreptococcales-Tissierellales Order	0.06	0.06	0.07
Myxococcota (Phylum) bacteriap25	0.06	0.09	0.10
Acetobacteraceae Family specie	0.06	0.04	0.04
Flavobacterium sp.	0.06	0.06	0.05
Bifidobacterium sp.	0.06	0.05	0.03
Candidatus *Kerfeldbacteria* sp.	0.06	0.08	0.08
Arcobacter sp.	0.06	0.10	0.12
Flavobacteriaceae Family specie	0.06	0.04	0.04
Sericytochromatia sp.	0.06	0.04	0.09
Clostridium sp.	0.06	0.04	0.02

Lewinella sp.	0.05	0.04	0.07
Candidatus *Komeilibacteria* sp.	0.05	0.05	0.04
Ideonella sp.	0.05	0.05	0.07
Caldisericales Order	0.05	0.04	0.03
Propionivibrio sp.	0.05	0.06	0.05
Williamwhitmania sp.	0.05	0.05	0.05
Altererythrobacter sp.	0.05	0.05	0.04
Xanthobacteraceae Family specie	0.05	0.03	0.00
Cloacimonadales Order	0.05	0.03	0.07
Ruminococcaceae Family specie	0.05	0.02	0.01
Actinobacteria (Class)	0.05	0.14	0.08
Oligosphaeraceae Family Z20	0.05	0.04	0.03
Hyphomicrobiaceae Family	0.05	0.03	0.00
Roseimicrobium sp.	0.05	0.07	0.04
Dokdonella sp.	0.05	0.03	0.02
Syntrophomonadaceae Family	0.05	0.03	0.03
Caulobacteraceae Family specie	0.05	0.03	0.02
Pseudarcobacter sp.	0.05	0.09	0.09
Desulfobulbus sp.	0.05	0.03	0.06
Candidatus *Vogelbacteria* sp.	0.04	0.06	0.05
Acidaminobacter sp.	0.04	0.05	0.00
Romboutsia sp.	0.04	0.06	0.04
Bradymonadales sp.	0.04	0.06	0.07
Opitutus sp.	0.04	0.04	0.04
Rhizobacter sp.	0.04	0.04	0.04
Ramlibacter sp.	0.04	0.08	0.10
Treponema sp.	0.04	0.06	0.00
Filomicrobium sp.	0.04	0.07	0.00
Nocardioides sp.	0.04	0.04	0.00
Tepidisphaeraceae sp.	0.04	0.06	0.02
Oscillospiraceae Family NK4A214_group	0.04	0.04	0.04
Fibrobacterales Order	0.04	0.05	0.02
Clostridia sp.	0.04	0.06	0.03
Marinoscillum sp.	0.04	0.06	0.05
Aminicenantales sp.	0.04	0.05	0.13
Candidatus *Raymondbacteria* sp.	0.04	0.02	0.03
Ruminiclostridium sp.	0.04	0.09	0.03
Verrucomicrobiae (Class) LD1-PB3	0.04	0.03	0.02
Firmicutes (phylum) BRH-c20a	0.04	0.02	0.00
Candidatus *Lloydbacteria* sp.	0.04	0.03	0.02
Methanoregula sp.	0.04	0.05	0.07

Nitrosomonas sp.	0.04	0.04	0.09
Acinetobacter sp.	0.04	0.04	0.00
Kryptoniales Order BSV26	0.04	0.06	0.04
Turneriella sp.	0.04	0.03	0.02
Fimbriimonadales Order	0.04	0.04	0.01
Pseudomonas sp.	0.04	0.04	0.02
Candidatus *Xiphinematobacter* sp.	0.04	0.01	0.02
Candidatus *Azambacteria* sp.	0.03	0.04	0.06
Veillonella sp.	0.03	0.04	0.05
Holophagaceae Family	0.03	0.05	0.03
Phycisphaerales Order AKAU3564_sediment_group	0.03	0.02	0.04
Thioalkalispiraceae Family specie	0.03	0.03	0.09
Oligosphaerales Order Lenti-02	0.03	0.05	0.03
Roseimarinus sp.	0.03	0.03	0.01
Erysipelatoclostridiaceae Family UCG-004	0.03	0.03	0.04
Monoglobus sp.	0.03	0.03	0.04
Gastranaerophilales sp.	0.03	0.06	0.00
Candidatus *Solibacter* sp.	0.03	0.05	0.03
Smithella sp.	0.03	0.00	0.00
Chitinivorax sp.	0.03	0.03	0.03
Sphingobium sp.	0.03	0.01	0.01
Sphingomonas sp.	0.03	0.00	0.01
Fluviicoccus sp.	0.03	0.05	0.05
Mesorhizobium sp.	0.03	0.01	0.01
Clostridium sp.	0.03	0.04	0.00
Ferribacterium sp.	0.03	0.03	0.00
Beijerinckiaceae Family specie	0.03	0.02	0.03
Subdoligranulum sp.	0.02	0.06	0.04
Acidibacter sp.	0.02	0.02	0.03
Acidaminococcaceae Family specie	0.02	0.04	0.04
Methyloparacoccus sp.	0.02	0.02	0.00
Moraxellaceae Family	0.02	0.03	0.05
Collinsella sp.	0.02	0.02	0.02
Desulfovibrio sp.	0.02	0.02	0.00
Reyranellaceae Family specie	0.02	0.02	0.00
Endomicrobium sp.	0.02	0.02	0.03
Pseudorhodoplanes sp.	0.02	0.04	0.00
Paludibacteraceae Family specie	0.02	0.01	0.00
Oligoflexaceae Family specie	0.02	0.00	0.00
Halomonadaceae Family HdN1	0.02	0.01	0.02
Dehalococcoidia (Class) S085	0.02	0.03	0.01

Aeromonas sp.	0.02	0.00	0.00
Immundisolibacter sp.	0.02	0.01	0.00
Cloacibacterium sp.	0.02	0.01	0.02
Kouleothrix sp.	0.02	0.02	0.01
Rhizobiaceae Family specie	0.02	0.04	0.02
Syntrophus sp.	0.02	0.00	0.04
Victivallales Order	0.02	0.03	0.00
Rickettsiales AB1	0.02	0.02	0.00
Ruminococcus sp.	0.02	0.02	0.02
Chthoniobacter sp.	0.02	0.01	0.01
Margulisbacteria sp.	0.02	0.03	0.01
*Defluviimona*s sp.	0.02	0.00	0.00
Streptococcus sp.	0.02	0.04	0.03
Sumerlaeia (Class) specie	0.02	0.04	0.05
Roseomonas sp.	0.02	0.02	0.02
Sediminispirochaeta sp.	0.02	0.01	0.01
Limnochordaceae sp.	0.02	0.01	0.02
Polyangiaceae Family	0.02	0.03	0.07
Crenothrix sp.	0.02	0.01	0.01
Telmatocola sp.	0.02	0.01	0.01
Actinomyces sp.	0.02	0.04	0.03
Pedomicrobium sp.	0.02	0.02	0.00
Candidatus *Adlerbacteria* sp.	0.02	0.02	0.03
Peredibacter sp.	0.02	0.03	0.01
Azovibrio sp.	0.02	0.01	0.02
Micavibrionales Order specie	0.02	0.03	0.03
Planctomicrobium sp.	0.02	0.02	0.01
Terrimicrobium sp.	0.02	0.00	0.00
Sulfurospirillum sp.	0.02	0.02	0.03
Lactococcus sp.	0.02	0.02	0.03
Candidatus *Peregrinibacteria* sp.	0.02	0.04	0.02
Stella sp.	0.02	0.03	0.01
Fimbriimonadales Order	0.02	0.03	0.00
Gimesiaceae Family specie	0.02	0.02	0.02
Alcanivorax sp.	0.01	0.00	0.00
Anaerocella sp.	0.01	0.01	0.00
Kiritimatiellaceae Family MSBL3	0.01	0.01	0.02
Spirochaeta sp.	0.01	0.00	0.00
Cloacimonadaceae Family C-2	0.01	0.02	0.00
Sorangium sp.	0.01	0.00	0.02
Aridibacter sp.	0.01	0.00	0.03

Methanosaeta sp.	0.01	0.06	0.00
Conexibacter sp.	0.01	0.03	0.03
Dongia sp.	0.01	0.02	0.01
Blautia sp.	0.01	0.02	0.00
Chlamydiales Order cvE6	0.01	0.01	0.02
Ilumatobacter sp.	0.01	0.01	0.02
Candidatus *Uhrbacteria* sp.	0.01	0.01	0.01
Geobacter sp.	0.01	0.01	0.00
*Caulobacte*r sp.	0.01	0.00	0.00
Azospira sp.	0.01	0.00	0.00
Saccharofermentans sp.	0.01	0.01	0.01
Gordonia sp.	0.01	0.03	0.01
Sterolibacterium sp.	0.01	0.00	0.00
Ethanoligenenaceae Family	0.01	0.01	0.02
Chlamydiae (Class) LD1-PA32	0.01	0.01	0.00
Syntrophomonas sp.	0.01	0.00	0.02
Bacteroides sp.	0.01	0.00	0.01
Omnitrophales sp.	0.01	0.01	0.02
Rhodospirillaceae Family specie	0.01	0.01	0.00
Candidatus *Yonathbacteria* sp.	0.01	0.00	0.00
Roseiflexaceae Family specie	0.01	0.03	0.01
Candidatus *Captivus* sp.	0.01	0.01	0.00
Izemoplasmatales Order	0.01	0.01	0.00
Candidatus *Megaira* sp.	0.01	0.01	0.01
Rhodobacteraceae Family	0.01	0.00	0.03
Fusibacter sp.	0.01	0.02	0.00
Brachyspira sp.	0.01	0.01	0.00
Candidatus *Koribacter* sp.	0.01	0.00	0.00
Brevinema sp.	0.01	0.01	0.00
Patescibacteria (Phylum) WWE3	0.01	0.01	0.00
Atopobium sp.	0.01	0.00	0.00
Papillibacter sp.	0.01	0.02	0.01
Methanobrevibacter sp.	0.01	0.04	0.01
Cryomorphaceae specie	0.01	0.00	0.00
Peptococcaceae specie	0.01	0.00	0.00
Acetobacterium sp.	0.01	0.00	0.00
Butyricicoccaceae UCG-009	0.01	0.00	0.00
Candidatus *Peribacteria* sp.	0.01	0.00	0.00
Candidatus *Berkiella* sp.	0.01	0.01	0.00
Woesearchaeales Order	0.00	0.03	0.02
Babeliales sp.	0.00	0.00	0.00

Azoarcus sp.	0.00	0.01	0.00
Firmicutes specie	0.00	0.01	0.02
Tundrisphaera sp.	0.00	0.00	0.01
Micrarchaeales sp.	0.00	0.01	0.00
Armatimonadota (Phylum) specie	0.00	0.02	0.02
Methylacidiphilaceae Family specie	0.00	0.00	0.01
Luteolibacter sp.	0.00	0.02	0.00
Salinispira sp.	0.00	0.00	0.01
Candidatus *Bealeia* sp.	0.00	0.00	0.01
Hyphomicrobium sp.	0.00	0.03	0.04
Planctopirus sp.	0.00	0.01	0.00
Dechlorosoma sp.	0.00	0.00	0.00
Rhodospirillales Order specie	0.00	0.00	0.04
Planctomycetes (Class) specie	0.00	0.01	0.00
Diplorickettsiaceae Family	0.00	0.00	0.02
Spirosomaceae Family	0.00	0.00	0.00
Eubacteriaceae (Famuly)	0.00	0.02	0.00
Moduliflexaceae Family	0.00	0.00	0.00
Caedibacter sp.	0.00	0.01	0.01
Diaphorobacter sp.	0.00	0.00	0.00
Hypnocyclicus sp.	0.00	0.00	0.00
Thermomonas sp.	0.00	0.01	0.00
Lentimicrobiaceae Family	0.00	0.02	0.02
Isosphaeraceae Family specie	0.00	0.01	0.00
Pseudoxanthomonas sp.	0.00	0.00	0.02
Vibrio sp.	0.00	0.04	0.04
Spirochaetota (Class) V2072-189E03	0.00	0.01	0.01
Candidatus *Yanofskybacteria* sp.	0.00	0.01	0.00
Cerasicoccus sp.	0.00	0.00	0.00
Rhodothermaceae Family specie	0.00	0.00	0.00
Corynebacterium sp.	0.00	0.02	0.00
Georgfuchsia sp.	0.00	0.03	0.03
Gallicola sp.	0.00	0.00	0.00
Thermovirga sp.	0.00	0.01	0.00
Latescibacteraceae sp.	0.00	0.00	0.00
Bacteriovoracaceae Family	0.00	0.01	0.00
Methylopilaceae Family	0.00	0.02	0.00
Vicinamibacter sp.	0.00	0.00	0.00
Victivallaceae sp.	0.00	0.01	0.00
Candidatus *Jorgensenbacteria* sp.	0.00	0.00	0.01
Dysgonomonadaceae Family specie	0.00	0.01	0.00

Levilinea sp.	0.00	0.01	0.00
Pseudoalteromonas sp.	0.00	0.00	0.02
Paracoccus sp.	0.00	0.02	0.00
Syntrophorhabdus sp.	0.00	0.01	0.01
Gaiellales Order specie	0.00	0.00	0.00
Fibrobacteraceae Family	0.00	0.01	0.00
Geminicoccaceae Family	0.00	0.00	0.00
Sulfurovum sp.	0.00	0.00	0.00
Candidatus *Abawacabacteria* sp.	0.00	0.01	0.00
Desulfatiferula sp.	0.00	0.00	0.00
Methanobacterium sp.	0.00	0.01	0.00
Methylosarcina sp.	0.00	0.01	0.00
Desulforegula sp.	0.00	0.00	0.00
Actibacter sp.	0.00	0.01	0.00
Carnobacteriaceae Family	0.00	0.00	0.01
Cytophaga sp.	0.00	0.00	0.00
Polyangium sp.	0.00	0.00	0.01
Simplicispira sp.	0.00	0.01	0.00
Ercella sp.	0.00	0.02	0.00
Methanomassiliicoccaceae Family specie	0.00	0.00	0.01
Eggerthellaceae Family specie	0.00	0.00	0.00
Holdemanella sp.	0.00	0.00	0.00
Acidobacteriota (Phylum) Subgroup_22	0.00	0.00	0.00
Acetoanaerobium sp.	0.00	0.01	0.00
Nannocystaceae Family	0.00	0.00	0.01
Neochlamydia sp.	0.00	0.00	0.00
Lachnospira sp.	0.00	0.01	0.00
Rhodovarius sp.	0.00	0.01	0.01
Thiothrix sp.	0.00	0.00	0.00
Oleiagrimonas sp.	0.00	0.01	0.00
Micavibrionaceae Family specie	0.00	0.00	0.01
Tolumonas sp.	0.00	0.02	0.00
Leptotrichia sp.	0.00	0.00	0.01
Proteiniphilum sp.	0.00	0.01	0.00
Cavicella sp.	0.00	0.01	0.00

5.6. References

[1] F. Di Capua, D. Spasiano, A. Giordano, F. Adani, U. Fratino, F. Pirozzi, G. Esposito, High-solid anaerobic digestion of sewage sludge: challenges and opportunities, Appl. Energy. 278 (2020) 115608. https://doi.org/10.1016/j.apenergy.2020.115608.

[2] L. Spinosa, A. Ayol, J.C. Baudez, R. Canziani, P. Jenicek, A. Leonard, W. Rulkens, G. Xu, L. van Dijk, Sustainable and innovative solutions for sewage sludge management, Water (Switzerland). 3 (2011) 702–717. https://doi.org/10.3390/w3020702.

[3] N. Di Costanzo, A. Cesaro, F. Di Capua, M.C. Mascolo, G. Esposito, Application of high-intensity static magnetic field as a strategy to enhance the fertilizing potential of sewage sludge digestate, Waste Manag. 170 (2023) 122–130. https://doi.org/10.1016/j.wasman.2023.08.005.

[4] V. Khanh Nguyen, D. Kumar Chaudhary, R. Hari Dahal, N. Hoang Trinh, J. Kim, S.W. Chang, Y. Hong, D. Duc La, X.C. Nguyen, H. Hao Ngo, W.J. Chung, D.D. Nguyen, Review on pretreatment techniques to improve anaerobic digestion of sewage sludge, Fuel. 285 (2021) 119105. https://doi.org/10.1016/j.fuel.2020.119105.

[5] A. Cesaro, The valorization of the anaerobic digestate from the organic fractions of municipal solid waste: Challenges and perspectives, J. Environ. Manage. 280 (2021) 111742. https://doi.org/10.1016/j.jenvman.2020.111742.

[6] N. Di Costanzo, A. Cesaro, F. Di Capua, G. Esposito, Exploiting the nutrient potential of anaerobically digested sewage sludge: A review, Energies. 14 (2021) 1–25. https://doi.org/10.3390/en14238149.

[7] N. Di Costanzo, F. Di Capua, A. Cesaro, M.C. Mascolo, F. Pirozzi, G. Esposito, Impact of High-Intensity Static Magnetic Field on Chemical Properties and Anaerobic Digestion of Sewage Sludge, Waste and Biomass Valorization. 14 (2023) 2469–2479. https://doi.org/10.1007/s12649-022-01891-x.

[8] M.C. Mascolo, Effect of magnetic field on calcium carbonate precipitated in natural waters with prevalent temporary hardness, J. Water Process Eng. 41 (2021) 102087. https://doi.org/10.1016/j.jwpe.2021.102087.

[9] H. Wang, L. Guo, X. Ren, M. Gao, C. Jin, Y. Zhao, J. Ji, Z. She, Enhanced aerobic granular sludge by static magnetic field to treat saline wastewater via simultaneous partial nitrification and denitrification (SPND) process, Bioresour. Technol. 350 (2022) 126891. https://doi.org/10.1016/j.biortech.2022.126891.

[10] M. Zieliński, M. Zielińska, A. Cydzik-Kwiatkowska, P. Rusanowska, M. Dębowski, Effect of static magnetic field on microbial community during anaerobic digestion, Bioresour. Technol. 323 (2021). https://doi.org/10.1016/j.biortech.2020.124600.

[11] M. Zielinski, M. Debowski, J. Kazimierowicz, The effect of static magnetic field on methanogenesis in the anaerobic digestion of municipal sewage sludge, Energies. 14 (2021). https://doi.org/10.3390/en14030590.

[12] B. Zhao, H. Sha, J. Li, S. Cao, G. Wang, Y. Yang, Static magnetic field enhanced methane production via stimulating the growth and composition of microbial community, J. Clean. Prod. 271 (2020) 122664. https://doi.org/10.1016/j.jclepro.2020.122664.

[13] A.P.H.A. American Public Health Association, A.W.W.A. American Water Works Association, W.E.F. Water Environment Federation, Standard Methods for the Examination of Water and Wastewater, 24th ed., APHA Press, Washington DC, 2023.

[14] APAT CNR IRSA, Analytical Methods for Water, 2003.

[15] F. Di Capua, M.C. Mascolo, F. Pirozzi, G. Esposito, Simultaneous denitrification, phosphorus recovery and low sulfate production in a recirculated pyrite-packed biofilter (RPPB), Chemosphere. 255 (2020) 126977. https://doi.org/10.1016/j.chemosphere.2020.126977.

[16] J. Doyle, DNA Protocols for Plants, Mol. Tech. Taxon. (1991) 283–293. https://doi.org/https://doi.org/10.1007/978-3-642-83962-7_18.

[17] A. Corniello, M. Guida, L. Stellato, M. Trifuoggi, F. Carraturo, E. Del Gaudio, C. Del Giudice, G. Forte, A. Giarra, M. Iorio, F. Marzaioli, M. Toscanesi, Hydrochemical, isotopic and microbiota characterization of telese mineral waters (Southern Italy), Environ. Geochem. Health. 44 (2022) 1949–1970.

https://doi.org/10.1007/s10653-021-00806-4.

[18] A.E. Tugtas, U. Tezel, S.G. Pavlostathis, An extension of the Anaerobic Digestion Model No. 1 to include the effect of nitrate reduction processes, Water Sci. Technol. 54 (2006) 41–49. https://doi.org/10.2166/wst.2006.524.

[19] Y. Chen, J.J. Cheng, K.S. Creamer, Inhibition of anaerobic digestion process: A review, Bioresour. Technol. 99 (2008) 4044–4064. https://doi.org/10.1016/j.biortech.2007.01.057.

[20] S.G. Arhin, A. Cesaro, F. Di Capua, G. Esposito, Recent progress and challenges in biotechnological valorization of lignocellulosic materials: Towards sustainable biofuels and platform chemicals synthesis, Sci. Total Environ. 857 (2023) 159333. https://doi.org/10.1016/j.scitotenv.2022.159333.

[21] Y.M. Amha, M.Z. Anwar, A. Brower, C.S. Jacobsen, L.B. Stadler, T.M. Webster, A.L. Smith, Inhibition of anaerobic digestion processes: Applications of molecular tools, Bioresour. Technol. 247 (2018) 999–1014. https://doi.org/10.1016/j.biortech.2017.08.210.

[22] Y. Yashiro, S. Sakai, M. Ehara, M. Miyazaki, T. Yamaguchi, H. Imachi, Methanoregula formicica sp. nov., a methane-producing archaeon isolated from methanogenic sludge, Int. J. Syst. Evol. Microbiol. 61 (2011) 53–59. https://doi.org/10.1099/ijs.0.014811-0.

[23] F. Di Maria, The Recovery of Energy and Materials From Food Waste by Codigestion with Sludge: Internal Environment of Digester and Methanogenic Pathway, Elsevier Inc., 2017. https://doi.org/10.1016/B978-0-12-811413-1.00003-6.

[24] T. Islam, V. Torsvik, Ø. Larsen, L. Bodrossy, L. Øvreås, N.K. Birkeland, Acid-tolerant moderately thermophilic methanotrophs of the class Gammaproteobacteria isolated from tropical topsoil with methane seeps, Front. Microbiol. 7 (2016) 1–12. https://doi.org/10.3389/fmicb.2016.00851.

[25] N. Doronina, E. Kaparullina, Y. Trotsenko, The Family Methylophilaceae BT - The Prokaryotes: Alphaproteobacteria and Betaproteobacteria, in: E. Rosenberg, E.F. DeLong, S. Lory, E. Stackebrandt, F. Thompson (Eds.), Springer Berlin Heidelberg, Berlin, Heidelberg, 2014: pp. 869–880.

https://doi.org/10.1007/978-3-642-30197-1_243.

CHAPTER 7

Headspace micro-oxygenation as a strategy for efficient biogas desulfurization and biomethane generation in a centralized sewage sludge digestion plant

The content of this chapter has been submitted to Biomass and Bioenergy in 2023/09/29 and accepted for publication in 2024/02/28.

Abstract

This chapter evaluated the biological desulfurization of hydrogen sulfide (H_2S) from the biogas produced in a centralized digestion plant treating high-solid sewage sludge under thermophilic conditions. The findings of this study will provide valuable insights that serve as a practical tool for the management and design of oxygenation systems tailored for full-scale thermophilic digester applications.

7.1. Introduction

Anaerobic digestion (AD) is a biological process by which complex organic substrates, such as sewage sludge, are transformed into biogas, an energy vector, and digestate, a semi-solid residue that is nowadays considered a valuable source of organic matter and nutrients and can be used as a fertilizer [1,2]. The biogas is a well-known energetically valuable product that can be further processed to produce biomethane and/or thermal/electrical energy [3]. It typically contains 55–65% of methane (CH_4), 35–45% of carbon dioxide (CO_2), and small concentrations of other gases, including hydrogen sulfide (H_2S) in the range 50 - 5000 ppm [4]. H_2S in biogas commonly occurs due to the anaerobic fermentation of sulfur-containing organic molecules (i.e., proteins) and the activity of sulfate-reducing bacteria [5]. The presence of H_2S in biogas is often a limitation for downstream processing to generate energy, as H_2S oxidation can release harmful sulfur oxides (SO_x) in flue gases and create corrosive condensates that reduce the operational life of gas pipelines, combined heat and power (CHP) units, boilers, and biogas upgrading systems [6]. Moreover, dissolved sulfide is toxic to methanogens already at concentrations above 50 mg/L and may cause the inhibition of the AD process [7].

Depending on the use of biogas and required desulfurization performance, several biogas desulfurization technologies have been proposed: biological systems, as biotrickling filters and microaeration [8–10], adsorption media such as granular activated carbon [11,12], or wet scrubbing systems [13,14]. Adsorption and scrubbing processes require the replacement and disposal of spent media and large amounts of water or chemicals, making operation and maintenance more complex and expensive [6,7]. In contrast, biological methods involve lower operational costs with no need for

chemical addition [15] even if H_2S is chemically oxidized by O_2 in rate much faster that biological processes. Among these methods, the in-situ biological desulfurization consists in the injection of a limited flux of air or oxygen (O_2) into the digester headspace, which triggers the biological oxidation of the H_2S contained in the biogas to sulfate (SO_4^{2-}) and/or elemental sulfur (S^0) by the sulfur-oxidizing bacteria (SOB) growing on the internal surfaces exposed to O_2 [16].

The redox reactions described above are shown by **Eqs. (1)** and **(2)** [5,17].

$$HS^- + 2\ O_2 \rightarrow SO_4^{2-} + H^+ \quad \Delta G^0 = -732.6\ kJ/mol \qquad (1)$$

$$HS^- + 0.5\ O_2 \rightarrow S^0 + OH^- \quad \Delta G^0 = -169.4\ kJ/mol \qquad (2)$$

Despite the use of air can be considered the most convenient option for headspace micro-aeration, it leads to the dilution of the CH_4 produced during the process mainly due to the presence of nitrogen gas (N_2). This can turn in an important challenge especially if the target is biogas upgrading to biomethane. Indeed, the technical specification UNI/TS 11537:2019 regulating biomethane injection in the natural gas network sets the higher heating value and Wobbe index of biomethane are respectively above 34.95 ÷ 45.28 MJ/Sm^3 and 47.31 ÷ 52.33 MJ/Sm^3. Moreover, standards for CO_2, O_2 and H_2S contents respectively to ≤ 2.5 $\%_{mol}$, ≤ 0.6 $\%_{mol}$, and ≤ 5 mg/Sm^3 (about 3.5 ppm), are required.

Several technologies are today commercially available and implemented for biogas upgrading at commercial biogas plants, including water scrubbing as well as pressure swing adsorption (PSA) and membrane-based technologies [18–20]. In the PSA process, the raw biogas is compressed at 4-10 bars and introduced into an adsorption column in which CH_4 can be separated from the impurities via selective adsorption on the filter media. However, this approach has some drawbacks, including significant treatment costs due to both a rapid saturation of the adsorbent, high CH_4 losses, and complicated process design [21–23]. Similarly, membrane separation is affected by the rapid contamination of the membranes in the presence of certain volatile organic compounds (VOCs) [24], the use of high pressures during the process, and the high maintenance costs, which add to the high price of the membrane [23,25]. Water scrubbing exploits the different solubilities of CH_4, CO_2, and H_2S in water. Specifically, H_2S has the highest solubility in water (3.93 g/L at 20°C) followed by

CO_2 (1.69 g/L at 20°C) and CH_4 (0.02 g/L at 20°C). The key parameters that govern the process efficiency are the liquid/gas ratio, pressure, and temperature. In detail, high pressure and low temperature are advantageous to the absorption of gas components into water. Typically, CO_2 is absorbed in the process water and then removed through an air stripper so that the regenerated water can be reused for the absorption process. H_2S in water acts as a weak acid, as it generates an HS^- ion and releases a proton. This last aspect is crucial because in the presence of an acidic environment the absorption of CO_2 into water is disadvantaged and the water solution cannot be easily regenerated [23], causing the production of significant amounts of wastewater and the need for frequent water make-up in the water circuit, which increases water consumption. It also should be noted that N_2 and O_2 cannot be separated by water scrubbing because of their low solubility in water [26]. In view of biogas upgrading to biomethane in AD plants, it is therefore recommended to remove H_2S upstream to optimize CO_2 elimination via water scrubbing and inject small amounts of pure O_2 (micro-oxygenation) instead of air in the digester headspace to prevent N_2 contamination of biogas. Oxygen requirements for desulfurization should take into account the amount incorporated by the process water during the air stripping process for water regeneration, in order to comply with the limits for O_2 content in biomethane.

The present study investigates biological biogas desulfurization via in-situ micro-oxygenation during the centralized digestion of sewage sludge and evaluates the impact of O_2 injection on biogas upgrading to biomethane. The desulfurization performance of three full-scale thermophilic digesters working in series was monitored for 84 days under different O_2 injection regimes. The response times of the biological desulfurization system were verified through intermittent O_2 injection. The impact of decreasing O_2 injection on the composition of the microbial communities responsible for H_2S oxidation and methane production was also evaluated.

7.2. Materials and methods

7.2.1. Full-scale plant description

The full-scale AD plant is located near Pavia in Northern Italy and consists of three thermophilic reactors working in series and treating a high-solid (about 18.5% dry

weight) feedstock mainly composed of sewage sludge. A flow scheme of the full-scale thermophilic digestion plant is reported in **Figure 7.1**.

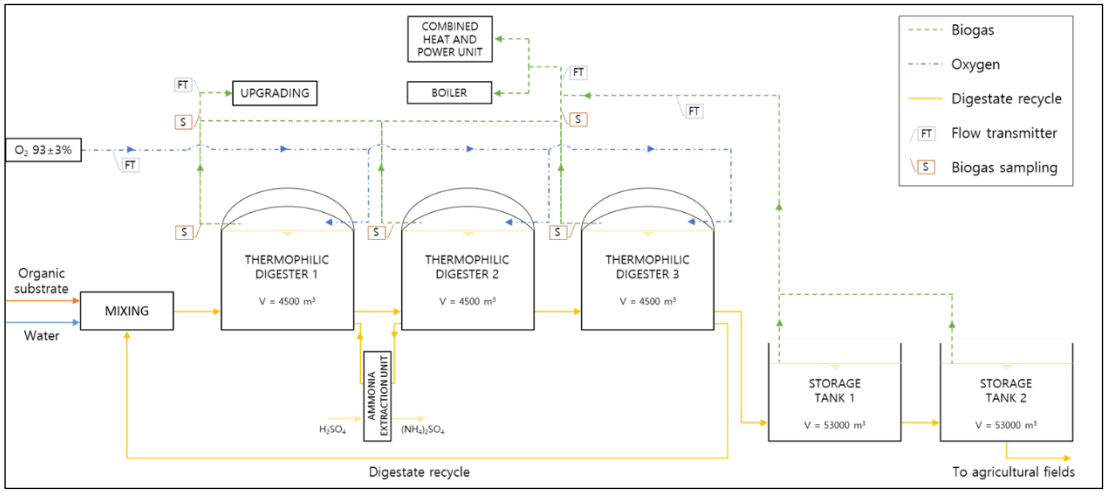

Figure 7.1 - Flow scheme of the full-scale thermophilic digestion plant. Biogas, oxygen, and digestate flows are indicated with lines of different colors.

The feedstock is heated by steam injection to 55(±2)°C and mixed with digestate coming from the third digester and water to reach a total solid (TS) content of 12-14% before being fed to the first digester. Mixing in the reactors is guaranteed by continuous digestate recirculation through external pumps. A side-stream ammonia air stripping unit is coupled to digester to control ammonia build-up in the system during the digestion process, as described by Di Capua et al. [27]. The digestate exiting from the third digester is collected in two 53,000 m^3 storage tanks prior to being used as fertilizer on agricultural fields. The biogas produced during the process is sent primarily to a CHP unit, which provides the electricity needed by the whole plant, and secondarily to a boiler which guarantees the heat to maintain thermophilic temperatures in the digesters. The excess biogas is sent to an upgrading unit to produce biomethane. Once the treatment capacity of the upgrading unit is filled, the possible surplus of biogas is sent to the CHP to generate electricity destined to the national grid. In-situ micro-oxygenation was performed by dosing O_2 with a 93(±3)% purity (the rest being N_2, argon and CO_2) in the headspace of the digesters, thus replacing the previous technique consisting in dosing air. O_2 was produced by feeding air to a PSA unit,

ensuring a continuous O_2 supply with a maximum flow rate of 3.5 Nm^3/h. The O_2 flow was controlled by glass tube flowmeters (ASA, Italy). The desulfurized biogas extracted from the digester was dewatered, compressed, and treated in an activated carbon filter prior to feeding the upgrading unit. The latter consisted of a water scrubbing unit with a maximum capacity of 600 Nm^3/h of raw biogas and was formed by three columns: an absorption column operating at 4.5-6.5 bar and liquid-gas ratio of 0.21(±0.04) v/v, a flash column operating at 1.1-1.4 bar, and a stripping column fed with air to regenerate the process water.

7.2.2. Experimental design

The study covered a period of 84 days divided in four different experimental periods. During the study, the plant treated about 34,500 ton of feedstock composed of 90% of sewage sludge from municipal and industrial (agrifood industry) wastewater treatment plants and 10% of co-products of source segregated domestic food waste. The main operational conditions of the AD plant, including O_2 supply, during the experimental campaign are described in **Table 7.1**.

Table 7.1 - Operational conditions of the full-scale thermophilic digesters during the study.

Parameter	Unit of measure	Start-up phase	Period 1	Period 2	Period 3	Period 4
Operational time	days	0-21	22-42	43-56	57-70	71-84
O_2 flow	m^3/week	86.4(±8.9)	94.4(±1.0)	74.1(±0.9)	53.8(±4.8)	27.5(±0.6)
HRT	d	27.5	26.7	22.0	21.5	22.1
OLR	kg VS/m^3d	3.3	3.4	4.3	4.4	4.4

After a start-up phase, dedicated to testing and validating the O_2 injection system, the O_2 flow rate injected in the digesters was gradually decreased from 94.4(±1.0) to 27.5(±0.6) m^3/week, and the desulfurization and digestion performances of the plant evaluated by daily and weekly measurements. During the study, the HRT and OLR were in the range of 21.5-27.5 d and 3.3-4.4 kg VS/m^3d, respectively (**Table 7.1**).

7.2.3. Monitoring and analytical methods

Biogas composition in the three digesters and upstream the main biogas pipeline was monitored five times/day using an Optima 7 portable biogas analyzer (MRU GmbH, Germany). The O_2 content in the biogas sent to the upgrading unit was continuously measured through an O_2 transmitter Senz-Tx (NTRON, Ireland). The composition of the biomethane produced with the upgrading unit was provided by an assembled skid (Endress+Hauser, Switzerland). This system is composed by two gas analysers with tunable diode laser absorption spectroscopy for monitoring H_2S (Mod. SS2100i-1) and water dew point (Mod. J22), an O_2 analyser (GPR1500 GB, MICHELL, UK), and a gas chromatograph (NGC8206, ABB, Switzerland).

Feedstock and digestate samples were periodically collected for volatile solids (VS) and TS analyses, which were carried out according to standard methods [28]. Volatile fatty acids (VFAs) and carbonate alkalinity (defined as the proton accepting capacity of the carbonate weak acid subsystem and indicated as H_2CO_3* alkalinity) concentrations in the digestate were measured as described by Lahav et al. [29].

The reported H_2S concentration was monitored upstream the main biogas pipeline and calculated as a weekly average concentration, according to Eq. (3), and reported with the corresponding standard deviation.

$$\overline{H_2S} = \sum_{i=1}^{n} H_2S_i / n \qquad (3)$$

with “n”, the number of measurements performed during the observation week.

7.2.4. Microbial community characterization using Next Generation Sequencing

Samples of 50 mL for the identification of microbial communities were collected in triplicate from the surface and the wall of the three thermophilic digesters (**Figure 7.2**) and stored at -20°C.

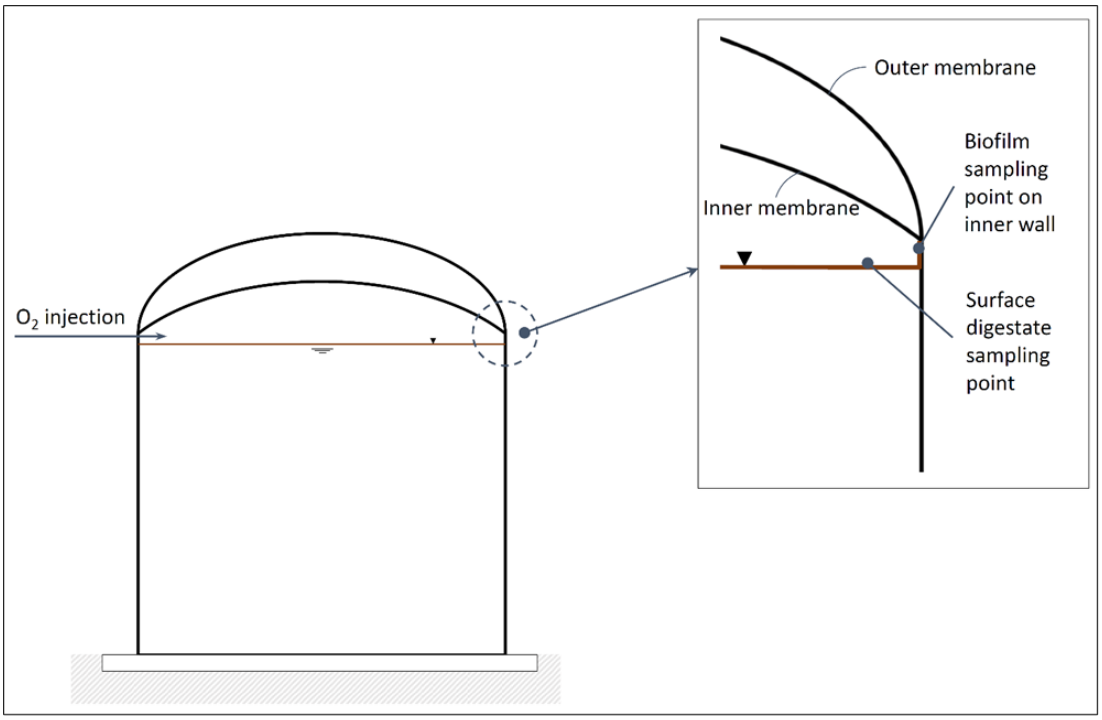

Figure 7.2 - Sampling point for the identification of microbial communities in the three thermophilic digesters.

Total DNA extraction was performed to sequence the genome of the whole microbiota, using Next Generation Sequencing (NGS), targeting bacterial 16S rRNA gene. For samples under analysis, 10 g were aliquoted and centrifuged to extract DNA, transferring 2 mL supernatant in sterile vials containing 0.5 g glass beads. The recovery of total DNA was performed using CTAB extraction protocol [30]; extracted DNA samples were amplified employing PCR, utilizing V3 and V4 primers, complementary to the V3-V4 variable region of 16S rRNA bacterial gene (V3: TCGTCGGCAGCGTCAGATGTGTATAAGAGACAGCCTACGGGNGGCWCGAG; V4: GTCTCGTGGGCTCGGAGATGTGTATAAGAGACAGGACTACHVGGGTATCTAATCC), and then sequenced with NGS analysis employing MiSeq Illumina platform, with 2 × 300 bp paired end, 600 cycles, according to manufacturer's instructions (Illumina MiSeq, USA). The diversities in the microbial communities data were evaluated, using weighted UniFrac distance and ANOVA (using Bray Curtis distance, Mothur), by anosim [31].

7.3. Results and discussion

7.3.1. Desulfurization performance of headspace micro-oxygenation

The temporal profiles of O_2 dosage, H_2S concentration, and biogas produced from the three thermophilic digesters monitored in this study are shown in **Figure 7.3**.

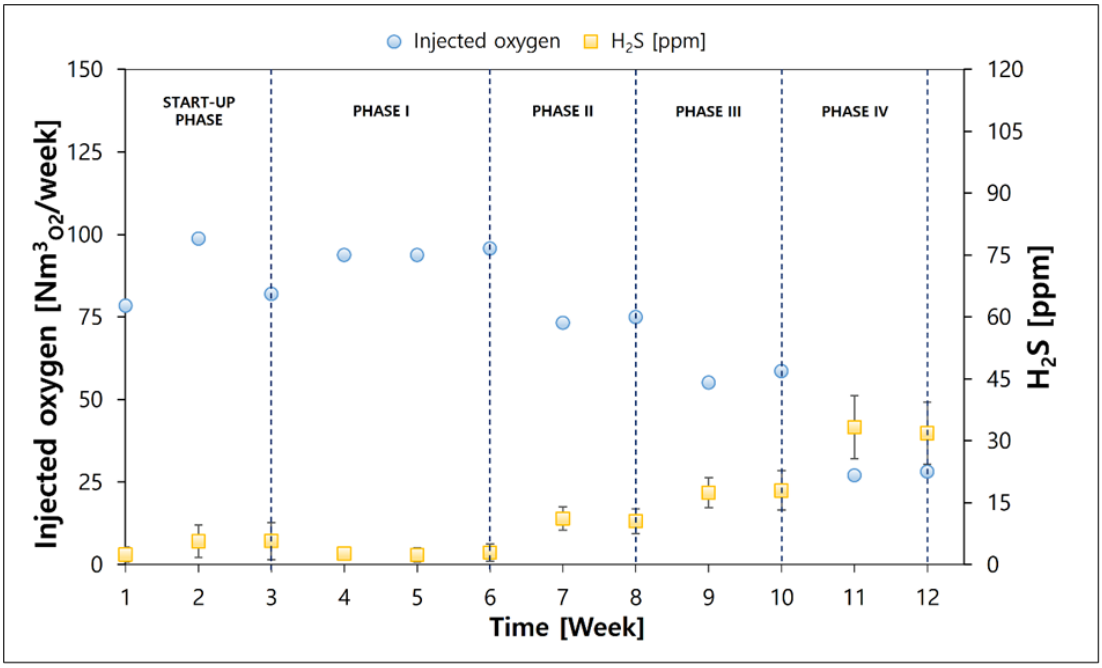

Figure 7.3 - Temporal profiles of injected O_2, biogas flows, and average H_2S levels in the produced biogas.

H_2S concentration in the produced biogas was 2.6(±0.3) ppm during the first experimental period, when O_2 was dosed at approximately 1 NL/Nm^3 biogas to the digester headspace. H_2S concentration in the biogas during this period was already compliant with the admissible limit for biomethane according to UNI/TS 11537:2019. Reducing the O_2 flow rate to 0.59(±0.03) NL/Nm^3 biogas in period 2 increased the H_2S levels in the biogas to >10 ppm and up to 32.6(±0.7) ppm in the last experimental period when O_2 dose was decreased to 0.19(±0.01) NL/Nm^3 biogas (**Figure 7.3**). Based on the obtained data, a linear relationship (R^2 = 0.97) between the logarithmic of the residual H_2S concentration in biogas and the oxygen dose was observed, as outlined in **Figure 7.4**.

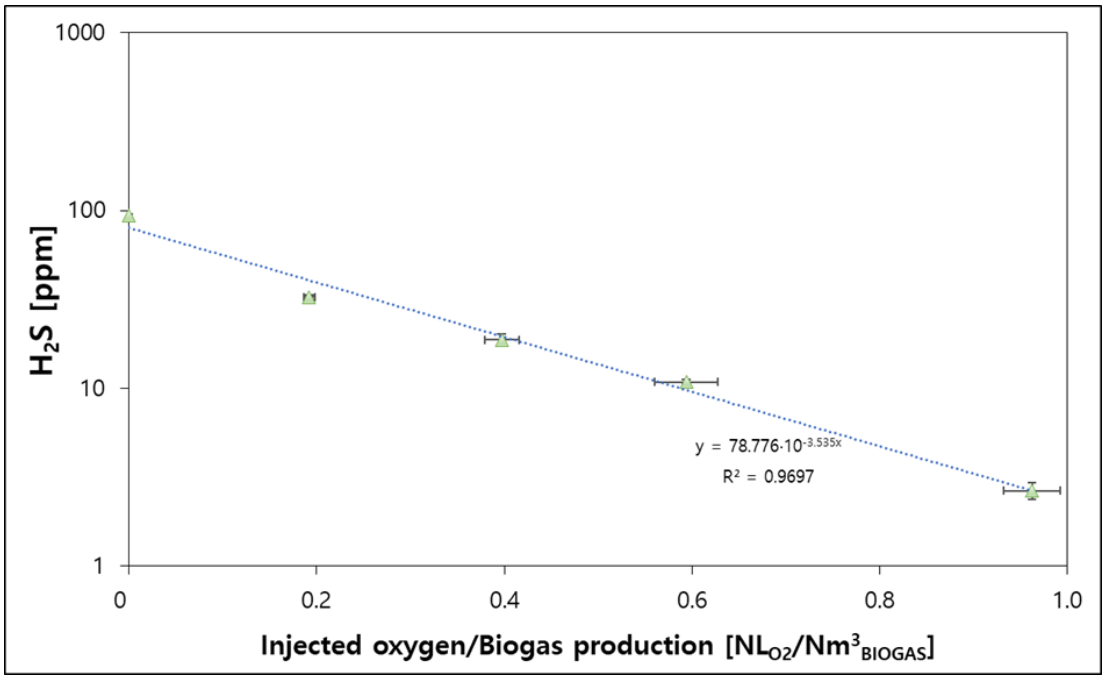

Figure 7.4 - Relationship between the residual H_2S concentration in biogas (logarithmic axis) and the ratio between injected O_2 and biogas produced from the three thermophilic digesters.

It should be pointed out that a specific logarithmic relationship between H_2S concentration and O_2 dosage can be defined for every plant, as it depends on the feedstock, operational conditions, and reactor configuration. This relationship can provide a decision-making tool indicating an optimal O_2 dosing for desulfurization, which takes into account the daily fluctuation of the produced biogas, and can help plant operators to reduce the costs for oxygenation while improving biogas quality.

Figure 7.4 also shows that the H_2S concentration without O_2 injection in the biogas was estimated to be around 100 ppm. This value is lower than that reported in other studies for AD plants treating sewage sludge [16,32,33], which could be related to the presence of the ammonia stripping unit. Specifically, during the AD process the ammonia content in the digestate is controlled via a side-stream ammonia stripping with air as stripping agent. Within this process, part of the H_2S contained in the digestate can be stripped together with ammonia and reduce the H_2S content of the

biogas. As a consequence of the low H_2S levels, the specific O_2 dosage was lower compared with previous experiences. For instance, Kraakman et al. [32] removed over 80% of the H_2S from the biogas under microaerobic condition at full scale by providing an amount of O_2 of about 0.26 – 0.70 L per L of feed sludge (i.e., 0.86 – 2.04 L of injected O_2 per Nm^3 of biogas produced). In another study, Jeníček et al. [33] reported that a H_2S removal efficiency of about 99% was achieved in 7 full-scale microaerobic digesters when 6.72 L of O_2 were fed per Nm^3 of biogas produced. Similarly, Kobayashi et al. [16] indicated a complete desulfurization at a O_2 dosage of 4.65 L per Nm^3 of biogas produced in a full-scale anaerobic digester. On the other hand, the mass of O_2 required per g of H_2S oxidized observed in this study was higher than that reported in previous experiences. Based on the data collected during the test, it was possible to estimate an O_2 mass required of 3.99 g per g of H_2S oxidized (4.25 mol O_2/mol H_2S). This ratio is approximately twice compared to that estimated according to the stoichiometry (**Eq. 1**) and to that reported by Jeníček et al. [33] for biogas desulfurization during conventional AD of sewage sludge, being respectively of 2 and 2.02 g O_2/g H_2S (on molar basis, 2 and 2.15 mol O_2/mol H_2S). This difference can be associated to the oxidation of organic compounds (i.e., VOCs including alkanes and aromatic hydrocarbons) in addition to H_2S within the biogas. Indeed, centralized AD can lead to the generation of higher concentrations of VOCs due the high solid content of the sludge entering the process [34]. The higher O_2/H_2S ratio estimated in this study is of fundamental importance for the design of the desulfurization system of full-scale centralized plants performing AD of high-solid (dewatered) sewage sludge, as it indicates that O_2 dosage should be doubled compared to conventional AD to ensure satisfactory biogas desulfurization.

The results of the intermittent O_2 feeding to the digester headspace are illustrated in **Figure 7.5**.

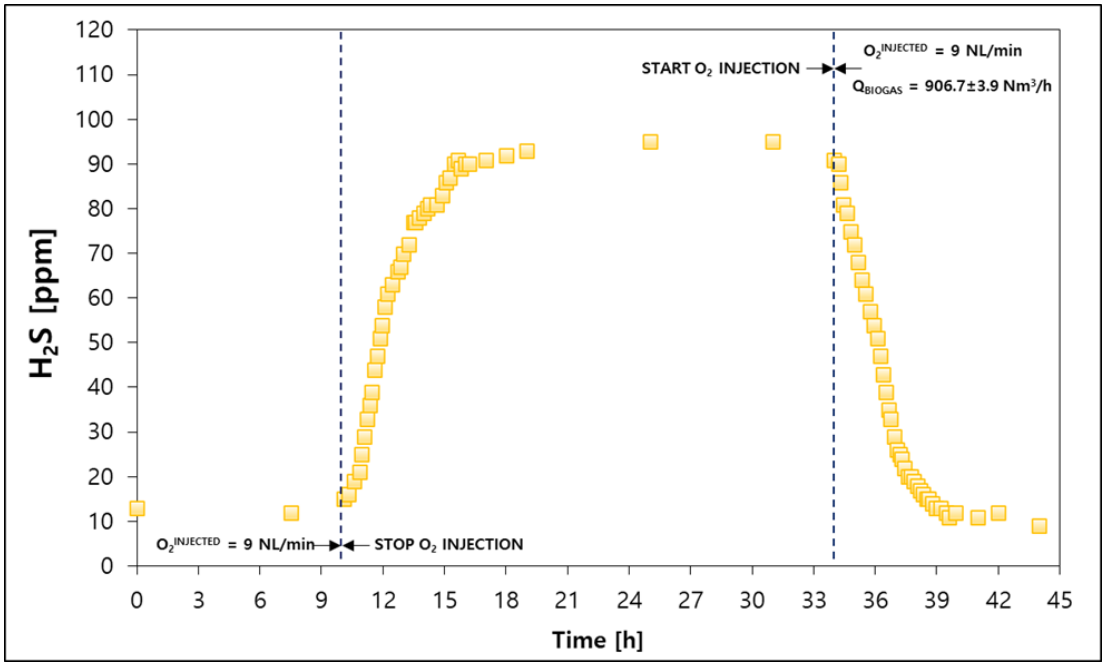

Figure 7.5 - H_2S build-up and consumption in the biogas collected from the three digesters during the intermittent oxygenation test.

After stopping O_2 injection, H_2S concentration in biogas increased gradually from about 13 ppm to a maximum of 95 ppm within 9 hours. After reinjecting O_2 at a flow rate of 0.55 NL/Nm^3 biogas, H_2S dropped to a stable value of about 10 ppm in 5 hours. The test revealed that H_2S build-up in the digester as well as the response time to the restart of oxygen feeding after a period of interruption occurred within 10 hours. This information is useful for plant operators as it indicates a time interval for interventions to prevent reaching high H_2S levels in the biogas which could deteriorate biogas quality in view of its upgrading to biomethane.

7.3.2. Impact of micro-oxygenation on AD process and biomethane quality

During the experimental campaign, no detrimental impact due to headspace micro-oxygenation or due to the anticipated reduction in redox potential within the reactor environment by the presence of sulfide in anaerobic digesters [35] were observed on the AD process (**Table 7.2**).

Table 7.2 - Biogas production and composition under the different conditions tested in this study.

Parameter	Unit of measure	Start-up phase	Period 1	Period 2	Period 3	Period 4
Operational time	days	0-21	22-42	43-56	57-70	71-84
Biogas production	Nm^3/week	96,207±6,305	98,276±4,094	125,278±8,611	138,788±2,226	143,315±292
Specific O_2 injection	NL O_2/Nm^3 biogas	0.95±0.15	0.96±0.03	0.59±0.03	0.40±0.02	0.19±0.01
CH_4	%	63.9±0.9	63.7±1.1	64.8±0.9	64.2±0.9	63.8±1.5
CO_2	%	36±0.7	36.3±0.8	35.3±0.8	35.6±0.5	36±0.9
H_2S	ppm	5.7±0.1	2.6±0.3	10.8±0.3	18.7±1.5	32.6±0.7
H_2S removal	%	95.4±1.5	98.2±1.3	89.2±0.3	81.3±1.5	67.4±0.7
Residual O_2	%	< 0.2	< 0.2	< 0.2	< 0.2	< 0.2
VFAs [a]	g HAc/kg digestate	0.49±0.08	0.55±0.05	0.72±0.06	0.78±0.05	0.82±0.04
Alkalinity [a]	g $CaCO_3$/kg digestate	10.4±0.5	10.7±0.2	10.7±0.1	10.7±0.2	11.1±0.3

The total VFA and carbonate alkalinity at the outlet of the third digester remained stable at a daily average of 0.68(±0.14) g HA_c/kg digestate and 10.7(±0.4) g $CaCO_3$/kg digestate. Similar results were reported in previous studies [36–38], indicating that injecting small quantities of oxygen in the digester headspace does not inhibit the anaerobic degradation of the organic matter contained in the sludge. Besides the limited amount of injected oxygen, O_2 diffusion limitation into the digestate and the rapid O_2 consumption by autotrophic SOB and facultative or aerobic microorganisms thriving closer to the surface can also play a role in protecting strictly anaerobic microorganisms. Also, some methanogens (e.g., the genera *Methanosarcina* and *Methanocella*) have shown the ability to survive to the presence of O_2 [39]. Specifically, as reported by Nguyen and Khanal [40] these microorganisms could survive after exposure of up to 500 μM H_2O_2, 1 h of aeration, and O_2 in headspace at 5% v/v, or dissolved oxygen up to 5.6 mg/L.

Biogas upgrading to biomethane started at an O_2 dosage of 0.7±0.1 NL/Nm^3 biogas in the headspace of the three full-scale digesters, and the quality and composition of the produced biomethane was monitored for 30 days. The applied O_2 dosage (0.7±0.1 NL/Nm^3 biogas) ensured the production of biomethane complying with the specifications required for its use (**Table 7.3**).

Table 7.3 - Composition and properties of biomethane generated by the upgrading unit compared with UNI/TS 11537:2019 specifications.

Parameter	Unit	This study	UNI/TS 11537:2019
Higher Heating Value	MJ/Sm^3	36.86±0.1	34.95 ÷ 45.28
Wobbe Index	MJ/Sm^3	48.73±0.36	47.31 ÷ 52.33
CH_4	%mol	97.7±0.21	≥ 96
CO_2	%mol	1.32±0.31	≤ 2.5
O_2	%mol	0.33±0.05	≤ 0.6
H_2S	mg/Sm^3	0.03±0.02	≤ 5

Reducing O_2 dosage would increase H_2S concentration above the limits imposed by the technical specification (UNI/TS 11537:2019) for biomethane quality, while increasing O_2 dosage above the tested range (≥1 NL O_2/Nm^3 biogas) may result in excess residual O_2. It should be noted that the O_2 content (0.33±0.05%) reported in **Table 7.3** is due to the contribution of the air stripping column for CO_2 removal, since the residual O_2 in the raw biogas fed to the upgrading unit was constantly below the detection limit of 0.1%.

7.3.3. Sulfur-oxidizing communities in the digester headspace

The taxonomic composition at family level of the microbial communities within the three digesters (**Figure 7.6, Supplementary Table 7.1)** included 5 main groups (with relative abundances above 1%) that can be classified as SOB: *Lentimicrobiaceae*, *Caldicoprobacteraceae*, *DTU014 (Firmicutes)*, *Syntrophomonadaceae*, and *Rhodobacteraceae*.

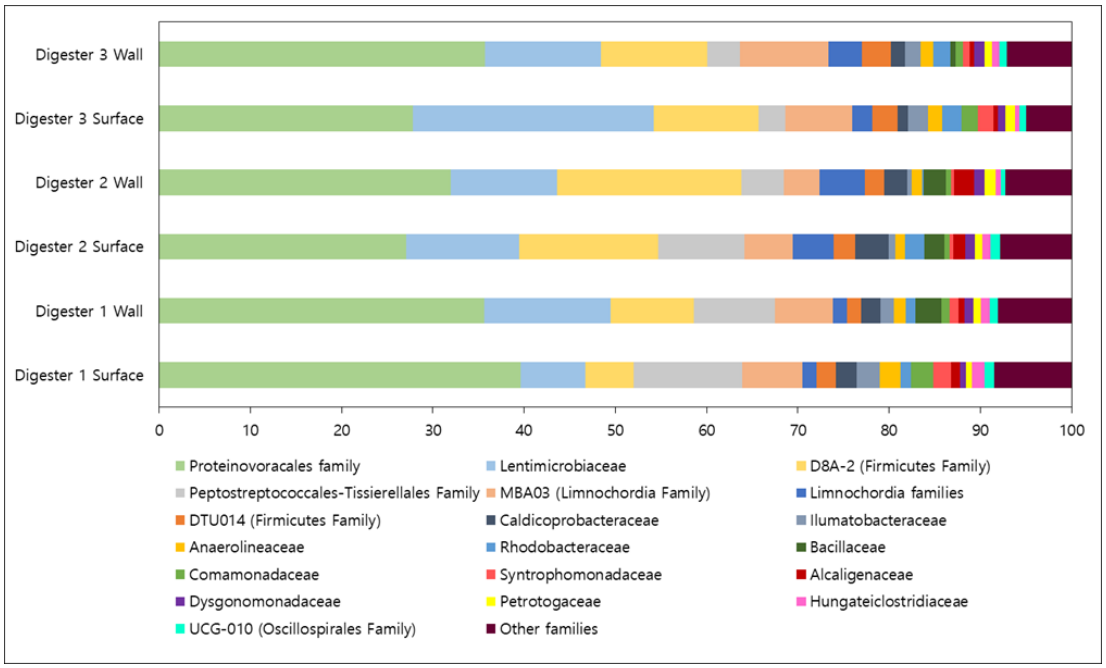

Figure 7.6 - Microbial community composition characterized in the three digesters at family level (relative abundances >1%).

Lentimicrobiaceae, represented by the genus *Lentimicrobium* (**Supplementary Table 7.2**), was the dominant family, among those classified as SOB [41,42], in all collected samples collected being present at relative abundances between 7.1% and 26.4%. With reference to the Digester 2 and Digester 3, *Lentimicrobiaceae* showed higher relative abundances in the samples collected from the surface (12.4% and 26.4%, respectively), compared to those sampled from the inner walls (11.6% and 12.7%, respectively). The higher concentration of macro- and micro-nutrients in the digestate likely stimulated the growth of SOB and may explain the higher relative abundance of these bacteria on the digestate surface then on the internal walls. Indeed, the intake of water and nutrients necessary for the optimal growth of SOB is continuously provided by the digested sludge and, therefore, more available on the surface compared to the walls of the digester [16]. Conversely, the relative abundance of SOB on the digestate surface of Digester 1 was half (7.1%) than that on the internal walls (13.9%). *Caldicoprobacteraceae*, represented by the genus *Caldicoprobacter* (**Supplementary Table 7.2**), were detected in all samples with similar relative abundances of 1.2-3.6%.

Bacteria belonging to *Caldicoprobacteraceae* are classified as autotrophic and capable of oxidizing sulfide and thiosulfate and of accumulating S^0 extracellularly [43]. The *DTU014* family was present in the three digesters with roughly comparable values ranging from 1.5% to 3.2%. Microorganisms belonging to this family have been previously described as syntrophic acetate oxidizing bacteria [44,45] and typically found in full-scale anaerobic digesters even with high ammonia levels [46]. Two other families of SOB, i.e., *Syntrophomonadaceae* and *Rhodobacteraceae,* referred as responsible for H_2S oxidation in biogas [47,48], were also present. Both were found to be predominant in the samples collected from the digestate surface (0.4-2% and 1.1-2.1%, respectively) compared to the samples from the digester wall (0.4-1% and 0.2-1.9%, respectively). Interestingly, none of the main SOB identified by Kobayashi et al. [16] as responsible for H_2S oxidation in anaerobic digesters and populating the digester walls, i.e., *Halothiobacillus neapolitanus* and *Sulfurimonas denitrificans*, were detected in the microbial communities of the three digesters analyzed in this study. It should be noted that the two applications referred to AD performed at different temperatures (thermophilic vs mesophilic) and with a different feedstock (sewage sludge vs cow manure). These differences were most likely responsible for the different composition of the microbial communities in the digesters. As an example, *Caldicoprobacter* is a thermophilic bacterium, while *Sulfurimonas* and Halothiobacillus prefer moderate temperatures (28-35°C) [49].

Besides SOB, other bacteria involved in the sulfur cycle were observed in the digesters, although at relative abundances less than 0.5% (**Supplementary Table 7.1 – 7.2**). For instance, sulfur-reducing bacteria including *Desulfitobacteriaceae*, *Desulfuribacillaceae*, and *Dethiobacteraceae* [50] were identified. These bacteria are strictly anaerobes and can reduce oxidized sulfur compounds to H_2S or S^0. The internal walls were also rich in fermentative microorganisms, whose presence should be attributed to digestate spraying. In terms of fermentative microorganisms, the most abundant families found on both surface and internal walls (27.1-39.6%) of the three digesters belong to the class of *Proteinovoracales*, gathering well-known haloalkaliphilic anaerobic bacteria able to ferment proteinaceous substrates to produce VFAs and hydrogen [51].

7.3.4. Energy demand and operational remarks

In this study, calculations on the energetic need of the descried in-situ desulfurization system were quantified based on an observation period of two months. The specific energy consumption was estimated, based on data collected by the electricity meter, as 5.9 Wh per Nm^3 of produced biogas when applying an O_2 dose of 0.7(±0.1) NL/Nm^3 biogas. This value is lower than that of 9.4 Wh per Nm^3 of produced biogas, required for the injection of concentrated O_2 from PSA generators, reported by Díaz et al. [52], who compared this scenario to other microaerobic scenarios (injection of pure O_2 from cryogenic tanks and air injection) in industrial-scale 5,000 m^3 anaerobic digesters. The energy demand for in-situ biological desulfurization by pure O_2 injection was found to be slightly higher than that established by Giordano et al. [5] with the same AD plant by using air to remove H_2S. Indeed, the authors reported that headspace microaeration performed by side channel blowers required a specific electric consumption of 4.1 Wh per Nm^3 of produced biogas. Despite the slightly higher energy demand of micro-oxygenation compared to microaeration, dosing pure O_2 can be preferred in view of the subsequent biogas upgrading to biomethane, as CH_4 dilution by N_2 is prevented.

7.4. Conclusions

Micro-oxygenation provided biogas complying with O_2 and H_2S specifications for biomethane in a centralized AD plant treating sewage sludge. An O_2 dose of 0.96(±0.03) NL/Nm^3 biogas was estimated for complete biogas desulfurization. The response to intermittent O_2 injection for full recovery of desulfurization performance was within 10 hours. H_2S oxidation was driven by SOB developed both on the digester surface and internal walls. No negative impact on AD was observed at varying O_2 dose. Although energy demand for micro-oxygenation was estimated to be slightly higher than for microaeration, using O_2 is strongly recommended if biogas upgrading to biomethane is targeted.

7.6. Supplementary materials

Supplementary Table 7.1 - Microbial community percentage composition, at family level, of the digestate surface and internal walls of the three digesters.

Family (Order/Phylum)	Dig. 1 Surface	Dig. 1 Wall	Dig. 2 Surface	Dig. 2 Wall	Dig. 3 Surface	Dig. 3 Wall
Proteinovoracales	39.60	35.64	27.08	31.98	27.83	35.73
Peptostreptococcales-Tissierellales	11.93	8.92	9.40	4.61	2.95	3.56
Lentimicrobiaceae	7.10	13.86	12.39	11.61	26.37	12.71
MBA03 (Limnochordia)	6.54	6.32	5.28	3.94	7.36	9.74
D8A-2 (Firmicutes)	5.29	9.06	15.25	20.21	11.47	11.63
Ilumatobacteraceae	2.56	1.45	0.78	0.49	2.16	1.67
Comamonadaceae	2.43	0.84	0.54	0.56	1.78	0.80
Anaerolineaceae	2.28	1.30	0.99	1.17	1.55	1.38
Caldicoprobacteraceae	2.27	2.14	3.62	2.50	1.18	1.59
DTU014 (Firmicutes)	2.08	1.54	2.37	2.13	2.70	3.16
Syntrophomonadaceae	2.03	1.03	0.44	0.40	1.72	0.77
(Limnochordia)	1.59	1.58	4.54	4.95	2.19	3.65
Hungateiclostridiaceae	1.34	0.99	0.89	0.62	0.56	0.85
Rhodobacteraceae	1.12	1.03	2.13	0.16	2.14	1.90
UCG-010 (Oscillospirales)	1.06	0.89	1.02	0.48	0.70	0.79
Alcaligenaceae	0.91	0.66	1.28	2.15	0.50	0.46
SRB2 (Thermoanaerobacterales)	0.87	0.92	1.22	0.76	0.51	0.58
Halanaerobiaceae	0.78	0.36	0.07	0.06	0.63	0.37
M55-D21 (Limnochordia)	0.77	0.59	0.39	0.50	0.69	1.22
Dysgonomonadaceae	0.73	0.91	1.05	1.12	0.86	1.12
Petrotogaceae	0.62	0.84	0.85	1.23	0.98	0.80
Rhodocyclaceae	0.60	0.29	0.00	0.05	0.03	0.15
Thermovenabulales	0.55	0.37	0.24	0.39	0.42	0.74
Thermovenabulales	0.43	0.43	0.61	0.36	0.29	0.36
Sporichthyaceae	0.42	0.17	0.00	0.00	0.00	0.05
Lachnospiraceae	0.38	0.13	0.00	0.04	0.08	0.10
Thermacetogeniaceae	0.33	0.74	0.57	1.24	0.34	0.67
Izemoplasmatales	0.28	0.27	0.24	0.07	0.10	0.24
SC-I-84 (Burkholderiales)	0.26	0.05	0.00	0.00	0.00	0.00
Planctomycetales	0.22	0.11	0.00	0.06	0.00	0.00
[Eubacterium]_Coprostanoligenes_group	0.21	0.44	0.37	0.17	0.27	0.26
Acidaminococcaceae	0.21	0.12	0.00	0.00	0.00	0.08
Anaerovoracaceae	0.20	0.19	0.00	0.05	0.00	0.09
Microtrichaceae	0.20	0.04	0.00	0.00	0.00	0.00
Caldatribacteriaceae	0.18	0.46	1.44	0.49	0.36	0.37
Synergistaceae	0.18	0.28	0.48	0.82	0.38	0.84

Sphingomonadaceae	0.15	0.08	0.00	0.00	0.00	0.05
Pirellulaceae	0.14	0.21	0.06	0.20	0.31	0.25
Saprospiraceae	0.14	0.06	0.00	0.00	0.06	0.06
RBG-13-54-9 (Anaerolinaeae Order)	0.11	0.03	0.00	0.00	0.00	0.00
Syntrophobacteraceae	0.11	0.07	0.03	0.00	0.11	0.06
Peptostreptococcaceae	0.10	0.08	0.00	0.00	0.00	0.00
Labraceae	0.09	0.00	0.00	0.00	0.00	0.00
Methylopilaceae	0.09	0.00	0.00	0.00	0.00	0.00
Symbiobacteraceae	0.09	0.09	0.06	0.00	0.00	0.04
Oscillospiraceae	0.08	0.04	0.00	0.00	0.00	0.00
Fimbriimonadaceae	0.07	0.11	0.00	0.06	0.07	0.06
Saccharimonadales	0.07	0.06	0.00	0.00	0.06	0.06
Burkholderiaceae	0.04	0.10	0.18	0.14	0.00	0.05
Methanosarcinaceae	0.04	0.00	0.00	0.00	0.00	0.00
Bacteroidaceae	0.04	0.02	0.00	0.00	0.00	0.00
0319-6G20 (Oligoflexia)	0.03	0.00	0.00	0.00	0.00	0.00
Methanoregulaceae	0.03	0.02	0.00	0.00	0.00	0.00
Syntrophorhabdaceae	0.03	0.00	0.00	0.00	0.02	0.00
Peptococcaceae	0.02	0.17	0.00	0.00	0.00	0.00
A0839 (Rhizobiales)	0.00	0.04	0.00	0.00	0.00	0.05
A4b (Anaerolinaeae)	0.00	0.05	0.00	0.00	0.00	0.00
Alphaproteobacteria	0.00	0.00	0.00	0.00	0.05	0.00
Bacillaceae	0.00	2.90	2.25	2.43	0.00	0.57
Beggiatoaceae	0.00	0.03	0.41	0.27	0.00	0.00
Beijerinckiaceae	0.00	0.09	0.00	0.16	0.00	0.10
Corynebacteriaceae	0.00	0.05	0.00	0.04	0.00	0.04
Coxiellaceae	0.00	0.03	0.00	0.04	0.00	0.00
Desulfitibacteraceae	0.00	0.00	0.00	0.08	0.00	0.00
Desulfitobacteriaceae	0.00	0.51	0.35	0.40	0.00	0.06
Desulfotomaculales_Incertae_Sedis	0.00	0.00	0.68	0.33	0.00	0.00
Desulfuribacillaceae	0.00	0.01	0.00	0.33	0.00	0.00
Dethiobacteraceae	0.00	0.04	0.00	0.00	0.00	0.04
Devosiaceae	0.00	0.00	0.00	0.00	0.00	0.00
Diplorickettsiaceae	0.00	0.00	0.02	0.00	0.00	0.00
Erysipelatoclostridiaceae	0.00	0.00	0.00	0.00	0.00	0.00
Ethanoligenenaceae	0.00	0.02	0.00	0.00	0.00	0.00
Geminicoccaceae	0.00	0.00	0.02	0.00	0.00	0.00
Gemmataceae	0.00	0.00	0.00	0.00	0.00	0.04
Geobacteraceae	0.00	0.00	0.00	0.00	0.00	0.00
Haloplasmataceae	0.00	0.00	0.00	0.00	0.03	0.00
Hydrogenedensaceae	0.00	0.02	0.00	0.00	0.00	0.00

Hyphomicrobiaceae	0.00	0.02	0.00	0.00	0.00	0.00
Intrasporangiaceae	0.00	0.00	0.00	0.00	0.10	0.00
Methylococcaceae	0.00	0.00	0.08	0.00	0.00	0.00
Nocardioidaceae	0.00	0.00	0.06	0.00	0.00	0.00
PeM15 (Actinobacteria)	0.00	0.00	0.11	0.13	0.00	0.00
Porphyromonadaceae	0.00	0.00	0.00	0.00	0.00	0.00
Rhizobiales_Incertae_Sedis	0.00	0.00	0.02	0.00	0.00	0.00
Rikenellaceae	0.00	0.00	0.00	0.00	0.02	0.00
Ruminococcaceae	0.00	0.04	0.00	0.00	0.04	0.04
Solirubrobacteraceae	0.00	0.00	0.07	0.00	0.00	0.00
Tannerellaceae	0.00	0.07	0.00	0.00	0.00	0.00
Thermicanaceae	0.00	0.00	0.05	0.00	0.00	0.00
Thermodesulfovibrionia	0.00	0.00	0.02	0.00	0.00	0.00

Supplementary Table 7.2 - Microbial community percentage composition, at genus level, of the digestate surface and internal walls of the three digesters.

Genus and specie	**Dig. 1 Surface**	**Dig. 1 Wall**	**Dig. 2 Surface**	**Dig. 2 Wall**	**Dig. 3 Surface**	**Dig. 3 Wall**
Proteinivoracaceae specie	31.34	29.30	19.70	17.82	23.99	28.39
Lentimicrobium sp.	5.68	11.46	9.11	6.38	22.73	9.78
Izemoplasmatales specie	0.22	0.23	0.18	0.04	0.08	0.19
MBA03 specie	4.99	4.96	3.24	1.88	5.90	7.31
D8A-2 specie	1.17	1.23	2.66	1.31	3.36	3.12
Proteiniphilum sp.	0.58	0.75	0.77	0.62	0.75	0.86
DTU014 specie	1.52	1.19	1.68	1.10	2.34	2.45
D8A-2 specie	3.06	6.26	8.56	9.80	6.63	5.83
uncultured	0.27	0.51	1.56	0.49	0.26	0.28
Family XI specie	4.38	2.97	0.69	0.28	0.65	0.59
Caldicoprobacter sp.	1.81	1.64	2.66	1.37	1.02	1.22
Tepidimicrobium sp.	5.17	4.40	6.22	2.25	1.89	2.15
[Eubacterium] coprostanoligenes	0.17	0.36	0.27	0.09	0.23	0.20
UCG-010 specie	0.85	0.65	0.66	0.27	0.61	0.61
Halocella sp.	0.63	0.29	0.05	0.03	0.54	0.28
Longilinea sp.	0.93	0.58	0.73	0.50	0.92	0.53
Izemoplasmatales specie	0.00	0.00	0.00	0.00	0.00	0.00
uncultured	0.83	0.46	0.00	0.11	0.35	0.50
Defluviitoga sp.	0.50	0.69	0.62	0.68	0.85	0.62
Limnochordaceae specie	0.34	0.26	0.92	1.85	0.48	1.47
Hungateiclostridiaceae specie	0.56	0.42	0.19	0.12	0.20	0.24
Rhodobacter sp.	0.90	0.85	1.37	0.09	1.79	1.46
Syntrophomonadaceae specie	0.00	0.00	0.00	0.00	0.00	0.00

Limnochordia specie	0.11	0.10	0.17	0.10	0.32	0.21
Ruminiclostridium sp.	0.43	0.35	0.41	0.19	0.29	0.36
Comamonadaceae specie	1.95	0.74	0.40	0.21	1.57	0.61
Acetomicrobium sp.	0.15	0.25	0.35	0.42	0.33	0.65
Syntrophomonadaceae specie	0.08	0.14	0.07	0.05	0.14	0.08
Ruminococcaceae specie	0.00	0.03	0.00	0.00	0.04	0.03
Caldicoprobacter sp.	0.00	0.13	0.00	0.00	0.00	0.00
UCG-010 specie	0.00	0.09	0.08	0.00	0.00	0.00
M55-D21 specie	0.62	0.49	0.29	0.28	0.60	0.94
Anaerovoracaceae specie	0.16	0.16	0.00	0.03	0.00	0.07
Hydrogenispora sp.	0.56	0.44	0.68	0.28	0.88	0.86
Tepidanaerobacter sp.	0.34	0.36	0.09	0.13	0.25	0.27
Defluviitoga sp.	0.00	0.00	0.00	0.00	0.00	0.00
SRB2 specie	0.70	0.76	0.90	0.42	0.44	0.45
DTU014 specie	0.15	0.08	0.06	0.07	0.19	0.16
Porphyromonas loveana	0.00	0.00	0.00	0.00	0.00	0.00
Macellibacteroides sp.	0.00	0.05	0.00	0.00	0.00	0.00
Haloplasma sp.	0.00	0.00	0.00	0.00	0.03	0.00
Ethanoligenenaceae specie	0.00	0.02	0.00	0.00	0.00	0.00
Limnochordales specie	0.44	0.30	0.18	0.21	0.36	0.57
Devosia sp.	0.00	0.00	0.00	0.00	0.00	0.00
Geobacteraceae specie	0.00	0.00	0.00	0.00	0.00	0.00
Syntrophomonas sp.	1.53	0.72	0.24	0.17	1.36	0.51
Syntrophaceticus sp.	0.26	0.61	0.42	0.68	0.29	0.51
CL500-29 marine group specie	2.05	1.20	0.57	0.27	1.86	1.29
Bacteroides sp.	0.03	0.02	0.00	0.00	0.00	0.00
Saprospiraceae specie	0.05	0.00	0.00	0.00	0.00	0.00
HN-HF0106 specie	0.08	0.03	0.00	0.03	0.00	0.04
Fastidiosipila sp.	0.00	0.01	0.05	0.00	0.00	0.02
Acidaminococcaceae specie	0.17	0.10	0.00	0.00	0.00	0.06
Candidatus Caldatribacterium sp.	0.15	0.38	1.06	0.27	0.31	0.28
UCG-004 specie	0.00	0.00	0.00	0.00	0.00	0.00
Oscillospirales specie	0.00	0.00	0.00	0.00	0.00	0.00
MBA03 speice	0.02	0.05	0.49	0.15	0.00	0.00
01-20 specie	0.00	0.04	0.00	0.00	0.00	0.00
Azospira sp.	0.03	0.00	0.00	0.00	0.00	0.00
Rhodobacteraceae specie	0.00	0.00	0.08	0.00	0.04	0.00
Pir4 lineage specie	0.11	0.00	0.02	0.00	0.00	0.00
Hyphomicrobiaceae specie	0.00	0.01	0.00	0.00	0.00	0.00
Nocardioides sp.	0.00	0.00	0.04	0.00	0.00	0.00
01-20 specie	0.00	0.00	0.00	0.00	0.05	0.00

Peptostreptococcus sp.	0.08	0.07	0.00	0.00	0.00	0.00
01-20 specie	0.08	0.03	0.00	0.00	0.00	0.00
Tetrasphaera sp.	0.00	0.00	0.00	0.00	0.02	0.00
PeM15 specie	0.00	0.00	0.08	0.07	0.00	0.00
Burkholderiaceae specie	0.00	0.00	0.03	0.00	0.00	0.00
Dechlorosoma sp.	0.00	0.00	0.00	0.00	0.03	0.00
Pirellula sp.	0.06	0.04	0.00	0.00	0.00	0.00
Paenalcaligenes sp.	0.00	0.00	0.08	0.81	0.00	0.00
Candidatus Berkiella sp.	0.00	0.03	0.00	0.02	0.00	0.00
SC-I-84 specie	0.21	0.04	0.00	0.00	0.00	0.00
Hungateiclostridium saccincola	0.14	0.12	0.00	0.00	0.00	0.00
Alistipes indistinctus	0.00	0.00	0.00	0.00	0.02	0.00
Rhizobiales specie	0.00	0.00	0.02	0.00	0.00	0.00
Desulfallas-Sporotomaculum sp.	0.00	0.00	0.04	0.18	0.00	0.00
Pir4 lineage specie	0.00	0.00	0.09	0.00	0.15	0.00
Planctomycetales specie	0.18	0.09	0.00	0.04	0.00	0.00
Methylococcaceae specie	0.00	0.00	0.06	0.00	0.00	0.00
Conexibacter sp.	0.00	0.00	0.05	0.00	0.00	0.00
Aminobacterium sp.	0.00	0.00	0.00	0.03	0.00	0.00
Dechloromonas sp.	0.25	0.00	0.00	0.00	0.00	0.00
Microtrichaceae specie	0.16	0.03	0.00	0.00	0.00	0.00
SJA-28 specie	0.02	0.06	0.00	0.00	0.00	0.00
Rhodobacter capsulatus	0.00	0.00	0.11	0.00	0.00	0.00
Anaerovoracaceae specie	0.00	0.05	0.00	0.00	0.00	0.00
DS-100 specie	0.00	0.02	0.00	0.00	0.00	0.00
Methylocystis sp.	0.00	0.00	0.00	0.09	0.00	0.00
Peptococcaceae specie	0.01	0.00	0.00	0.00	0.00	0.00
Hydrogenispora sp.	0.00	0.00	0.00	0.00	0.00	0.00
Candidatus Alysiosphaera sp.	0.00	0.00	0.02	0.00	0.00	0.00
Clostridiaceae specie	0.00	0.00	0.00	0.00	0.02	0.00
WD2101 soil group specie	0.03	0.00	0.00	0.00	0.00	0.00
SJA-28 specie	0.06	0.02	0.00	0.00	0.00	0.00
SJA-15 specie	0.00	0.00	0.05	0.00	0.00	0.00
Paenalcaligenes sp.	0.00	0.00	0.00	0.00	0.02	0.00
Gemmataceae specie	0.00	0.06	0.00	0.04	0.00	0.00
Other species	21.83	22.22	30.86	47.70	14.83	23.97

7.6. References

[1] N. Di Costanzo, A. Cesaro, F. Di Capua, G. Esposito, Exploiting the nutrient potential of anaerobically digested sewage sludge: A review, Energies. 14 (2021) 1–25. https://doi.org/10.3390/en14238149.

[2] A. Pigoli, M. Zilio, F. Tambone, S. Mazzini, M. Schepis, E. Meers, O. Schoumans, A. Giordano, F. Adani, Thermophilic anaerobic digestion as suitable bioprocess producing organic and chemical renewable fertilizers: A full-scale approach, Waste Manag. 124 (2021) 356–367. https://doi.org/10.1016/j.wasman.2021.02.028.

[3] N. Di Costanzo, A. Cesaro, F. Di Capua, M.C. Mascolo, G. Esposito, Application of high-intensity static magnetic field as a strategy to enhance the fertilizing potential of sewage sludge digestate, Waste Manag. 170 (2023) 122–130. https://doi.org/10.1016/j.wasman.2023.08.005.

[4] N. Di Costanzo, F. Di Capua, A. Cesaro, M.C. Mascolo, F. Pirozzi, G. Esposito, Impact of High-Intensity Static Magnetic Field on Chemical Properties and Anaerobic Digestion of Sewage Sludge, Waste and Biomass Valorization. 14 (2023) 2469–2479. https://doi.org/10.1007/s12649-022-01891-x.

[5] A. Giordano, F. Di Capua, G. Esposito, F. Pirozzi, Long-term biogas desulfurization under different microaerobic conditions in full-scale thermophilic digesters co-digesting high-solid sewage sludge, Int. Biodeterior. Biodegrad. 142 (2019) 131–136. https://doi.org/10.1016/j.ibiod.2019.05.017.

[6] C. Muller, K. Guevarra, A. Summers, L. Pierce, P. Shahbaz, P.E. Zemke, K. Woodland, V. Hollingsworth, G. Nakhla, K. Bell, E. Bronstad, A review of the practical application of micro-aeration and oxygenation for hydrogen sulfide management in anaerobic digesters, Process Saf. Environ. Prot. 165 (2022) 126–137. https://doi.org/10.1016/j.psep.2022.07.009.

[7] L. Krayzelova, J. Bartacek, I. Díaz, D. Jeison, E.I.P. Volcke, P. Jenicek, Microaeration for hydrogen sulfide removal during anaerobic treatment: a review, Rev. Environ. Sci. Biotechnol. 14 (2015) 703–725. https://doi.org/10.1007/s11157-015-9386-2.

[8] R. Khanongnuch, F. Di Capua, A.M. Lakaniemi, E.R. Rene, P.N.L. Lens, H2S

removal and microbial community composition in an anoxic biotrickling filter under autotrophic and mixotrophic conditions, J. Hazard. Mater. 367 (2019) 397–406. https://doi.org/10.1016/j.jhazmat.2018.12.062.

[9] R. Khanongnuch, F. Di Capua, A.M. Lakaniemi, E.R. Rene, P.N.L. Lens, Transient–state operation of an anoxic biotrickling filter for H2S removal, J. Hazard. Mater. 377 (2019) 42–51. https://doi.org/10.1016/j.jhazmat.2019.05.043.

[10] Y. Cheng, T. Yuan, Y. Deng, C. Lin, J. Zhou, Z. Lei, K. Shimizu, Z. Zhang, Use of sulfur-oxidizing bacteria enriched from sewage sludge to biologically remove H2S from biogas at an industrial-scale biogas plant, Bioresour. Technol. Reports. 3 (2018) 43–50. https://doi.org/10.1016/j.biteb.2018.01.006.

[11] H.W. Ou, M.L. Fang, M.S. Chou, H.Y. Chang, T.F. Shiao, Long-term evaluation of activated carbon as an adsorbent for biogas desulfurization, J. Air Waste Manag. Assoc. 70 (2020) 641–648. https://doi.org/10.1080/10962247.2020.1754305.

[12] M. Farooq, M.N. Almustapha, M. Imran, M.A. Saeed, J.M. Andresen, In-situ regeneration of activated carbon with electric potential swing desorption (EPSD) for the H2S removal from biogas, Bioresour. Technol. 249 (2018) 125–131. https://doi.org/10.1016/j.biortech.2017.09.198.

[13] S. Kurella, P.K. Bhukya, B.C. Meikap, Removal of H2S pollutant from gasifier syngas by a multistage dual-flow sieve plate column wet scrubber, J. Environ. Sci. Heal. - Part A Toxic/Hazardous Subst. Environ. Eng. 52 (2017) 515–523. https://doi.org/10.1080/10934529.2017.1281690.

[14] A. Manmeen, P. Kongjan, T. Rattanaya, B. Cheirsilp, N. Raybut, R. Jariyaboon, Desulfurization of H2S-rich biogas using water scrubbing: Performance in pilot scale scrubber and scale-up estimation for the concentrated latex factory, Environ. Prog. Sustain. Energy. (2022). https://doi.org/10.1002/ep.14034.

[15] F. Almenglo, J.J. González-Cortés, M. Ramírez, D. Cantero, Recent advances in biological technologies for anoxic biogas desulfurization, Chemosphere. 321 (2023). https://doi.org/10.1016/j.chemosphere.2023.138084.

[16] T. Kobayashi, Y.Y. Li, K. Kubota, H. Harada, T. Maeda, H.Q. Yu,

Characterization of sulfide-oxidizing microbial mats developed inside a full-scale anaerobic digester employing biological desulfurization, Appl. Microbiol. Biotechnol. 93 (2012) 847–857. https://doi.org/10.1007/s00253-011-3445-6.

[17] E. Tilahun, E. Sahinkaya, B. Çalli, A hybrid membrane gas absorption and bio-oxidation process for the removal of hydrogen sulfide from biogas, Int. Biodeterior. Biodegrad. 127 (2018) 69–76. https://doi.org/10.1016/j.ibiod.2017.11.015.

[18] F. Bauer, T. Persson, C. Hulteberg, D. Tamm, Biogas upgrading – technology overview, comparison and perspectives for the future, Biofuels, Bioprod. Biorefining. 7 (2013) 499–511. https://doi.org/10.1002/BBB.

[19] A.I. Adnan, M.Y. Ong, S. Nomanbhay, K.W. Chew, P.L. Show, Technologies for biogas upgrading to biomethane: A review, Bioengineering. 6 (2019) 1–23. https://doi.org/10.3390/bioengineering6040092.

[20] M.U. Khan, J.T.E. Lee, M.A. Bashir, P.D. Dissanayake, Y.S. Ok, Y.W. Tong, M.A. Shariati, S. Wu, B.K. Ahring, Current status of biogas upgrading for direct biomethane use: A review, Renew. Sustain. Energy Rev. 149 (2021) 111343. https://doi.org/10.1016/j.rser.2021.111343.

[21] S.F. Ahmed, M. Mofijur, K. Tarannum, A.T. Chowdhury, N. Rafa, S. Nuzhat, P.S. Kumar, D.V.N. Vo, E. Lichtfouse, T.M.I. Mahlia, Biogas upgrading, economy and utilization: a review, Environ. Chem. Lett. 19 (2021) 4137–4164. https://doi.org/10.1007/s10311-021-01292-x.

[22] S. Cavenati, C.A. Grande, A.E. Rodrigues, Upgrade of methane from landfill gas by pressure swing adsorption, Energy and Fuels. 19 (2005) 2545–2555. https://doi.org/10.1021/ef050072h.

[23] N. Aryal, L.D. Mørck Ottosen, M.V. Wegener Kofoed, D. Pant, Emerging Technologies and Biological Systems for Biogas Upgrading, 2021. https://doi.org/10.1016/B978-0-12-822808-1.00019-2.

[24] M. Kárászová, Z. Sedláková, P. Izák, Review: Gas permeation processes in biogas upgrading: A short review, Chem. Pap. 69 (2015) 1277–1283. https://doi.org/10.1515/chempap-2015-0141.

[25] P. Shao, M. Dal-Cin, A. Kumar, H. Li, D.P. Singh, Design and economics of a

hybrid membrane-temperature swing adsorption process for upgrading biogas, J. Memb. Sci. 413–414 (2012) 17–28. https://doi.org/10.1016/j.memsci.2012.02.040.

[26] O.W. Awe, Y. Zhao, A. Nzihou, D.P. Minh, N. Lyczko, A review of biogas utilisation, purification and upgrading technologies, Waste and Biomass Valorization. 8 (2017) 267–283. https://doi.org/10.1007/s12649-016-9826-4.

[27] F. Di Capua, F. Adani, F. Pirozzi, G. Esposito, A. Giordano, Air side-stream ammonia stripping in a thin film evaporator coupled to high-solid anaerobic digestion of sewage sludge: Process performance and interactions, J. Environ. Manage. 295 (2021) 113075. https://doi.org/10.1016/j.jenvman.2021.113075.

[28] (APHA) American Public Health Association, (AWWA) American Water Works Association, (WEF) Water Environment Federation, Standard Methods for the Examination of Water and Wastewater Standard Methods for the Examination of Water and Wastewater, Public Health. 51 (1999) 940–940. https://doi.org/10.2105/AJPH.51.6.940-a.

[29] O. Lahav, B.E. Morgan, R.E. Loewenthal, Rapid, simple, and accurate method for measurement of VFA and carbonate alkalinity in anaerobic reactors, Environ. Sci. Technol. 36 (2002) 2736–2741. https://doi.org/10.1021/es011169v.

[30] J. Doyle, DNA Protocols for Plants, Mol. Tech. Taxon. (1991) 283–293. https://doi.org/https://doi.org/10.1007/978-3-642-83962-7_18.

[31] A. Corniello, M. Guida, L. Stellato, M. Trifuoggi, F. Carraturo, E. Del Gaudio, C. Del Giudice, G. Forte, A. Giarra, M. Iorio, F. Marzaioli, M. Toscanesi, Hydrochemical, isotopic and microbiota characterization of telese mineral waters (Southern Italy), Environ. Geochem. Health. 44 (2022) 1949–1970. https://doi.org/10.1007/s10653-021-00806-4.

[32] N.J.R. Kraakman, I. Diaz, M. Hierholzer, J.M. Friel, R. Muñoz, Full-scale digester micro-aeration pilot study to improve biogas quality for energy recovery, WEFTEC 2019 - 92nd Annu. Water Environ. Fed. Tech. Exhib. Conf. (2019) 4112–4123.

[33] P. Jeníček, J. Horejš, L. Pokorná-Krayzelová, J. Bindzar, J. Bartáček, Simple

biogas desulfurization by microaeration – Full scale experience, Anaerobe. 46 (2017) 41–45. https://doi.org/10.1016/j.anaerobe.2017.01.002.

[34] F. Di Capua, D. Spasiano, A. Giordano, F. Adani, U. Fratino, F. Pirozzi, G. Esposito, High-solid anaerobic digestion of sewage sludge: challenges and opportunities, Appl. Energy. 278 (2020) 115608. https://doi.org/10.1016/j.apenergy.2020.115608.

[35] S. Shakeri Yekta, R.M. Ziels, A. Björn, U. Skyllberg, J. Ejlertsson, A. Karlsson, M. Svedlund, M. Willén, B.H. Svensson, Importance of sulfide interaction with iron as regulator of the microbial community in biogas reactors and its effect on methanogenesis, volatile fatty acids turnover, and syntrophic long-chain fatty acids degradation, J. Biosci. Bioeng. 123 (2017) 597–605. https://doi.org/10.1016/j.jbiosc.2016.12.003.

[36] W. Mulbry, K. Selmer, S. Lansing, Effect of liquid surface area on hydrogen sulfide oxidation during micro-aeration in dairy manure digesters, PLoS One. 12 (2017) 1–12. https://doi.org/10.1371/journal.pone.0185738.

[37] J.P. Sheets, X. Ge, Y. Li, Effect of limited air exposure and comparative performance between thermophilic and mesophilic solid-state anaerobic digestion of switchgrass, Bioresour. Technol. 180 (2015) 296–303. https://doi.org/10.1016/j.biortech.2015.01.011.

[38] I. Ramos, R. Pérez, M. Fdz-Polanco, The headspace of microaerobic reactors: Sulphide-oxidising population and the impact of cleaning on the efficiency of biogas desulphurisation, Bioresour. Technol. 158 (2014) 63–73. https://doi.org/10.1016/j.biortech.2014.02.001.

[39] S. Fu, S. Lian, I. Angelidaki, R. Guo, Micro-aeration: an attractive strategy to facilitate anaerobic digestion, Trends Biotechnol. (2022) 1–13. https://doi.org/10.1016/j.tibtech.2022.09.008.

[40] D. Nguyen, S.K. Khanal, A little breath of fresh air into an anaerobic system: How microaeration facilitates anaerobic digestion process, Biotechnol. Adv. 36 (2018) 1971–1983. https://doi.org/10.1016/j.biotechadv.2018.08.007.

[41] S. Li, Z. Jiang, G. Ji, Effect of sulfur sources on the competition between denitrification and DNRA, Environ. Pollut. 305 (2022) 119322.

https://doi.org/10.1016/j.envpol.2022.119322.

[42] J.J. González-Cortés, F. Almenglo, M. Ramírez, D. Cantero, Simultaneous removal of ammonium from landfill leachate and hydrogen sulfide from biogas using a novel two-stage oxic-anoxic system, Sci. Total Environ. 750 (2021) 141664. https://doi.org/10.1016/j.scitotenv.2020.141664.

[43] Y. Song, A. Mahdy, Z. Hou, M. Lin, W. Stinner, W. Qiao, R. Dong, Air Supplement as a Stimulation Approach for the in Situ Desulfurization and Methanization Enhancement of Anaerobic Digestion of Chicken Manure, Energy and Fuels. 34 (2020) 12606–12615. https://doi.org/10.1021/acs.energyfuels.0c01724.

[44] C. Li, L. Hao, F. Lü, H. Duan, H. Zhang, P. He, Syntrophic Acetate-Oxidizing Microbial Consortia Enriched from Full-Scale Mesophilic Food Waste Anaerobic Digesters Showing High Biodiversity and Functional Redundancy, MSystems. 7 (2022). https://doi.org/10.1128/msystems.00339-22.

[45] E. Perman, A. Schnürer, A. Björn, J. Moestedt, Serial anaerobic digestion improves protein degradation and biogas production from mixed food waste, Biomass and Bioenergy. 161 (2022). https://doi.org/10.1016/j.biombioe.2022.106478.

[46] C. Li, P. He, L. Hao, F. Lü, L. Shao, H. Zhang, Diverse acetate-oxidizing syntrophs contributing to biogas production from food waste in full-scale anaerobic digesters in China, Renew. Energy. 193 (2022) 240–250. https://doi.org/10.1016/j.renene.2022.04.143.

[47] S. Haosagul, P. Prommeenate, G. Hobbs, N. Pisutpaisal, Sulfide-oxidizing bacteria community in full-scale bioscrubber treating H2S in biogas from swine anaerobic digester, Renew. Energy. 150 (2020) 973–980. https://doi.org/10.1016/j.renene.2019.11.139.

[48] H. Kambara, H.T.T. Dinh, S. Matsushita, Y. Aoi, T. Kindaichi, N. Ozaki, A. Ohashi, New microbial electrosynthesis system for methane production from carbon dioxide coupled with oxidation of sulfide to sulfate, J. Environ. Sci. (China). 125 (2023) 786–797. https://doi.org/10.1016/j.jes.2022.02.029.

[49] R. Borja, B. Rincón, Biogas Production, Ref. Modul. Life Sci. (2017).

https://doi.org/10.1016/B978-0-12-809633-8.09105-6.

[50] H. Tian, P. Gao, Z. Chen, Y. Li, Y. Li, Y. Wang, J. Zhou, G. Li, T. Ma, Compositions and abundances of sulfate-reducing and sulfur-oxidizing microorganisms in water-flooded petroleum reservoirs with different temperatures in China, Front. Microbiol. 8 (2017) 1–14. https://doi.org/10.3389/fmicb.2017.00143.

[51] I. Owusu-Agyeman, E. Plaza, Z. Cetecioglu, Long-term alkaline volatile fatty acids production from waste streams: Impact of pH and dominance of Dysgonomonadaceae, Bioresour. Technol. 346 (2022) 126621. https://doi.org/10.1016/j.biortech.2021.126621.

[52] I. Díaz, I. Ramos, M. Fdz-Polanco, Economic analysis of microaerobic removal of H2S from biogas in full-scale sludge digesters, Bioresour. Technol. 192 (2015) 280–286. https://doi.org/10.1016/j.biortech.2015.05.048.

CHAPTER 8

Conclusions and future perspectives

The core objective of this doctoral thesis was to develop an integrated approach to enhance the anaerobic digestion (AD) process of sewage sludge, specifically focusing on boosting biomethane (CH_4) production, nutrient recovery, the removal of inhibitory compounds, and the agronomic quality of the digestate. Achieving this goal entailed examining the impact of static magnetic fields (SMF) on AD process and digestate characteristics as well as evaluating the viability and the advantages towards biomethane generation of biological biogas desulfurization via in situ micro-oxygenation in full-scale anaerobic digesters. This section highlights the main findings of this doctoral thesis (**Figure 8.1**) and discusses their relevance. Recommendations for future studies are also expressed in this chapter.

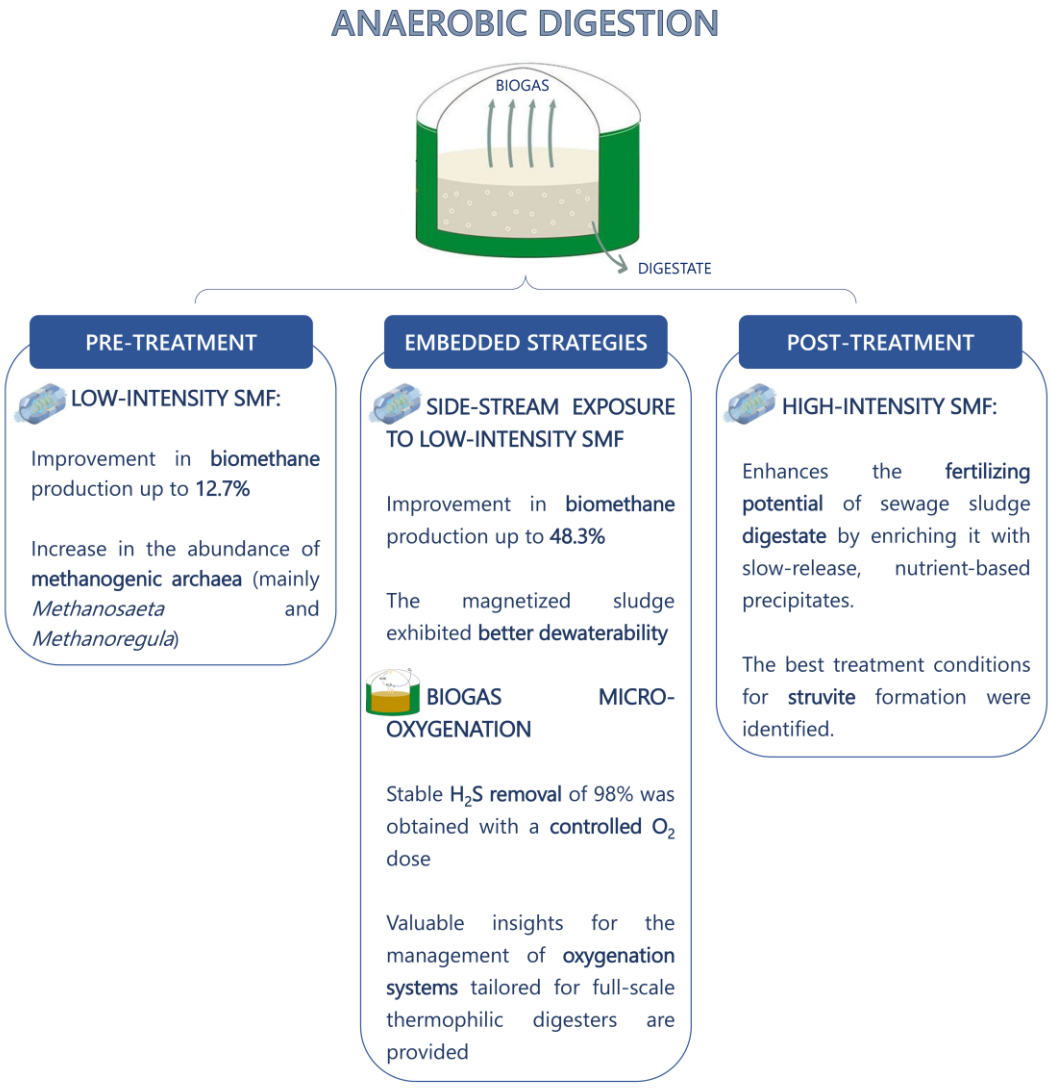

Figure 8.1 - Main findings of this doctoral thesis.

8.1. Chapters overview

The huge amounts of sewage sludge produced by municipal wastewater treatment plants induce major environmental and economic issues that demands seeking effective, environmentally friendly and sustainable handling. In this context, the present doctoral thesis firstly (*Chapter 2*) showed the potential valorization routes of sewage sludge treated via AD, highlighting the possible reuse of anaerobically digested sewage sludge (ADS) for fertilizing purposes due to its remarkable macronutrient content, especially when the solid content is high. Specifically, *Chapter 2* provides an overview of the state of the art of nutrient recovery from ADS, critically reviewing and comparing the technologies used for this purpose, with a focus on recent technological advances, in order to identify their application status at industrial level, the main pros and cons, and to address future research directions.

Based on the literature review, this thesis proposes the development of an integrated approach aimed at improving AD of sewage sludge, both in terms of CH_4 production and chemical composition of the digestate, through the application of a novel strategy such as the application of SMF. In detail, *Chapter 3* reveals that an extensive exposure of the sewage sludge to the high-intensity SMF resulted in a 24% decrease of CH_4 production and in a reduced concentration of the monitored ionic species (up to 19.1% for NH_4^+, 35.7% for NO_3^-, 13% PO_4^{3-}, 41.2% SO_4^{2-} and 23.9% Mg^{2+}) in the liquid phase of sewage sludge, promoting the precipitation of compounds with valuable fertilizing properties, e.g., struvite. Based on this result, *Chapter 4* demonstrates how the precipitation effect induced by high-intensity SMF on digestates originating from both AD and high-solid AD (HSAD) of sewage sludge can be further improved through certain operating conditions, e.g. by exploiting the paramagnetism of the oxygen (O_2) molecule, thus promoting the formation of struvite and that of other nutrient-based compounds with potential fertilizing value. Subsequently, this thesis work moved further along this line of research by evaluating the effect induced by a low-intensity SMF in terms of AD performance and evolution of fermentative and methanogenic communities (*Chapter 5*). Our study demonstrates that low-intensity (20 mT) SMF pretreatment is an effective technique for enhancing AD performance, attaining 12.7% improvement of CH_4 production at

20 mT compared to the untreated sewage sludge. Conversely, the use of 1.5 T had a negative impact on cumulative CH_4 production, resulting in a decrease of 15.1%. In addition, microbial community analysis indicated that low-intensity (20 mT) SMF pretreatment results in differences in the microbiota structure, increasing the relative abundance of the species involved in the CH_4 production.

Based on these results, it appeared interesting to evaluate the effect induced by a continuous exposure of the digesting sludge to a low-intensity (20 mT) SMF during mesophilic AD (*Chapter 6*) to determine whether CH_4 production can be further increased under continuous magnetic exposure. The obtained results showed that continuous side-stream magnetization significantly enhanced CH_4 production, resulting in a 48.3% increase compared to the control reactor. The SMF-treated sludge also exhibited better dewaterability, potentially leading to reduced sludge handling costs and improved sludge storage and transport.

Finally, *Chapter 7* investigates the application of in-situ micro-oxygenation for biogas desulfurization and CH_4 generation in a full-scale centralized sewage sludge digestion plant. The study demonstrates that headspace micro-oxygenation can effectively remove hydrogen sulfide (H_2S) from biogas with high removal efficiencies (>98%) under different O_2 dosages. The results also show that the response time of the biological H_2S oxidation is within 10 hours. Moreover, the microbial community analysis reveals the dominant families involved in H_2S oxidation (*Lentimicrobiaceae*, *Caldicoprobacteraceae*, DTU014, *Syntrophomonadaceae*, and *Rhodobacteraceae*). The study also estimates the specific energy consumption of the in-situ desulfurization system to be 5.9 Wh per Nm^3 of produced biogas, which is lower than that required for the injection of concentrated air. These findings indicate that headspace micro-oxygenation is a promising technology for biogas desulfurization and CH_4 generation in full-scale sewage sludge digestion plants, offering operational flexibility, economic efficiency, and environmental benefits.

8.2. Impact of magnetization on CH_4 production and microbial community dynamics

In the context of waste management and renewable energy production, sewage sludge stands as a resource with both environmental burdens and unexploited potential. While its high organic content presents challenges in terms of pathogen load and environmental impact, it also has the capability to be transformed into a valuable energy source – biogas, primarily CH_4. AD, a natural process that breaks down organic matter in the absence of O_2, is the most established method for converting sewage sludge into biogas. However, optimizing AD processes to maximize CH_4 production remains a crucial goal.

By manipulating key SMF influencing parameters, i.e., flow rate, mixing ratio, pumping cycles, and total solid content, it is possible to differently address the SMF effects to differently enhance AD yields. Extensive exposure to the high-intensity SMF, as described in *Chapter 3*, achieved by increasing flow rate, mixing ratio and pumping cycles, resulted in a noticeable decrease of CH_4 production by approximately 24%. This finding aligns with previously published data where using an intensity higher than 1 T results in a biochemical processes inhibition [1] and could be likely due to a lower intake of micro- and macro-nutrients available to microorganisms during the digestion process, which can be linked to the formation of precipitates in the ADS solid phase (this topic will be addressed more in detail in the next section). However, since the findings of this chapter suggest that low SMF exposure (achieved by reducing flow rate, mixing ratio and pumping cycles) has less pronounced effects, and a weak SMF may even enhance the biological decomposition of organic compounds [2], *Chapter 5* and *Chapter 6* focus on the effects of sewage sludge exposure to low-intensity SMF (20 mT) as either AD pretreatment (*Chapter 5*) or AD-integrated treatment (*Chapter 6*). Magnetic pretreatment at 20 mT demonstrated remarkable efficacy, boosting CH_4 production by up to 12.7% over the untreated sludge. Noteworthy, low-intensity SMF pretreatment induces distinct microbiota compositions, elevating the relative abundance of species crucial for CH_4 production, principally *Methanosaeta* and *Methanoregula*, further solidifying low-intensity SMF pretreatment ability to enhance sewage sludge AD performance. However, the pretreatment approach results in a time-limited exposure (ranging from 0.2 to 200 min in the experimental

conditions described in *Chapter 3* and *Chapter 5*) of sewage sludge to the SMF, which may lead to a diminishing effect over time during the following AD stage, particularly in the context of integrating this pretreatment with real plant configurations where magnetic systems must be efficient from an energy point of view, so as not to increase the operating costs of the plant. Therefore, to try to prolong sludge exposure to the SMF and evaluate the resulting impact, in *Chapter 6* the low-intensity SMF of 20 mT was applied during the AD process by installing the magnetic polarizer on the sludge recycle line, thereby ensuring a continuous magnetization (1440 $min \cdot d^{-1}$) to bench-scale digesters operated in batch mode in a continuously stirred tank reactor. The choice to adopt this specific reactor configuration is related to remarks suggested in previous studies that highlighted the need for future investigations into the practical SMF scalability at industrial level. Specifically, the metallic structures and large volumes of industrial digesters can disrupt the uniform distribution of the SMF within the reactor, necessitating innovative approaches to ensure consistent exposure. Therefore, side-stream magnetization appeared as a smart strategy for continuous magnetization of digesting sludge, since the installation and maintenance of SMF placed outside of the digester looks straightforward and minimally intrusive. Notably, our study demonstrates that continuous side-stream magnetization is a promising and sustainable approach for enhancing CH_4 production and dewaterability from sewage sludge. The significant increase in specific CH_4 production (+48.3% compared to the control reactor) observed in the SMF-treated sludge could be attributed to the improved hydrolysis and methanogenesis processes induced by the SMF. The enhanced dewaterability of the SMF-treated sludge further contributes to its overall economic viability as an energy resource. More comprehensive research is required to corroborate these findings and evaluate the protracted ramifications of implementing SMF in large-scale facilities. Therefore, continuous side-stream magnetization emerges as a compelling strategy for optimizing sewage sludge AD and promoting the sustainable utilization of this valuable bioresource.

8.3. SMF promoting the nutrient recovery from sewage sludge

With growing population and increasing wastewater generation, finding ways to manage nutrients efficiently is crucial. ADS, a byproduct of wastewater treatment, holds nutrients like nitrogen, phosphorus, and potassium that can be recovered and reutilized for sustainable purposes. Based on this, recovering these nutrients from ADS presents a promising path towards resource conservation and sustainable development. *Chapter 2* delves into the current situation of nutrient recovery from ADS, exploring the potential and challenges of this sludge valorization strategy. Various approaches can be employed to extract nutrients from ADS. These can broadly be categorized into two strategies: selective and simultaneous nutrient recovery. Selective techniques focus on recovering a single nutrient, such as ammonia stripping for nitrogen retrieval. Simultaneous nutrient recovery techniques aim to recover multiple nutrients from ADS in a single process. In this context, struvite (a crystalline mineral composed of Mg^{2+}, NH_4^+, and PO_4^{3-}) precipitation stands out as a prominent example [3], as it allows simultaneous recovery of nitrogen and phosphorus. Struvite can be effectively precipitated and separated for a subsequent reuse [4–6]. However, in certain instances, such as ADS from HSAD, it can be challenging to isolate struvite [7]. Notwithstanding these difficulties, the presence of struvite in the produced ADS enhances its fertilizing potential, being a valuable slow-release source of soil nutrients. In light of this, identifying innovative strategies that improve struvite precipitation (and other valuable fertilizer compounds) aligns well with a circular economy and sustainable development paradigm. Consequently, *Chapter 4* explores the effects of high-intensity SMF treatment on the chemical composition of anaerobic digestate in order to improve its fertilizing potential, rendering it a more sustainable and valuable resource for agricultural applications. To this end, various strategies were employed to optimize the SMF treatment, including varying the number of magnetization cycles, incorporating different magnesium sources and quantities, and conducting digestate aeration. The results demonstrated that a synergistic combination of these strategies significantly reduced the concentrations of NH_4^+, NO_3^-, PO_4^{3-}, SO_4^{2-}, and Mg^{2+} in the liquid phase by up to 28%, 38%, 34%, 39%, and 31%, respectively, resulting in the formation of nutrient-containing precipitates that remain mostly entrapped in the

sludge matrix. X-ray diffraction (XRD) analysis of the solid phase of the magnetized digestate samples revealed an enhanced presence of crystalline and amorphous phases of nitrogen and phosphorus compounds with high fertilizing value such as struvite. In this context, exploring the impact of alternative magnesium sources on struvite precipitation, particularly those derived from recycled materials, holds the key to augmenting process competitiveness and sustainability. Moreover, it should be noted that the combination of digestate oxygenation and SMF significantly enhances the precipitation of valuable compounds in digestate. This is of particular interest in the context of integrating this system into existing plants. As discussed in *Chapter 7* and as will be further elaborated in the next section, oxygenation can also be a feasible strategy for biological desulfurization of biogas. Within full-scale digesters, pre-oxygenation of digesting sludge within the recirculation stream can effectively manage H_2S production, thereby curtailing its presence in biogas Therefore, by identifying a strategic positioning that is able to integrate SMF and micro-oxygenation, it would be possible to meet both the needs of increasing the fertilizing power of the ADS and improving the biological desulfurization of the biogas. In addition, it is crucial to take into account the substantial difference in impact that exists between digestate from conventional AD and HSAD. Firstly, owing to its significantly less intricate matrix, the effect elicited by SMF on the digestate from conventional AD is more salient than that observed on the digestate from HSAD. Additionally, in the prospect of a future scale-up of SMF application, it is imperative to acknowledge that the type of matrix being processed can significantly influence its efficacy. The passage through the polarizer is suitable for fluids of low viscosity, whereas for fluids of high viscosity it could lead to rapid clogging and requires more pumping energy. Consequently, the total solids content plays a pivotal role in selecting the most suitable SMF configuration, as it impinges on the rheological properties of the fluid. To mitigate this challenge, configurations for SMF application specifically tailored to digestates originating from HSAD should be considered.

8.4. Micro-oxygenation for effective H_2S removal during AD

AD process inevitably generates H_2S, a noxious gas with a characteristic rotten egg odor, which poses a significant challenge for biogas puritification. While small amounts of H_2S can be tolerated, excessive concentrations can lead to safety hazards, corrosion issues, and environmental concerns. Therefore, effective H_2S removal is paramount for ensuring the safe, efficient, and environmentally responsible production of biogas.

Conventional H_2S removal techniques, such as scrubbing [8] with alkaline solutions [9] or membrane separation [10], often rely on complex equipment and involve high operational costs [11], making them less attractive options. In contrast, providing a limited amount of pure oxygen (micro-oxygenation) to the digester headspace offers a promising solution for H_2S management in anaerobic digesters while biogas dilution due to N_2 input. This controlled oxygenation creates a favorable environment for the growth of specialized bacteria known as sulfur-oxidizing bacteria [12]. These microorganisms, unlike methanogenic bacteria responsible for biogas production, can oxidize H_2S, converting it into either elemental sulfur (S^0) or sulfate (SO_4^{2-}) [13]. The delicate microbiota of an anaerobic digester is sensitive to O_2 intrusion, which can disrupt methanogenesis. *Chapter 7* investigates, for the first time, the effects of pure O_2 desulfurization on biomethane quality after biogas upgrading in full-scale thermophilic digesters in a centralized sludge treatment plant. Specifically, in this chapter the desulfurization performance of the system under different inlet O_2 flows and how these flows impact the generation of CH_4 were evaluated. The response times of the biological desulfurization system were also verified through intermittent O_2 injection. In addition, the impact of the O_2 injection on the evolution of microbial communities responsible for H_2S oxidation, on energy demand for desulfurization, and on the AD process performance was evaluated. Micro-oxygenation emerged as a robust and effective desulfurization strategy, effectively desulfurizing biogas to meet stringent CH_4 quality standards. An O_2 dose of 0.96(±0.03) NL/Nm^3 of biogas was determined to eliminate all traces of H_2S, rendering the gas suitable for CH_4 production. This remarkable efficiency was further demonstrated by the system ability to rapidly regain desulfurization performance following intermittent O_2 injections, achieving full recovery within 10

hours. The underlying mechanism driving this result was the proliferation of sulfur-oxidizing bacteria (i.e., *Lentimicrobiaceae, Caldicoprobacteraceae, DTU014, Syntrophomonadaceae*, and *Rhodobacteraceae)* on both the digester surface and within its interior walls. Notably, the AD process remained unaffected even under varying O_2 dosages, highlighting the compatibility of micro-oxygenation with the delicate anaerobic environment. Furthermore, a key advantage of this technology lies in the fact that biological desulfurization occurs directly within the anaerobic digester itself, eliminating the need for a separate desulfurization unit and the use of additional chemicals, thus providing a straightforward, highly efficient, and stable approach to removing hydrogen sulfide from biogas. Therefore, this chapter delves into the development of a decision-making tool that provides an optimal O_2 dosage for desulfurization, considering the dynamic nature of biogas production. This tool emerges as a valuable resource for plant operators, enabling them to optimize aeration processes and enhance biogas quality while simultaneously minimizing aeration costs. While micro-oxygenation's energy consumption is marginally higher than microaeration, the strategic utilization of pure-O_2 offers a compelling advantage in the context of subsequent biogas upgrading to biomethane, effectively preventing CH_4 dilution by nitrogen.

8.5. Conclusions and future perspectives

This thesis work suggested that by adopting innovative technologies and sustainable practices, it is possible optimize the environmental and economic benefits of sewage sludge management, contributing to a more sustainable and resource-efficient wastewater treatment paradigm.

SMF have emerged as a promising technology for sewage sludge treatment, offering potential benefits in enhancing sludge dewatering and nutrient recovery. Further research is warranted to optimize the application of SMFs, exploring their impact on various sludge types, and investigating their long-term effects on sludge properties and nutrient recovery mechanisms. Additionally, comprehensive evaluation of the feasibility and effectiveness of SMFs in full-scale sewage sludge digestion plants is

essential. This includes factors such as field strength requirements, operational parameters, and economic considerations.

In-situ micro-oxygenation systems demonstrate potential for improving sludge desulfurization efficiency, enhancing CH_4 production during AD. Further research is needed to optimize the design and operation of in-situ micro-oxygenation systems, investigating their performance under varying conditions and assessing their economic viability compared to conventional desulfurization methods.

These proposed future research directions underscore the ongoing efforts to enhance sewage sludge treatment and valorize this valuable resource, contributing to establish a more sustainable and environmentally responsible approach.

8.6. References

[1] J. Miyakoshi, Effects of static magnetic fields at the cellular level, Prog. Biophys. Mol. Biol. 87 (2005) 213–223. https://doi.org/10.1016/j.pbiomolbio.2004.08.008.

[2] J. Filipič, B. Kraigher, B. Tepuš, V. Kokol, I. Mandic-Mulec, Effects of low-density static magnetic fields on the growth and activities of wastewater bacteria Escherichia coli and Pseudomonas putida, Bioresour. Technol. 120 (2012) 225–232. https://doi.org/10.1016/j.biortech.2012.06.023.

[3] L. Shi, W.S. Simplicio, G. Wu, Z. Hu, H. Hu, X. Zhan, Nutrient Recovery from Digestate of Anaerobic Digestion of Livestock Manure: a Review, Curr. Pollut. Reports. 4 (2018) 74–83. https://doi.org/10.1007/s40726-018-0082-z.

[4] N. Morales, M.A. Boehler, S. Buettner, C. Liebi, H. Siegrist, Recovery of N and P from urine by struvite precipitation followed by combined stripping with digester sludge liquid at full scale, Water (Switzerland). 5 (2013) 1262–1278. https://doi.org/10.3390/w5031262.

[5] O. Lahav, M. Telzhensky, A. Zewuhn, Y. Gendel, J. Gerth, W. Calmano, L. Birnhack, Struvite recovery from municipal-wastewater sludge centrifuge supernatant using seawater NF concentrate as a cheap Mg(II) source, Sep. Purif. Technol. 108 (2013) 103–110. https://doi.org/10.1016/j.seppur.2013.02.002.

[6] K.S. Le Corre, E. Valsami-Jones, P. Hobbs, S.A. Parsons, Phosphorus recovery from wastewater by struvite crystallization: A review, 2009. https://doi.org/10.1080/10643380701640573.

[7] F. Di Capua, D. Spasiano, A. Giordano, F. Adani, U. Fratino, F. Pirozzi, G. Esposito, High-solid anaerobic digestion of sewage sludge: challenges and opportunities, Appl. Energy. 278 (2020) 115608. https://doi.org/10.1016/j.apenergy.2020.115608.

[8] A. Manmeen, P. Kongjan, T. Rattanaya, B. Cheirsilp, N. Raybut, R. Jariyaboon, Desulfurization of H2S-rich biogas using water scrubbing: Performance in pilot scale scrubber and scale-up estimation for the concentrated latex factory, Environ. Prog. Sustain. Energy. (2022).

https://doi.org/10.1002/ep.14034.

[9] Y. Cheng, T. Yuan, Y. Deng, C. Lin, J. Zhou, Z. Lei, K. Shimizu, Z. Zhang, Use of sulfur-oxidizing bacteria enriched from sewage sludge to biologically remove H2S from biogas at an industrial-scale biogas plant, Bioresour. Technol. Reports. 3 (2018) 43–50. https://doi.org/10.1016/j.biteb.2018.01.006.

[10] E. Tilahun, E. Sahinkaya, B. Çalli, A hybrid membrane gas absorption and bio-oxidation process for the removal of hydrogen sulfide from biogas, Int. Biodeterior. Biodegrad. 127 (2018) 69–76. https://doi.org/10.1016/j.ibiod.2017.11.015.

[11] F. Almenglo, J.J. González-Cortés, M. Ramírez, D. Cantero, Recent advances in biological technologies for anoxic biogas desulfurization, Chemosphere. 321 (2023). https://doi.org/10.1016/j.chemosphere.2023.138084.

[12] L. Krayzelova, J. Bartacek, I. Díaz, D. Jeison, E.I.P. Volcke, P. Jenicek, Microaeration for hydrogen sulfide removal during anaerobic treatment: a review, Rev. Environ. Sci. Biotechnol. 14 (2015) 703–725. https://doi.org/10.1007/s11157-015-9386-2.

[13] A. Giordano, F. Di Capua, G. Esposito, F. Pirozzi, Long-term biogas desulfurization under different microaerobic conditions in full-scale thermophilic digesters co-digesting high-solid sewage sludge, Int. Biodeterior. Biodegrad. 142 (2019) 131–136. https://doi.org/10.1016/j.ibiod.2019.05.017.